



**FCTUC DEPARTAMENTO DE ENGENHARIA CIVIL**

FACULDADE DE CIÊNCIAS E TECNOLOGIA  
UNIVERSIDADE DE COIMBRA

# **Comparison Between Analytical Expressions for Determination of Elastic Critical Moment of Steel Beams**

**Dissertaçāo apresentada para a obtenção do grau de Mestre em Engenharia Civil  
na Especialidade de Mecânica Estrutural**

**Autor**

**João Luís Pinelo Esteves Canha**

**Orientadores**

**Luís Alberto Proença Simões da Silva**

**Liliana Raquel Simões Marques**

Esta dissertação é da exclusiva responsabilidade do seu autor, não tendo sofrido correcções após a defesa em provas públicas. O Departamento de Engenharia Civil da FCTUC declina qualquer responsabilidade pelo uso da informação apresentada

**Coimbra, Outubro, 2013**

## AGRADECIMENTOS

O meu agradecimento ao Professor Doutor Luís Simões da Silva, pela orientação, motivação, e partilha do seu vasto conhecimento.

À Professora Doutora Liliana Marques, pela motivação, interesse, compreensão e especialmente pela disponibilidade independente do dia ou da hora.

À minha família e amigos.

Muito obrigado.

## RESUMO

Em elementos submetidos à flexão, é habitual a utilização de secções com maior resistência e rigidez no plano onde as cargas são aplicadas, permitindo uma maior economia de material. Normalmente, para esta consideração, opta-se por secções abertas de paredes finas como secções em I ou H. Contudo, estas secções são mais susceptíveis à rotura por encurvadura lateral.

Este fenómeno caracteriza-se por um deslocamento da parte comprimida da secções em relação à parte traccionada, e é previsto no processo de dimensionamento pelo Eurocódigo 3 (CEN, 2007) no cálculo do momento resistente à encurvadura lateral,  $M_{b,Rd}$ .

A determinação de  $M_{b,Rd}$  depende fundamentalmente do momento crítico,  $M_{cr}$ . Este é o resultado de uma interacção entre variados factores como a geometria da secções e do elemento, as propriedades do material, as condições fronteira, o tipo de carga aplicada e a posição desta em relação ao centro de corte. Assim se comprehende a complexidade do seu cálculo e a necessidade da utilização de métodos mais complexos como o Métodos dos Elementos Finitos para a sua exacta determinação. Apesar da evolução ao longo dos últimos anos, a utilização de *software* baseado em elementos finitos ainda não atingiu a rapidez e a simplicidade de cálculo exigida para a sua aplicação em ambiente de projecto, prevalecendo expressões analíticas com um maior sentido prático e rapidez. De referir que apesar de este valor entrar no seu procedimento de cálculo, a versão do Eurocódigo 3 em vigor não apresenta nenhuma alternativa de cálculo.

Nesta tese, são confrontadas várias destas expressões e factores de calibração propostos por diversos autores para o cálculo do momento crítico elástico. Na primeira parte são sintetizadas as soluções disponíveis mais utilizadas e consensuais, descrevendo: (i) âmbito de aplicação; (ii) a metodologia e (iii) considerações necessárias na sua aplicação. Por fim é apresentado (i) o estudo paramétrico realizado e (ii) análise e discussão de resultados.

## ABSTRACT

In elements subject to bending, usually one uses sections with greater strength and stiffness in the plane in which loads are applied, allowing greater savings of material. For this reason, open thin-wall cross sections such as I-sections beams are normally adopted. This can lead to failure by lateral-torsion buckling.

This phenomenon happens when the compression flange has a tendency to bend sideways while the remainder of the cross section restrains it from doing so, and it is quantified in Eurocode 3 (CEN, 2007) verification procedure by the design buckling resistance moment,  $M_{b,Rd}$ .

The design buckling resistance moment,  $M_{b,Rd}$ , depends essentially on the critical moment,  $M_{cr}$ . This value is the result of an interaction of various factors such as geometric properties of the cross-section; of the element; material proprieties; restrictions at supports; and loading type and loading position relative to the section shear center. This variety of factors increases the complexity of the calculation leading to an accurate value, usually requiring the utilization of numerical techniques such as the Finite Element Method. On the other hand, the complexity of the software involved and the time spent to compute the values makes analytical expressions more attractive and practical for structural designers and general use. It is important to mention that although the critical moment is used in safety verification of Eurocode 3, there is no way for calculate it in the procedure.

In this thesis, various expressions and calibration factors proposed by different authors for determination of the elastic critical moment are compared. Firstly, the available solutions more commonly used and accepted are presented, describing: (i) scope; (ii) theoretical background; and (iii) considerations for its application. Then the following is presented: (i) the parametric study and (ii) analysis and discussion of the results.

## TABLE OF CONTENTS

1 INTRODUCTION.....	1
1.1 Motivation and Objectives .....	1
1.1 Outline of the Dissertation.....	3
2 THEORETICAL BACKGROUND AND EUROCODE 3 VERIFICATION.....	4
2.1 Equilibrium and Bifurcation Buckling.....	4
2.2 Critical Moment - Basic Case.....	5
2.3 Eurocode 3 .....	6
3 ANALYTICAL EXPRESSIONS FOR DETERMINATION OF CRITICAL MOMENT ....	8
3.1 General Expressions.....	8
3.2 C Factors.....	12
3.2.1 Baláž and Koleková .....	16
3.2.2 ECCS – Basis Load cases .....	17
3.2.3 Galéa .....	18
3.2.4 Andrade <i>et al.</i> .....	18
3.2.5 Lindner .....	18
3.2.6 Trahair .....	21
3.2.7 Serna <i>et al.</i> .....	22
3.3 Final Remarks.....	22
4 PARAMETRIC STUDY .....	23
4.1 Numerical Model.....	23
4.2 Parametric Study .....	23
4.3 Methodology.....	25
4.4 Results.....	25
4.4.1 Baláž and Koleková .....	25
4.4.1.1 Case 1 .....	26
4.4.1.2 Case 2 .....	27
4.4.1.3 Case 3 .....	28
4.4.1.4 Case 4 .....	29
4.4.1.5 Case 5 .....	30
4.4.1.6 Case 6 .....	31
4.4.1.7 Case 7 .....	32
4.4.1.8 Case 9 .....	33
4.4.1.9 Case 10 .....	34

4.4.2 ECCS - Basis Load Cases .....	35
4.4.2.1 Case 1 .....	35
4.4.2.2 Case 2 .....	37
4.4.2.3 Case 3 .....	38
4.4.2.4 Case 4 .....	39
4.4.3 Galéa .....	39
4.4.3.1 Case 1 and 2 .....	40
4.4.3.2 Case 3 and 5 .....	41
4.4.3.3 Case 6 and 7 .....	42
4.4.3.4 Case 8 .....	43
4.4.4 Andrade <i>et al.</i> .....	43
4.4.4.1 Case 9 .....	44
4.4.4.2 Case 10 .....	44
4.4.5 Lindner .....	45
4.4.5.1 Case 9 .....	45
4.4.5.2 Case 10 .....	46
4.4.5.3 Additional Case .....	47
4.4.6 Trahair .....	48
4.4.6.1 Case 1 and 2 .....	48
4.4.6.2 Case 3 .....	49
4.4.6.3 Case 4 .....	50
4.4.6.4 Case 5 .....	51
4.4.6.5 Case 6 .....	52
4.4.6.6 Case 7 .....	53
4.4.6.7 Case 8 .....	54
4.4.6.8 Case 9 .....	54
4.4.6.9 Case 10 .....	55
4.4.7 Serna <i>et al.</i> .....	56
4.4.7.1 Case 1 and 2 .....	56
4.4.7.2 Case 3 and 4 .....	57
4.4.7.3 Case 5 and 6 .....	58
4.4.7.4 Case 7 .....	59
4.4.7.5 Case 8 .....	60
4.5 Comparison .....	61
4.5.1 Case 1 .....	61
4.5.2 Case 2 .....	62
4.5.3 Case 3 .....	64
4.5.4 Case 4 .....	66
4.5.5 Case 5 .....	68
4.5.6 Case 6 .....	69

4.5.7 Case 7 .....	71
4.5.8 Case 8 .....	72
4.5.9 Case 9 .....	73
4.5.10 Case 10 .....	74
4.6 Final Remarks .....	75
<b>5 CONCLUSION AND FUTURE RESEARCH .....</b>	<b>78</b>
5.1 Conclusion .....	78
5.2 Future Research .....	78
5.3 Original Contributions .....	79
<b>6 REFERENCES .....</b>	<b>80</b>
<b>ANNEX .....</b>	<b>82</b>
<b>ANNEX A – C Factors .....</b>	<b>1</b>
A.1 – General Formulae .....	1
A.2 – Baláž and Koleková .....	2
A.3 – ECCS – Basis Load Cases .....	7
A.4 – Galéa .....	8
A.5 – Andrade <i>et al.</i> .....	21
A.6 – Lindner .....	23
A.7 – Trahair .....	24
A.8 – Serna <i>et al.</i> .....	29
<b>ANNEX B – Statistical Analysis .....</b>	<b>1</b>
B.1 – Baláž and Koleková .....	1
B.2 – ECCS - Basis Load Cases .....	10
B.3 – Galéa .....	15
B.4 – Andrade <i>et al.</i> .....	17
B.5 – Lindner .....	19
B.6 – Trahair .....	21
B.7 – Serna <i>et al.</i> .....	25

## LIST OF FIGURES

Figure 1.1 – Lateral-torsional buckling in cantilever loaded on the tip .....	1
Figure 2.1 – Generic equilibrium path of a lateral-torsion buckling of a beam.....	4
Figure 2.2 – Basic case. ....	5
Figure 3.1 – Sign convention for $z_g$ . ....	12
Figure 3.2 – Polynomial test of the chart a). ....	19
Figure 4.1 – Baláž and Koleková – Case 1.....	26
Figure 4.2 – Baláž and Koleková – Case 2.....	27
Figure 4.3 – Baláž and Koleková – Case 3.....	28
Figure 4.4 – Baláž and Koleková – Case 4.....	29
Figure 4.5 – Baláž and Koleková – Case 5.....	30
Figure 4.6 – Baláž and Koleková – Case 6.....	31
Figure 4.7 – Baláž and Koleková – Case 7.....	32
Figure 4.8 – Baláž and Koleková – Case 9.....	33
Figure 4.9 – Baláž and Koleková – Case 10. ....	34
Figure 4.10 – ECCS – Case 1 – Double symmetric cross sections.....	35
Figure 4.11 – ECCS – Case 1 – Mono symmetric cross sections. ....	36
Figure 4.12 – ECCS – Basis Load Cases – Case 2. ....	37
Figure 4.13 – ECCS – Basis Load Cases – Case 3. ....	38
Figure 4.14 – ECCS – Basis Load Cases – Case 4. ....	39
Figure 4.15 – Galéa – Case 1 and 2. ....	40
Figure 4.16 – Galéa – Case 3 and 5. ....	41
Figure 4.17 – Galéa – Case 6 and 7. ....	42
Figure 4.18 – Galéa – Case 8.....	43
Figure 4.19 – Andrade <i>et al.</i> – Case 9.....	44
Figure 4.20 – Andrade <i>et al.</i> – Case 10. ....	45
Figure 4.21 – Lindner – Case 9. ....	46
Figure 4.22 – Lindner – Case 10. ....	47
Figure 4.23 – Lindner – Additional case. ....	48
Figure 4.24 – Trahair – Case 1 and 2.....	49
Figure 4.25 – Trahair – Case 3. ....	50
Figure 4.26 – Trahair – Case 4. ....	51

Figure 4.27 – Trahair – Case 5.....	51
Figure 4.28 – Trahair – Case 6.....	52
Figure 4.29 – Trahair – Case 7.....	53
Figure 4.30 – Trahair – Case 8.....	54
Figure 4.31 – Trahair – Case 9.....	55
Figure 4.32 – Trahair – Case 10.....	56
Figure 4.33 – Serna <i>et al.</i> – Case 1 and 2 .....	57
Figure 4.34 – Serna <i>et al.</i> – Case 3 and 4 .....	58
Figure 4.35 – Serna <i>et al.</i> – Case 5 and 6 .....	59
Figure 4.36 – Serna <i>et al.</i> – Case 7 .....	60
Figure 4.37 – Serna <i>et al.</i> – Case 8 .....	60
Figure A.1 – Loading case.....	A.6
Figure A.2 – C <sub>1</sub> for end moments with uniformly distributed load q .....	A.9
Figure A.3 – C <sub>2</sub> for end moments with uniformly distributed load q .....	A.10
Figure A.4 – C <sub>1</sub> for end moments with concentrated load F .....	A.11
Figure A.5 – C <sub>2</sub> for end moments with concentrated load F .....	A.12
Figure A.6 – Values of k for single double symmetric beams with cantilever .....	A.23
Figure A.7 – Moment diagram and moment values.....	A.29

## LIST OF TABLES

Table 3.1 – Relations between the alternatives 3-factors formulae. ....	10
Table 3.2 – C Factor values analyzed. ....	13
Table 3.3 – C Factors (Case 1 to 6) – Ranges. ....	14
Table 3.4 – C Factors (Case 7 to 10) – Ranges. ....	15
Table 3.5 – Variables A to R. ....	20
Table 4.1 – Parametric Study. ....	24
Table 4.2 – Lindner – Parameter L Study....	24
Table 4.3 – Baláž and Koleková – Case 1....	26
Table 4.4 – Baláž and Koleková – Case 2....	27
Table 4.5 – Baláž and Koleková – Case 3....	28
Table 4.6 – Baláž and Koleková – Case 4....	29
Table 4.7 – Baláž and Koleková – Case 5....	30
Table 4.8 – Baláž and Koleková – Case 6....	31
Table 4.9 – Baláž and Koleková – Case 7....	32
Table 4.10 – Baláž and Koleková – Case 9 – Non-linear....	33
Table 4.11 – Baláž and Koleková – Case 10 – Non-linear....	35
Table 4.12 – ECCS – Basis Load Cases – Case 1 – Without $k_z=0,7$ ....	36
Table 4.13 – ECCS – Basis Load Cases – Case 2....	38
Table 4.14 – ECCS – Basis Load Cases – Case 3....	38
Table 4.15 – ECCS – Basis Load Cases – Case 4....	39
Table 4.16 – Galéa – Case 1....	40
Table 4.17 – Galéa – Case 2....	40
Table 4.18 – Galéa – Case 3....	41
Table 4.19 – Galéa – Case 5....	41
Table 4.20 – Galéa – Case 6....	42
Table 4.21 – Galéa – Case 7....	42
Table 4.22 – Galéa – Case 8....	43
Table 4.23 – Andrade <i>et al.</i> – Case 9....	44
Table 4.24 – Andrade <i>et al.</i> – Case 10....	45
Table 4.25 – Lindner – Case 9. ....	46
Table 4.26 – Lindner – Case 10. ....	47

Table 4.27 – Galéa – Case 1.....	48
Table 4.28 – Galéa – Case 2.....	49
Table 4.29 – Trahair – Case 3.....	50
Table 4.30 – Trahair – Case 4.....	50
Table 4.31 – Trahair – Case 5.....	52
Table 4.32 – Trahair – Case 6.....	53
Table 4.33 – Trahair – Case 7.....	53
Table 4.34 – Trahair – Case 8.....	54
Table 4.35 – Trahair – Case 9.....	55
Table 4.36 – Trahair – Case 10.....	55
Table 4.37 – Serna <i>et al.</i> – Case 1.....	56
Table 4.38 – Serna <i>et al.</i> – Case 2.....	57
Table 4.39 – Serna <i>et al.</i> – Case 3.....	57
Table 4.40 – Serna <i>et al.</i> – Case 4.....	58
Table 4.41 – Serna <i>et al.</i> – Case 5.....	58
Table 4.42 – Serna <i>et al.</i> – Case 6.....	59
Table 4.43 – Serna <i>et al.</i> – Case 7.....	59
Table 4.44 – Serna <i>et al.</i> – Case 8.....	61
Table 4.45 – Comparisons – Case 1.....	61
Table 4.46 – Comparison 1.....	62
Table 4.47 – Comparison 2.....	62
Table 4.48 – Comparisons – Case 2.....	62
Table 4.49 – Comparison 3.....	63
Table 4.50 – Comparison 4.....	63
Table 4.51 – Comparison 5.....	63
Table 4.52 – Comparison 6.....	64
Table 4.53 – Comparisons – Case 3.....	64
Table 4.54 – Comparison 7.....	65
Table 4.55 – Comparison 8.....	65
Table 4.56 – Comparison 9.....	65
Table 4.57 – Comparison 10.....	66
Table 4.58 – Comparison 11.....	66
Table 4.59 – Comparisons – Case 4.....	66
Table 4.60 – Comparison 12.....	67
Table 4.61 – Comparison 13.....	67
Table 4.62 – Comparison 14.....	67
Table 4.63 – Comparison 15.....	68
Table 4.64 – Comparison 16.....	68

Table 4.65 – Comparisons – Case 5.....	68
Table 4.66 – Comparison 17. ....	69
Table 4.67 – Comparison 18. ....	69
Table 4.68 – Comparison 19. ....	69
Table 4.69 – Comparisons – Case 6.....	70
Table 4.70 – Comparison 20. ....	70
Table 4.71 – Comparison 21. ....	70
Table 4.72 – Comparison 22. ....	71
Table 4.73 – Comparison – Case 7. ....	71
Table 4.74 – Comparison 23. ....	71
Table 4.75 – Comparison 24. ....	72
Table 4.76 – Comparison 25. ....	72
Table 4.77 – Comparisons – Case 8.....	72
Table 4.78 – Comparison 26. ....	73
Table 4.79 – Comparison 27. ....	73
Table 4.80 – Comparisons – Case 9.....	73
Table 4.81 – Comparison 28. ....	74
Table 4.82 – Comparison 29. ....	74
Table 4.83 - Comparison 29. ....	74
Table 4.84 – Comparison 30. ....	75
Table 4.85 – Comparison 31. ....	75
Table 4.86 – Overview for double symmetric cross section. ....	76
Table 4.87 – Overview for mono symmetric cross section. ....	77
Table A.1 – Values of factors $C_1$ and $C_3$ corresponding to various end moment ratio $\psi$ , values of buckling length factor $k_z$ and cross-section parameters $\psi_f$ and $k_{wt}$ ( $k_w=1$ ). ....	A.2
Table A.2 – Values of factors $C_1$ , $C_2$ and $C_3$ corresponding to various transverse loading cases, values of buckling length factors $k_y$ , $k_z$ and $k_w$ , cross section mono symmetry factor $\psi_f$ and torsion parameter $k_{wt}$ . ....	A.3
Table A.3 – Relative non-dimensional critical moment $\mu_{cr}$ for cantilever loaded by concentrated tip load $F$ ( $k_z=k_w=2$ ). ....	A.4
Table A.4 – Relative non-dimensional critical moment $\mu_{cr}$ for cantilever loaded by uniformly distributed load $q$ ( $k_z=k_w=2$ ). ....	A.5
Table A.5 – Values of factor $C_1$ ( $k_{wt} = 0.235$ ; $\psi$ ; $M_0/M$ ) ( $k_z=k_w=1$ ). ....	A.6
Table A.6 – Values of factors $C_1$ and $C_3$ corresponding to various end moment ratio $\psi$ , values of buckling length factor $k_z$ and cross-section parameters $\psi_f$ and $k_{wt}$ ( $k_w=1$ ). ....	A.7

Table A.7 – Values of factors $C_1$ , $C_2$ and $C_3$ corresponding to various transverse loading cases, values of buckling length factor $k_z$ , cross section mono symmetry and torsion parameter $k_{wt}$ ( $k_w=1$ ). ....	A.8
Table A.8 – $C_1$ for end moments with uniformly distributed load $q$ ( $\mu \geq 0$ ). ....	A.13
Table A.9 – $C_1$ for end moments with uniformly distributed load $q$ ( $\mu \leq 0$ ) ....	A.14
Table A.10 – $C_2$ for end moments with uniformly distributed load $q$ ( $\mu \geq 0$ ). ....	A.15
Table A.11 – $C_2$ for end moments with uniformly distributed load $q$ ( $\mu \leq 0$ ). ....	A.16
Table A.12 – $C_1$ for end moments with concentrated load $F$ ( $\mu \geq 0$ ). ....	A.17
Table A.13 – $C_1$ for end moments with concentrated load $F$ ( $\mu \leq 0$ ). ....	A.18
Table A.14 – $C_2$ for end moments with concentrated load $F$ ( $\mu \geq 0$ ). ....	A.19
Table A.15 – $C_2$ for end moments with concentrated load $F$ ( $\mu \leq 0$ ). ....	A.20
Table A.16 – Values of $C_1$ and $C_2$ for cantilevers with warping prevent at the fixed end....	A.21
Table A.17 – Values of $C_3$ for cantilevers with warping prevent at the fixed end.....	A.21
Table A.18 – Values of $C_1$ and $C_2$ for cantilevers with warping free at the fixed end. ....	A.22
Table A.19 – Values of $C_3$ for cantilevers with warping free at the fixed end.....	A.22
Table A.20 – Values of $\alpha_m$ for doubly symmetric beams with loads at shear center ( $k_z=k_w=1$ ). ....	A.24
Table A.21 – Critical moment for mono symmetric beams with loads at shear center ( $k_z=k_w=1$ ).....	A.25
Table A.22 – Critical moment for doubly and mono symmetric beams with loads out of shear center ( $k_z=k_w=1$ ). ....	A.26
Table A.23 – Critical moment for doubly and mono symmetric beams with loads out shear center and subjected to uniform bending moment.....	A.27
Table A.24 – Critical moment for doubly symmetric cantilevers.....	A.28
Table B.1 – Baláž and Koleková – Case 1. ....	B.1
Table B.2 – Baláž and Koleková – Case 2. ....	B.2
Table B.3 – Baláž and Koleková – Case 2 – $\psi_f$ limits analysis.....	B.2
Table B.4 – Baláž and Koleková – Case 3. ....	B.3
Table B.5 – Baláž and Koleková – Case 3 – $\psi_f$ limits analysis.....	B.3
Table B.6 – Baláž and Koleková – Case 4. ....	B.4
Table B.7 – Baláž and Koleková – Case 4 – $\psi_f$ limits analysis.....	B.4
Table B.8 – Baláž and Koleková – Case 5. ....	B.5
Table B.9 – Baláž and Koleková – Case 5 – $\psi_f$ limits analysis.....	B.5
Table B.10 – Baláž and Koleková – Case 6. ....	B.6
Table B.11 – Baláž and Koleková – Case 6 – $\psi_f$ limits analysis. ....	B.6
Table B.12 – Baláž and Koleková – Case 7. ....	B.7
Table B.13 – Baláž and Koleková – Case 7 – $C_2$ analysis. ....	B.7

Table B.14 – Baláž and Koleková – Case 9 .....	B.8
Table B.15 – Baláž and Koleková – Case 9 – Interpolation analysis.....	B.8
Table B.16 – Baláž and Koleková – Case 10.....	B.9
Table B.17 – Baláž and Koleková – Case 10 – Interpolation analysis.....	B.9
Table B.18 – ECCS – Basis Load Cases – Case 1.....	B.10
Table B.19 – ECCS – Basis Load Cases – Case 1 – $k_z = 0,7$ Method.....	B.11
Table B.20 – ECCS – Basic Load Cases – Case 2.....	B.12
Table B.21 – ECCS – Basic Load Cases – Case 2 – $\psi_f$ limits analysis .....	B.12
Table B.22 – ECCS – Basic Load Cases – Case 3.....	B.13
Table B.23 – ECCS – Basic Load Cases – Case 3 – $\psi_f$ limits analysis .....	B.13
Table B.24 – ECCS – Basic Load Cases – Case 4.....	B.14
Table B.25 – ECCS – Basic Load Cases – Case 4 – $\psi_f$ limits analysis .....	B.14
Table B.26 – Galéa – Case 1 to 6.....	B.15
Table B.27 – Galéa – Case 7 .....	B.16
Table B.28 – Galéa – Case 8 .....	B.16
Table B.29 – Andrade <i>et al.</i> – Case 9 .....	B.17
Table B.30 – Andrade <i>et al.</i> – Case 9 – $\psi_f$ limits analysis.....	B.17
Table B.31 – Andrade <i>et al.</i> – Case 10 .....	B.18
Table B.32 – Andrade <i>et al.</i> – Case 10 – $\psi_f$ limits analysis .....	B.18
Table B.33 – Lindner – Case 9.....	B.19
Table B.34 – Lindner – Case 10.....	B.20
Table B.35 – Trahair – Case 1 to 4 .....	B.21
Table B.36 – Trahair – Case 5 to 6 .....	B.22
Table B.37 – Trahair – Case 3 to 6 – $h_l$ analysis .....	B.22
Table B.38 – Trahair – Case 7 and 8.....	B.23
Table B.39 – Trahair – Case 9 and 10 .....	B.24
Table B.40 – Serna <i>et al.</i> – Case 1 and 6 .....	B.25
Table B.41 – Serna <i>et al.</i> – Case 5 and 6 .....	B.26
Table B.42 – Serna <i>et al.</i> – Case 7 and 8 .....	B.27

## NOTATIONS

### Lowercases

b – Cross section width;

$b_{fc}$ ,  $b_{ft}$  – Compression and tension flanges width

c – Parameter

d – Distance between the mid-span and the load position along the beam; Ratio between the real d value and the total length of the beam

$f_y$  – Yield stress

$f_1$ ,  $f_2$ ,  $f_3$  – Parameter related to mono symmetric cross section

h – Cross section height

$h_m$  – Distance between flanges centroids

$h_w$  – Web height

$h_{load}$ ,  $h_l$  – Distance between the point of application of the load and bottom face of the cross section; Ratio between the real  $h_l$  and total height of the cross section

k – Lindner Factor

$k_z$  – Length factor related to rotations about the weak axis z

$k_w$  – Length factor related to warping restriction

$k_{wt}$  – Non-dimensional parameter

$k_1$ ,  $k_2$ ,  $k_\phi$  – Length factors

m – Parameter

n – Parameter

q – Uniform distributed load

t – Cross section thickness

$t_f$  – Flange thickness

$t_{fc}$ ,  $t_{ft}$  – Compression and Tension flange thickness

$t_w$  – Web thickness

$\bar{z}$  – Distance between the centroid of the cross section and the centroid of the compressed flange.

$z_a$  – Distance between the point of the application of the loads and the centroid of the cross section

- $z_g$  – Distance between the point of the application of loads and the shear center of the cross section
- $z_j$  – Parameter that reflects the degree of asymmetry of the cross section in relation to the y axis
- $z_s$  – Distance between the shear center and the centroid of the cross section
- $z_p$  - Distance between the point of the application of loads and the centroid of the cross section
- x-x – Axis along the element
- y-y – Cross section axis parallel to the flanges
- z-z – Cross section axis perpendicular to the flanges
- $x'-x'$ ,  $y'-y'$ ,  $z'-z'$  – Local system

### Uppercases

- $C_1$  – Factor related to the bending moment shape and can be related to torsion properties
- $C_2$  – Factor related to the position of loading relatively to the shear center
- $C_3$  – Factor related to the shape of the cross section
- $D_i$  – Integration constant
- $E$  – Modulus of elasticity
- $F$  – Concentrated load
- $G$  – Shear modulus
- $I$  – Second moment of area
- $I_{fc}$  – Second moment of area of compression flange about z
- $I_{ft}$  – Second moment of area of tension flange about z
- $I_{fz}$  – Second moment of area of flange about z
- $I_y$ ,  $I_z$  – Second moment of area, y-y and z-z axis
- $I_w$  – Warping constant
- $I_T$  – Torsional constant
- $K$  – Torsion parameter
- $\bar{K}$  – Parameter related to mechanical properties
- $L$  – Element length
- $L_1$  – Length of the simply supported beam part
- $M$  – Bending moment
- $M_{b,Rd}$  – Design buckling resistance moment
- $M_{cr}$  – Elastic moment for lateral-torsion buckling, critical moment
- $M_{cr}^{Basic}$  – Critical moment of the basic case
- $M_{Ed}$  – Design bending moment
- $M_{Ki,y}$  – Elastic moment for lateral-torsion buckling
- $M_{max}$  – Maximum value of the bending moment diagram
- $M_{pl}$  – Plastic resistance to bending moment

$M_y, M_{y'}$  – Bending moment, y-y axis and  $y'-y'$  axis  
 $M_0$  – Moment due to transverse load  
 $N_{cr,z}$  – Elastic critical force for out-of-plane buckling  
 $N_{Ki,z}$  – Elastic critical force for out-of-plane buckling  
 $T$  – Torsion  
 $T_t$  – Uniform torsional component  
 $T_w$  – Non-uniform torsional component  
 $W_y$  – Bending modulus, y-y axis

#### Lowercases Greek letters

$\alpha_{LT}$  – Imperfection factor  
 $\alpha_m$  – Trahair Factor  
 $\alpha_z$  – Stiffness of the bending restriction about z  
 $\alpha_w$  – Stiffness of warping restraints  
 $\alpha_x$  – Stiffness of the bending restriction about x  
 $\beta$  – Ratio between the maximum and minimum bending moment, for a linear bending moment distribution  
 $\beta_y, \beta_y^*$  – Parameter that reflects the degree of asymmetry of the cross section in relation to the y axis  
 $\beta_0, \beta_1, \beta_2$  – Mrázik Factors  
 $\gamma$  – Parameter  
 $\gamma_{M1}$  – Partial safety factor for resistance of members to instability assessed by member checks  
 $\xi$  – Moment factor applicable to fork restraint at the supports  
 $\xi_g, \xi_{j,0}$  – Non-dimensional parameter related to the load position  
 $\xi_j, \xi_{g,0}$  – Non-dimensional parameter related to the asymmetry of the cross section  
 $\bar{\lambda}_{LT}$  – Non-dimensional slenderness for lateral-torsion buckling  
 $\bar{\lambda}_{LT,0}$  – Plateau length of the lateral torsional buckling curves  
 $\mu$  – Ratio of the moment due to transverse load to the maximum moment  
 $\mu_{cr}$  – Non-dimensional critical moment; eigenvalue  
 $v$  – Displacement out of plane  
 $\chi_{LT}$  – Reduction factor to lateral-torsion buckling  
 $\phi$  – Angle of rotation;  
 $\phi_{LT}$  – Value to determine the reduction factor  $\chi_{LT}$   
 $\chi_t$  – Torsion coefficient  
 $\psi$  – Ratio between the maximum and minimum bending moment, for a linear bending moment distribution  
 $\psi_f$  – Parameter that reflects the degree of asymmetry of the flanges  
 $\omega$  – Displacement in the load plane

## 1 INTRODUCTION

### 1.1 Motivation and Objectives

Typically, elements subject to bending have much greater strength and stiffness in the plane in which loads are applied, such as I-section beams, allowing greater savings of material. This consideration can lead to failure by lateral-torsional buckling (or flexural-torsion buckling) of such elements before their maximum capacity of the cross section in the plane of loading is reached. This can be easily seen in Figure 1.1, which represents lateral-torsion buckling of a cantilever vertically loaded at the tip. In the Figure, the compression flange has a tendency to bend sideways while the remainder of the cross section restrains it from doing so. This phenomenon is a bifurcation-type instability and its critical buckling mode involves bending and torsion deformation. The critical buckling point corresponds to a critical moment,  $M_{cr}$ , representing the maximum moment that the element can support without lateral-torsional buckling. This value is not only a characteristic of the material or cross section, but it is a result from an interaction of various factors such as geometric properties of the cross section; of the element; of the material; restriction at supports; loading type and loading position relatively to the cross section shear center.

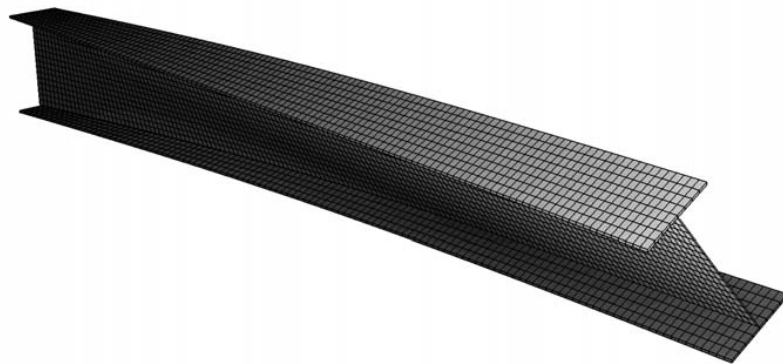


Figure 1.1 – Lateral-torsional buckling in cantilever loaded on the tip.

The study of the general theory of lateral-torsion buckling, such as the study of the stability theory, was started by Euler in 1759 on column flexural buckling, which presented the first

analytical theory to predict the reduced of the maximum strength of slender columns. Years later, in 1855, the research of Sanit-Venant on uniform torsion gave the first description of the response of elements to torsion. However, it was only in 1899 that lateral-torsion buckling appears published by Michell and Prandtl. In their research, they considered only beams with rectangular cross section, therefore only with uniform torsion. Based on this, Timoshenko in 1905 presented his research about I-section beams, including the effects of the warping torsion on these elements. More research such as Wagner in 1929 led to the development of a general theory of lateral-torsion buckling, which was published in many textbook used and accepted nowadays (Trahair, 1993).

However, the complexity of the calculation needed to this analysis limits the manual analysis of variables. Only in the 60's with the advent of the modern digital computer was it possible to eliminate some barriers, allowing for the appearance of a huge number of published researches about lateral-torsional buckling. In 1970, the extension of the general finite element method of structural analysis to lateral-torsion buckling problems by Barsoum and Gallagher, allows all complex hypotheses with various load cases and boundary conditions to be automatically computed (Trahair, 1993). On the other hand, 40 years have passed, and despite the significant evolution of the software based in Finite Element Method in the last decade, they remain too complex and slow to compute accurate values, making simplified and approximated analytical expression more attractive and practical for structural designers and general use. There is a variety of these expressions and calibration factors values in result of the extensive research over the years, but all follow the same principle. This variety is due to their low consistency or limitation, which leads to different codes adopting different ways or simply do not present no procedure for its calculation. Eurocode 3 (CEN, 2007) is the latter: the critical moment is used in its safety verification procedure but no way for its calculation is proposed. There is an analytical expression in Annex F (informative) of its pre-standard version (CEN, 2003). However some authors have shown that its calibration factors can lead to incorrect values of the critical moment (Baláz, et al., 1999) (Baláz, et al., 2012), creating some disagreement and results in to its removal from the current version of the code. Therefore the main objective of this thesis is to start a selection process of the most complete expression, and the most accurate calibration factors. Allowing the creation of a standardized procedure based on the best results in future research. For this purpose the established goals are: (i) present the theoretical background of this analytical expression; (ii) present and analyze the most used expressions and factors' values; (iii) compare them with numerical models considering a wide parametric study in order to know its accuracy; and (iv) compare and discuss results from the different solutions among them.

## 1.1 Outline of the Dissertation

This thesis is divided in 5 chapters.

- In **Chapter 1** the phenomenon of lateral-torsional buckling is presented as well as the importance of an accurate critical moment value. The research evolution and the current situation of the methods for its evaluation are also described inserting the objective of the thesis on that.
- In **Chapter 2** the theoretical background of the analytical expressions and its concepts are presented. The link of the elastic critical moment value with the Eurocode 3 procedure is also made.
- In **Chapter 3** all expressions and proposed factors values analyzed here are presented and discussed. Firstly, the alternatives general expressions are described and then all solutions for factors' values are analyzed and discussed.
- In **Chapter 4** the parametric study and its results are presented and discussed. Firstly, the comparison between each solution is made with numerical model. Then, the results are compared for each analyzed case and discussed among them.
- And in **Chapter 5** some general conclusions are taken as well as the important subjects to be further developed.

And finally, the thesis has two **Annex** parts. In the first part, Annex A, all the analyzed and discussed solutions for the factors values are presented, and then in Annex B the statistical analysis for each one relative to the numerical models results is presented.

## 2 THEORETICAL BACKGROUND AND EUROCODE 3 VERIFICATION

### 2.1 Equilibrium and Bifurcation Buckling

In structural analysis, the “Stability” concept is always associated to the equilibrium concept, once it is used for classification of the equilibrium position of a structure under load. This structure may be stable, neutral or unstable. At the transition from stable to unstable equilibrium, it is assumed that a state of neutral equilibrium exists. Bifurcation-type instability is characterized by a primary equilibrium path, and in a bifurcation point this path may suddenly branch or bifurcate creating a postbuckling path. This point corresponds to the intersection between these paths and it is where the equilibrium of the primary path changes from stable to unstable. Which means that after passing the bifurcation load, the original path is unstable and any small disturbance will be cause a snap to the lower path.

The lateral-torsional buckling involves both transversal displacements and twist rotations and is resisted by combinations of the bending resistance and the torsional resistances. Thus, it is possible to realize that for lateral-torsional buckling of a beam, the equilibrium path must be a 3D graph with four variables:  $M$  is the moment applied;  $\omega$  is the displacement in the load plane;  $v$  is displacement out of plane and  $\varphi$  is the angle of rotation. Therefore, a generic equilibrium path of a lateral-torsion buckling of a beam is presented in Figure 2.1.

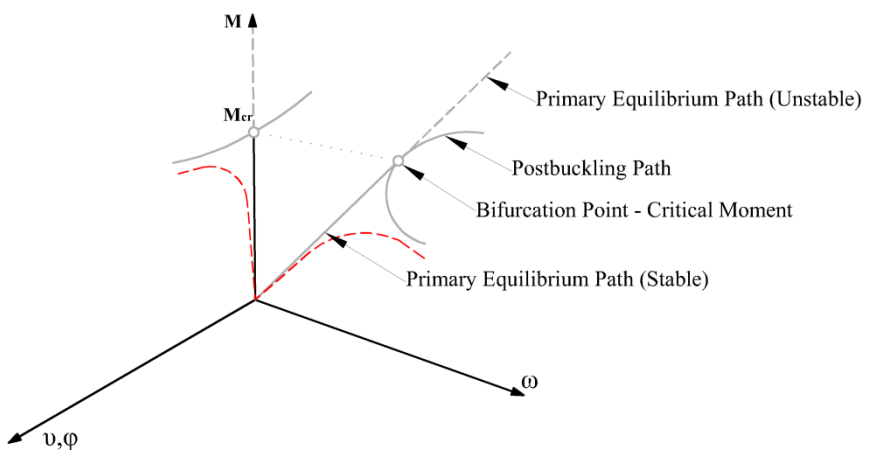
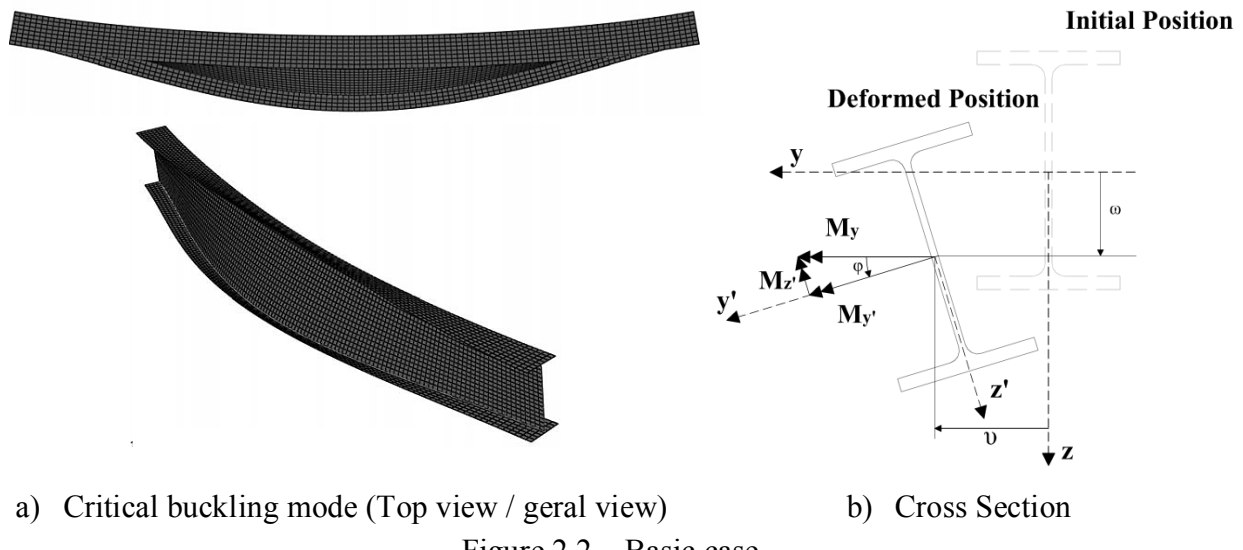


Figure 2.1 – Generic equilibrium path of a lateral-torsion buckling of a beam.

As seen in the figure above, the bifurcation point corresponds to a “critical bifurcation moment”, which is called Critical Moment. Real elements present a variety of initial geometrical imperfections like an initial deformed configuration, geometric cross section imperfection or residual stress. This has a huge impact on the primary equilibrium path, as can be easily seen in red in the figure above. However in this thesis it is only studied elements without imperfections and with elastic behavior. These variables are included on the structural design process by the Eurocode 3 (CEN, 2007).

## 2.2 Critical Moment - Basic Case

The analytical expressions to calculate the elastic critical moment used in this study are based in a basic case with easy and precise formulation. To understand this formulation, the governing differential equation for lateral torsional buckling of the basic case is summarized. In this case, the beam has a by-symmetrical I-section and it is subjected to constant bending moment. At the supports, lateral displacements and twist in the cross section are prevented, but warping and bending rotations around the cross sectional axes are allowed. The formulation is obtained from the differential equation of equilibrium in the deformed configuration, as seen in Figure 2.2.



a) Critical buckling mode (Top view / geral view)

b) Cross Section

Figure 2.2 – Basic case.

The local system is  $x', y', z'$  at the center of cross section. The deformation of the element is defined by the components  $v$ ,  $\omega$  of the displacement and by the angle of rotation  $\varphi$ . The equilibrium equation for bending in  $y'$  direction with  $M_{y'} = M_y \cos \varphi \approx M_y$  is given by

$$EI_y \frac{d^2\omega(x)}{dx^2} + M_y = 0 \quad (1)$$

Similarly, for bending in z' direction with  $M_{z'} = M_y \sin \varphi \approx \varphi M_y$  is given by

$$EI_z \frac{d^2v(x)}{dx^2} + \varphi(x)M_y = 0 \quad (2)$$

The equilibrium equation for torsion in x' direction with  $T = M_y \sin(dv/dx) \approx M_y(dv/dx)$  is given by

$$EI_w \frac{d^3\varphi(x)}{dx^3} - GI_T \frac{d\varphi(x)}{dx} + M_y \frac{dv(x)}{dx} = 0 \quad (3)$$

Eq. (1) is independent from Eq. (2) and Eq. (3). Differentiating Eq. (3) once and combining it with Eq. (2), Eq. (4) is obtained:

$$EI_w \frac{d^4\varphi(x)}{dx^4} - GI_T \frac{d^2\varphi(x)}{dx^2} - \frac{M_y^2}{EI_z} \varphi(x) = 0 \quad (4)$$

Eq. (4) is a fourth order differential equation with constants coefficients, the general solution is of the type

$$\varphi(x) = D_1 \sin(mx) + D_2 \cos(mx) + D_3 e^{nx} + D_4 e^{-nx} \quad (5)$$

where m and n are positive real quantities. The constants  $D_1$ ,  $D_2$ ,  $D_3$  and  $D_4$  may be obtained by the boundary conditions of the problem, leading to the Critical Moment of the basic case

$$M_{cr} = \frac{\pi}{L} \sqrt{GI_T EI_z \left( 1 + \frac{\pi^2 EI_w}{L^2 GI_T} \right)} \quad (6)$$

Eq. (6) represents the solution of the basic case and this is the basis for the expressions that are analyzed here. These expressions combine this equation with one or more calibrated factors to take into account the real conditions of the hypothesis in study, such as different loading type and load position; different support conditions; and different cross sections.

### 2.3 Eurocode 3

Real beams are conditioned by plasticity phenomena and imperfections such as initial lateral displacements, initial torsional rotations, eccentricity of the transversal loads and residual stresses. These variables are included in the design process by Eurocode 3 (CEN, 2007). The collapse of the beams composed by an elasto-plastic material is originated by a combination between phenomena of plasticity and instability and it depends on the slenderness of the beam, plastic resistance of the cross section and the imperfections. Thus, it is easily understood that the resistance capacity of low slenderness beams is limited by the plastic moment  $M_{pl}$  and for high slenderness beams the limit is the critical moment. For intermediate

slenderness beams, the resistance capacity is limited by an interaction of both, plastic moment and critical moment. Thus, the procedure to the design of an element has to involve all of these factors. As a result, the procedure adopted by the Eurocode 3 to verification of resistance of uniform beams in bending consists of the verification of the Eq. (7) (Clause 6.3.2.1 (1)).

$$\frac{M_{Ed}}{M_{b,Rd}} \leq 1.0 \quad (7)$$

Where  $M_{Ed}$  is the design bending moment and  $M_{b,Rd}$  is the design buckling resistant moment which is given by

$$M_{b,Rd} = \chi_{LT} W_y f_y / \gamma_{M1} \quad (8)$$

where  $W_y$  is the bending modulus about strong axis and its calculation depends on the class of the cross section, in other words, depends on the capacity and ability of the cross section to form rotational plastic hinges;  $f_y$  is the yield strength;  $\gamma_{M1}$  is the partial factor for resistance of members to instability; and  $\chi_{LT}$  is the reduction factor for lateral-torsion bulking. The value of  $\chi_{LT}$  (clause 6.3.2.2) is based on a non-dimensional slenderness for lateral torsional buckling, which is given by

$$\bar{\lambda}_{LT} = \sqrt{\frac{W_y f_y}{M_{cr}}} \quad (9)$$

Where  $M_{cr}$  is the critical moment of the beam, which is based on gross cross sectional properties, and takes into account the loading conditions, the real moment distribution and the lateral restraints (clause 6.3.2.2 (2)). As said, the current version of the Eurocode 3 does not include a procedure for the calculation of this critical moment. And it is on this issue procedure that this thesis focuses. The relation between  $\chi_{LT}$  and  $\bar{\lambda}_{LT}$  is given by

$$\chi_{LT} = \frac{1}{\phi_{LT} + \sqrt{\phi_{LT}^2 - \bar{\lambda}_{LT}^2}} \quad \text{with } \chi_{LT} \leq 1 \quad (10)$$

where the parameter  $\phi_{LT}$  is given by

$$\phi_{LT} = 0.5 [1 + \alpha_{LT} (\bar{\lambda}_{LT} - 0.2) + \bar{\lambda}_{LT}^2] \quad (11)$$

$\alpha_{LT}$  is the imperfection factor which depends on the buckling curve. Standard European lateral-torsional buckling curves do not yet exist (ECCS, 2006), hence the Eurocode 3 adopted the same curves used for  $\chi$ , reduction factor for relevant buckling mode in columns.

### 3 ANALYTICAL EXPRESSIONS FOR DETERMINATION OF CRITICAL MOMENT

In Chapter 2, the formulation of the critical moment of a beam with double-symmetrical I-section and fork conditions subjected to constant bending moment is defined, Eq. (6), i.e., the basic case. This case is a particular case with an easy and precise formulation. However, many situations in reality have different conditions, such as different symmetry of the cross section; different restrictions at the supports; different loading type and loading position. And it is understandable that, it is not practical to compute an exact equation for each situation, since this implies the computation of differential equations with different complexity. Another approach for that is the use of software based on numerical techniques such as the Finite Element Method. However the complexity of the software and the time spent to compute makes analytical expressions more attractive and practical for structural designers and general use. There is a variety of these expressions in result of the extensive research over the years, but all following the same principle. As said in the Chapter 2, these expressions are all based in the basic case equation that is multiplied by calibrated factors to take the different conditions into account, being the main difference between them the values of the factors. In this chapter each analyzed proposal is presented, as well as some considerations that are necessary to establish for each one in order to overcome some issues/inconsistencies in each procedures. Thus, firstly the general expressions are presented, which basically is the modification of Eq. (6) in order to include the factors, and then all solutions for factors' values are analyzed.

#### 3.1 General Expressions

One of the most commonly employed expression to estimate the elastic critical moment is the so-called 3-factor formula. This formula was first proposed by Mrázik in 1958 (Mrázik, et al., 1958) (Baláz, et al., 1999), with three factors,  $\beta_0$ ,  $\beta_1$ , and  $\beta_2$  depending on loading, symmetry of cross section and boundary conditions, given by

$$M_{cr} = \beta_0 \frac{\pi^2 EI_z}{(k_z L)^2} \left\{ \sqrt{\beta_2 \left[ \frac{I_w}{I_z} \left( \frac{k_z}{k_w} \right)^2 + \frac{G I_T}{E I_z} \left( \frac{k_z L}{\pi} \right)^2 \right]} + (z_g + \beta_1 z_j)^2 + (z_g + \beta_1 z_j) \right\} \quad (12)$$

Other authors proposed similar formulae like Clark and Hill in 1960 (Clark, et al., 1960) Eq. (13), and Djalaly in 1974 (Djalaly, 1974) Eq. (14) (Baláz, et al., 1999)

$$M_{cr} = C_1 \frac{\pi^2 EI_z}{(kL)^2} \left\{ \sqrt{\frac{I_w}{I_z} \left( 1 + \frac{GI_T(kL)^2}{\pi^2 EI_w} \right)} + (C_2 g + C_3 K)^2 + (C_2 g + C_3 K) \right\} \quad (13)$$

$$M_{cr} = C_1 \frac{\pi^2 EI_z}{k_z k_w L^2} \left\{ \sqrt{\frac{I_w}{I_z} + \frac{GI_T}{EI_z} \left( \frac{k_w L}{\pi} \right)^2} + (C_2 z_g + C_3 z_j)^2 + (C_2 z_g + C_3 z_j) \right\} \quad (14)$$

Based on these researches the ENV version of Eurocode 3 (CEN, 2003) adopted the following formula with three factors,  $C_1$ ,  $C_2$  and  $C_3$  depending be related to bending moment shape, position of loading relatively to the shear center, and shape of the cross section respectively. This formula is currently one of the most well-known and widely employed formula.

$$M_{cr} = C_1 \frac{\pi^2 EI_z}{(k_z L)^2} \left( \sqrt{\left[ \left( \frac{k_z}{k_w} \right)^2 \frac{I_w}{I_z} + \frac{(k_z L)^2 GI_t}{\pi^2 EI_z} + (C_2 z_g - C_3 z_j)^2 \right]} - [C_2 z_g - C_3 z_j] \right) \quad (15)$$

Where  $k_z$  and  $k_w$  are effective length factor that depend on the support conditions at the end sections,  $k_z$  is related to rotations about the weak axis  $z$ , and  $k_w$  refers to the warping restriction;  $z_g$  is the distance between the point of the application of the loads and the shear center of the cross section; and  $z_j$  is a parameter that reflects the degree of asymmetry of the cross section in relation to the  $y$  axis. Some authors use  $C_1$  also related to the torsion properties. Note that if all factors in Eq. (15) are equal to 1, results in Eq. (6), the basis case. Some authors consider other equivalent formulae to Eq. (15). Baláz and Koleková (Baláz, et al., 2012) (CEN, 2007) consider Eq. (16) for determination of the elastic critical moment

$$M_{cr} = \mu_{cr} \frac{\pi \sqrt{EI_z GI_t}}{L} \quad (16)$$

where

$$\mu_{cr} = \frac{C_1}{k_z} \left( \sqrt{1 + k_{wt}^2 + (C_2 \zeta_g - C_3 \zeta_j)^2} - (C_2 \zeta_g - C_3 \zeta_j) \right) \quad (17)$$

And the three non-dimensional parameters are

$$k_{wt} = \frac{\pi}{k_w L} \sqrt{\frac{EI_w}{GI_t}} \quad \zeta_g = \frac{\pi z_g}{k_z L} \sqrt{\frac{EI_z}{GI_t}} \quad \zeta_j = \frac{\pi z_j}{k_z L} \sqrt{\frac{EI_z}{GI_t}} \quad (18)$$

Note that replacing Eq. (17) and Eq. (18) in Eq. (16) leads to Eq. (15). The use and calculation separately of these three non-dimensional parameters allows the inclusion of more specific conditions of the hypothesis in study in the calculation process of the  $C$  factors. This results in

more customized, varied and perhaps more accurate C values. Apart from how the factors are presented and calibrated, all formulae can be synthetized in similar format, yet they are not exactly equivalent. It is seen in the following that an attempt to find an equivalency between the formulae is not as straightforward as it may seem at first. In summary, when one compares Eq. (15) to other formulae for  $M_{cr}$ , the following can be said:

- In Eq. (12),  $\beta_0\sqrt{(\beta_2)}$  could be said to be related to bending moment shape as  $C_1$  of Eq. (15);  $-1/\sqrt{(\beta_2)}$  to position of loading as  $C_2$  of Eq. (15); and  $\beta_1/\sqrt{(\beta_2)}$  to the asymmetry of cross section in the plane of loading as  $C_3$  of Eq. (15). Thus, Eq. (12) can be rearranged as

$$M_{cr} = \sqrt{\beta_2}\beta_0 \frac{\pi^2 EI_z}{(k_z L)^2} \left\{ \sqrt{\left(\frac{k_z}{k_w}\right)^2 \frac{I_w}{I_z} + \frac{(k_z L)^2 GI_t}{\pi^2 EI_z} + \left(\frac{-z_g - \beta_1 z_j}{\sqrt{\beta_2}}\right)^2} - \frac{-z_g - \beta_1 z_j}{\sqrt{\beta_2}} \right\} \quad (19)$$

- In Eq. (13),  $C_2$  holds an opposite sign to  $C_2$  in Eq. (15). Regarding the length factors  $k_z$  and  $k_w$ , which are here somehow represented by a factor  $k$ , these are not considered in a same manner as in Eq. (15). However if  $k_w=k_z=k$  the formula is equivalent to Eq. (15). Thus, considering  $k_z=k_w=k$ , Eq. (13) can be rearranged as

$$M_{cr} = C_1 \frac{\pi^2 EI_z}{(k_z L)^2} \left\{ \sqrt{\frac{I_w}{I_z} + \frac{(k_z L)^2 GI_t}{\pi^2 EI_z} + (-C_2 g - C_3 K)^2} - (-C_2 g - C_3 K) \right\} \quad (20)$$

- In Eq. (14),  $C_2$  also hold an opposite sign to  $C_2$  in Eq. (15). Regarding the length factors  $k_z$  and  $k_w$ , they are again not considered in a same manner as in Eq. (15) as they are not considered the same exact terms in the equation as in Eq (15). Thus, Eq. (14) can be rearranged as

$$M_{cr} = C_1 \frac{\pi^2 EI_z}{k_z k_w L^2} \left\{ \sqrt{\frac{I_w}{I_z} + \frac{(k_w L)^2 GI_t}{\pi^2 EI_z} + \left(\frac{k_w}{k_z}\right)^2 (-C_2 z_g + C_3 z_j)^2} - \frac{k_w}{k_z} (-C_2 z_g + C_3 z_j) \right\} \quad (21)$$

- The Eq. (16), as mentioned previously, is equivalent to Eq. (15).

The relations between the formulae are summarized in Table 3.1.

Table 3.1 – Relations between the alternatives 3-factors formulae.

Eq. (15)	$C_1$	$C_2$	$C_3$	$k_w$	$k_z$
Eq. (12)	$\beta_0\sqrt{(\beta_2)}$	$-1/\sqrt{(\beta_2)}$	$\beta_1/\sqrt{(\beta_2)}$	$k_w$	$k_z$
Eq. (13)	$C_1$	$-C_2$	$C_3$	$k^*$	$k^*$
Eq. (14)	$C_1$	$-C_2 \frac{k_w}{k_z}$	$C_3 \frac{k_w}{k_z}$	$k_w$	$k_z$
Eq. (16)	$C_1$	$C_2$	$C_3$	$k_w$	$k_z$

\* This assumption is only possible if  $k_z=k_w=k$

Some authors, as Lindner (ECCS, 2006) and Trahair (Trahair, 1993) consider 1-factor formulae. These formulae are obviously simpler but also more limited than the 3-factor formulae. This type of formula is also used in some modern steel structures codes as the American AISC LRFD (AISC, 1994). There are some differences between Lindner and Trahair formula. Lindner considers the equation given by (ECCS, 2006)

$$M_{cr} = \frac{k}{L} \sqrt{EI_z GI_t} \quad (22)$$

Where k is a lateral torsional buckling coefficient depending on the torsion coefficient  $\chi_t$  given by

$$\chi_t = \frac{EI_w}{L^2 GI_t} \quad (23)$$

This formula is limited to double symmetric cross sections. And the k value is given in charts as a function of  $\chi_t$ . Trahair formula is the simplest one; it is basically the multiplication of Eq. (6) by a factor  $\alpha_m$ , which leads to (Trahair, 1993)

$$M_{cr} = \alpha_m \frac{\pi}{L} \sqrt{GI_T EI_z \left(1 + \frac{\pi^2 EI_w}{L^2 GI_T}\right)} \quad (24)$$

This equation is equal to Eq. (15) with the length factors equal to 1;  $C_2$  and  $C_3$  equal to zero; and considering  $\alpha_m$  equal to  $C_1$ . As seen in Annex A.7, the author uses this equation as base equation and contours its limitation by changing the equation depending of the specific situation, based on numerical results. This leads to a huge number of limited equations and transformations in order to include all possible situations permitted.

As a final note, it is important to mention the formulation and sign convention for  $z_g$  and  $z_j$  adopted by the Eq. (15) and Eq. (16) and the values of the length factors adopted by most authors. The  $z_j$  parameter that as stated is a parameter that reflects the degree of asymmetry of the cross section in relation to the y axis, is given by

$$z_j = z_s - 0.5 \int_A (y^2 + z^2) \frac{z}{I_y} dA \quad (25)$$

This parameter is equal to zero for doubly symmetric cross sections. For mono symmetrical I section the Eq. (25) can be simplified as

$$z_j = \frac{1}{2I_y} \left[ (h_m - \bar{z}) \left\{ \frac{b_{ft}^3 t_{ft}}{12} + b_{ft} t_{ft} (h_m - \bar{z})^2 \right\} - \bar{z} \left\{ \frac{b_{fc}^3 t_{fc}}{12} + b_{fc} t_{fc} \bar{z}^2 \right\} \right. \\ \left. + \left\{ \left( h_m - \bar{z} - \frac{t_{ft}}{2} \right)^4 - \left( \bar{z} - \frac{t_{fc}}{2} \right)^4 \right\} \frac{t_w}{4} \right] - z_s \quad (26)$$

where  $\bar{z}$  is the distance between the centroid of the cross section and the centroid of the compressed flange. For the sign convention, this parameter takes positive values when the flange with the largest second moment of area about  $z$  is the compressed flange. The parameter  $z_g$  that as mentioned is the distance between the point of the application of the loads and the shear center of the cross section, and is given by

$$z_g = z_a - z_s \quad (27)$$

where  $z_a$  and  $z_s$  are respectively the coordinates of the point of application of the load and of the shear center relative to the centroid of the cross section. The parameter  $z_g$  is positive if gravity loads are located above the shear center and negative if located below the shear center, as seen in the Figure 3.1.

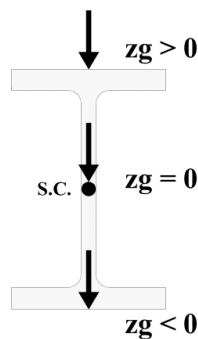


Figure 3.1 – Sign convention for  $z_g$ .

And finally relatively to the length factors  $k_z$  and  $k_w$ , they vary from 0.5 for full restraint to 1.0 for no restraint, with 0.7 for one end fixed and one end free, in the general of the cases and solutions. Nevertheless in cases such as cantilevers, these factors depend of the considerations made by each author.

### 3.2 C Factors

In this section, the C values or equivalent factors values from several authors are compared, all their C values or its formulation are presented in Annex A. The main differences between each solution are the possibilities of considering different type of loading; boundary conditions; type of cross-section and the respective values of the factors. The C values presented by Baláz and Koleková which were adopted in Eurocode 9 (CEN, 2007) as well as the values for combination of loads presented by the same authors (Baláz, et al., 2012) are considered here. The values presented in ECCS publication number 119 (ECCS, 2006) are also considered, namely the C values of the publication for simply supported beams with a single type of loads, the C values by Galéa (Galéa, 2002) for combination of loads, the C

values by Andrade *et al.* (Andrade, et al., 2006) for I-section cantilevers and the values by Lindner for overhanging beams. Finally the values by Trahair (Trahair, 1993) and the C values by Serna *et al.* (Serna, et al., 2006) are also considered. The analyzed C values are listed in Table 3.2 by author. Each solution has distinct limitations of cross-sections types, loading types or restrictions at supports as seen in Tables 3.3 and 3.4. In these tables the analyzed cases in this thesis as well as the numeration adopted are also presented.

Table 3.2 – C Factor values analyzed.

C Factors	Reference
Baláž and Koleková	(Baláž, et al., 2012) (CEN, 2007)
ECCS – Basis Load Cases	(ECCS, 2006)
Galéa	(ECCS, 2006) (Galéa, 2002)
Andrade <i>et al.</i>	(ECCS, 2006) (Andrade, et al., 2006)
Lindner	(ECCS, 2006)
Trahair	(Trahair, 1993)
Serna <i>et al.</i>	(Serna, et al., 2006)

For Tables 3.3 and 3.4, it is important to mention that for Trahair factors his book from 1993 (Trahair, 1993) is used, in which he presents several formulations for different cases. However, Annex A.7 presents in a summarized way only formulations for the cases analyzed here. As can be seen in Tables A.21 and A.23 the formulations presented for mono symmetric cross sections or for different support conditions are very limited and restrictive in number of cases and possibilities. In this sense, the author makes a vast number of references to papers with even more formulations including more cases and hypotheses than in his book. Since this is not practical and following the purpose of these analytical expressions, for simplification Tables A.21 and Table A.23 are neither considered, nor included in the following tables. In the same way, in ECCS publication (ECCS, 2006) a huge number of papers by Lindner *et al.* involving cases with special support conditions are presented in a summarized way. Since most of them are too specific, in this thesis only factors for cases with overhanging beams are analyzed, since this factors takes into account the stiffness of the simple supported beam as a variable. Note that all other factors analyzed in these thesis for cantilevers with free warping, i.e. the overhanging cases, have the rotation about z axis restricted, which means that they consider the simply supported beams as infinitely rigid.

As a final note regarding the following tables, it is important to mention that the figures only have a schematic sense: for instance the boundary condition in the cantilevers may not be fixed in all directions as shown in the figures.

Table 3.3 – Factors (Case 1 to 6) – Ranges.

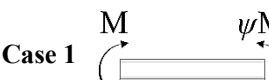
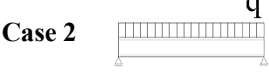
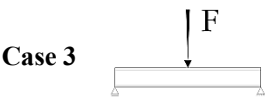
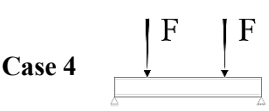
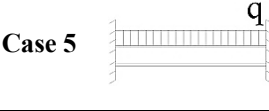
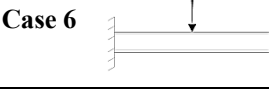
		Baláž and Kolekova	ECCS – Basis Load Cases	Galea	Andrade <i>et al.</i>	Trahair	Lindner	Serra <i>et al.</i>	
<b>Case 1</b>		$k_w$ 1 {0,5; 0,7L; 0,7R; 1} $k_z$ $\psi_f$ $\psi$ $k_w$ $k_z$ $\psi_f$ $z_g$ $d$	$k_w$ 1 {0,5; 1} $k_z$ $\psi_f$ $z_g$ $d$	n.a.	n.a.	n.a.	n.a.	n.a.	{0,5; 0,7; 1}
<b>Case 2</b>		$k_w$ 1 {0,5; 1} $k_z$ $\psi_f$ $z_g$ $d$	$k_w$ 1 {0,5; 1} $k_z$ $\psi_f$ $z_g$ $d$	n.a.	n.a.	n.a.	n.a.	n.a.	{0,5; 0,7; 1}
<b>Case 3</b>		$k_w$ 1 {0,5; 1} $k_z$ $\psi_f$ $z_g$ $d$	$k_w$ 1 {0,5; 1} $k_z$ $\psi_f$ $z_g$ $d$	n.a.	n.a.	n.a.	n.a.	n.a.	{0,5; 0,7; 1}
<b>Case 4</b>		$k_w$ 1 {0,5; 1} $k_z$ $\psi_f$ $z_g$ $d$	$k_w$ 1 {0,5; 1} $k_z$ $\psi_f$ $z_g$ $d$	n.a.	n.a.	n.a.	n.a.	n.a.	{0,5; 0,7; 1}
<b>Case 5</b>		$k_w$ 1 {0,5; 1} $k_z$ $\psi_f$ $z_g$ $d$	$k_w$ 1 {0,5; 1} $k_z$ $\psi_f$ $z_g$ $d$	n.a.	n.a.	n.a.	n.a.	n.a.	{0,5; 0,7; 1}
<b>Case 6</b>		$k_w$ 1 {0,5; 1} $k_z$ $\psi_f$ $z_g$ $d$	$k_w$ 1 {0,5; 1} $k_z$ $\psi_f$ $z_g$ $d$	n.a.	n.a.	n.a.	n.a.	n.a.	{0,5; 0,7; 1}

Table 3.4 – Factors (Case 7 to 10) – Ranges.

Case 7		Case 8		Case 9		Case 10		Balkz and Koldovský		Andrade et al.		Galea		ECCS - Basis Load Cases		Lindner		Trahair		Senna da M.	
$k_w$		$k_w$		$k_w$		$k_w$		$\zeta_{j0} \leftrightarrow \psi_f$		1	1							1	1	{0,5; 0,7; 1}	
$k_z$		$k_z$		$k_z$		$k_z$		$\zeta_{g0} \leftrightarrow z_g$		1	0							0	0	0	
$\psi_f$		$\psi_f$		$\psi_f$		$\psi_f$		$\bar{K}$		0	0							<-1 <sup>(\psi=0)</sup>	<-1,5 <sup>(\psi=1)</sup>		
$\Psi$		$\Psi$		$\Psi$		$\Psi$		$L_1/L_2$		0	0							<0	0		
$M_0/M \leftrightarrow \mu$		$M_0/M \leftrightarrow \mu$		$\chi_t$		$\chi_t$		$\zeta_{j0} \leftrightarrow \psi_f$		100%	100%							0	0		
$M$		$M$		$k_w$		$k_w$		$\zeta_{g0} \leftrightarrow z_g$		n.a.	n.a.							0	0		
$z_g$		$z_g$		$\zeta_{j0} \leftrightarrow \psi_f$		$\zeta_{j0} \leftrightarrow \psi_f$		$\bar{K}$										0	0		
$k_w$		$k_w$		$\zeta_{g0} \leftrightarrow z_g$		$\zeta_{g0} \leftrightarrow z_g$		$L_1/L_2$										0	0		
$k_z$		$k_z$		$\bar{K}$		$\bar{K}$		$\chi_t$										0	0		
$\psi_f$		$\psi_f$		$L_1/L_2$		$L_1/L_2$		$\chi_t$										0	0		
$\Psi$		$\Psi$		$\chi_t$		$\chi_t$												0	0		
$M_0/M \leftrightarrow \mu$																					

### 3.2.1 Baláž and Koleková

C factors proposed by Baláž and Koleková, see Annex A.2, are presented with Eq. (16). For its analysis the authors have presented 5 tables to obtain the solution for the three C factors for 9 different cases (Baláz, et al., 2012) (CEN, 2007):

- Simply supported beams with end moments, Table A.1.
- Simply supported or fixed beams with various transverse loading cases, Table A.2.
- Cantilevers with point load applied at the tip, Table A.3.
- Cantilevers with uniformly distributed load, Table A.4.
- Simply supported beams with the combination between end moments and uniformly distributed load, Table A.5.

It is important to notice that Table A.3 and A.4 give directly the non-dimensional critical moment  $\mu_{cr}$ , the direct value of Eq. (17), and not the C values. In addition to these tables an approximated formulation to calculate by the C factors is also presented, see note b). However this formulation is limited to  $C_1$  and  $C_2$  excluding mono symmetric cross sections, therefore it is not considered here. For the application it is necessary to establish some considerations:

- In Table A.1, if the maximum of the moment diagram is in a support, this support is to be considered on the left edge of the beam and all boundary conditions are defined with this orientation;
- For cantilevers, Table A.3 and A.4, three options are available, although they do not precisely coincide:
  - (i) Discrete coefficients of the tables. Intermediate values shall be further obtained by non-linear interpolation;
  - (ii) For double symmetrical cross-sections with the loads applied on shear center, the authors suggest an equation for point load applied at the tip, Table A.3 note a), and an equation for uniform distributed load, Table A.4 note a);
  - (iii) For double symmetrical cross section, as it was said, a specific formulae may be used as an alternative to the values obtained from i) and ii), using an approximation to the C factor values, note b).

Here option ii) for double symmetrical cross-section with the loads applied at the shear center, and option ii) for all other cases are considered. For the interpolation in the option i), in the paper (Baláz, et al., 2012) nothing is said, however in the Eurocode 9 (CEN, 2007) is recommended the use of non-linear interpolation. Thus, it is adopted a polynomial equation of degree four for  $k_{wt}$  and  $\xi_{g0}$  and a polynomial equation of degree six for  $\xi_{j0}$ .

- In what concerns beams with combination of distributed loading and end moments, see Table A.5, the authors calibrated  $C_1$  factors for the case of  $k_{wt}=0,235$ . These factors may

nonetheless be used for other values of  $k_{wt}$ , according to the authors. This is taken into account here.

- In the same table, the consideration of uniformly distributed load acting at a distance from the shear center ( $\xi_g \neq 0$ ) combined with end moment loading is to be accounted for by the factor  $C_2$ . Since the authors do not have relevant values of  $C_2$ , as a simplification it is recommended by the authors that  $C_2=0,5$  as done in DIN 18800 (DIN, 1990). In this code the expression for the critical moment is given by Eq. (28) for double symmetric sections, in which the value for  $C_2$  is fixed and is equal to 0,5.

$$M_{Ki,y} = \xi N_{Ki,z} \left( \sqrt{c^2 + 0,25z_p^2} + 0,5z_p \right) \quad (28)$$

- An approximated formula for  $C_1$  is given in Annex I (Informative) of the Eurocode 9 (CEN, 2007), when  $k_z=1$ . This formula is not considered here.

$$C_1 = (0,310 + 0,428\psi + 0,262\psi^2)^{-0,5} \quad (29)$$

- In all tables, except for the cantilevers, a linear interpolate is considered whenever necessary.

### 3.2.2 ECCS – Basis Load cases

$C$  factors values proposed by ECCS publication for simply supported beams with a single kind of load, see Annex A.3, are presented with Eq. (15). For its analysis 2 tables to obtain the solution for the three  $C$  factors for 4 different loading cases (ECCS, 2006) are proposed:

- Simply supported beams with end moments, Table A.6;
- Simply supported beams with various transverse loading cases, Table A.7.

As it happens in the previous solution, for its application it is necessary to establish some consideration:

- For  $k_z=1$  and end moments cases of the Table A.6, Eq. (30) may be approximately used for any ratio end moment loading as an alternative to the table. This expression is considered here;

$$C_1 = (0,310 + 0,428\psi + 0,262\psi^2)^{-0,5} \quad (30)$$

- In Table A.6 only values for  $C_1$  and  $C_3$  for cases with  $k_z=1$  or  $k_z=0,5$  are presented. For cases with  $k_z=0,7$  it is here analyzed two possible ways: the first one and more trivial one, is to conservatively use the values of  $C_1$  and  $C_3$  from the tables for the case  $k_z=1$  and replace  $k_z=0,7$  in the main equation, and the second way is to use a linear interpolation of the  $C_1$  and  $C_3$  values;

- Still regarding end conditions, a note concerning the applicability of C factors is attached to the tables, imposing that these are to be applied for  $k_z=k_w=1$ . This aspect is clearly contradicting and is disregarded for the purpose of this study;
- When necessary, a linear interpolation considering the discrete values from tables is carried out.

### 3.2.3 Galéa

C factors proposed by Galéa are presented with Eq. (15), see Annex A.4. For its analysis the authors has proposed 8 charts, Figure A.2 to Figure A.5, or equivalent 8 tables, Table A.8 to Table A.15, to obtain the solution for  $C_1$  and  $C_2$  for 2 different combinations between end moments and transversal loads (Galéa, 2002) (ECCS, 2006), comprising:

- Simply supported beams with the combinations between end moments and uniformly distributed load, Figure A.2 and Figure A.3 or Table A.8 to Table A.11;
- Simply supported beams with the combination between end moments and point load applied at mid-span, Figure A.4 and Figure A.5 or Table A.12 to Table A.15.

For computing the C factors, the values from the referred tables are considered and results are linearly interpolated whenever necessary. This is considered as the discrete values that are obtained from the table are exact in comparison to the values to be obtained from the charts. In addition, since the original expression is not available, programming of C factors from the tables is more convenient.

### 3.2.4 Andrade *et al.*

C factors proposed by Andrade *et al.* are presented with Eq. (15), see Annex A.5. For its analysis the authors have proposed 4 tables to obtain the solution for the three C factors to cantilevers for 2 different load cases (ECCS, 2006) (Andrade, et al., 2006):

- Cantilevers with uniformly distributed load, Table A.16 and Table A.17;
- Cantilevers with point load applied at the tip, Table A.18 and Table A.19.

### 3.2.5 Lindner

This solution proposed by Lindner uses a k factor in alternative to C factors and is presented with Eq. (22), see Annex A.6. For its analysis the author has proposed 5 charts, Figure A.6, to obtain the k value to overhanging beams for 3 different loading cases (ECCS, 2006):

---

- Overhanging beam with uniformly distributed load only in the suspended part, Figure A.6 a) and b);
- Overhanging beam with a point load applied at the tip, Figure A.6 c) and d);
- Overhanging beam with an end moment applied at the tip, Figure A.6 e).

As can be easily seen in Figure A.6, an inconsistency is noticed in the presentation of charts c) and e), which, for distinct cases, give exactly the same results. Since no information is given in ECCS (2006) regarding the source of such charts, both cases are considered here, also with the aim to detect to which case they correspond. In order to compute the procedure, an approximated equation for each chart is previously obtained. Each line of the charts is divided in 20 parts, resulting in 21 points per line. With these 21 points, and by the least squares method, the polynomial regression function with best relation between lowest degree and accuracy is obtained for each line, as seen in the Figure 3.2 for chart a).

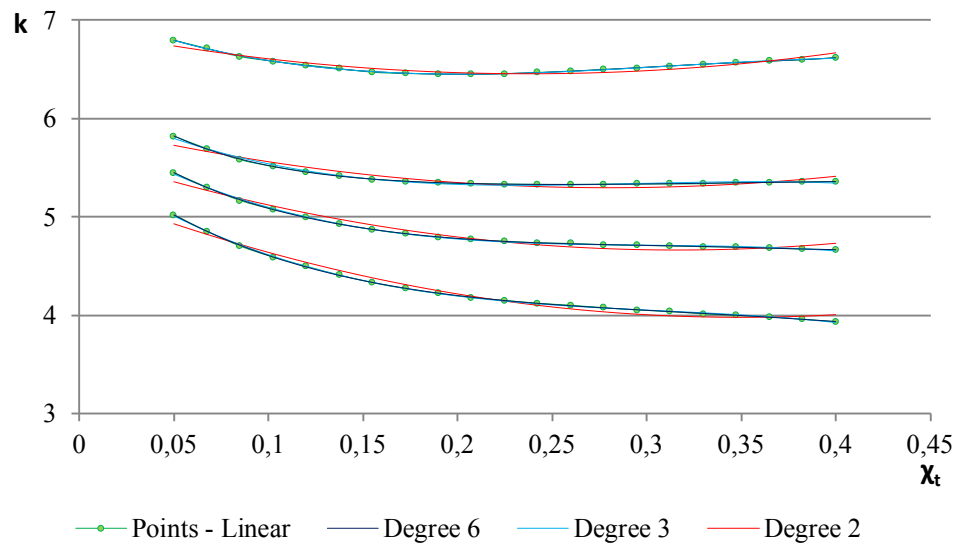


Figure 3.2 – Polynomial test of the chart a).

As easily observed, all the polynomial equations have a good accuracy, however the polynomial equation of degree two can lead to some visible unsafe values, thus in order to simplified the final formula polynomial equation of degree three is adopted. These results are similar in all charts. Since there are 4 lines in each chart and they are dependent of only one variable,  $L_1/L_2$ , the final equation of each chart it is obtained by polynomial equation of three degree involving the 4 previous polynomial equations. This leads to an equation of  $k$  per charts. Thus, combining Eq. (22) and Eq. (15) with these equations it is possible to obtain an equation of  $C_1$  to each chart, which leads to:

$$\begin{aligned}
 C_1 = & \left[ G^3 L^6 I_T^3 \left( A \left( \frac{L_1}{L} \right)^3 + B \left( \frac{L_1}{L} \right)^2 + C \left( \frac{L_1}{L} \right) + D \right) \right. \\
 & + E G^2 L^4 I_T^2 I_w \left( E \left( \frac{L_1}{L} \right)^3 + F \left( \frac{L_1}{L} \right)^2 + H \left( \frac{L_1}{L} \right) + I \right) \\
 & + E^2 G L^2 I_T I_w^2 \left( J \left( \frac{L_1}{L} \right)^3 + K \left( \frac{L_1}{L} \right)^2 + M \left( \frac{L_1}{L} \right) + N \right) \\
 & \left. + E^3 I_w^3 \left( O \left( \frac{L_1}{L} \right)^3 + P \left( \frac{L_1}{L} \right)^2 + Q \left( \frac{L_1}{L} \right) + R \right) \right] \\
 & / \left( 10000 G^{5/2} L^5 \pi I_T^{5/2} \sqrt{G L^2 I_T + E \pi^2 I_w} \right)
 \end{aligned} \quad (31)$$

Where L is the length of the suspended part; L<sub>1</sub> is the length of the simply supported beam part; and the variables A to R in the Table 3.5.

Table 3.5 – Variables A to R.

Charts	a)	b)	c) and e)	d)
<b>A</b>	-48454	-105887	-17620	-46620
<b>B</b>	89122	158109	34528	78577
<b>C</b>	-56143	-83409	-22402	-38579
<b>D</b>	71178	92075	44501	50899
<b>E</b>	122315	-324386	64456	213569
<b>F</b>	-131256	722686	-104028	-197780
<b>H</b>	-43814	-855949	21975	-184331
<b>I</b>	-78308	702707	-107516	306196
<b>J</b>	-171344	1088135	-131793	-1051420
<b>K</b>	89282	-2088732	237474	1219393
<b>M</b>	194212	2036119	-77253	219713
<b>N</b>	285820	-1509090	355558	-679840
<b>O</b>	-31633	-1869003	74928	597563
<b>P</b>	268191	3272871	-159640	-439532
<b>Q</b>	-365161	-2549774	50611	-591853
<b>R</b>	-304128	1636538	-386419	754651

Note that the difference between the chart a) and b) or c) and d) is the load position relatively to the shear center; in this sense it would be logic to use C<sub>1</sub> and C<sub>2</sub> factors. This was indeed done, however it is not presented here: firstly, C<sub>1</sub> factors were calibrated for cases b) and d), therefore isolating the position of the load relatively to the shear center of the cross section; secondly, C<sub>2</sub> factors were calibrated for cases a) and c), with reference to cases b) and d), respectively, thus making it possible to isolate the loading position in the C<sub>2</sub> factors. This

approach has the advantage of being consistent with the 3-factor formula (apart from the mono-symmetry of the cross section, represented by  $C_3$  – not considered here). However, it is not presented here for the following reason: (i) it led to a non-practical equation of  $C_2$ , for which more attention needs to be paid to simplifying it; (ii) to associate this broader  $C_2$  factor with the 3-factor formula, it is assumed that it is validated to any position of load relatively to the shear center. This was also noted here and will definitely be considered in a further step of this study; (iii) the main objective of this study is to compare different alternatives for calculation of the critical moment – for this reason, and for the time being, factors  $C_1$  were calibrated specifically for cases a) and c), thus allowing for programming of the referred charts.

### 3.2.6 Trahair

The solution proposed by Trahair uses a  $\alpha_m$  factor, which can be considered as a  $C_1$  factor, and is presented with Eq. (24), see Annex A.7. For its analysis the author has proposed one Table, for simple supported beams with the most current loading cases, Table A.20; an upgrade to the formula in order to include the load location relatively to the shear center, Table A.22; and 4 specific formulae for cantilevers with 2 differences loading cases, Table A.24, thus in a summarized way it is covered: (Trahair, 1993):

- Simply supported beams with end moments;
- Simply supported beams with various transverse loading cases;
- Simply supported beams with the combination between end moments and uniformly distributed load or point load applied at the mid-span;
- Cantilevers with uniformly distributed load;
- Cantilevers with point load applied at the tip.

As above mentioned, in the 1993 book by Trahair (Trahair, 1993) a huge number of formulations for other various cases is presented. However, here only the formulations related to the cases presented in Tables 3.3 and 3.4 are studied, and also presented in Annex A.7. Some of these formulations are very limited or restrictive, and therefore some considerations are made:

- Since the expressions presented in Table A.21 are only for 3 of the 10 cases analyzed here, these expressions are disregarded and thus it is only analyzed double symmetric cross sections.
  - Since the mono symmetric cross sections are disregarded, the corresponding expression presented in Table A.22 is also not considered. As seen in this table, for this type of cross sections with loads not applied at the shear center it is only possible to analyze one case, which gives further support to the previous consideration.
-

- As one can see in Table A.23, the proposal for restrictions at the supports is only applicable to load and section conditions of the basic case, which it is very restrictive. This table is therefore also disregarded.

As a final note, it is important to state that the same book makes a huge number of references to papers with more solutions than the ones mentioned above – also most likely including a non-practical number of new different and independent equations. These papers are not considered for the purpose of this study.

### 3.2.7 Serna *et al.*

C factors proposed by Serna *et al.* are presented with Eq. (15) with  $C_2$  and  $C_3$  equal to zero (Serna, et al., 2006). The procedure to calculate the  $C_1$  factor is described in Annex A.8. This solution is based in the moment diagram geometry which gives the possibility to cover a huge number of cases. On the other hand, the solution only covers double symmetric cross sections with loads applied at the shear center. Relatively to the support conditions, only rotations and warping free or fixed at the same time in each support are allowed. If the support conditions are different between supports the authors has values for  $C_1$  factor, thought they do not say which value to use for the length factors in the main formula. Nevertheless, it is the only solution that allows one support totally fixed (both warping and weak axis rotation) and the other support with fork conditions. Given these two previous considerations, the possibility to consider supports with different conditions is disregarded here.

## 3.3 Final Remarks

As discussed in section 3.1, almost all expressions are equivalent or simplification of the Eq. (15). There are however 2 exceptions: the Lindner formula and the sets of formulae by Trahair. The first exception can be easily converted in a C factors format as showed in section 3.2.5. Relatively to the second exception, the Eq. (24) for simply supported beams with basic load cases is equivalent to Eq. (15) as already seen; the problem are the complex and different formulations for loads not applied at shear center and cantilevers. However, as seen in section 3.2.6, these formulations do not permit more solutions than the already existent in C factor format proposed by others authors becoming an accuracy matter. Considering this, Eq. (15) seems to be the most practical and complete expression.

Relatively to the C factors values and to the different solutions for those factors, its accuracy is tested and compared in Chapter 4 by a wide parametric study.

## 4 PARAMETRIC STUDY

### 4.1 Numerical Model

All results in this study are compared to numeric results with very good accuracy, in order to better understand the accuracy level given by each analyzed solution. The software used is LTBeam (Galéa, 2010), based in Finite Element Method. This software was developed by Centre Technique Industriel de la Construction Métallique (CTICM) in the frame of a European research project supported by the European Coal and Steel Community (ECSC) to deal specifically with elastic lateral torsional buckling of steel and composite beams. This software essentially computes an accurate value of the lowest eigenvalue,  $\mu_{cr}$ , and thus the critical moment value,  $M_{cr}$ , of a beam with various possible cross sections; restrictions or load cases.

In its validation report (Galéa, 2002) 65 test were performed between LTBeam and ANSYS V5.6 (ANSYS) leading to differences lower than 1% for most of the cases. The description of these and other validation tests are given in the mentioned document. The program allows for the use of a discretization with 50 to 300 elements. For all cases 200 elements are used following the author's recommendation for cantilevers, the most sensitive case to loading and restrain conditions, with a precision of  $1 \cdot 10^{-4}$  and 70 as maximum number of interactions.

To compute the analyses, the same values of cross section proprieties and element conditions are used in numerical model and in C factor value definition.

### 4.2 Parametric Study

In Table 4.1 the variables and ranges analyzed in this study for all cases of the Tables 3.3 and 3.4 are concisely presented. These ranges are the base ranges used in the study, for the study of the range limitation relatively to parameter  $\psi_f$  by 0,9 or 0,5, both mono symmetric cross sections are added.

Table 4.1 – Parametric Study.

Variable	Range	
E [GPa]	210	
G [GPa]	81	
L [m]	{5;10}	
k <sub>w</sub>	{5;10}	
k <sub>z</sub>	{5;0,7;10}	
ψ	[-1;-0,95;...0,95;1]	
d [%]	[0;0,05;...0,45;0,5]	
h <sub>load</sub> [%]	[0;0,05...0,95;1]	
μ	[-20;-10;-8;-6;-4;-3,75;-3,25;-2;-1,9; ...;1,9;2;2,25;2,75;3,25;4;6;8;20]	
Double Symmetric	IPE HEB	{100;200;300;400;500}
Mono Symmetric - ψ <sub>f</sub>	h = 300 h = 500	[-1;-0,8;...;0,8;1]
L <sub>1</sub> /L <sub>2</sub>	[0;0,125;...; 0,875;1]	
Nº Cases	<b>10</b>	
Nº of Tests	<b>107034</b>	

Other important note is that the Lindner solution is very restrictive about the slenderness; therefore the L range is changed. Thus, for the same double symmetric cross sections, all the possible hypotheses are analyzed and are presented in Table 4.2.

Table 4.2 – Lindner – Parameter L Study.

L [m]	1	2	3	4	5	6	7	8
Profile	IPE100	IPE200	IPE200	IP300	IP300	IPE400	IPE400	IPE500
	HEB100	HEB200	HEB300	IPE400	IPE400	IPE500	IPE500	HEB500
			IPE400	IPE500	IPE500	HEB300	HEB400	
			IPE200	HEB300	HEB300	HEB400	HEB500	
			HEB300	HEB400	HEB400	HEB500		
			HEB400	HEB500	HEB500			
			HEB500					

Finally, the parametric study compromises more than 100.000 tests involving the 10 cases. As previously seen, each solution has distinct limitations of cross sections types, loading types or restrictions at the supports. In this sense, firstly all solutions are analyzed separately, and then they are compared between them in the ranges of variables that they have in common.

### 4.3 Methodology

For better interpretation of the results, the ten cases presented in Tables 3.3 and 3.4 are divided in double symmetric and mono-symmetric cross sections. For these groups two types of analysis are performed:

- Graphical analysis: Using normalized values according to the Eq. (32). This scale is chosen only for visualization purposes in order to be able to view different cross section (which present different levels of  $M_{cr}$ ) in a same scale range.

$$\left\{ \begin{array}{l} \text{Results from expressions: } \sqrt{\frac{M_{cr}^{\text{Author}}}{M_{pl,y}}} = \frac{1}{\bar{\lambda}^{\text{Author}}} \\ \text{Results from LTBeam: } \sqrt{\frac{M_{cr}^{\text{LTBeam}}}{M_{pl,y}}} = \frac{1}{\bar{\lambda}^{\text{LTBeam}}} \end{array} \right. \quad (32)$$

- Statistical analysis: Statistical evaluation concerning the ratio  $M_{cr}^{\text{Author}}/M_{cr}^{\text{LTBeam}}$  for the analyzed solution. In these table the CoV column is the coefficient of variation given by the ratio between the standard deviation and the mean; and the <0,9 and >1,03 columns are percentage of cases that exceed more than 10% of conservatism and more than 3% of unconservatism relatively to the LTBeam values, all tables are presented in Annex B.

This chapter first presents the results for each solution, in section 4.5, and then the possible comparisons between them, section 4.5.

### 4.4 Results

As above referred, all solutions have C values for distinct limitations and it is impossible to compare all variables between them. In addition, in few of them it is necessary to analyze some considerations made in their procedure and some variables only included in each one. In this sense, in this section each solution is separately discussed, in order to exclude some variables or procedure with worst results; give an overview about all; and analyze incomparable variables. The statistical analysis of all solutions and variables is presented in Annex B, and all tables mentioned with A or B numerations are from annexes.

#### 4.4.1 Baláž and Koleková

In this solution all variables of all cases are analyzed here. As it seen in Tables 3.3 and 3.4 this is very complete and it only has not C values for Case 8.

#### 4.4.1.1 Case 1

Figure 4.1 presents the graphical analysis of the Case 1 for double and mono symmetric cross sections and Table 4.3 presents a summary of the Table B.1. Relatively to the double symmetric cross sections, see a), the C values obtain very good results relatively to LTBeam, with a CoV value of 1,948% and only 0,6% of the results above the 3% unsafe mark with a maximum value of 1,036 (0,6% above the 3% unsafe mark). In Table B.1, it is possible to see that these unsafe results have  $\psi$  as a member of [0;0,5[ with  $k_z$  equal to 0,7, essentially when the restriction is on the right side, 0,7R.

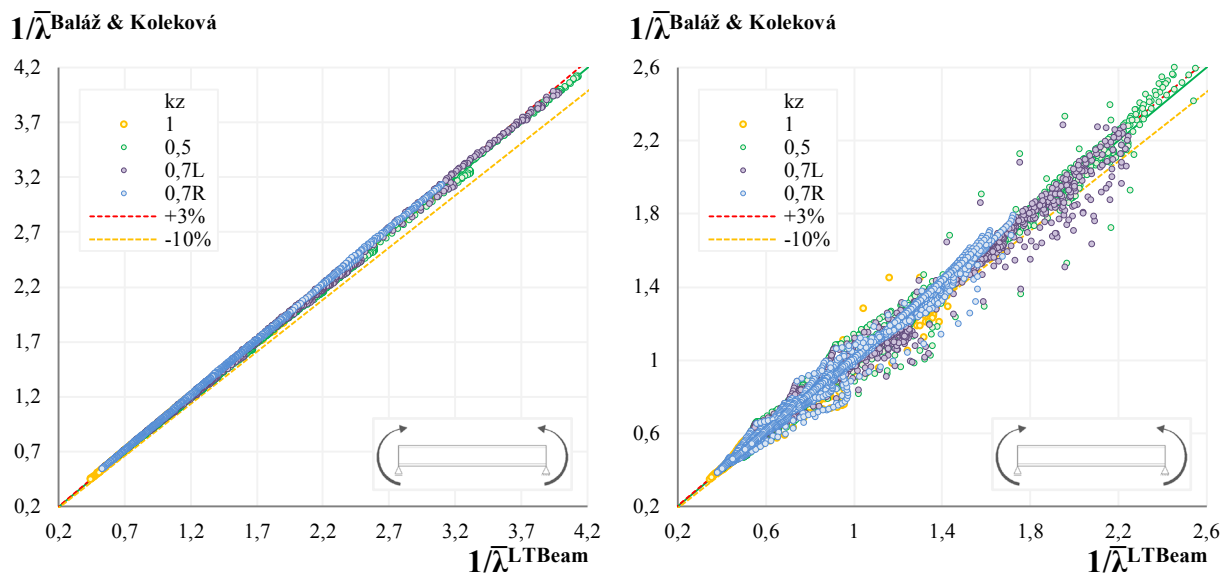


Figure 4.1 – Baláž and Koleková – Case 1.

Relatively to mono symmetric cross sections, see b), the C values obtain worst results, presenting a CoV value approximately of 7,817 with 20,8% of the results above the 3% unsafe mark, and a maximum value 55,6% above the LTBeam results. In Table B.1, it is possible to see that most of the unsafe tests are in sections with  $\psi_f$  near to the limits of its range, [-0,9;0,9], and increase following the variation of  $\psi = 1$  to -1. Since the analytical expressions are based in the basic case with  $\psi_f = 0$  and  $\psi = 1$  these results would be expected. Note that for all section with  $\psi_f$  between -0,9 and 0,9 the solution only propose one or two  $C_3$  value, on the other hand, for T-sections,  $\psi_f$  equal to 1 or -1, there are specific values, and this is why there is a decrease of unsafe results for 0,9 to 1 and for -0,9 to -1.

Table 4.3 – Baláž and Koleková – Case 1.

Baláž & Koleková		n	Mean	St. Dev.	CoV%	Min.	Max.	<0,9%	>1,03%
Case 1	Double Symmetric	3280	0,998	0,019	1,948	0,944	1,036	0,0	0,6
	Mono Symmetric	8528	1,003	0,078	7,817	0,571	1,556	6,1	20,8

#### 4.4.1.2 Case 2

Figure 4.2 presents the graphical analysis of the Case 2 for double and mono symmetric cross sections and Table 4.4 presents a summary of the Table B.2. For double symmetric cross sections, see a), the C values obtain a CoV value of 1,03% and only 0,9% of the results above the 3% mark with a maximum value of 1,044 (1,4% above the 3% mark) which are good results. As can be seen in Table B.2 and in green in a) the unsafe results are in sub-set of  $k_w=1$  and  $k_z=0,5$ .

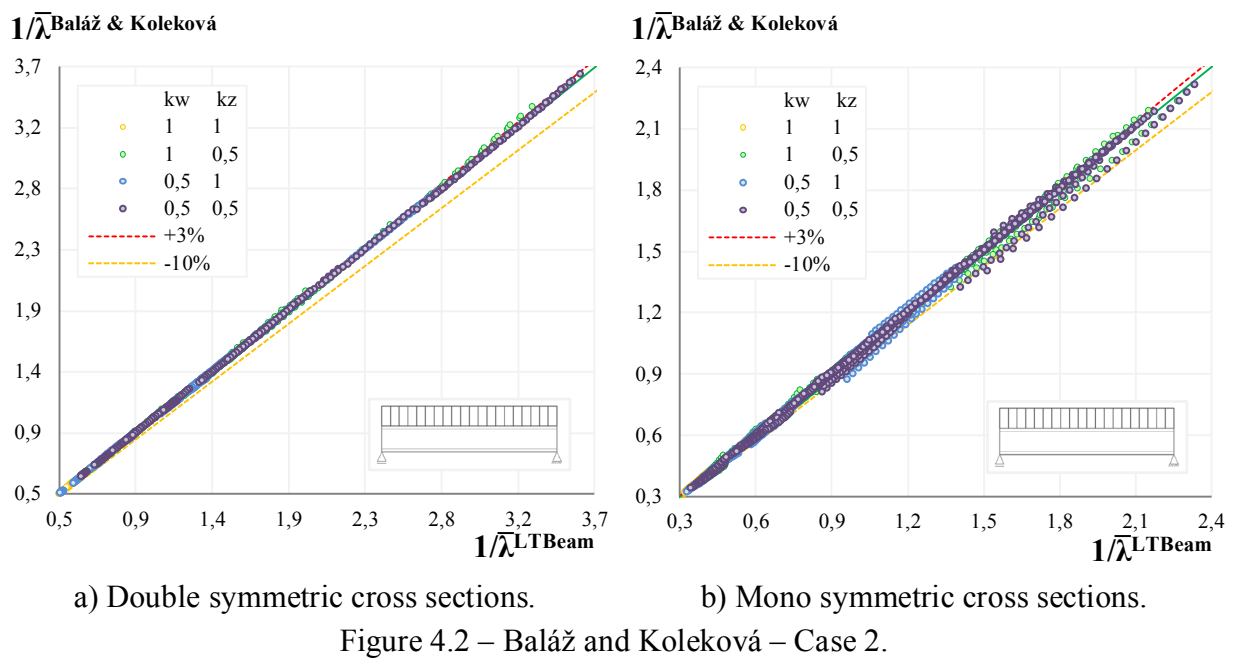


Figure 4.2 – Baláž and Koleková – Case 2.

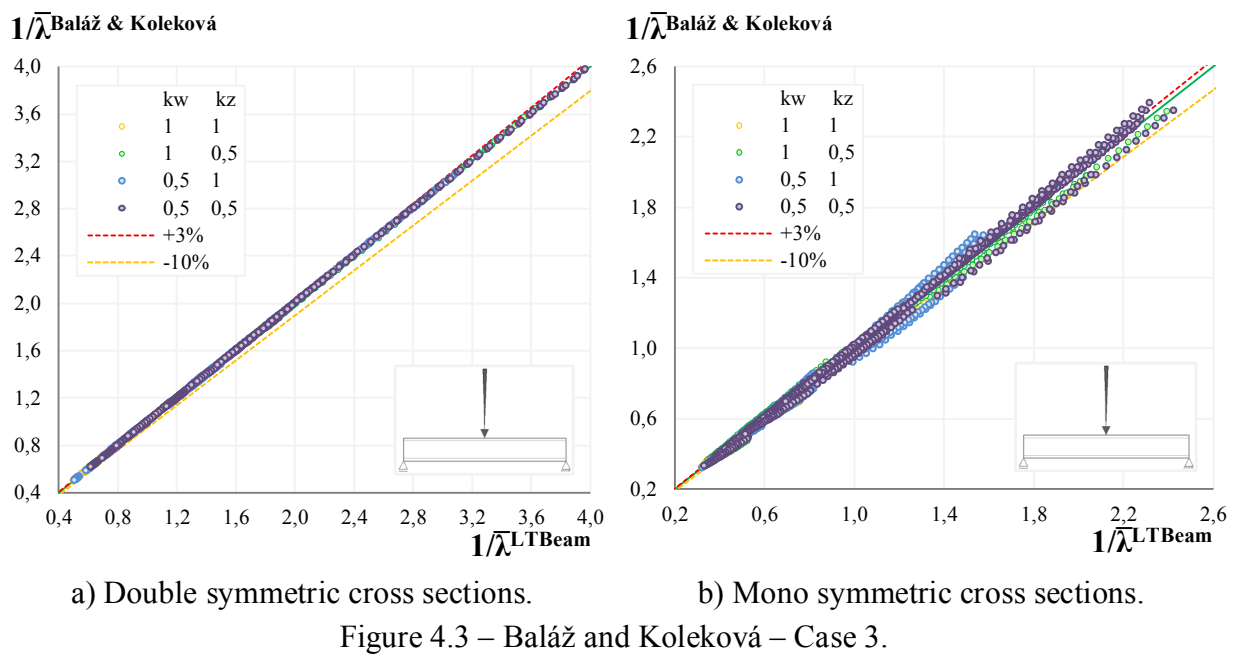
For mono symmetric cross sections, see b), the C values have better results comparatively to the previously case, presenting a CoV value of 2,76% with 3,8% of the results above the 3% unsafe mark, and a maximum value 11,6% above the LTBeam results. As previously, the results are worst for  $\psi_f$  near to the limits of its range, [-0,9;0,9], and for  $k_w=1$  and  $k_z=0,5$  as happens for double symmetric cross sections. Table B.3 presents the results for the 3  $\psi_f$  values (of the parametric study) nearest of the range limits, in order to understand the distribution of the accuracy in this range. In this table, it is possible to see that there is a gap between  $\psi_f = -0,8$  with only 6,8% unsafe results with maximum value of 1,074 (7% above the LTBeam) and  $\psi_f = -0,9$  with 19% unsafe results with maximum value of 1,116 (11,6 % above LTBeam).

Table 4.4 – Baláž and Koleková – Case 2.

Baláž & Koleková		n	Mean	St. Dev.	CoV%	Min.	Max.	<0,9%	>1,03%
Case 2	Double Symmetric	1680	0,998	0,010	1,030	0,972	1,044	0,0	0,9
	Mono Symmetric	4368	0,994	0,027	2,760	0,827	1,116	1,0	3,8

#### 4.4.1.3 Case 3

Figure 4.3 presents the graphical analysis of the Case 3 for double and mono symmetric cross sections and Table 4.5 presents a summary of the Table B.4. In an overview of this case, these C values obtain very similar results relatively to the previous case, possibly because the moment diagram shape is similar between these cases. For double symmetric sections, see a), the C values obtain a CoV value of 0,733% and has no unsafe testes or conservative testes, which are very good results.



On the other hand, for mono symmetric cross sections, the C values obtain a CoV value of 4,283% with 11,8% of the results above the 3% unsafe mark, and a maximum value 13,8% above the LTBeam results. All unsafe results have  $\psi_f$  as a member of [-0,9;-0,6] or [0,6;0,9]. As previously, in Table B.5 this sub-sets are divided, and it is possible to see the huge gap between the percentage of unsafe results with  $\psi_f$  equal to 0,9 or -0,9 (26,8% and 74,4% respectively) and with  $\psi_f$  equal to 0,8 or -0,8 (17,9% and 20,8% respectively). And note that, for  $\psi_f$  equal to 0,6 or -0,6 the percentage of unsafe tests is 2,4% and 7,1%, which is very low comparing with  $\psi_f = -0,9$  results. For this table, the maximum values varies between 11,9% ( $\psi_f = -0,9$ ) and 3,6% ( $\psi_f = -0,6$ ) above the LTBeam results. As a final note, the T-section obtains approximately 30% of tests below the 10% conservative mark.

Table 4.5 – Baláž and Koleková – Case 3.

Baláž & Koleková		n	Mean	St. Dev.	CoV%	Min.	Max.	<0,9%	>1,03%
Case 3	Double Symmetric	1680	0,997	0,007	0,733	0,978	1,009	0,0	0,0
	Mono Symmetric	4368	0,994	0,043	4,283	0,811	1,138	5,3	11,8

#### 4.4.1.4 Case 4

Figure 4.4 presents the graphical analysis of the Case 4 for double and mono symmetric cross sections and Table 4.6 presents a summary of the Table B.6. For double symmetric cross sections, see a), the C values obtain a CoV value of 2,216% and 8,8% of the results above the 3% unsafe mark with a maximum value 12,7% above the LTBeam results. As one can see in Table B.6 and in green and purple in the chart a), these unsafe results are in  $k_z = 0,5$  sub-sets and for  $h_l$  as a member of  $[0;0,5[$  (load applied in the bottom and tension part of the cross section). Coincidentally these 2 sub-sets combined lead to highest critical moment values, and thus the  $\bar{\lambda}_{LTBeam}$  sub-set with lower value has almost all unsafe results.

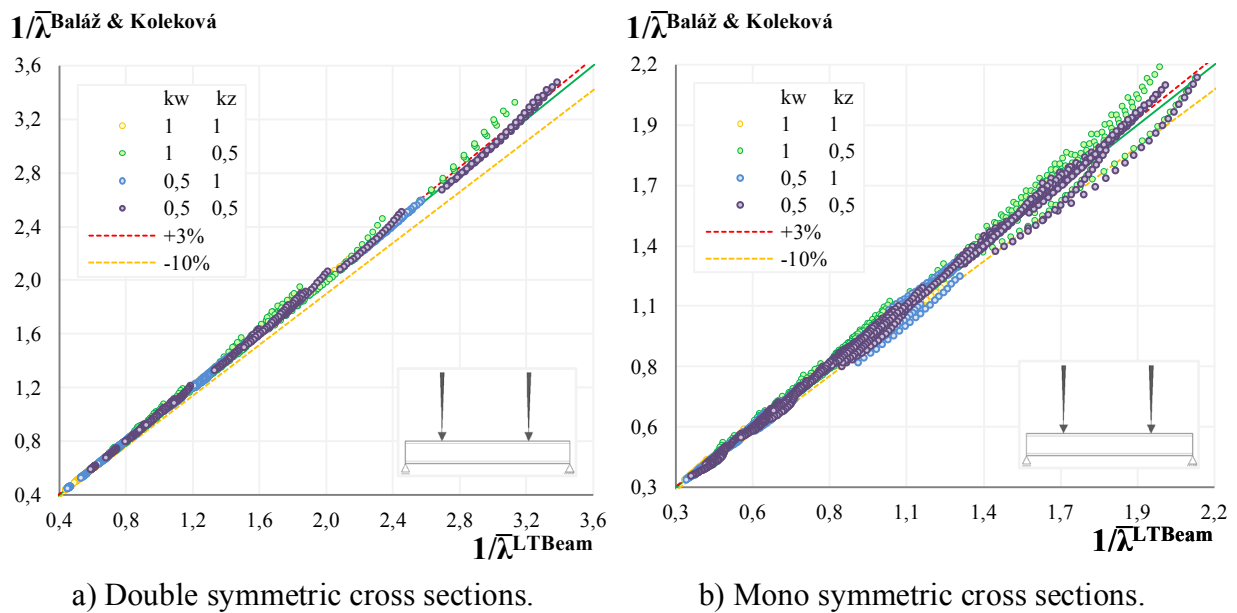


Figure 4.4 – Baláž and Koleková – Case 4.

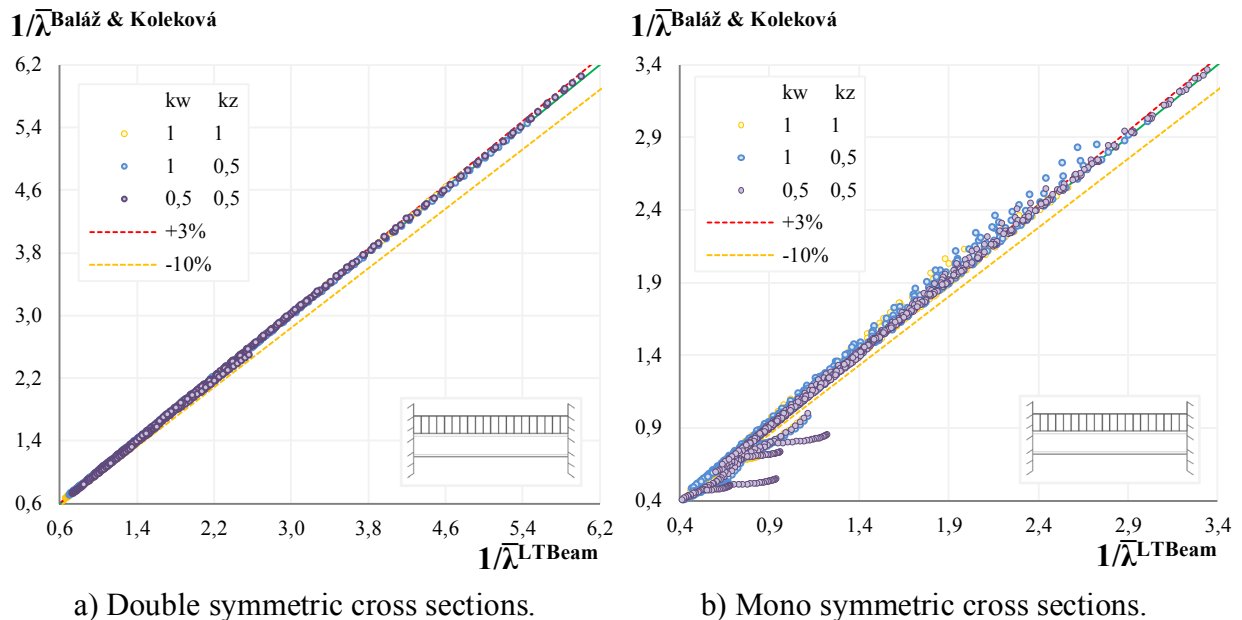
For mono symmetric cross sections, see b), the C values obtain a CoV value of 4,213% with 12,2% of the results above the 3% unsafe mark, and a maximum value 19% above the LTBeam results. The results are worst for the same variables and ranges of the double symmetric cross sections, however now there is also the  $\psi_f$  parameter. The analysis of this parameter is presented in Table B.7, and the results are similar to the previous cases. Note that the percentage of unsafe results decrease 10% for positives  $\psi_f$  values and 3% for negatives values. For T-sections, the C values obtain approximately 20% of results below the 10% conservative mark, and no unsafe tests.

Table 4.6 – Baláž and Koleková – Case 4.

Baláž & Koleková		n	Mean	St. Dev.	CoV%	Min.	Max.	<0,9%	>1,03%
<b>Case 4</b>	<b>Double Symmetric</b>	1680	1,002	0,022	2,216	0,963	1,127	0,0	8,8
	<b>Mono Symmetric</b>	4368	0,995	0,042	4,213	0,826	1,190	3,5	12,2

#### 4.4.1.5 Case 5

Figure 4.5 presents the graphical analysis of the Case 5 for double and mono symmetric cross sections and Table 4.7 presents a summary of the Table B.8. For double symmetric cross sections, see a), the C values obtain a CoV value of 1,518% and had no unsafe tests or conservative tests, which are very good results.



a) Double symmetric cross sections.

b) Mono symmetric cross sections.

Figure 4.5 – Baláž and Koleková – Case 5.

For mono symmetric cross sections, see b), the C values obtain a CoV value of 13,447%, with 22% of the results above the 3% unsafe mark and 19,1% below the 10% conservative mark. With a maximum value 19,8% above the LTBeam results and a minimum value 66,3% below. Almost all unsafe results, as seen in Table B.8, have  $\psi_f$  as a member of  $[-0,5;0[$ ; on the other hand, all conservative results correspond to T-section.

Table 4.7 – Baláž and Koleková – Case 5.

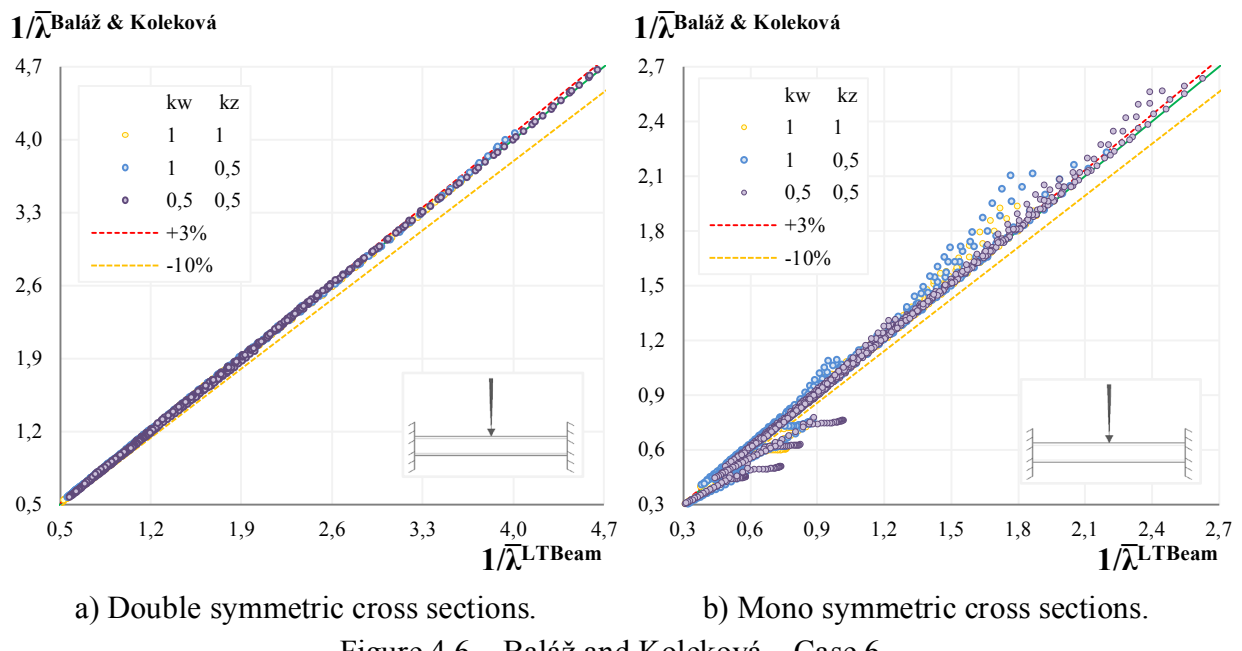
Baláž & Koleková		n	Mean	St. Dev.	CoV%	Min.	Max.	<0,9%	>1,03%
<b>Case 5</b>	<b>Double Symmetric</b>	1260	0,996	0,015	1,518	0,944	1,019	0,0	0,0
	<b>Mono Symmetric</b>	2268	0,963	0,130	13,447	0,337	1,198	19,1	22,0

Given the huge difference between the results of double and mono symmetrical cross sections, the variable  $\psi_f$  is analyzed in a more detailed way in the Table B.9. Firstly it is important to mention that this solution only have C values for  $\psi_f$  equal to 1 or -1 and for values between -0,5 to 0,5, as can be seen in Table A.2. As nothing is said in this table and for an overview of the problem, the interpolation between these values is analyzed separately of the analysis above in order to get a solution for  $\psi$  as a member of  $[-0,9;-0,5[$  and  $]0,5;0,9]$ , as

can be seen in the first part of Table B.9. This interpolation gives bad results, with percentages of unsafe values over 70%, in this sense, these interpolations are disregarded. In the second part of this table, a more detailed analysis of the limits proposed by the solution is presented. Beyond the same conclusions given in the previous cases, it is possible to see that for  $\psi_f = -0,5$  the C values obtain 83,3% unsafe results with a maximum value 19,8% above LTBeam results.

#### 4.4.1.6 Case 6

Figure 4.6 presents the graphical analysis of the Case 6 for double and mono symmetric cross sections and Table 4.8 presents a summary of the Table B.10. For double symmetric cross sections, see a), the C values obtain a CoV value of 1,598% and only 0,2% of the results above the 3% mark with a maximum value approximately 3% above the LTBeam results.



a) Double symmetric cross sections.

b) Mono symmetric cross sections.

Figure 4.6 – Baláž and Koleková – Case 6.

For mono symmetric cross sections, see b), the C values obtain a CoV value of 12,911% with 29,2% of the results above the 3% unsafe mark and 18,7% below the 10% conservative mark. With a maximum value 41% above the LTBeam results, and a minimum value 53% below the LTBeam results. A similar analysis as the presented in the previously case is performed with similar results, as can be seen in Table B.11

Table 4.8 – Baláž and Koleková – Case 6.

Baláž & Koleková		n	Mean	St. Dev.	CoV%	Min.	Max.	<0,9%	>1,03%
<b>Case 6</b>	<b>Double Symmetric</b>	1260	0,999	0,016	1,598	0,961	1,030	0,0	0,2
	<b>Mono Symmetric</b>	2268	0,972	0,126	12,911	0,470	1,410	18,7	29,2

#### 4.4.1.7 Case 7

For this case, firstly, the consideration made in section 3.2.1 for cases with the uniformly distributed load acting at a distance from the shear center is analyzed. In which it was decided to use  $C_2=0,5$  as it is done in DIN 18800 (DIN, 1990). This consideration leads to bad results as seen in Figure 4.7 a) and in Table B.13. For loads applied at top flange the CoV values is 20,551% with 48% of the results above the 3% unsafe mark and 7,5% below the 10% conservative mark, and a maximum value 150% the LTBeam results. And for loads applied at the bottom flange the CoV value is 14,684% with 25,6% of the results above the 3% unsafe mark and 21,5% below the 10% conservative mark, and a minimum value 60% below the LTBeam results. Since this consideration obtains very bad results, for the analysis of the C values all loads are applied at shear center, disregarding the  $C_2$  values.

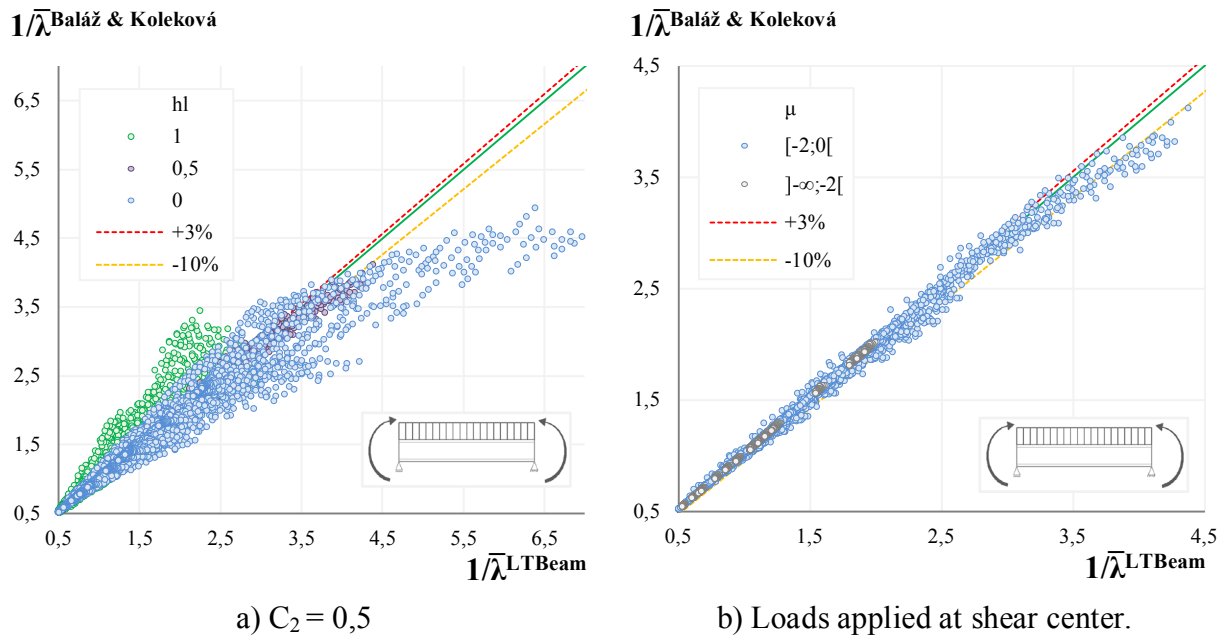


Figure 4.7 – Baláž and Koleková – Case 7.

Thus, Figure 4.7 b) presents the graphical analysis of the Case 7 for double symmetric cross sections with the loads applied at shear center and Table 4.9 presents a summary of the Table B.12. For this case the C values obtain a CoV value of 4,034% and 12,6% of the results above the 3% unsafe mark and 3,5% of the tests below the 10% conservative mark. With a maximum value approximately 24% above the LTBeam results and a minimum value 21,1% below. Almost all of the unsafe results have  $\psi$  as a member of  $]0,5;1]$ .

Table 4.9 – Baláž and Koleková – Case 7.

Baláž & Koleková	n	Mean	St. Dev.	CoV%	Min.	Max.	<0,9%	>1,03%
Case 7 $C_2 = 0$	5220	1,003	0,040	4,034	0,789	1,241	3,5	12,6

#### 4.4.1.8 Case 9

For this case, firstly, a comparison between non-linear interpolations with linear interpolations is performed. The considerations about the use of non-linear interpolation are already discussed in section 3.2.1. However, since the use of this type of interpolations in tables with 3 variables is not practical and it is the opposite behind the philosophy of these analytical expressions this comparison is performed. This analysis is presented in Table B.15 and as can be seen, for double symmetrical cross sections, the difference is insignificant, the CoV value decrease about 1%. On other hand, for mono symmetric cross sections, the CoV value increases about 1% but with half of unsafe results. Although it is not a significant improvement, the non-linear interpolation is adopted for the case analysis.

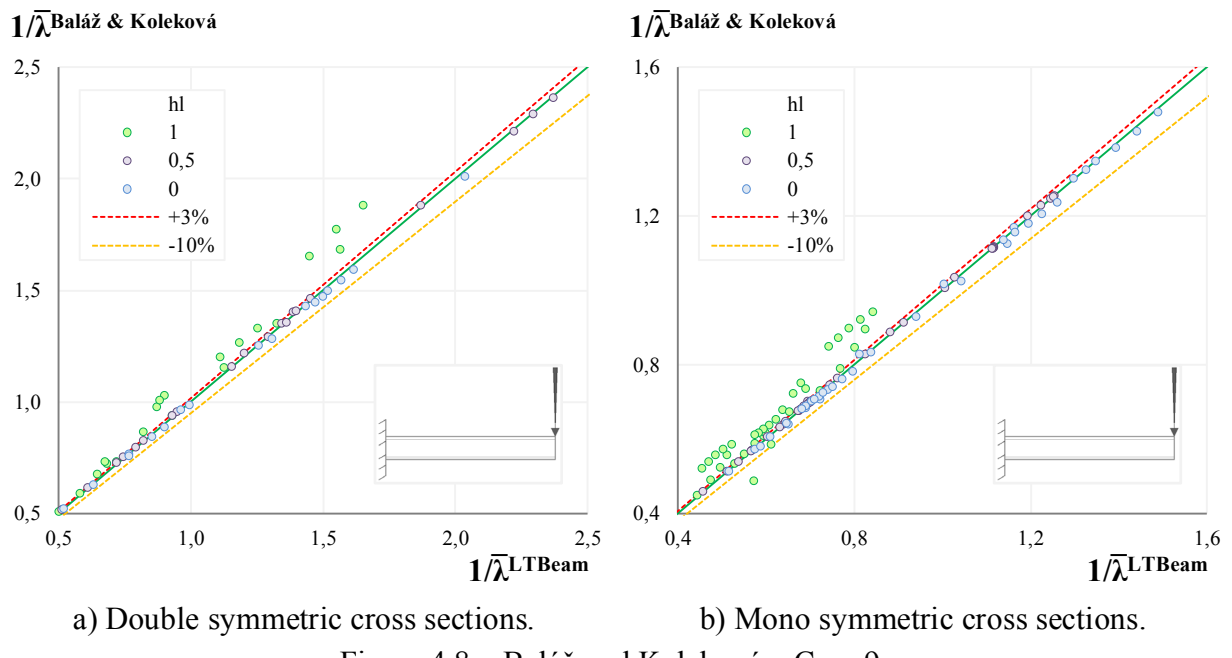


Figure 4.8 – Baláž and Koleková – Case 9.

Figure 4.8 presents the graphical analysis of the Case 9 for double and mono symmetric cross sections and Table 4.10 presents a summary of the Table B.14. For double symmetric cross section, see a), the C value obtains a CoV value of 9,314% and 28,3% of the results above the 3% unsafe mark with a maximum value 30,2% above the LTBeam results. As seen in Table B.14 and in green in a), all unsafe results are tests with the load applied at the top flange.

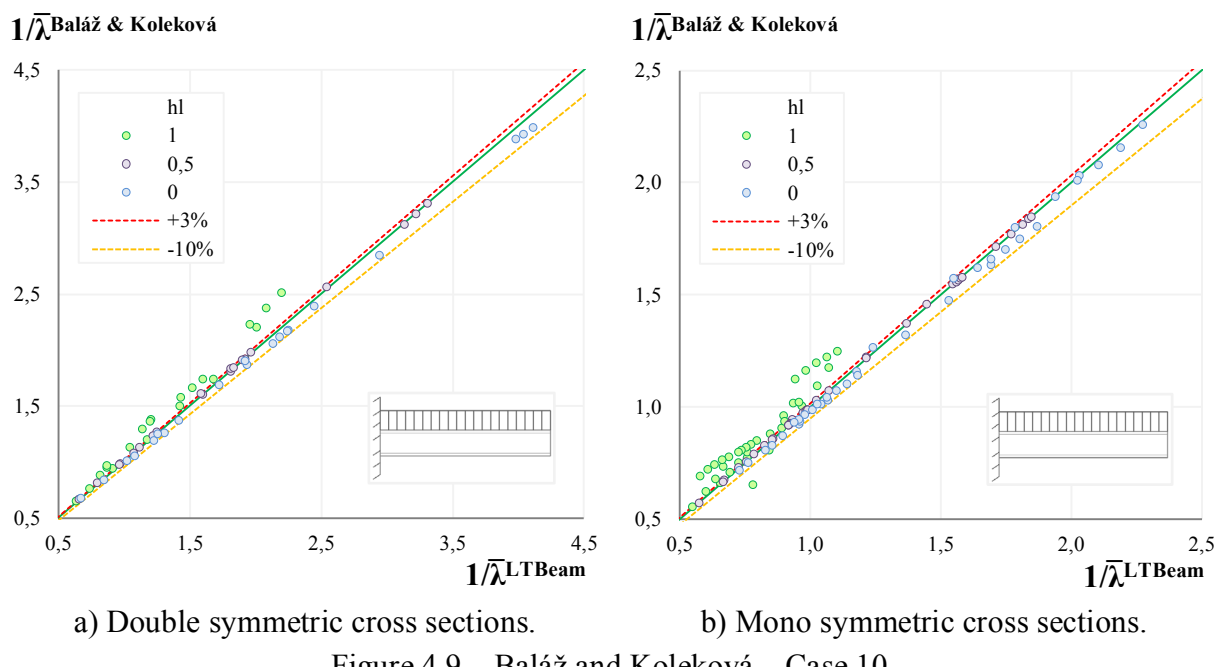
Table 4.10 – Baláž and Koleková – Case 9 – Non-linear.

Baláž & Koleková		n	Mean	St. Dev.	CoV%	Min.	Max.	<0,9%	>1,03%
Case 9	Double Symmetric	60	1,045	0,097	9,314	0,960	1,302	0,0	28,3
	Mono Symmetric	108	1,034	0,115	11,131	0,445	1,310	1,9	27,8

For mono symmetric cross sections, see b), the C values obtains a CoV value of 11,131% and 27,8% of the results above the 3% unsafe mark with a maximum value 31% above the LTBeam results. The results are worst for the same type of tests, with the load applied at the top flange.

#### 4.4.1.9 Case 10

For the same reason, as it was done in the previous case, a comparison between non-linear interpolations with linear interpolations is performed, and the results are very similar. This analysis is present in Table B.17, for double symmetrical cross section the CoV value decreases about 3%. On the other hand, for mono symmetrical cross section the CoV value increases 1% but with half of unsafe results. In the same way, the non-linear interpolation is adopted for the case analysis.



a) Double symmetric cross sections.      b) Mono symmetric cross sections.

Figure 4.9 – Baláž and Koleková – Case 10.

Figure 4.9 presents the graphical analysis of the Case 9 for double and mono symmetric cross sections and Table 4.11 presents a summary of the Table B.16. For double symmetric cross sections, see a), the C values obtain a CoV value of 10,691% and 33,3% of the results above the 3% unsafe mark with a maximum value 29,7% above the LTBeam results. As one can see in Table B.16 and in green in a), all unsafe results are tests with the load applied at the top flange. For mono symmetric cross sections, see b), the C values obtain a CoV value of 13,691% and 28,7% of the results above the 3% unsafe mark with a maximum value 42,4% above the LTBeam results. And the results are worst for the same type of tests.

Table 4.11 – Baláž and Koleková – Case 10 – Non-linear.

Baláž & Koleková		n	Mean	St. Dev.	CoV%	Min.	Max.	<0,9%	>1,03%
Case 10	Double Symmetric	60	1,047	0,112	10,691	0,929	1,297	0,0	33,3
	Mono Symmetric	108	1,035	0,142	13,691	0,348	1,424	1,9	28,7

#### 4.4.2 ECCS - Basis Load Cases

In this solution all variable of all cases are analyzed here. As it seen in Tables 3.3 and 3.4 this only has C values for 4 cases.

##### 4.4.2.1 Case 1

For this case, a preliminary analysis is performed in order to choose a way to take in account the  $k_z=0,7$  tests as discussed in section 3.2.2. In that section, it is presented two possible ways: use the C factors values of the tables for case  $k_z=1$  and only replace  $k_z=0,7$  in the main equation, or use a linear interpolation between the C factors. The comparative analysis between these two methods is presented in Table B.19, and as can be seen, there is not a significant difference between them. However, in order to decide which method to use, it is given preference to the method with lower CoV value, since this method may be more consistent. Figure 4.10 presents the graphical analysis of the Case 1 for double symmetric cross sections and Table 4.12 presents a summary of the Table B.18.

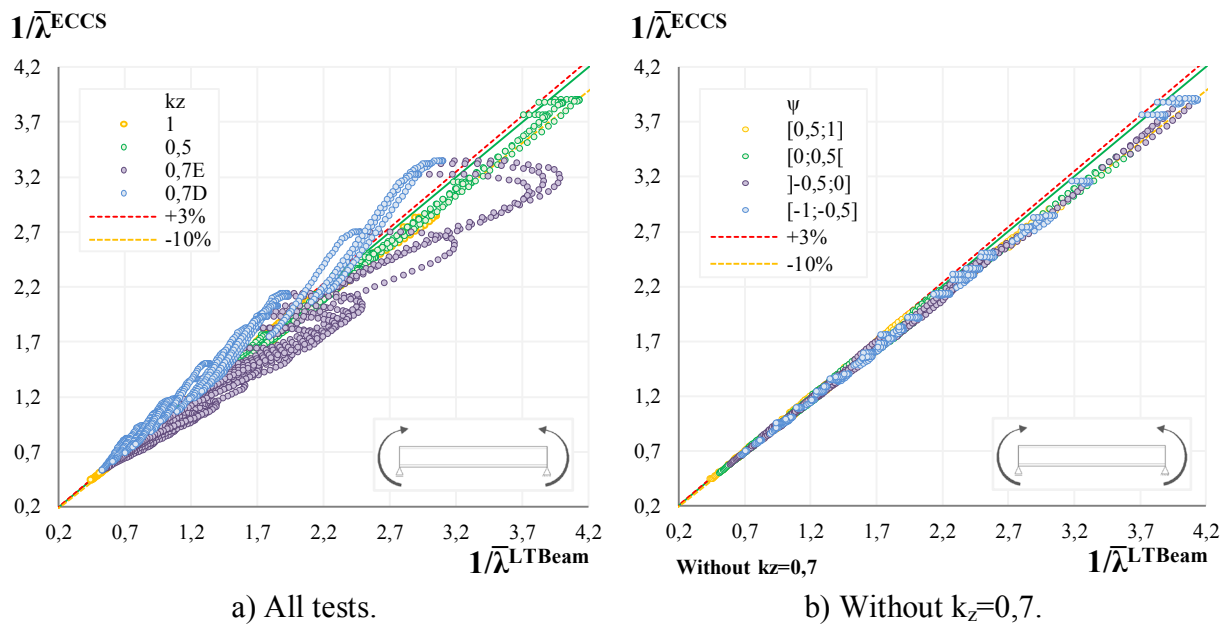


Figure 4.10 – ECCS – Case 1 – Double symmetric cross sections.

In a) and b), the results are presented differentiating the  $k_z$  by colors. In a), it is easily noticed that the results for  $k_z=0,7L$  (in purple) are too conservative, with 73,5% of the tests below the 10% conservative mark. The opposite is noticed for  $k_z=0,7R$  (in blue), with the results too unconservative with 75,5% of the test above the 3% unsafe mark. In these sense, for the C values analysis, the tests with different boundary conditions,  $k_z=0,7$ , are disregarded. Thus, for double symmetric cross sections without  $k_z = 0,7$  tests, the C values obtain a CoV value of 3,445% with only 0,1% of the results above the 3% mark and 16,2% below the 10% conservative mark. The maximum value is 3,2% above the LTBeam results and the minimum value is 13,5% below the LTBeam results. As seen in Table B.18, the number of conservative results increase following the variation of  $\psi = 1$  to -1, leading to the sub-set with  $\psi$  as a member of [-1;-0,5] with 26,6% conservative tests.

Table 4.12 – ECCS – Basis Load Cases – Case 1 – Without  $k_z=0,7$ .

ECCS – Basis Load Cases		n	Mean	St. Dev.	CoV%	Min.	Max.	<0,9%	>1,03%
Case 1	Double Symmetric	1640	0,934	0,032	3,445	0,865	1,032	16,2	0,1
	Mono Symmetric	3608	0,957	0,079	8,214	0,752	1,381	17,8	10,0

Figure 4.11 presents the graphical analysis of the Case 1 for mono symmetric cross sections. For this type of cross sections, as seen in a) and b), the  $k_z=0,7$  tests obtain the same problem already seen for double symmetric cross sections, with  $k_z=0,7L$  (in purple) too conservative, with 59,6% of the tests below the 10% conservative mark. And  $k_z=0,7R$  (in blue), too unconservative with 73,5% of the test above the 3% unsafe mark. In the same way, for the C values analysis, the tests with different boundary conditions,  $k_z=0,7$ , are disregarded.

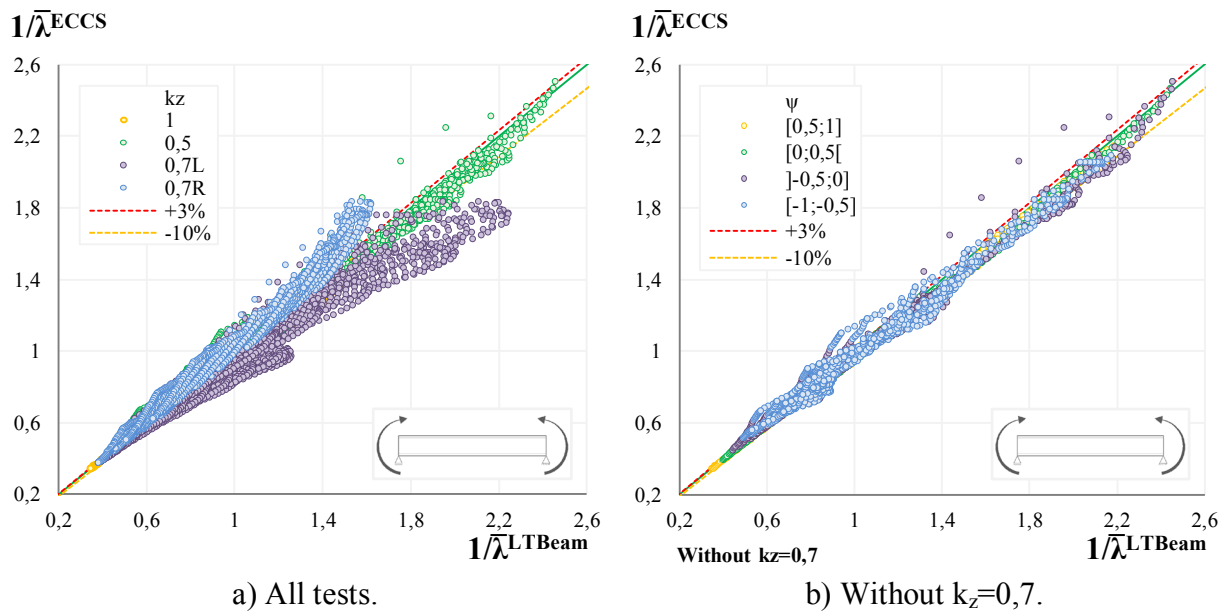


Figure 4.11 – ECCS – Case 1 – Mono symmetric cross sections.

Thus, for mono symmetric cross sections without  $k_z = 0,7$  tests, the C values obtain a CoV value of 8,214% with 10% of the results above the 3% unsafe mark and 17,8% below the 10% conservative mark. The maximum value is 3,81% above the LTBeam results and the minimum value is 24,8% below the LTBeam results. The number of conservative results increase following the variation of  $\psi = 1$  to -1 and  $\psi_f = -0,9$  to 0,9, and the unsafe results have  $\psi_f$  as a member of [-0,9;-0,6] and [0,6;0,9] and increase following the variation of  $\psi = 1$  to -1.

#### 4.4.2.2 Case 2

Figure 4.12 presents the graphical analysis of the Case 2 for double and mono symmetric cross sections and Table 4.13 presents a summary of the Table B.20. For double symmetric cross sections, seen a), the C values obtain very good results relatively to LTBeam, with a CoV value of 1,486% and only 0,2% of the results above the 3% unsafe mark with a maximum value of 1,031 (0,1% above the 3% unsafe mark). The unsafe results are in  $k_z=0,5$  sub-set.

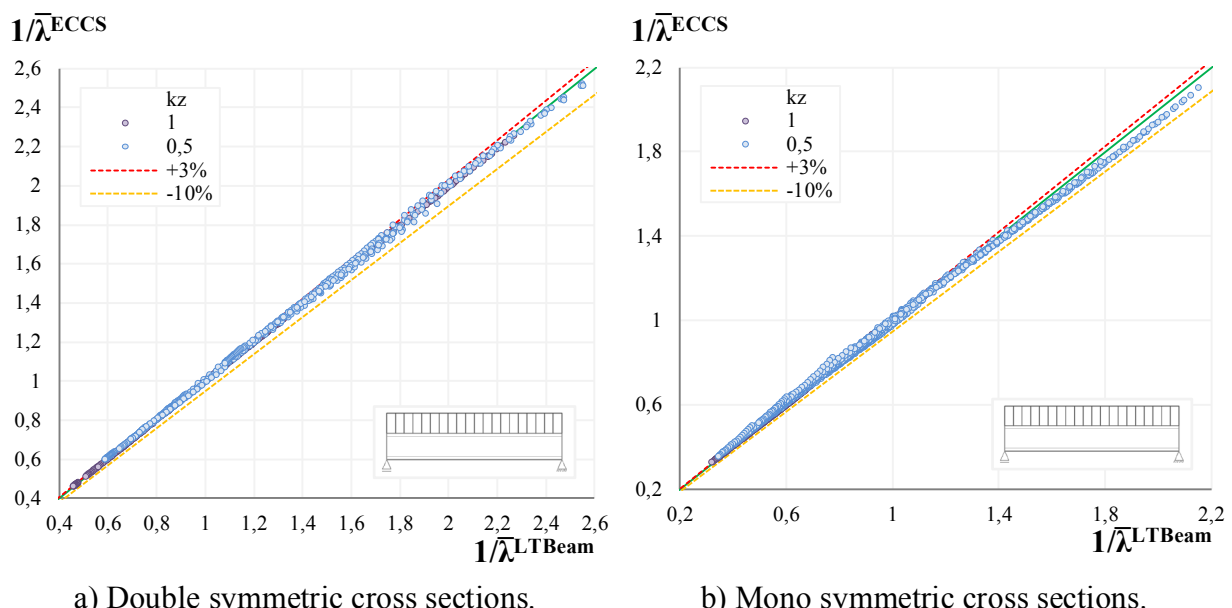


Figure 4.12 – ECCS – Basis Load Cases – Case 2.

Relatively to mono symmetric cross sections, seen b), the C values obtain a CoV value of 2,780% with 11,1% of the results above the 3% unsafe mark, and a maximum value 12,2% above the LTBeam results. These unsafe results, are essentially in the  $k_z=0,5$  sub-set and have the  $\psi_f$  as a member of [-0,9;-0,6]. This  $\psi_f$  range is detailed in Table B.21, and one can see that there is a huge difference between the values of the range. For  $\psi_f = -0,8$ , the unsafe results are half those obtained for  $\psi_f = -0,9$ . And [-0,9;-0,6] have no conservative or unsafe result.

Table 4.13 – ECCS – Basis Load Cases – Case 2.

ECCS – Basis Load Cases	n	Mean	St. Dev.	CoV%	Min.	Max.	<0,9%	>1,03%	
Case 2	<b>Double Symmetric</b>	840	0,993	0,015	1,486	0,949	1,031	0,0	0,2
	<b>Mono Symmetric</b>	1848	0,996	0,028	2,780	0,935	1,122	0,0	11,1

#### 4.4.2.3 Case 3

Figure 4.13 presents the graphical analysis of the Case 3 for double and mono symmetric cross sections and Table 4.14 presents a summary of the Table B.22. For double symmetric cross sections, see a), the C values obtain a CoV value of 1,770% and has no unsafe or conservative tests, which are very good results.

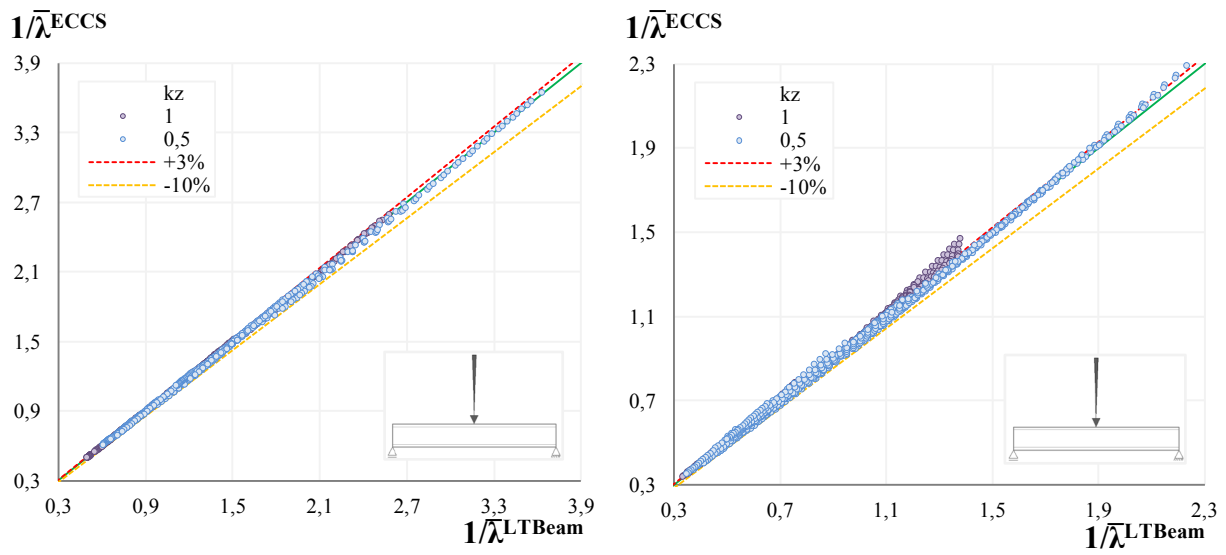


Figure 4.13 – ECCS – Basis Load Cases – Case 3.

For mono symmetric cross sections, see b), the C values obtain a CoV value of 2,997% with 13,7% of the results above the 3% unsafe mark, and a maximum value 13,8% above the LTBeam results. These unsafe results have  $\psi_f$  as a member of [-0,9;-0,6] and [0,6;0,9]. These ranges are detailed in Table B.23, and it is possible to see that they follow the same conclusions of the previous cases, however it is important to note the huge gap between  $\psi_f = -0,9$  with 74,4% of the unsafe results and  $\psi_f = -0,8$  with only 20,8%.

Table 4.14 – ECCS – Basis Load Cases – Case 3.

ECCS – Basis Load Cases	n	Mean	St. Dev.	CoV%	Min.	Max.	<0,9%	>1,03%	
Case 3	<b>Double Symmetric</b>	840	0,990	0,018	1,770	0,931	1,017	0,0	0,0
	<b>Mono Symmetric</b>	1848	1,000	0,030	2,997	0,925	1,138	0,0	13,7

#### 4.4.2.4 Case 4

Figure 4.14 presents the graphical analysis of the Case 4 for double and mono symmetric cross sections and Table 4.15 presents a summary of the Table B.24. For double symmetric cross sections, see a), the C values obtain a CoV value of 2,122% and 13% of the results above the 3% mark with a maximum value 10,7% above the 3% unsafe mark. The unsafe values are in  $k_z=0,5$  sub-set as can be easily seen in the blue in Figure 4.14 a).

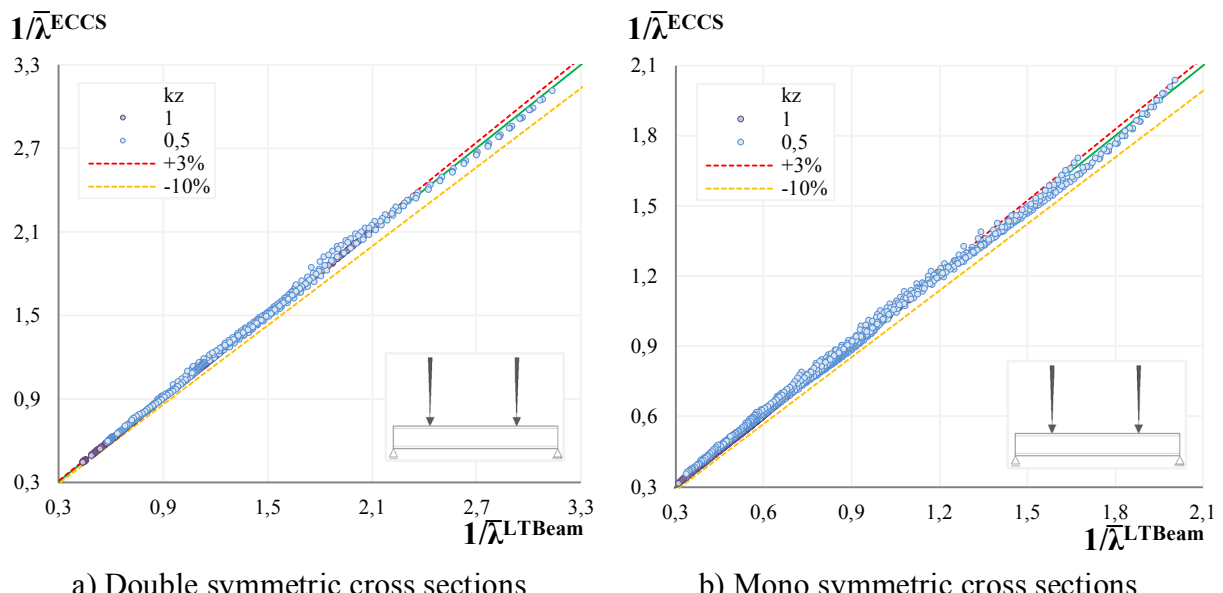


Figure 4.14 – ECCS – Basis Load Cases – Case 4.

For mono symmetric cross sections, see a), the C values obtain a CoV value of 3,397% and 22,2% of the results above the 3% unsafe mark with a maximum 16% above the LTBeam results. The unsafe values are in  $k_z=0,5$  sub-set and the number increase following the variation of  $\psi_f$  = 0,9 to -0,9. In which the  $\psi_f$  = -0,9 sub-set has 61,3% unsafe results, see Table B.25.

Table 4.15 – ECCS – Basis Load Cases – Case 4.

ECCS – Basis Load Cases	n	Mean	St. Dev.	CoV%	Min.	Max.	<0,9%	>1,03%	
<b>Case 4</b>	<b>Double Symmetric</b>	840	1,009	0,021	2,122	0,960	1,107	0,0	13,0
	<b>Mono Symmetric</b>	1848	1,015	0,034	3,397	0,942	1,160	0,0	22,2

#### 4.4.3 Galéa

In this solution all variable of all cases are analyzed here. As seen in Tables 3.3 and 3.4 this only has not C values for Case 4 and cantilevers cases.

#### 4.4.3.1 Case 1 and 2

Figure 4.15 presents the graphical analysis of Case 1 and 2 for double symmetric cross sections and Tables 4.16 and 4.17 presents a summary of the Table B.26 for these cases respectively.

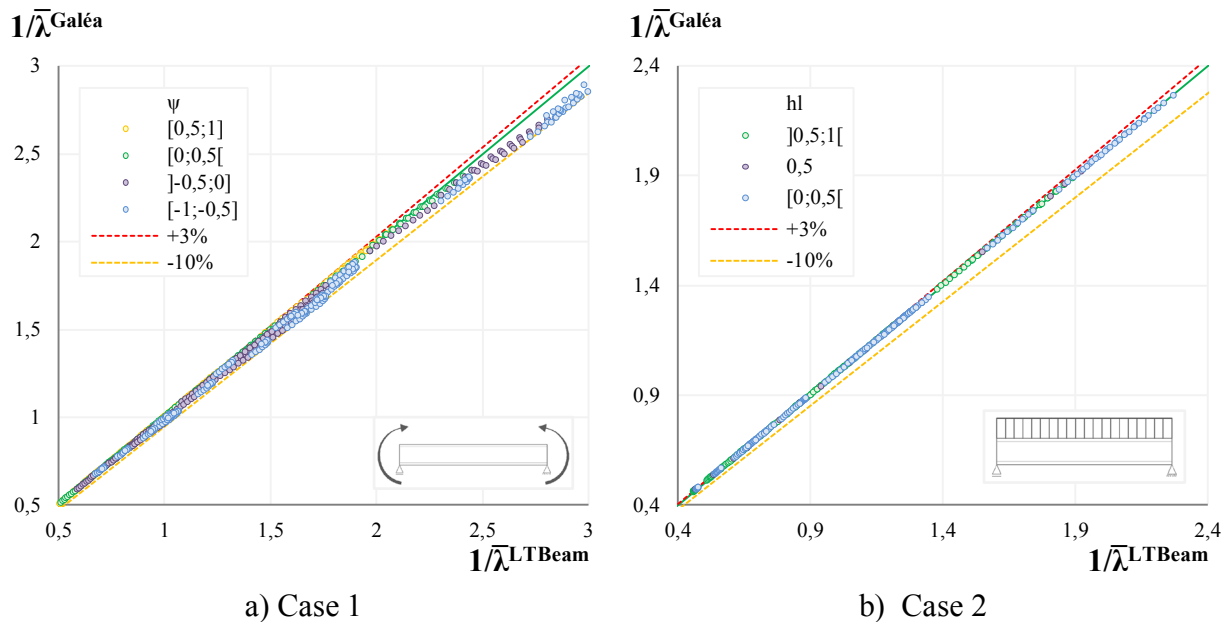


Figure 4.15 – Galéa – Case 1 and 2.

For Case 1, the C values obtain a CoV value of 3,032% and 0,6% of the results below the 10% conservative mark with a minimum value 0,2% below the 10% conservative mark which are very good results. This low number of unsafe tests have the  $\psi$  as a member of [-1;0,5], see Table B.26.

Table 4.16 – Galéa – Case 1.

Galéa		n	Mean	St. Dev.	CoV%	Min.	Max.	<0,9%	>1,03%
Case 1	Double Symmetric	820	0,973	0,029	3,032	0,898	1,001	0,6	0,0

For Case 2, the C values obtain a CoV value of 0,203% and has no unsafe tests or conservative tests, which are very good results.

Table 4.17 – Galéa – Case 2.

Galéa		n	Mean	St. Dev.	CoV%	Min.	Max.	<0,9%	>1,03%
Case 2	Double Symmetric	420	1,000	0,002	0,203	0,995	1,003	0,0	0,0

#### 4.4.3.2 Case 3 and 5

Figure 4.16 presents the graphical analysis of Case 3 and 5 for double symmetric cross sections and Tables 4.18 and 4.19 presents a summary of the Table B.26 for these cases respectively.

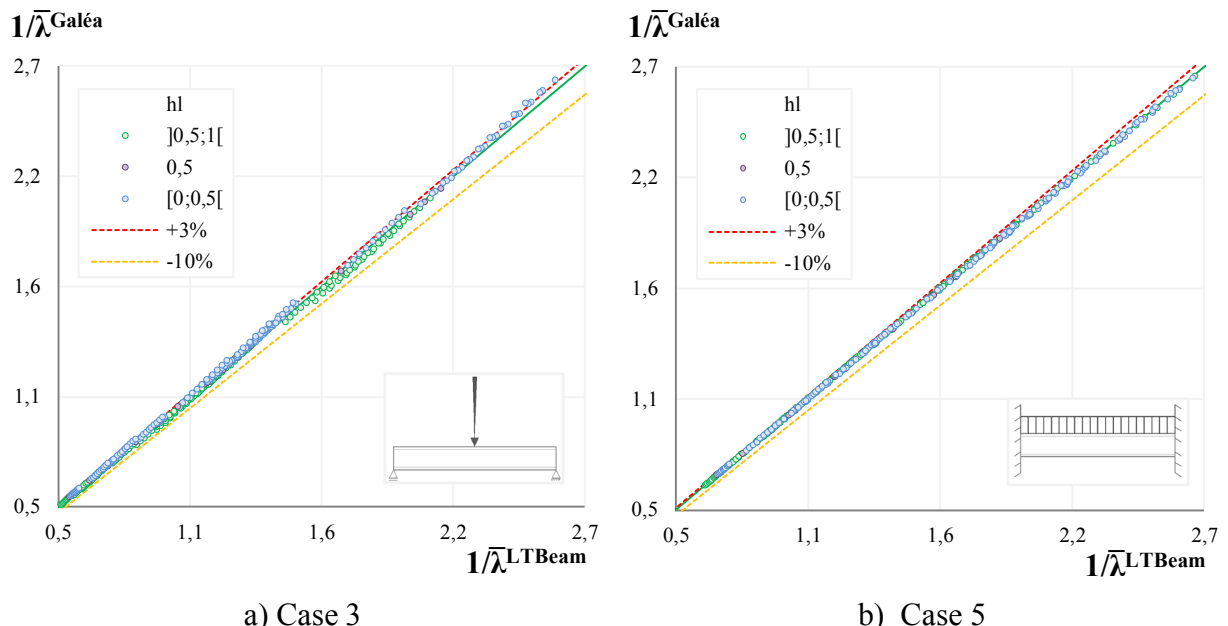


Figure 4.16 – Galéa – Case 3 and 5.

For Case 3, the C values obtain a CoV value of 2,014% and 4% of the results above the 3% unsafe mark with a maximum value 4,5% above the LTBeam results. This unsafe tests, as can be seen in Table B.26 and in blue in the Figure 4.16 a), have the load applied at the in the bottom and tension part of the cross section.

Table 4.18 – Galéa – Case 3.

Galéa		n	Mean	St. Dev.	CoV%	Min.	Max.	<0,9%	>1,03%
Case 4	Double Symmetric	420	0,994	0,020	2,014	0,943	1,045	0,0	4,0

For Case 5, the C values obtain a CoV value of 0,482% and has no unsafe tests or conservative tests, which are very good results.

Table 4.19 – Galéa – Case 5.

Galéa		n	Mean	St. Dev.	CoV%	Min.	Max.	<0,9%	>1,03%
Case 5	Double Symmetric	420	0,995	0,005	0,482	0,983	1,004	0,0	0,0

#### 4.4.3.3 Case 6 and 7

Figure 4.17 presents the graphical analysis of Case 6 and 7 for double symmetric cross sections. Table 4.20 presents a summary of the Table B.26 for Case 6.

Table 4.20 – Galéa – Case 6.

Galéa		n	Mean	St. Dev.	CoV%	Min.	Max.	<0,9%	>1,03%
Case 6	Double Symmetric	420	0,987	0,053	5,400	0,876	1,112	6,0	20,5

For this case, the C values obtain a CoV value of 5,4% with 20,5% of the results above the 3% unsafe mark and 6% of the results below the 10% conservative mark. With a maximum value 11,2% above the LTBeam results and a minimum value 12,4% below.

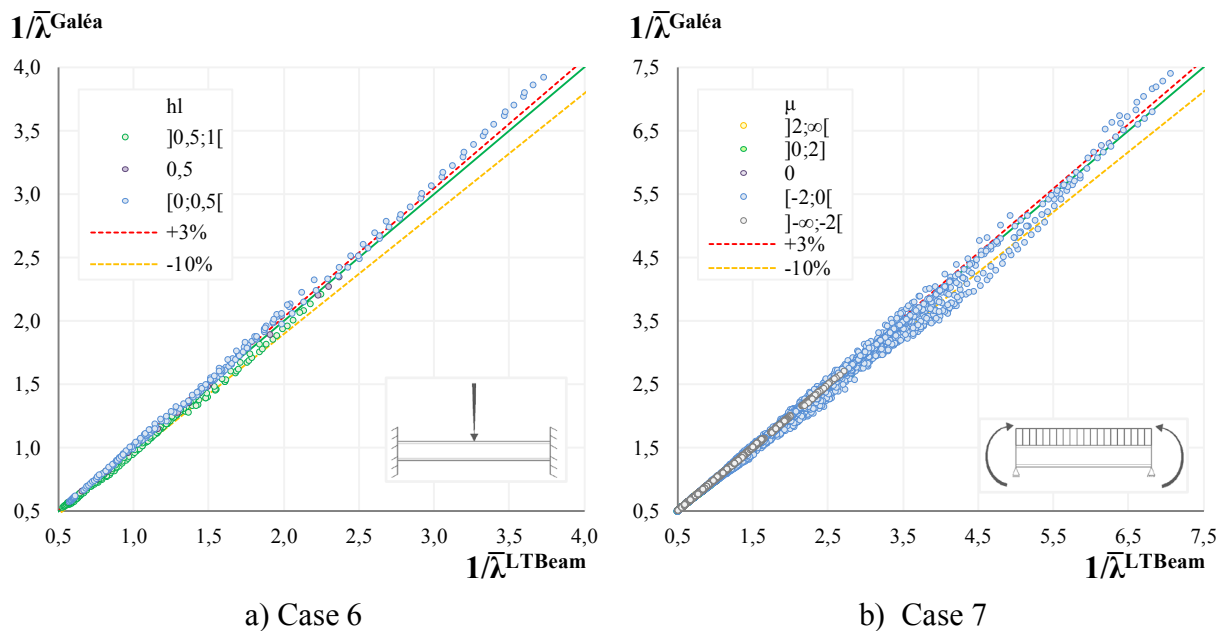


Figure 4.17 – Galéa – Case 6 and 7.

The unsafe tests, as can be seen in Table B.26 and in blue in the Figure 4.17 a), have the load applied at the bottom and tension part of the cross section, with  $h_l$  as a member of  $[0;0,5[$  sub-set with 43% unsafe results. On the other hand, the conservative tests, in green in the Figure 4.17 a), have the load applied at the top and compression part of the cross section, with  $h_l$  as a member of  $]0,5;1]$  sub-set with 12,5% conservative results. Table 4.21 presents a summary of the Table B.27 for Case 7.

Table 4.21 – Galéa – Case 7.

Galéa		n	Mean	St. Dev.	CoV%	Min.	Max.	<0,9%	>1,03%
Case 7	Double Symmetric	31860	0,990	0,023	2,305	0,773	1,113	1,3	0,7

For this case, the C values obtain a CoV value of 2,305% with 0,7% of the results above the 3% unsafe mark and 1,3% of the result below the 10% conservative mark. With a maximum value 11,3% above the LTBeam results and a minimum value 22,7% below. The unsafe and conservative tests have  $\mu$  as a member of  $[-2;0[$ , as seen in blue in the Figure 4.17 b).

#### 4.4.3.4 Case 8

Figure 4.18 presents the graphical analysis of the Case 8 for double symmetric cross sections and Table 4.22 presents a summary of the Table B.28.

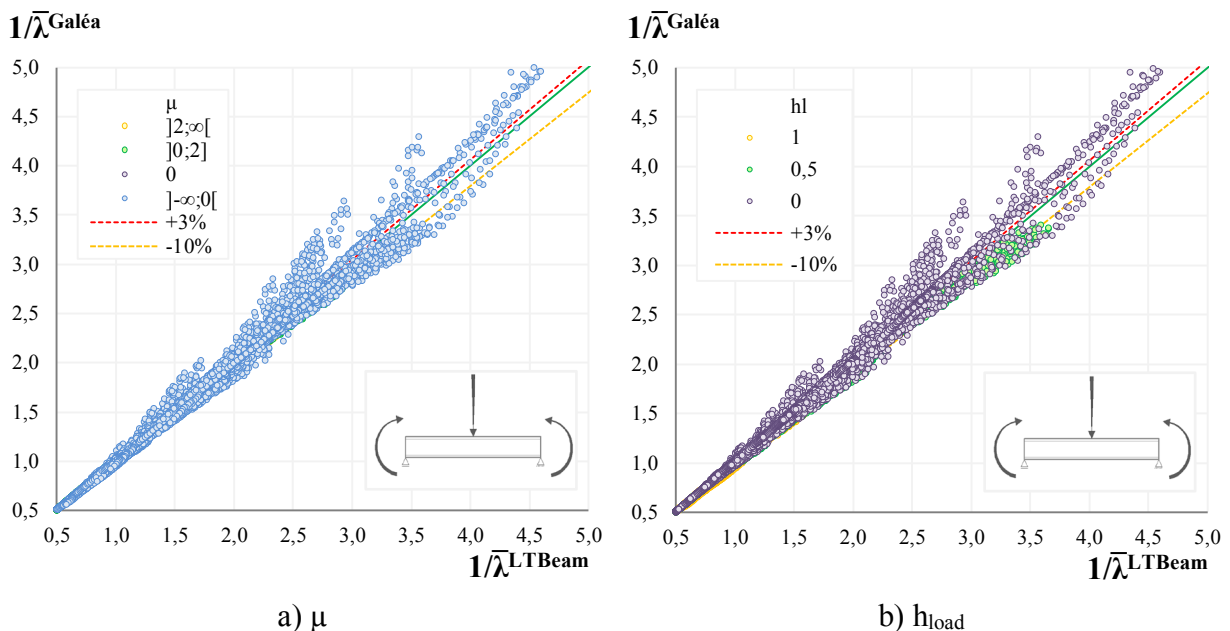


Figure 4.18 – Galéa – Case 8.

The C values obtain a CoV value of 4,640% with 8,1% of the results above the 3% unsafe mark and 1,9% of the result below the 10% conservative mark. With a maximum 55,8% above the LTBeam results and a minimum value 20,6% below. The unsafe and conservative tests, have essentially  $\mu$  as a member of  $]-\infty; 0[$ , as can be seen in blue in the figure a).

Table 4.22 – Galéa – Case 8.

Galéa		n	Mean	St. Dev.	CoV%	Min.	Max.	<0,9%	>1,03%
Case 7	Double Symmetric	31860	0,992	0,046	4,640	0,794	1,558	1,9	8,1

#### 4.4.4 Andrade et al.

In this solution all variables of all cases are analyzed here. As seen in Tables 3.3 and 3.4 this has only C values for cantilevers cases.

#### 4.4.4.1 Case 9

Figure 4.19 presents the graphical analysis of the Case 9 for double and mono symmetric cross sections and Table 4.23 presents a summary of the Table B.29. For double symmetric cross sections, see a), the C values obtain very good results, with a CoV value of 0,971% and has no unsafe tests or conservative tests.

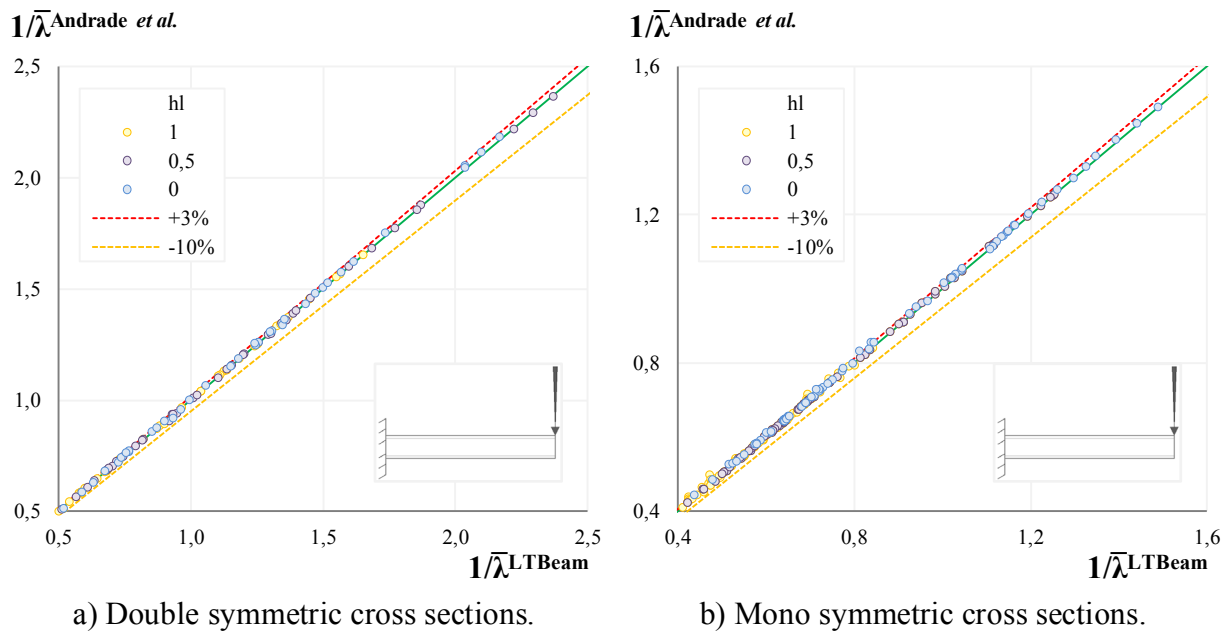


Figure 4.19 – Andrade *et al.* – Case 9.

For mono symmetric cross sections, the C values obtain a CoV of 1,49 with 6,9% of the results above the 3% unsafe mark with a maximum value 11,8% above the LTBeam results. In Table B.29 and Table B.30, it is possible to see that all of the unsafe tests are in sections with  $\psi_f$  near to the limits of its range, [-0,8;0,8] and with loads not applied at shear center.

Table 4.23 – Andrade *et al.* – Case 9.

	<b>Andrade <i>et al.</i></b>	<b>n</b>	<b>Mean</b>	<b>St. Dev.</b>	<b>CoV%</b>	<b>Min.</b>	<b>Max.</b>	<b>&lt;0,9%</b>	<b>&gt;1,03%</b>
<b>Case 9</b>	<b>Double Symmetric</b>	120	1,001	0,010	0,971	0,969	1,018	0,0	0,0
	<b>Mono Symmetric</b>	216	1,007	0,015	1,490	0,968	1,118	0,0	6,9

#### 4.4.4.2 Case 10

Figure 4.20 presents the graphical analysis of the Case 10 for double and mono symmetric cross sections and Table 4.24 presents a summary of the Table B.31. For double symmetric cross sections, see a), the C values obtain a CoV value of 1,091% and has no unsafe tests or conservative tests, which are very good results.

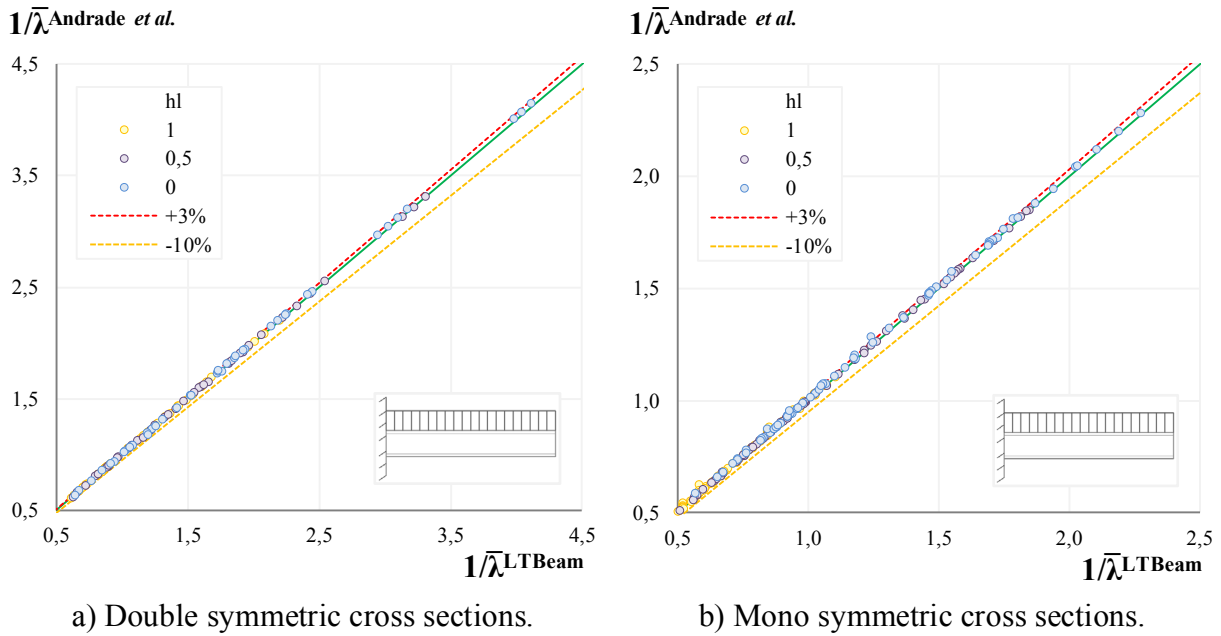


Figure 4.20 – Andrade *et al.* – Case 10.

For mono symmetric cross sections, see b), the C values obtain a CoV value of 1,670% with 7,9% of the results above the 3% unsafe mark with a maximum value 13,2% above the LTBeam results. In Table B.30 and Table B.31, it is possible to see that all of the unsafe tests are in sections with  $\psi_f$  near to the limits of its range, [-0,8;0,8] and with loads not applied at shear center, as in the previous case.

Table 4.24 – Andrade *et al.* – Case 10.

Andrade <i>et al.</i>		n	Mean	St. Dev.	CoV%	Min.	Max.	<0,9%	>1,03%
Case 10	Double Symmetric	120	1,003	0,011	1,091	0,963	1,018	0,0	0,0
	Mono Symmetric	216	1,009	0,017	1,670	0,974	1,132	0,0	7,9

#### 4.4.5 Lindner

In this solution all variable of all cases are analyzed here. As seen in Tables 3.3 and 3.4 this only has values for cantilevers cases. As it was said in section 3.2.5, the values are computed by 2 ways: the first one is the use of k values by direct linear interpolation between points of the charts, and the second one is the use of  $C_1$  values computed by the Eq. (31).

##### 4.4.5.1 Case 9

Figure 4.21 presents the graphical analysis of the Case 9 for double symmetric cross sections by the 2 calculation ways and Table 4.25 presents a summary of the Table B.33. As seen in

these tables and as would be expected, for the curves values of the solution charts both ways have the same results. However, since the Eq. (31) was obtained by a non-linear interpolation, the C<sub>1</sub> method has a slight improvement in values between the curves.

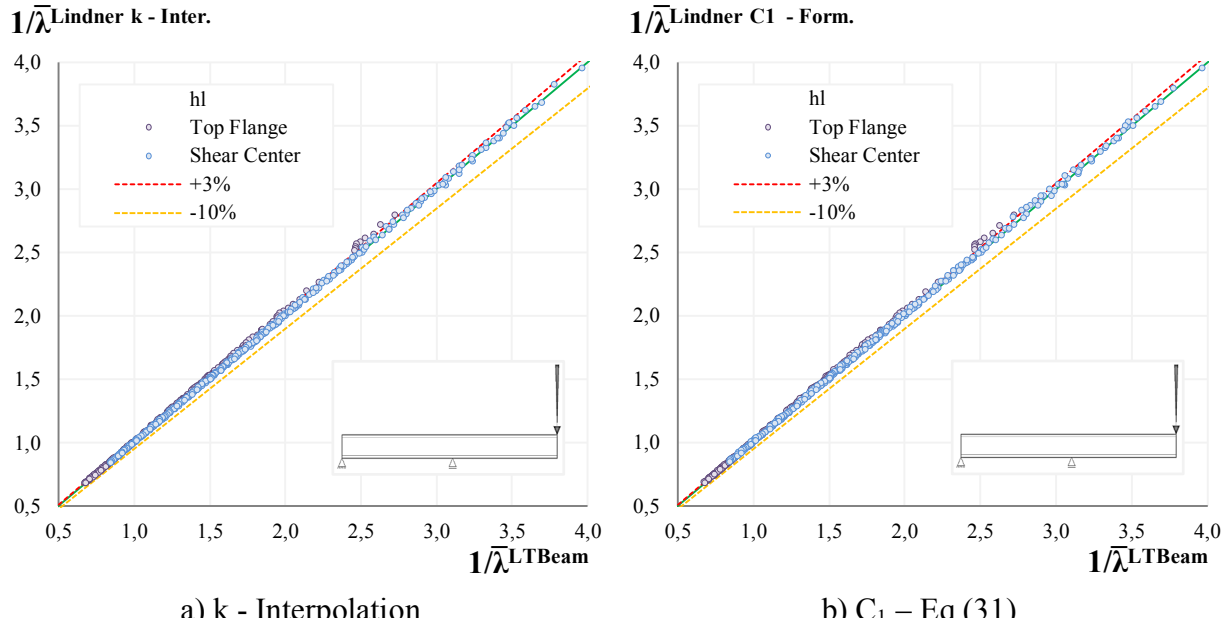


Figure 4.21 – Lindner – Case 9.

For the two calculation ways, the charts obtain a CoV value approximately of 1,6% with 14% of the results above the 3% unsafe mark and a maximum value 7% above the LTBeam results. Almost all of these unsafe results are based in values between curves for tests with the load applied at the top flange and in HEB profiles. Note that, the HEB profiles have less slenderness relatively to the IPE profiles.

Table 4.25 – Lindner – Case 9.

Lindner	n	Mean	St. Dev.	CoV%	Min.	Max.	<0,9%	>1,03%
Case 9	Interpolation	612	1,012	0,016	1,606	0,976	1,074	0,0
	Formula	612	1,012	0,017	1,656	0,975	1,077	0,0

#### 4.4.5.2 Case 10

Figure 4.22 presents the graphical analysis of the Case 10 for double symmetric sections by the 2 calculation ways and Table 4.26 presents a summary of the Table B.34. As can be easily seen in these tables, the results are very similar to the previous case. Note that in this case the differences between the calculation methods results are bigger. The Eq. (31) is more accurate for almost all values intervals between curves, thought for values between ]0,5;1[ the linear

interpolation is better. And in this case the profile and the  $h_l$  parameter have not a so evident influence in the unsafe tests numbers.

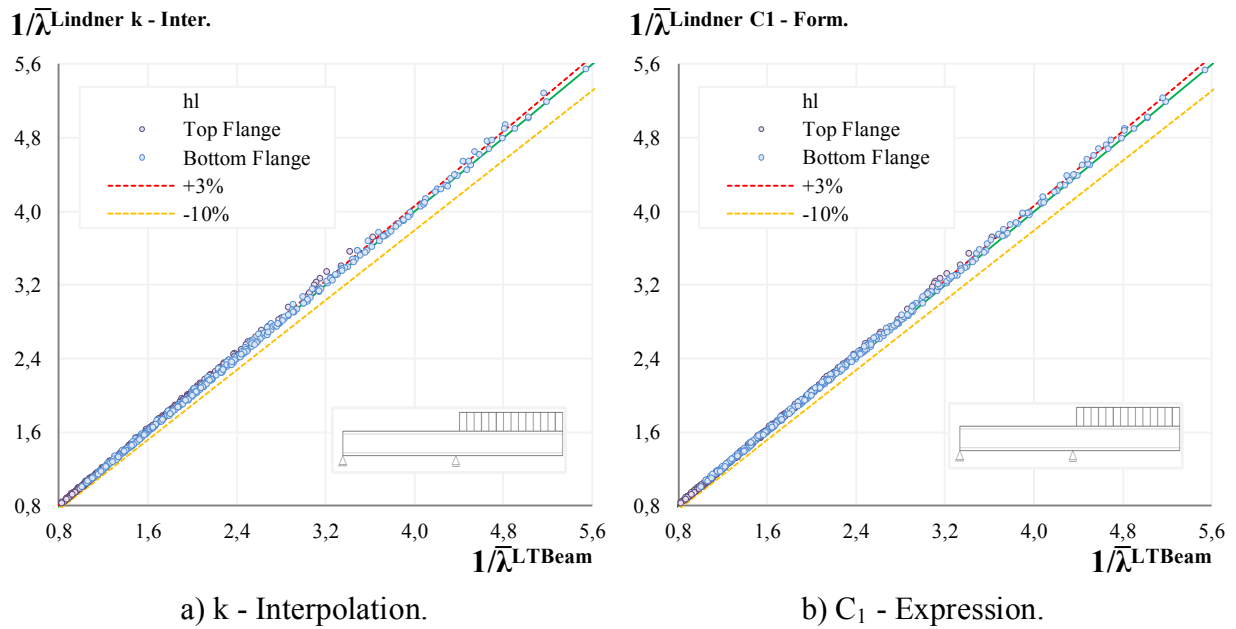


Figure 4.22 – Lindner – Case 10.

For the 2 calculation ways, the charts obtain a CoV value of 1,9% with 30% of the results above the 3% unsafe mark and a maximum value 8,5% above the LTBeam results.

Table 4.26 – Lindner – Case 10.

Andrade <i>et al.</i>		n	Mean	St. Dev.	CoV%	Min.	Max.	<0,9%	>1,03%
<b>Case 9</b>	<b>Interpolation</b>	612	1,016	0,020	1,970	0,985	1,089	0,0	24,0
	<b>Formula</b>	612	1,022	0,017	1,710	0,991	1,086	0,0	34,2

#### 4.4.5.3 Additional Case

As discussed in section 3.2.5 this case of an overhanging beam with a load moment at the tip, it is analyzed in order to make sure that this is the case with the inconsistent chart in the ECCS publication (ECCS, 2006), which can be easily concluded in Figure 4.23. Since this case is not considered by any solution, it is disregarded from the study.

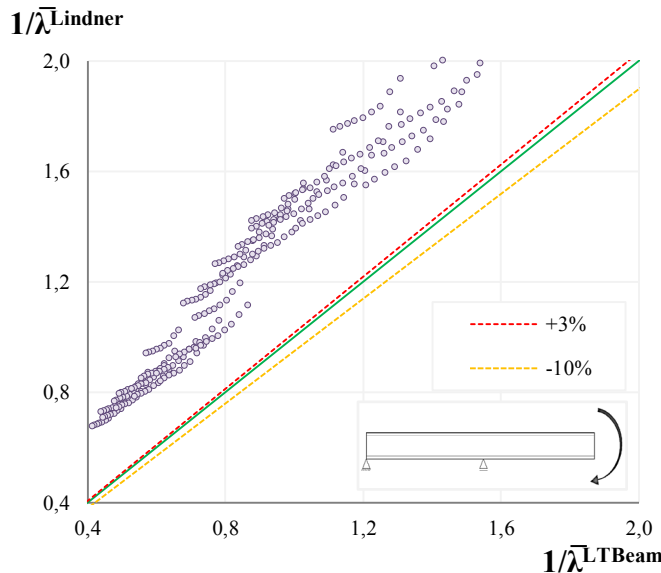


Figure 4.23 – Lindner – Additional case.

#### 4.4.6 Trahair

In this solution all variables (taking to account what was discussed in section 3.2.6) are analyzed here. As seen in Tables 3.3 and 3.4 this is the only one with all cases, however only for double symmetrical cross sections and with the limitations presented in these tables.

##### 4.4.6.1 Case 1 and 2

Figure 4.24 presents the graphical analysis of Case 1 and 2 for double symmetric cross sections and Tables 4.27 and 4.28 presents a summary of the Table B.35 both cases respectively. For Case 1, the expression obtain a CoV value of 3,412% and 6,2% of the results below the 10% conservative mark with a minimum value 12,5% below the LTBeam results.

Table 4.27 – Galéa – Case 1.

	Trahair	n	Mean	St. Dev.	CoV%	Min.	Max.	<0,9%	>1,03%
Case 1	Double Symmetric	820	0,963	0,033	3,412	0,875	1,015	6,2	0,0

As seen in Table B.35 and in blue in Figure 4.24 a), all the conservative results have  $\psi$  as a member of [-1;-0,5].

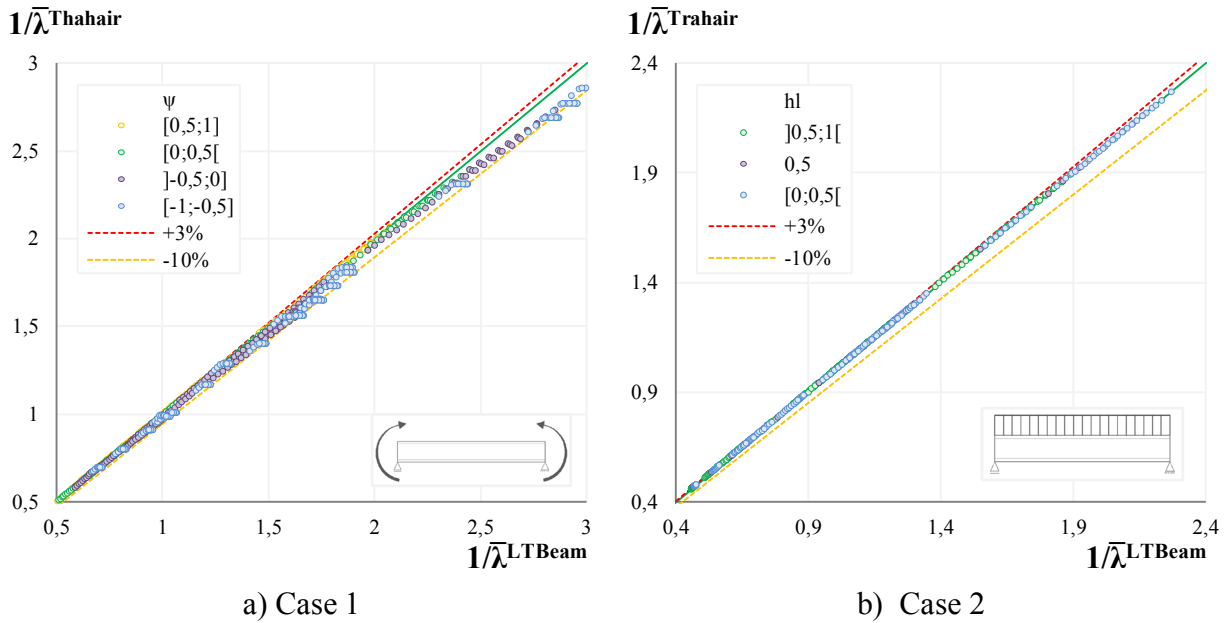


Figure 4.24 – Trahair – Case 1 and 2.

For Case 2, the formulations obtain a CoV value of 0,203% and has no unsafe tests or conservative tests, which are very good results.

Table 4.28 – Galéa – Case 2.

	Trahair	n	Mean	St. Dev.	CoV%	Min.	Max.	<0,9%	>1,03%
<b>Case 2</b>	<b>Double Symmetric</b>	420	1,000	0,002	0,203	0,995	1,003	0,0	0,0

#### 4.4.6.2 Case 3

For this case, the possibility to combine the variable  $d$  from the Table A.20 with the formulation of the Table A.22 is first analyzed, in order to take into account tests with the load not applied at the shear center and a nonzero value of the parameter  $d$ . As easily seen in Figure 4.25 a) and the Table B.37, this consideration obtains bad results, with too conservative results when the load is applied at the top flange and  $d$  as a member of  $[0,25;0,5[$ , in green in a), and too unconservative with the load applied at the bottom flange and  $d$  as a member of  $]0;0,5[$ , in blue in a). Note that,  $d$  is the distance between the mid-span and the load position along the beam, however, in order to use normalized values,  $d$ , is represented as the ratio between the real value of  $d$  and the total length of the beam in the analysis. In this sense, these combinations are disregarded from the analysis and the parameter  $h_l$  is only analyzed for loads applied at the mid-span of the beams.

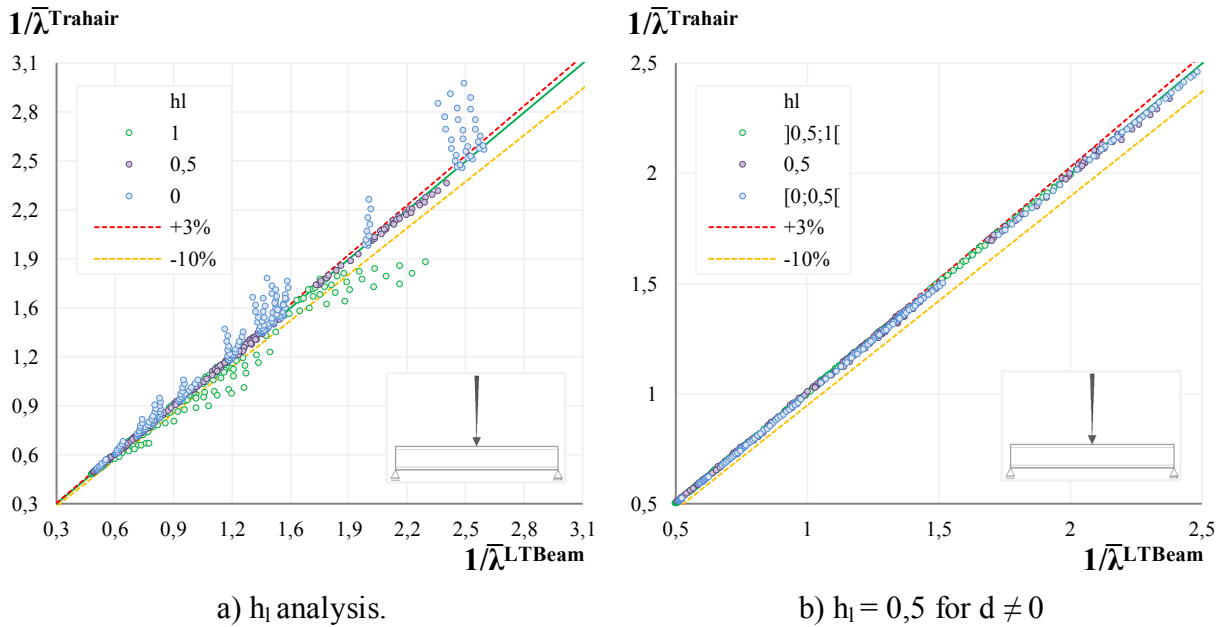


Figure 4.25 – Trahair – Case 3.

Thus, Figure 4.25 b) presents the graphical analysis of the Case 3 for double symmetric cross sections and Table 4.29 presents a summary of the Table B.35 for this case.

Table 4.29 – Trahair – Case 3.

	Trahair	n	Mean	St. Dev.	CoV%	Min.	Max.	<0,9%	>1,03%
<b>Case 3</b>	<b>Double Symmetric</b>	600	0,995	0,010	1,035	0,963	1,020	0,0	0,0

The formulations obtain a CoV value of 1,035% and has no unsafe tests or conservative tests, which are very good results.

#### 4.4.6.3 Case 4

A similar comparison between the parameter  $d$  and the parameter  $h_l$  is performed. As easily seen in Figure 4.26 a) and the Table B.37, these combinations obtain bad results. In this sense, they are disregarded from the analysis and the parameter  $h_l$  is only analyzed for loads applied at  $0,25L$  of the mid-span. Thus, Figure 4.26 b) presents the graphical analysis of the Case 4 for double symmetric cross sections and Table 4.30 presents a summary of the Table B.35 for this case.

Table 4.30 – Trahair – Case 4.

	Trahair	n	Mean	St. Dev.	CoV%	Min.	Max.	<0,9%	>1,03%
<b>Case 4</b>	<b>Double Symmetric</b>	580	1,044	0,013	1,269	1,003	1,068	0,0	87,6

The formulations obtains a CoV value of 1,269% and 87,2% of the results above the 3% unsafe mark, however, with a maximum value only 6,8% above the LTBeam results. Note that, there is not an influential variable to the worst results.

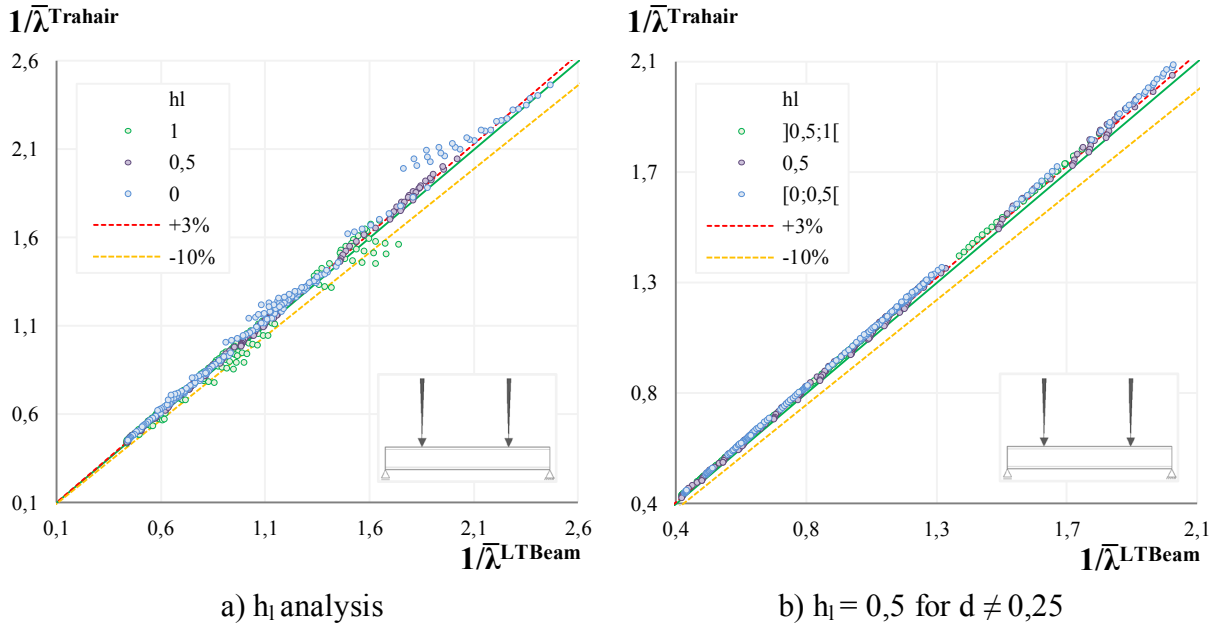


Figure 4.26 – Trahair – Case 4.

#### 4.4.6.4 Case 5

For this case the application of the formulation of the Table A.22 is also analyzed and the results of that are presented in Figure 4.27 a) and in Table B.37.

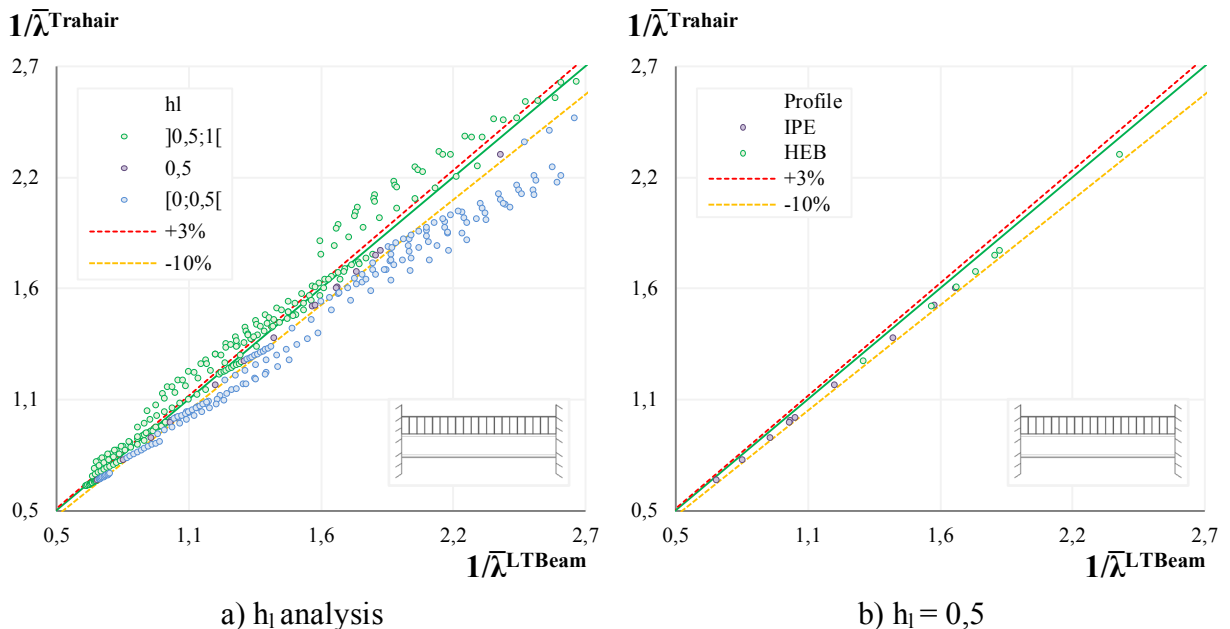


Figure 4.27 – Trahair – Case 5.

As possible to see in a), the results are too conservatives when the load is applied at the bottom part of the cross section (blue), and they are too unconservative when the load is applied at top part (green). In this sense, this formulation is disregarded and all tests have the loads applied at the shear center. Thus, Figure 4.27 b) presents the graphical analysis of the Case 5 for double symmetric cross sections and Table 4.31 presents a summary of the Table B.36 for this case.

Table 4.31 – Trahair – Case 5.

	Trahair	n	Mean	St. Dev.	CoV%	Min.	Max.	<0,9%	>1,03%
<b>Case 5</b>	<b>Double Symmetric</b>	20	0,931	0,003	0,367	0,927	0,938	0,0	0,0

The formulations obtain a CoV value of 0,367% and has no unsafe tests or conservative tests, which are very good results.

#### 4.4.6.5 Case 6

A similar analysis is performed for this case, testing the formulation of the Table A.22. The results are presented in the Figure 4.28 a) and in Table B.37. As can be seen in a), the results are too conservatives when the load is applied at the bottom part of the cross section (blue), and they are too unconservative when the load is applied at top part (green). In this sense, this formulation is disregarded and all tests have the loads applied at the shear center.

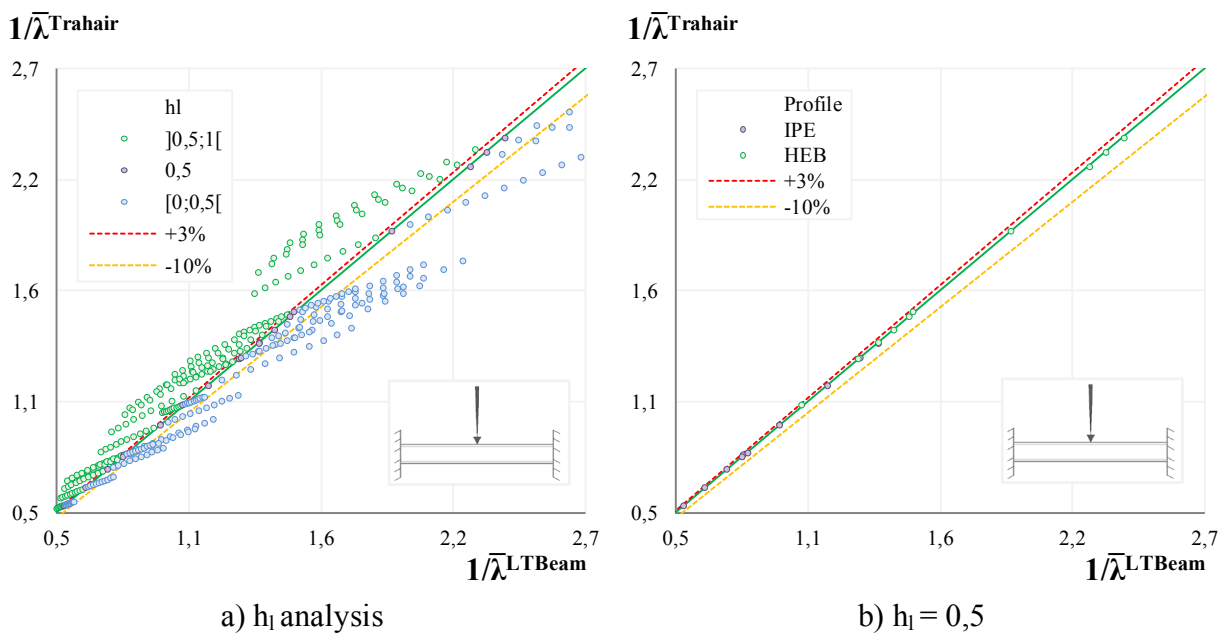


Figure 4.28 – Trahair – Case 6.

Thus, Figure 4.28 b) presents the graphical analysis of the Case 6 for double symmetric cross sections and Table 4.32 presents a summary of the Table B.36 for this case.

Table 4.32 – Trahair – Case 6.

Trahair		n	Mean	St. Dev.	CoV%	Min.	Max.	<0,9%	>1,03%
Case 6	Double Symmetric	20	0,999	0,007	0,736	0,991	1,014	0,0	0,0

The formulations obtain a CoV value of 0,736% and has no unsafe tests or conservative tests, which are very good results.

#### 4.4.6.6 Case 7

As in the previous cases, the formulation of the Table A.22 is firstly analyzed. As possible to see in Figure 4.29 a), this formula has bad results in this case. Thus, it is disregarded from the case analysis. Figure 4.29 b) presents the graphical analysis of the Case 7 for double symmetric cross sections and Table 4.33 presents a summary of the Table B.38 for this case.

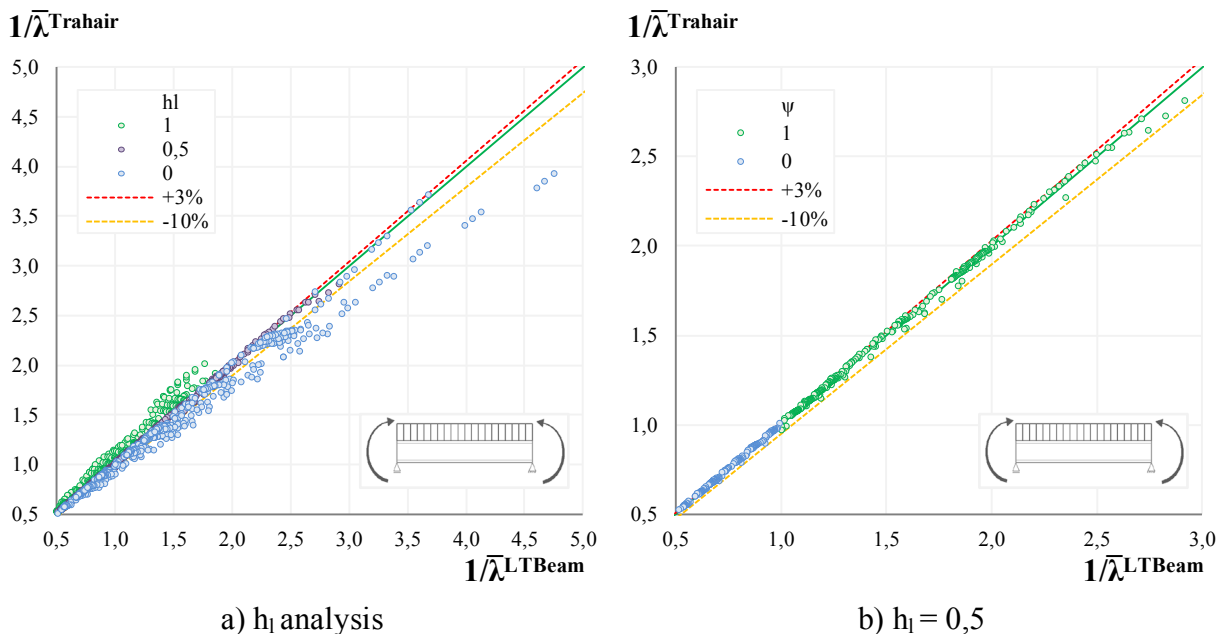


Figure 4.29 – Trahair – Case 7.

The formulation obtains a CoV value of 1,561% and only 0,7% of the results above the 3% unsafe mark with a maximum value 3,5% above the LTBeam results, which are good results.

Table 4.33 – Trahair – Case 7.

Trahair		n	Mean	St. Dev.	CoV%	Min.	Max.	<0,9%	>1,03%
Case 7	Double Symmetric	700	1,000	0,016	1,561	0,927	1,035	0,0	0,7

#### 4.4.6.7 Case 8

The formulation of the Table A.22 is firstly analyzed in this case, and as can be easily seen in Figure 4.30 a), this formula has bad results in this case. Thus, it is disregarded from the case analysis.

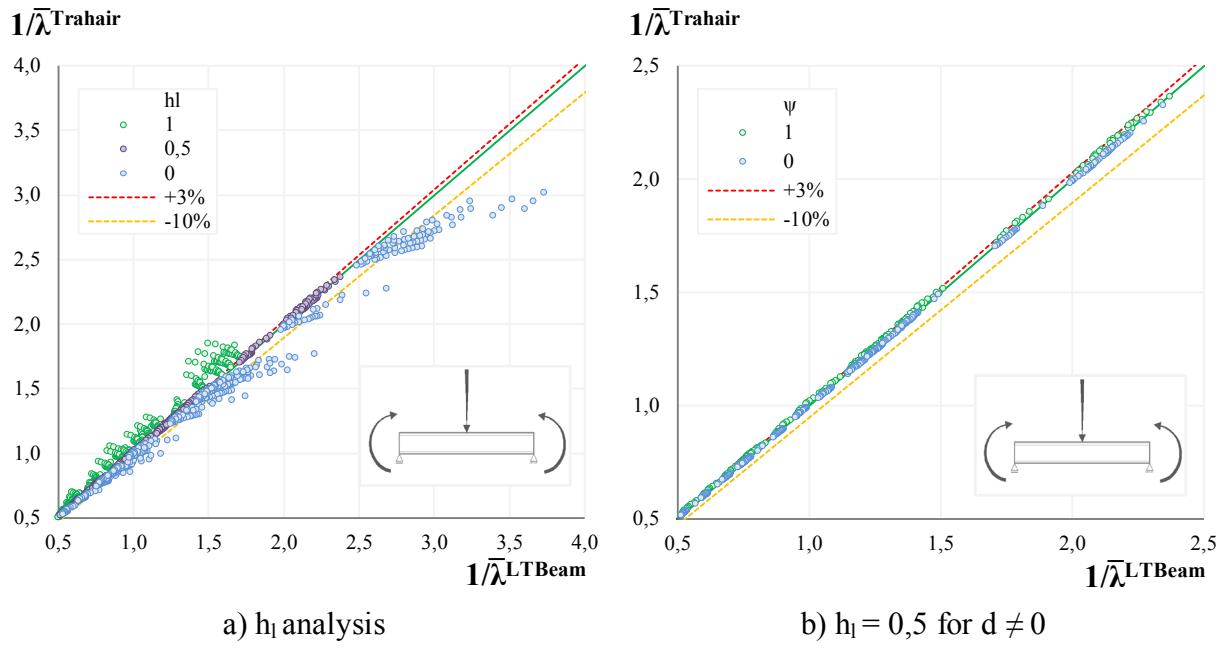


Figure 4.30 – Trahair – Case 8.

Figure 4.34 b) presents the graphical analysis of the Case 8 for double symmetric cross sections and Table 4.34 presents a summary of the Table B.38 for this case.

Table 4.34 – Trahair – Case 8.

	Trahair	n	Mean	St. Dev.	CoV%	Min.	Max.	<0,9%	>1,03%
<b>Case 8</b>	<b>Double Symmetric</b>	520	1,000	0,014	1,431	0,981	1,036	0,0	3,5

The solution obtains a CoV value of 1,431% and 3,5% of the results above the 3% unsafe mark with a maximum value 3,6% above the LTBeam results, which are good results.

#### 4.4.6.8 Case 9

Figure 4.31 presents the graphical analysis of the Case 9 for double symmetric cross sections and Table 4.35 presents a summary of the Table B.39 for this case. The formulations obtains a CoV value of 6,814% and 40% of the results above the 3% unsafe mark with a maximum value 33,8% above the LTBeam results.

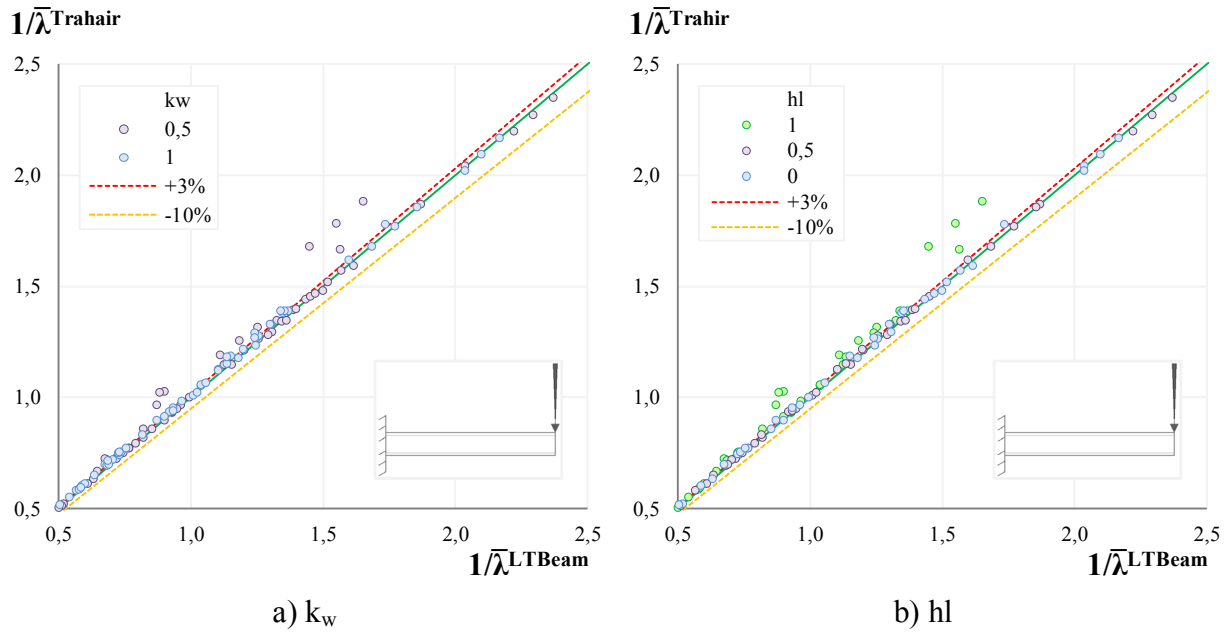


Figure 4.31 – Trahair – Case 9.

The worst unsafe results, as easily seen in Figure 4.35 (in purple in a), and in the Table.35 are tests with the load applied at the top flange and the rotation about z restricted,  $k_z=0,5$ .

Table 4.35 – Trahair – Case 9.

Trahair		n	Mean	St. Dev.	CoV%	Min.	Max.	<0,9%	>1,03%
Case 9	Double Symmetric	120	1,039	0,071	6,814	0,966	1,338	0,0	40,0

#### 4.4.6.9 Case 10

Figure 4.32 presents the graphical analysis of the Case 10 for double symmetric cross sections and Table 4.36 presents a summary of the Table B.39 for this case. The formulations obtain a CoV value of 7,637% with 11,7% of the results above the 3% unsafe mark 10,0% below the 10% conservative mark. The maximum value is 22,3% the LTBeam results and the minimum value is 15% below the LTBeam results.

Table 4.36 – Trahair – Case 10.

Trahair		n	Mean	St. Dev.	CoV%	Min.	Max.	<0,9%	>1,03%
Case 10	Double Symmetric	120	0,964	0,074	7,637	0,850	1,223	10,0	11,7

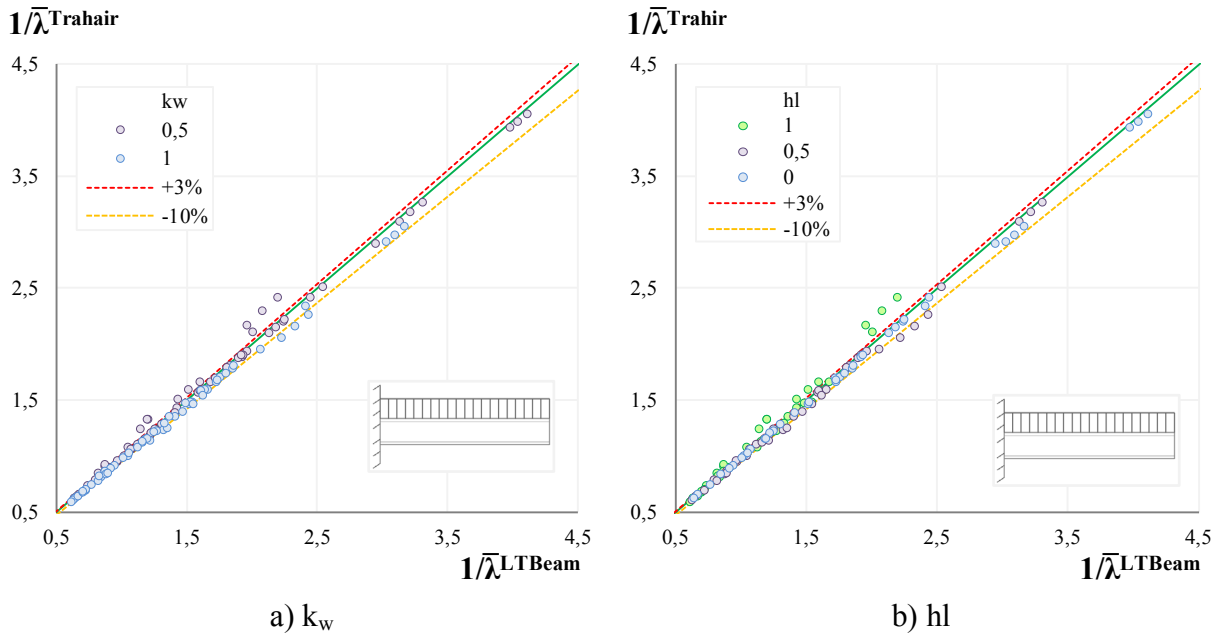


Figure 4.32 – Trahair – Case 10.

All unsafe tests have the load applied at the top flange, in green in b), and with  $k_z=0,5$ , in purple in a). On the other hand, all conservative tests have the load applied at the shear center, in purple in b), and with  $k_z=1$ , in blue in a)

#### 4.4.7 Serna et al.

In this solution all variables (taking to account what was discussed in section 3.2.7) are analyzed here. As seen in Tables 3.3 and 3.4, this only has not C values for Case 8.

##### 4.4.7.1 Case 1 and 2

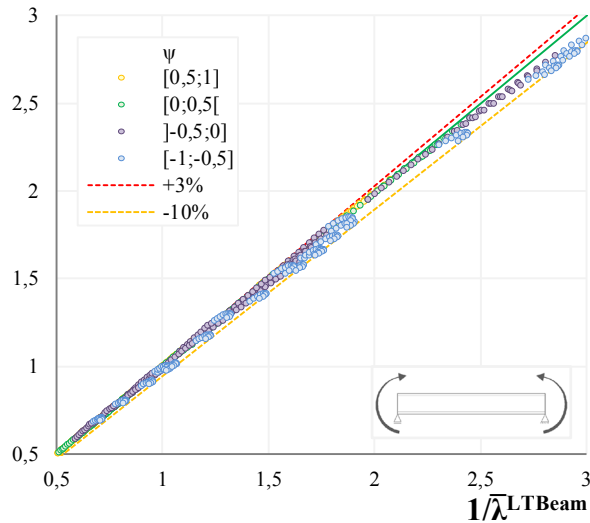
Figure 4.33 presents the graphical analysis of Case 1 and 2 for double symmetric cross sections and Tables 4.37 and 4.38 present a summary of the Table B.40 for both cases respectively. For Case 1, the C values obtain a CoV value of 3,203% and 3,8% of the results below the 10% conservative mark with a minimum value 11% below the 10% conservative mark which are good results.

Table 4.37 – Serna et al. – Case 1.

Serna et al.		n	Mean	St. Dev.	CoV%	Min.	Max.	<0,9%	>1,03%
Case 1	Double Symmetric	820	0,973	0,031	3,203	0,890	1,026	3,8	0,0

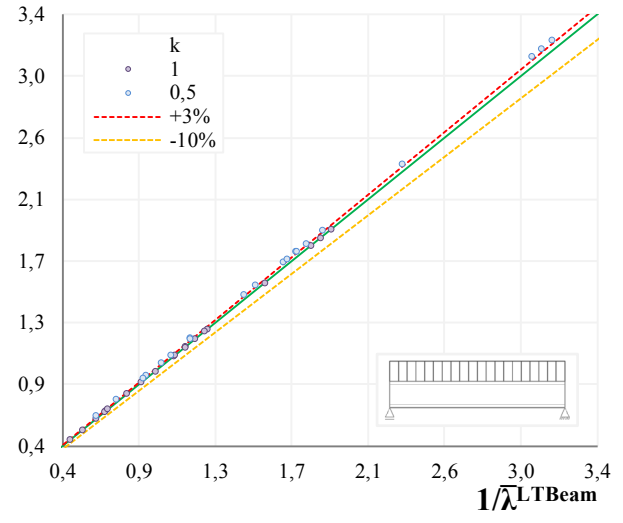
This low number of conservative tests have the  $\psi$  as a member of [-1;-0,5], as seen in blue in Figure 4.33 a) and in Table B.40.

$1/\bar{\lambda}_{\text{Serna et al.}}$



a) Case 1

$1/\bar{\lambda}_{\text{Serna et al.}}$



b) Case 2

Figure 4.33 – Serna *et al.* – Case 1 and 2.

For Case 2, the C values obtain a CoV value of 2,585% and 50% of the results above the 3% unsafe mark with a maximum value 5,6% above the LTBeam results.

Table 4.38 – Serna *et al.* – Case 2.

Serna <i>et al.</i>	n	Mean	St. Dev.	CoV%	Min.	Max.	<0,9%	>1,03%
Case 2    Double Symmetric	40	1,020	0,026	2,585	0,993	1,056	0,0	50,0

The unsafe testes have  $k_w=k_z=0,5$ , as it is possible to see in blue in Figure 4.33 b) and in Table B.40.

#### 4.4.7.2 Case 3 and 4

Figure 4.34 presents the graphical analysis of Case 3 and 4 for double symmetric cross sections and Table 4.39 and 4.40 presents a summary of the Table B.40 both cases respectively. For Case 3, the C values obtain a CoV value of 3,326% and 9,1% of the results above the 3% unsafe mark with a maximum value 5,5% above the LTBeam results.

Table 4.39 – Serna *et al.* – Case 3.

Serna <i>et al.</i>	n	Mean	St. Dev.	CoV%	Min.	Max.	<0,9%	>1,03%
Case 3    Double Symmetric	220	0,988	0,033	3,326	0,915	1,055	0,0	9,1

All the unsafe tests have  $k_w=k_z=1$  and  $d$  as a member of  $]0;0,25]$  as is possible to see in purple in Figure 4.34 a) and in Table B.40.

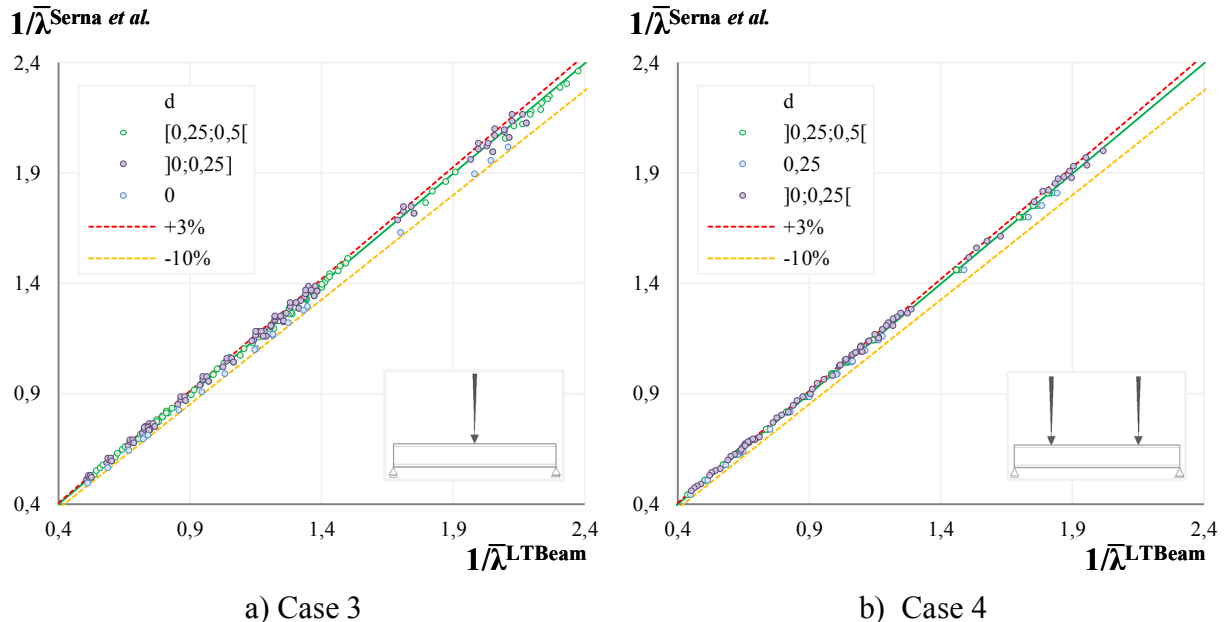


Figure 4.34 – Serna *et al.* – Case 3 and 4.

For Case 4, the C values obtain a CoV value of 2,378% and 14% of the results above the 3% unsafe mark with a maximum value 5,3% above the LTBeam results.

Table 4.40 – Serna *et al.* – Case 4.

Serna <i>et al.</i>		n	Mean	St. Dev.	CoV%	Min.	Max.	<0,9%	>1,03%
Case 4	Double Symmetric	200	1,002	0,024	2,378	0,962	1,053	0,0	14,0

Almost all of the unsafe tests have  $k_w=k_z=0,5$  and  $d$  as a member of  $]0;0,25[$  as it is possible to see in purple in Figure 4.34 b) and in Table B.40.

#### 4.4.7.3 Case 5 and 6

Figure 4.35 presents the graphical analysis of Case 5 and 6 for double symmetric cross sections and Table 4.41 and 4.42 presents a summary of the Table B.41 for both cases respectively. For Case 5, the C values obtain a CoV value of 2,759% and has no unsafe tests or conservative tests, which are very good results.

Table 4.41 – Serna *et al.* – Case 5.

Serna <i>et al.</i>		n	Mean	St. Dev.	CoV%	Min.	Max.	<0,9%	>1,03%
Case 5	Double Symmetric	40	0,940	0,026	2,759	0,918	1,024	0,0	0,0

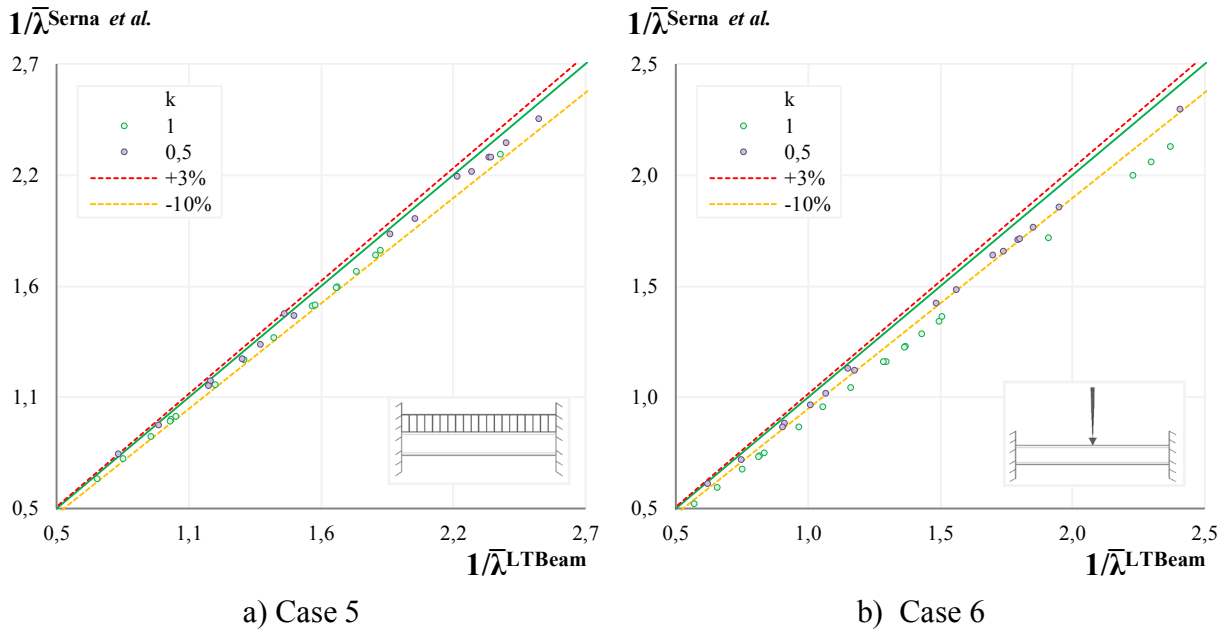


Figure 4.35 – Serna *et al.* – Case 5 and 6.

For Case 6, the C values obtain a CoV value of 6,579% and 50% of the results below the 10% conservative mark with a minimum value 19,9% below the LTBeam results. All the conservative tests have  $k_w=k_z=1$ , as easily seen in green in Figure 4.35 b) and in Table B.41.

Table 4.42 – Serna *et al.* – Case 6.

Serna <i>et al.</i>		n	Mean	St. Dev.	CoV%	Min.	Max.	<0,9%	>1,03%
<b>Case 5</b>	<b>Double Symmetric</b>	40	0,861	0,057	6,579	0,801	0,965	50,0	0,0

#### 4.4.7.4 Case 7

Figure 4.36 presents the graphical analysis of the Case 7 for double symmetric cross sections and Table 4.43 presents a summary of the Table B.42 for this case. The C values obtain a CoV value of 5,366% with 8% of the results below the 10% conservative mark and 0,8% of the results above the 3% unsafe mark. The minimum value is 33,4% below the LTBeam results and the maximum value is 4,7% above the LTBeam results. All conservative tests as  $\mu$  as a member of [-2;0] as seen in blue in a), and all unsafe tests has  $\psi$  as a member of [-1;0[.

Table 4.43 – Serna *et al.* – Case 7.

	Trahair	n	Mean	St. Dev.	CoV%	Min.	Max.	<0,9%	>1,03%
Case 7	Double Symmetric	10620	0,979	0,053	5,366	0,666	1,047	8,0	0,8

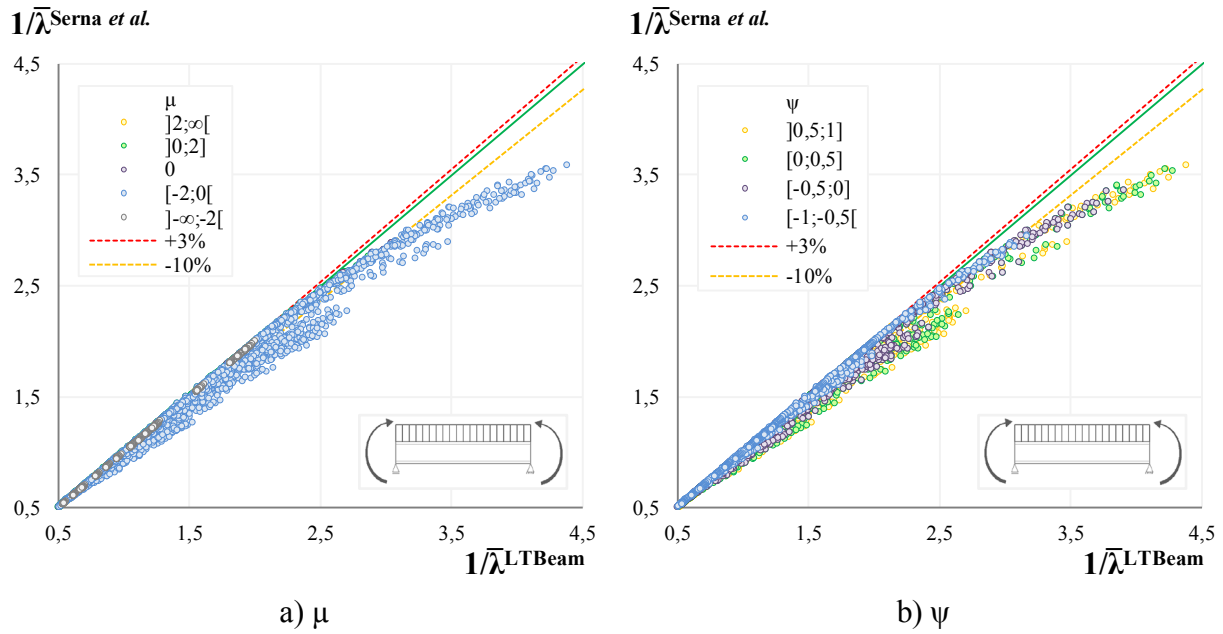


Figure 4.36 – Serna *et al.* – Case 7.

#### 4.4.7.5 Case 8

Figure 4.37 presents the graphical analysis of the Case 8 for double symmetric cross sections and Table 4.44 presents a summary of the Table B.42 for this case.

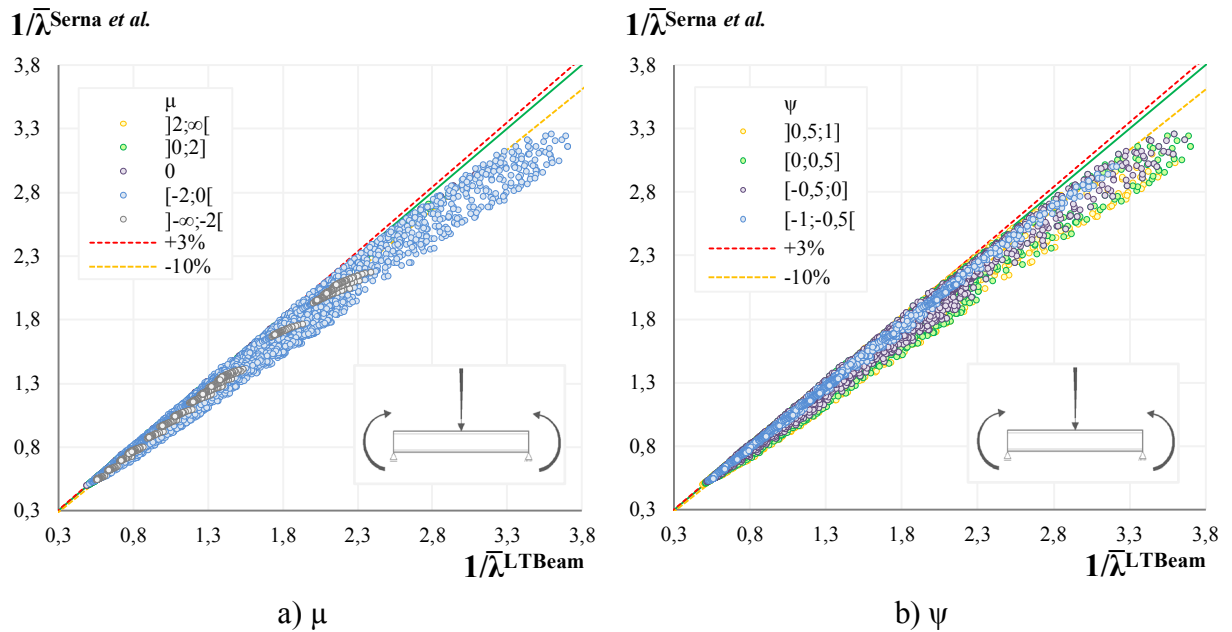


Figure 4.37 – Serna *et al.* – Case 8.

The C values obtain a CoV value of 6,365% with 21,7% of the results below the 10% conservative mark and 0,1% of the results above the 3% unsafe mark. The minimum value is 30,9% below the LTBeam results and the maximum value is 4,2% above the LTBeam results. All conservative tests as  $\mu$  as a member of  $[-\infty; 0]$  as seen in blue and grey in a).

Table 4.44 – Serna *et al.* – Case 8.

	Trahair	n	Mean	St. Dev.	CoV%	Min.	Max.	<0,9%	>1,03%
<b>Case 8</b>	<b>Double Symmetric</b>	10620	0,922	0,059	6,365	0,691	1,042	21,7	0,1

## 4.5 Comparison

As easily seen in Tables 3.3 and 3.4, since all solution present values for different possible conditions and have distinct limitations among them, it is impossible to say directly which solution is better or worst. However, it is possible to compare for each case the variables ranges that are common to all solutions or sets of solution.

### 4.5.1 Case 1

For Case 1, the comparable variables and solutions involved are described in Table 4.45. As seen, two different comparisons can be made.

Table 4.45 – Comparisons – Case 1.

	Case 1	Serna <i>et al.</i>	
		Trahair	Galéa
ECCS		ECCS	ECCS
Baláž & Koleková		Baláž & Koleková	Baláž & Koleková
$k_w$		1	1
$k_z$		{0,5; 1}	1
$\psi_f$		[-0,9;0,9]	0
$\psi$		[-1;1]	[-1;1]
		Comparison 1	Comparison 2

- **Comparison 1**

A summary of the statistical analysis to the comparison 1, for double and mono symmetric cross sections between Baláž and Koleková and ECCS is given in Table 4.46. For double symmetric cross sections, Baláž and Koleková obtain better results with no unsafe and conservative tests.

Table 4.46 – Comparison 1.

Comparison 1		n	Mean	St. Dev.	CoV%	Min.	Max.	<0,9%	>1,03%
<b>Double Symmetric</b>	Baláž & Koleková	1640	0,988	0,017	1,728	0,944	1,009	0,0	0,0
	ECCS	1640	0,934	0,032	3,445	0,865	1,032	16,2	0,1
<b>Mono Symmetric</b>	Baláž & Koleková	3608	1,014	0,069	6,832	0,791	1,467	2,9	23,4
	ECCS	3608	0,957	0,079	8,214	0,752	1,381	17,8	10,0

Relatively to mono symmetric cross sections both solutions present bad results, with Baláž and Koleková with a lower CoV value and lower conservative results. However, as already seen, these bad results can be opposed by a bigger limitation on the  $\psi_f$  parameter, or possibly creating more  $C_3$  values for smaller ranges of  $\psi_f$ .

#### • Comparison 2

A summary of the statistical analysis to the comparison 2, for double symmetric cross sections between Baláž and Koleková, ECCS, Galéa, Trahair and Serna *et al.* is given in Table 4.47.

Table 4.47 – Comparison 2.

Comparison 2		n	Mean	St. Dev.	CoV%	Min.	Max.	<0,9%	>1,03%
<b>Double Symmetric</b>	Baláž & Koleková	820	0,997	0,010	1,044	0,960	1,009	0,0	0,0
	ECCS	820	0,937	0,030	3,217	0,865	1,004	13,2	0,0
	Galéa	820	0,973	0,029	3,032	0,898	1,001	0,6	0,0
	Trahair	820	0,963	0,033	3,412	0,875	1,015	6,2	0,0
	Serna <i>et al.</i>	820	0,973	0,031	3,203	0,890	1,026	3,8	0,0

As possible to see, Baláž and Koleková obtain better results with lower CoV value and no unsafe and conservative tests.

#### 4.5.2 Case 2

For Case 2, the comparable variables and solutions involved are described in Table 4.48. As seen, four different comparisons can be made.

Table 4.48 – Comparisons – Case 2.

Case 2	Baláž & Koleková	Trahair		Serna <i>et al.</i>		Serna <i>et al.</i>	
		ECCS	ECCS	ECCS	ECCS	Trahair	Galéa
	$k_w$	1	1			{0,5; 1}	1
	$k_z$	{0,5; 1}	1			{0,5; 1}	1
	$\psi_f$	[-0,9; 0,9]	0			0	0
	$z_g$	100%	100%			0	0
		Comparison 3	Comparison 4	Comparison 5	Comparison 6		

### • Comparison 3

A summary of the statistical analysis to the comparison 3, for double and mono symmetric cross sections between Baláž and Koleková and ECCS is given in Table 4.49.

Table 4.49 – Comparison 3.

Comparison 3		n	Mean	St. Dev.	CoV%	Min.	Max.	<0,9%	>1,03%
Double Symmetric	Baláž & Koleková	840	0,999	0,011	1,116	0,972	1,044	0,0	1,8
	ECCS	840	0,993	0,015	1,486	0,949	1,031	0,0	0,2
Mono Symmetric	Baláž & Koleková	1848	1,002	0,017	1,688	0,962	1,116	0,0	5,7
	ECCS	1848	0,996	0,028	2,780	0,935	1,122	0,0	11,1

For double symmetric cross sections, Baláž and Koleková obtain better CoV value, and ECCS obtains lower number of unsafe results. However, the maximum value of Baláž and Koleková is 4,4% the LTBeam results and the maximum value of ECCS is 3,1%, which means that there is not a big difference between them. For mono symmetric cross section, Baláž and Koleková obtain better results, with a lower CoV value and lower unsafe results.

### • Comparison 4

A summary of the statistical analysis to the comparison 4, for double and mono symmetric cross sections between Baláž and Koleková, ECCS, Galéa and Trahair is given in Table 4.50.

Table 4.50 – Comparison 4.

Comparison 4		n	Mean	St. Dev.	CoV%	Min.	Max.	<0,9%	>1,03%
Double Symmetric	Baláž & Koleková	420	1,000	0,001	0,083	0,998	1,002	0,0	0,0
	ECCS	420	0,991	0,003	0,253	0,984	0,996	0,0	0,0
	Galéa	420	0,997	0,002	0,161	0,993	1,000	0,0	0,0
	Trahair	420	1,000	0,002	0,203	0,995	1,003	0,0	0,0

All solutions obtain very good results with very low CoV values and no unsafe or conservative tests. Note that Baláž and Koleková present the lowest CoV value.

### • Comparison 5

A summary of the statistical analysis to the comparison 5, for double symmetric cross sections between Baláž and Koleková and Serna *et al.* is given in Table 4.51.

Table 4.51 – Comparison 5.

Comparison 5		n	Mean	St. Dev.	CoV%	Min.	Max.	<0,9%	>1,03%
Double Symmetric	Baláž & Koleková	40	0,998	0,003	0,331	0,990	1,000	0,0	0,0
	Serna <i>et al.</i>	40	1,020	0,026	2,585	0,993	1,056	0,0	50,0

As possible to see, Baláž and Koleková obtain better results with lower CoV value and no unsafe and conservative tests.

- **Comparison 6**

A summary of the statistical analysis to the comparison 6, for double symmetric cross sections between Baláž and Koleková, ECCS, Galéa, Trahair and Serna *et al.* is given in Table 4.52.

Table 4.52 – Comparison 6.

Comparison 6	n	Mean	St. Dev.	CoV%	Min.	Max.	<0,9%	>1,03%
Double Symmetric	Baláž & Koleková	20	1,000	0,001	0,050	0,999	1,000	0,0
	ECCS	20	0,991	0,001	0,134	0,990	0,994	0,0
	Galéa	20	0,997	0,001	0,134	0,996	1,000	0,0
	Trahair	20	1,000	0,001	0,134	0,998	1,002	0,0
	Serna <i>et al.</i>	20	0,994	0,001	0,134	0,993	0,997	0,0

All solutions obtain very good results, with very low CoV values, and no unsafe or conservative tests. Note that, Baláž and Koleková present perfect results, with the values almost equal to the LTBeam results.

#### 4.5.3 Case 3

For Case 3, the comparable variables and solutions involved are described in Table 4.53. As seen, five different comparisons can be made.

Table 4.53 – Comparisons – Case 3.

Case 3	ECCS	Baláž & Koleková	Trahair	Galéa	Serna <i>et al.</i>	ECCS	Baláž & Koleková	Trahair	Galéa	Serna <i>et al.</i>	Trahair
	k <sub>w</sub>	1	1		{0,5; 1}		1		1		1
	k <sub>z</sub>	{0,5; 1}		1				1			1
	ψ <sub>f</sub>	[-0,9; 0,9]		0		0		0		0	
	z <sub>g</sub>	100%		100%		0		0		0	
		Comparison 7	Comparison 8	Comparison 9	Comparison 10	Comparison 11					

- **Comparison 7**

A summary of the statistical analysis to the comparison 7, for double and mono symmetric cross sections between Baláž and Koleková and ECCS is given in Table 4.54. For double symmetric cross sections, both solutionss present very good results with no unsafe or conservative tests. Note that Baláž and Koleková obtain better CoV value of 0,596%.

Table 4.54 – Comparison 7.

Comparison 7		n	Mean	St. Dev.	CoV%	Min.	Max.	<0,9%	>1,03%
<b>Double Symmetric</b>	Baláž & Koleková	840	0,997	0,006	0,596	0,984	1,008	0,0	0,0
	ECCS	840	0,990	0,018	1,770	0,931	1,017	0,0	0,0
<b>Mono Symmetric</b>	Baláž & Koleková	1848	1,008	0,026	2,554	0,961	1,108	0,0	16,8
	ECCS	1848	1,000	0,030	2,997	0,925	1,138	0,0	13,7

Relatively to mono symmetric cross sections both solutions presents unsafe results, with Baláž and Koleková with a lower CoV value and ECCS with lower unsafe results. However, as already seen, these bad results can be opposed by a bigger limitation on the  $\psi_f$  parameter, or possibly creating more  $C_3$  values for smaller ranges of  $\psi_f$ .

#### • Comparison 8

A summary of the statistical analysis to the comparison 8, for double symmetric cross sections between Baláž and Koleková, ECCS, Galéa and Trahair is given in Table 4.55.

Table 4.55 – Comparison 8.

Comparison 8		n	Mean	St. Dev.	CoV%	Min.	Max.	<0,9%	>1,03%
<b>Double Symmetric</b>	Baláž & Koleková	420	1,000	0,004	0,413	0,993	1,008	0,0	0,0
	ECCS	420	0,995	0,009	0,862	0,972	1,017	0,0	0,0
	Galéa	420	0,994	0,020	2,014	0,943	1,045	0,0	4,0
	Trahair	420	0,995	0,008	0,817	0,980	1,010	0,0	0,0

All solutions obtain very good results, with very low CoV values, and only Galéa obtains unsafe results. Note that Baláž and Koleková present the lowest CoV value.

#### • Comparison 9

A summary of the statistical analysis to the comparison 9, for double symmetric cross sections between Baláž and Koleková and Serna *et al.* is given in Table 4.56.

Table 4.56 – Comparison 9.

Comparison 9		n	Mean	St. Dev.	CoV%	Min.	Max.	<0,9%	>1,03%
<b>Double Symmetric</b>	Baláž & Koleková	40	0,998	0,004	0,419	0,987	1,001	0,0	0,0
	Serna <i>et al.</i>	40	0,944	0,026	2,765	0,915	0,983	0,0	0,0

Both solutions obtain very good results. Baláž and Koleková obtain the lowest CoV value of 0,419%.

#### • Comparison 10

Table 4.57 gives a summary of the statistical analysis to the comparison 10, for double symmetric cross sections between Baláž and Koleková, ECCS, Galéa, Trahair and Serna *et al.*

Table 4.57 – Comparison 10.

Comparison 9		n	Mean	St. Dev.	CoV%	Min.	Max.	<0,9%	>1,03%
Double Symmetric	Baláž & Koleková	20	0,999	0,001	0,130	0,997	1,000	0,0	0,0
	ECCS	20	0,994	0,003	0,346	0,991	1,001	0,0	0,0
	Galéa	20	0,993	0,003	0,346	0,989	0,999	0,0	0,0
	Trahair	20	0,994	0,003	0,346	0,991	1,001	0,0	0,0
	Serna et al.	20	0,919	0,003	0,346	0,915	0,925	0,0	0,0

All solutions obtain very good results with very lower CoV values and no unsafe or conservative tests. Note that Baláž and Koleková present the lowest CoV value.

#### • Comparison 11

A summary of the statistical analysis to the comparison 11, for double symmetric cross sections between Trahair and Serna *et al.* is given in Table 4.58.

Table 4.58 – Comparison 11.

Comparison 11		n	Mean	St. Dev.	CoV%	Min.	Max.	<0,9%	>1,03%
Double Symmetric	Trahair	200	0,996	0,013	1,351	0,963	1,020	0,0	0,0
	Serna <i>et al.</i>	200	0,990	0,034	3,422	0,915	1,055	0,0	10,0

As possible to see, Trahair obtain better results with lower CoV value and no conservative tests.

#### 4.5.4 Case 4

For Case 4, the comparable variables and solutions involved are described in Table 4.59. As seen, five different comparisons can be made.

Table 4.59 – Comparisons – Case 4.

Case 4	ECCS	Trahair		Serna <i>et al.</i>	
		Baláž & Koleková	Baláž & Koleková	Baláž & Koleková	Baláž & Koleková
	$k_w$	1	1	{0,5; 1}	1
	$k_z$	{0,5; 1}	1	{0,5; 1}	1
	$\psi_f$	[-0,9; 0,9]	0	0	0
	$z_g$	100%	100%	0	0
		Comparison 12	Comparison 13	Comparison 14	Comparison 15
					Comparison 16

### • Comparison 12

A summary of the statistical analysis to the comparison 12, for double and mono symmetric cross sections between Baláž and Koleková and ECCS is given in Table 4.60.

Table 4.60 – Comparison 12.

Comparison 12		n	Mean	St. Dev.	CoV%	Min.	Max.	<0,9%	>1,03%
<b>Double Symmetric</b>	<b>Baláž &amp; Koleková</b>	840	1,005	0,027	2,715	0,963	1,127	0,0	12,5
	<b>ECCS</b>	840	1,009	0,021	2,122	0,960	1,107	0,0	13,0
<b>Mono Symmetric</b>	<b>Baláž &amp; Koleková</b>	1848	1,011	0,034	3,408	0,959	1,190	0,0	17,0
	<b>ECCS</b>	1848	1,015	0,034	3,397	0,942	1,160	0,0	22,2

Both solutions have very similar results, presenting for double and mono symmetric cross sections approximately 13% and 20% of unsafe results respectively. As seen in 4.4.1.4 and 4.4.2.4 the problem is in tests with  $k_z=0,5$ .

### • Comparison 13

A summary of the statistical analysis to the comparison 13, for double symmetric cross sections between Baláž and Koleková, ECCS and Trahair is given in Table 4.61.

Table 4.61 – Comparison 13.

Comparison 13		n	Mean	St. Dev.	CoV%	Min.	Max.	<0,9%	>1,03%
<b>Double Symmetric</b>	<b>Baláž &amp; Koleková</b>	420	1,001	0,005	0,522	0,995	1,019	0,0	0,0
	<b>ECCS</b>	420	1,002	0,002	0,231	1,000	1,010	0,0	0,0
	<b>Trahair</b>	420	1,048	0,007	0,633	1,038	1,068	0,0	100,0

Note that, unlike the previous comparison, in this one there are only cases with  $k_z=1$ , and Baláž and Koleková and ECCS obtain very good results, with ECCS with lower CoV value. And Trahair have all tests above the 3% mark.

### • Comparison 14

A summary of the statistical analysis to the comparison 14, for double symmetric cross sections between Baláž and Koleková, and Serna *et al.* is given in Table 4.62.

Table 4.62 – Comparison 14.

Comparison 14		n	Mean	St. Dev.	CoV%	Min.	Max.	<0,9%	>1,03%
<b>Double Symmetric</b>	<b>Baláž &amp; Koleková</b>	40	0,999	0,003	0,323	0,990	1,001	0,0	0,0
	<b>Serna <i>et al.</i></b>	40	1,003	0,041	4,117	0,962	1,053	0,0	50,0

As possible to see, Baláž and Koleková obtain better results with lower CoV value and no conservative tests.

### • Comparison 15

A summary of the statistical analysis to the comparison 15, for double symmetric cross sections between Baláž and Koleková, ECCS, Trahair and Serna *et al.* is given in Table 4.63.

Table 4.63 – Comparison 15.

Comparison 15	n	Mean	St. Dev.	CoV%	Min.	Max.	<0,9%	>1,03%
Double Symmetric	Baláž & Koleková	20	1,000	0,000	0,024	0,999 1,000	0,0	0,0
	ECCS	20	1,001	0,001	0,052	1,000 1,002	0,0	0,0
	Trahair	20	1,046	0,001	0,052	1,046 1,047	0,0	100,0
		20	0,962	0,000	0,052	0,962 0,963	0,0	0,0

As possible to see, all solutions obtain very good results. However, Baláž and Koleková obtain lowest CoV value and no conservative tests. Note that, the maximum value obtained by Trahair is only 4,7% above the LTBeam results.

### • Comparison 16

A summary of the statistical analysis to the comparison 16, for double symmetric cross sections between Trahair and Serna *et al.* is given in Table 4.64.

Table 4.64 – Comparison 16.

Comparison 16	n	Mean	St. Dev.	CoV%	Min.	Max.	<0,9%	>1,03%
Double Symmetric	Trahair	180	1,035	0,018	1,777	1,003 1,060	0,0	60,0
	Serna <i>et al.</i>	180	0,997	0,020	2,040	0,962 1,034	0,0	4,4

Both solutions have unsafe results, however, Serna *et al.* obtain a lower number of these cases and with a maximum value only 3,4% above the LTBeam results.

#### 4.5.5 Case 5

For Case 5, the comparable variables and solutions involved are described in Table 4.65. As seen, three different comparisons can be made.

Table 4.65 – Comparisons – Case 5.

Case 5	<b>Galéa</b> <b>Baláž &amp; Koleková</b>	<b>Serna <i>et al.</i></b> <b>Baláž &amp; Koleková</b>	<b>Baláž &amp; Koleková</b>	<b>Serna <i>et al.</i></b>
				<b>Trahair</b>
k <sub>w</sub>	1	1		{0,5; 1}
	{0,5; 1}	1		
	[-0,9; 0,9]	0		
	100%	100%	0	
		<b>Comparison 17</b>	<b>Comparison 18</b>	<b>Comparison 19</b>

### • Comparison 17

A summary of the statistical analysis to the comparison 17, for double symmetric cross sections between Baláž and Koleková and Galéa is given in Table 4.66.

Table 4.66 – Comparison 17.

Comparison 17		n	Mean	St. Dev.	CoV%	Min.	Max.	<0,9%	>1,03%
Double Symmetric	Baláž & Koleková	420	1,001	0,004	0,424	0,996	1,013	0,0	0,0
	Galéa	420	0,995	0,005	0,482	0,983	1,004	0,0	0,0

As one can note, both solutions obtain very good results with very lower CoV values and no unsafe or conservative tests.

### • Comparison 18

A summary of the statistical analysis to the comparison 18, for double symmetric cross sections between Baláž and Koleková and Serna *et al.* is given in Table 4.67.

Table 4.67 – Comparison 18.

Comparison 18		n	Mean	St. Dev.	CoV%	Min.	Max.	<0,9%	>1,03%
Double Symmetric	Baláž & Koleková	40	0,992	0,017	1,705	0,949	1,008	0,0	0,0
	Serna <i>et al.</i>	40	0,940	0,026	2,759	0,918	1,024	0,0	0,0

Both solutions obtain very good results with no unsafe or conservative tests. However, Baláž and Koleková obtain lower CoV value.

### • Comparison 19

A summary of the statistical analysis to the comparison 19, for double symmetric cross sections between Baláž and Koleková, Galéa, Trahair and Serna *et al.* is given in Table 4.68.

Table 4.68 – Comparison 19.

Comparison 19		n	Mean	St. Dev.	CoV%	Min.	Max.	<0,9%	>1,03%
Double Symmetric	Baláž & Koleková	20	0,997	0,002	0,156	0,996	1,000	0,0	0,0
	Galéa	20	0,992	0,004	0,367	0,988	0,999	0,0	0,0
	Trahair	20	0,931	0,003	0,367	0,927	0,938	0,0	0,0
	Serna <i>et al.</i>	20	0,922	0,003	0,367	0,918	0,929	0,0	0,0

All solutions obtain very good results with very low CoV values and no unsafe or conservative tests. Note that Baláž and Koleková present the lowest CoV value.

### 4.5.6 Case 6

For Case 6, the comparable variables and solutions involved are described in Table 4.69. As seen, three different comparisons can be made.

Table 4.69 – Comparisons – Case 6.

	<b>Galéa</b> <b>Baláž &amp; Koleková</b>	<b>Serna et al.</b> <b>Baláž &amp; Koleková</b>	<b>Trahair</b> <b>Galéa</b> <b>Baláž &amp; Koleková</b>
<b>Case 6</b>	$k_w$ 1	1	{0,5; 1}
	$k_z$ {0,5; 1}	1	
	$\psi_f$ [-0,9; 0,9]	0	0
	$z_p$ 100%	100%	0
	<b>Comparison 20</b>	<b>Comparison 21</b>	<b>Comparison 22</b>

#### • Comparison 20

A summary of the statistical analysis to the comparison 20, for double symmetric cross sections between Baláž and Koleková and Galéa is given in Table 4.70.

Table 4.70 – Comparison 20.

<b>Comparison 20</b>		<b>n</b>	<b>Mean</b>	<b>St. Dev.</b>	<b>CoV%</b>	<b>Min.</b>	<b>Max.</b>	<b>&lt;0,9%</b>	<b>&gt;1,03%</b>
<b>Double Symmetric</b>	<b>Baláž &amp; Koleková</b>	420	1,000	0,014	1,351	0,977	1,025	0,0	0,0
	<b>Galéa</b>	420	0,987	0,053	5,400	0,876	1,112	6,0	20,5

As seen, Baláž and Koleková present very good results with better CoV value and with no unsafe or conservative tests.

#### • Comparison 21

A summary of the statistical analysis to the comparison 21, for double symmetric cross sections between Baláž and Koleková and Serna *et al.* is given in Table 4.71.

Table 4.71 – Comparison 21.

<b>Comparison 21</b>		<b>n</b>	<b>Mean</b>	<b>St. Dev.</b>	<b>CoV%</b>	<b>Min.</b>	<b>Max.</b>	<b>&lt;0,9%</b>	<b>&gt;1,03%</b>
<b>Double Symmetric</b>	<b>Baláž &amp; Koleková</b>	40	0,994	0,013	1,266	0,963	1,007	0,0	0,0
	<b>Serna et al.</b>	40	0,861	0,057	6,579	0,801	0,965	50,0	0,0

As one can see, Baláž and Koleková present very good results with better CoV value and with no conservative tests.

#### • Comparison 22

A summary of the statistical analysis to the comparison 22, for double symmetric cross sections between Baláž and Koleková, Galéa, Trahair and Serna *et al.* is given in Table 4.72. Almost all solutions obtain very good results with very lower CoV values and no unsafe or conservative tests. Note that Baláž and Koleková present the lowest CoV value.

Table 4.72 – Comparison 22.

Comparison 22		n	Mean	St. Dev.	CoV%	Min.	Max.	<0,9%	>1,03%
Double Symmetric	Baláž & Koleková	20	0,997	0,003	0,319	0,993	1,001	0,0	0,0
	Galéa	20	0,983	0,007	0,736	0,976	0,998	0,0	0,0
	Trahair	20	0,999	0,007	0,736	0,991	1,014	0,0	0,0
	Serna et al.	20	0,807	0,006	0,736	0,801	0,819	100,0	0,0

#### 4.5.7 Case 7

For Case 7, the comparable variables and solutions involved are described in Table 4.73. As seen, three different comparisons can be made.

Table 4.73 – Comparison – Case 7.

Case 7	Galéa Serna et al.	Serna et al.		Trahair Serna et al. Galéa
		Galéa Serna et al.	Baláž e Koleková	Baláž e Koleková
	$k_w$	1	1	1
	$k_z$	1	1	1
	$\Psi_f$	0	0	0
	$\Psi$	[-1;1]	[-1;1]	{0;1}
	$M_0/M$	>0 <0	>0	< -1
	$M$	>0 <0	<0	<0
	$z_g$	0	0	0
		Comparison 23	Comparison 24	Comparison 25

- Comparison 23

A summary of the statistical analysis to the comparison 23, for double symmetric cross sections between Galéa and Serna et al. is given in Table 4.74.

Table 4.74 – Comparison 23.

Comparison 23		n	Mean	St. Dev.	CoV%	Min.	Max.	<0,9%	>1,03%
Double Symmetric	Galéa	10620	0,987	0,026	2,653	0,773	1,040	2,4	0,1
	Serna et al.	10620	0,979	0,053	5,366	0,666	1,047	8,0	0,8

Both solutions present unsafe and conservative values. However, Galéa obtains lowest CoV value and lowest unsafe and conservative results number.

#### • Comparison 24

A summary of the statistical analysis to the comparison 24, for double symmetric cross sections between Baláž and Koleková, Galéa and Serna *et al.* is given in Table 4.75.

Table 4.75 – Comparison 24.

Comparison 24		n	Mean	St. Dev.	CoV%	Min.	Max.	<0,9%	>1,03%
Double Symmetric	Baláž & Koleková	5220	1,003	0,040	4,034	0,789	1,241	3,5	12,6
	Galéa	5220	0,981	0,033	3,412	0,773	1,040	4,8	0,3
	Serna <i>et al.</i>	5220	0,961	0,069	7,206	0,666	1,047	16,0	0,6

All solutions present unsafe and conservative results. However, Galéa obtains lowest CoV value and lowest unsafe results number.

#### • Comparison 25

A summary of the statistical analysis to the comparison 25, for double symmetric cross sections between Baláž and Koleková, Galéa, Trahair and Serna *et al.* is given in Table 4.76.

Table 4.76 – Comparison 25.

Comparison 25		n	Mean	St. Dev.	CoV%	Min.	Max.	<0,9%	>1,03%
Double Symmetric	Baláž & Koleková	700	1,016	0,015	1,513	0,987	1,047	0,0	20,1
	Galéa	700	0,994	0,004	0,442	0,982	1,013	0,0	0,0
	Trahair	700	1,000	0,016	1,561	0,927	1,035	0,0	0,7
	Serna <i>et al.</i>	700	0,990	0,018	1,857	0,918	1,012	0,0	0,0

Galéa and Serna *et al.* do not obtain unsafe or conservative values, and Galéa presents the lowest CoV value.

#### 4.5.8 Case 8

For Case 8, the comparable variables and solutions involved are described in Table 4.77. As can be seen, two different comparisons can be made.

Table 4.77 – Comparisons – Case 8.

Case 8	Serna <i>et al.</i> Galéa	Serna <i>et al.</i> Trahair Galéa	
$k_w$	1		1
$k_z$	1		1
$\psi_f$	0		0
$\psi$	[-1;1]		{0;1}
$\mu_{y=0}$	>0 <0		< -1,33
$\mu_{y=1}$			< -2
$M$	>0 <0		<0
$z_g$	0		0
		Comparison 26	Comparison 27

- **Comparison 26**

A summary of the statistical analysis to the comparison 26, for double symmetric cross sections between Galéa and Serna *et al.* is given in Table 4.78.

Table 4.78 – Comparison 26.

Comparison 26		n	Mean	St. Dev.	CoV%	Min.	Max.	<0,9%	>1,03%
<b>Double Symmetric</b>	<b>Galéa</b>	10620	0,984	0,024	2,468	0,814	1,040	2,3	0,0
	<b>Serna <i>et al.</i></b>	10620	0,922	0,059	6,365	0,691	1,042	21,7	0,1

Galéa has the lowest CoV value and lowest unsafe and conservative results number.

- **Comparison 27**

A summary of the statistical analysis to the comparison 27, for double symmetric cross sections between Galéa, Trahair and Serna *et al.* is given in Table 4.79.

Table 4.79 – Comparison 27.

Comparison 27		n	Mean	St. Dev.	CoV%	Min.	Max.	<0,9%	>1,03%
<b>Double Symmetric</b>	<b>Galéa</b>	520	0,988	0,006	0,626	0,973	1,001	0,0	0,0
	<b>Trahair</b>	520	1,000	0,014	1,431	0,981	1,036	0,0	3,5
	<b>Serna <i>et al.</i></b>	520	0,886	0,026	2,968	0,801	0,923	64,2	0,0

Galéa is the only one, without unsafe and conservative cases, and has the lowest CoV value.

#### 4.5.9 Case 9

For Case 9, the comparable variables and solutions involved are described in Table 4.80. As can be seen, two different comparisons can be made.

Table 4.80 – Comparisons – Case 9.

	Trahair		Trahair Andrade <i>et al.</i>
	Andrade <i>et al.</i>	Baláž & Koleková	
Case 9	$k_w$	0,5	1
	$\psi_f$	[-0,8; 0,8]	0
	$z_g$	{Top; Center; Bottom}	{Top; Center; Bottom}
		Comparison 28	Comparison 29

- **Comparison 28**

A summary of the statistical analysis to the comparison 28, for double and mono symmetric cross sections between Baláž and Koleková, Andrade *et al.* and Trahair is given in Table 4.81.

For double symmetric cross section, Andrade *et al.* obtain the lowest CoV value, and is the only one without unsafe or conservative results. For mono symmetrical cross section, Andrade *et al.* have the better results, with the lowest CoV value and the lowest unsafe results number.

Table 4.81 – Comparison 28.

Comparison 28		n	Mean	St. Dev.	CoV%	Min.	Max.	<0,9%	>1,03%
Double Symmetric	Baláž & Koleková	60	1,045	0,097	9,314	0,960	1,302	0,0	28,3
	Andrade <i>et al.</i>	60	1,003	0,007	0,713	0,982	1,013	0,0	0,0
	Trahair	60	1,045	0,097	9,312	0,966	1,338	0,0	25,0
Mono Symmetric	Baláž & Koleková	108	1,034	0,115	11,131	0,445	1,310	1,9	27,8
	Andrade <i>et al.</i>	108	1,006	0,012	1,152	0,979	1,044	0,0	5,6

#### • Comparison 29

A summary of the statistical analysis to the comparison 29, for double and mono symmetric cross sections between Andrade *et al.* and Trahair is given in Table 4.82.

Table 4.82 – Comparison 29.

Comparison 29		n	Mean	St. Dev.	CoV%	Min.	Max.	<0,9%	>1,03%
Double Symmetric	Andrade <i>et al.</i>	60	1,000	0,012	1,170	0,969	1,018	0,0	0,0
	Trahair	60	1,032	0,024	2,278	0,982	1,084	0,0	55,0

Andrade *el at.* have the better results with the lowest CoV value and no unsafe results number.

#### 4.5.10 Case 10

For Case 10, the comparable variables and solutions involved are described in Table 4.83. As seen, two different comparisons can be made.

Table 4.83 - Comparison 29.

Case 10	Trahair		Andrade <i>et al.</i>		Trahair		Andrade <i>et al.</i>	
	Andrade <i>et al.</i>		Baláž & Koleková		Trahair		Andrade <i>et al.</i>	
	$k_w$	0,5			1			
	$\psi_f$		[-0,8; 0,8]			0		
	$z_g$		{Top; Center; Bottom}		{Top; Center; Bottom}		Comparison 30	
							Comparison 31	

#### • Comparison 30

A summary of the statistical analysis to the comparison 30, for double and mono symmetric cross sections between Baláž and Koleková, Andrade *et al.* and Trahair is given in Table 4.84.

For double symmetric cross section, Andrade *et al.* obtain the lowest CoV value, and is the only one without unsafe or conservative results. For mono symmetrical cross section, Andrade *et al.* have the better results, with the lowest CoV value and the lowest unsafe results number.

Table 4.84 – Comparison 30.

Comparison 30		n	Mean	St. Dev.	CoV%	Min.	Max.	<0,9%	>1,03%
Double Symmetric	Baláž & Koleková	60	1,047	0,112	10,691	0,929	1,297	0,0	33,3
	Andrade <i>et al.</i>	60	1,005	0,006	0,589	0,993	1,014	0,0	0,0
	Trahair	60	1,006	0,080	7,985	0,940	1,223	0,0	23,3
Mono Symmetric	Andrade <i>et al.</i>	108	1,037	0,120	11,610	0,698	1,421	0,9	27,8
	Baláž & Koleková	108	1,117	0,156	13,970	0,916	1,578	0,0	60,2

### • Comparison 31

A summary of the statistical analysis to the comparison 31, for double and mono symmetric cross sections between Andrade *et al.* and Trahair is given in Table 4.85.

Table 4.85 – Comparison 31.

Comparison 31		n	Mean	St. Dev.	CoV%	Min.	Max.	<0,9%	>1,03%
Double Symmetric	Andrade <i>et al.</i>	60	1,000	0,014	1,393	0,963	1,018	0,0	0,0
	Trahair	60	0,921	0,029	3,097	0,850	0,975	20,0	0,0

Andrade *el at.* have the better results with the lowest CoV value and no unsafe cases.

## 4.6 Final Remarks

Since there are different limitations between the analyzed solutions, it is not simple to define the most accurate solution. In order to get an overview of all the accuracy of the solutions the Tables 4.86 and 4.87 are presented. The values in these tables include all possible variables in each solution, so it is not an exact comparison table; however it is possible to take some conclusion. In the row with the number of tests involved for each solution it is possible to understand the limitations of each one. The safest solutions according to this parametric study are marked with a check. Note that, since the C values used for mono symmetric cross section give worst results, this type of cross section is presented in a different table.

For each variable the most accurate C values are described along this Chapter. The assembly of these C factors with the best accuracy is left for Future Research, as described in Chapter 5.

Table 4.86 – Overview for double symmetric cross section.

	Baláž and Koleková	ECCS	Galéa	Andrade et al.	Lindner	Trahair	Serna et al.
<b>Case 1</b>	✓		✓				
>1,3[%]	0,6%	0,1	0,0%	-	-	0,0%	0,0%
<0,9[%]	0,0%	16,2	0,6	-	-	6,2%	3,8%
nº tests	<b>3280</b>	1640	820	0		820	820
<b>Case 2</b>	✓	✓	✓			✓	
>1,3[%]	0,9%	0,2%	0,0%	-	-	0,0%	50,0%
<0,9[%]	0,0%	0,0%	0,0%	-	-	0,0%	0,0%
nº tests	<b>1680</b>	840	420	0		420	40
<b>Case 3</b>	✓	✓				✓	
>1,3[%]	0,0%	0,0%	4,0%	-	-	0,0%	9,1%
<0,9[%]	0,0%	0,0%	0,0%	-	-	0,0%	0,0%
nº tests	<b>1680</b>	840	420	0		600	220
<b>Case 4</b>	✓						
>1,3[%]	8,8%	13,0%	-	-	-	87,6	14,0%
<0,9[%]	0,0%	0,0%	-	-	-	0,0%	0,0%
nº tests	<b>1680</b>	840	0	0		580	200
<b>Case 5</b>	✓		✓			✓	✓
>1,3[%]	0,0%	-	0,0%	-	-	0,0%	0,0%
<0,9[%]	0,0%	-	0,0%	-	-	0,0%	0,0%
nº tests	<b>1260</b>	0	420	0		20	40
<b>Case 6</b>	✓					✓	
>1,3[%]	0,2%	-	20,5%	-	-	0,0%	0,0%
<0,9[%]	0,0%	-	6,5%	-	-	0,0%	50%
nº tests	<b>1260</b>	0	0	0	0	20	40
<b>Case 7</b>			✓			✓	
>1,3[%]	12,6%	-	0,7%	-	-	0,7%	0,8%
<0,9[%]	3,5%	-	1,3%	-	-	0%	8%
nº tests	5520	0	<b>31860</b>	0	0	700	10620
<b>Case 8</b>			✓			✓	
>1,3[%]	-	-	8,1%	-	-	3,5%	0,1%
<0,9[%]	-	-	1,9%	-	-	0,0%	21,7%
nº tests	0	0	<b>31860</b>	0	0	520	10620
<b>Case 9</b>				✓			
>1,3[%]	28,3%	-	-	0,0%	13,2%	40,0%	-
<0,9[%]	0,0%	-	-	0,0%	0,0%	0,0%	-
nº tests	60	0	0	120	<b>612</b>	120	0
<b>Case 10</b>				✓			
>1,3[%]	33,3%	-	-	0,0%	34,2%	11,7%	-
<0,9[%]	0,0%	-	-	0,0%	0,0%	10,0%	-
nº tests	60	0	0	120	<b>612</b>	120	0

Table 4.87 – Overview for mono symmetric cross section.

	Baláž and Koleková	ECCS	Galéa	Andrade et al.	Lindner	Trahair	Serna et al.
<b>Case 1</b>							
>1,3[%]	20,8	10	-	-	-	-	-
<0,9[%]	6,1	17,8	-	-	-	-	-
nº tests	<b>8528</b>	3608	0	0	0	0	0
<b>Case 2</b>	✓						
>1,3[%]	3,8	11,1	-	-	-	-	-
<0,9[%]	1	0	-	-	-	-	-
nº tests	<b>4368</b>	1848	0	0	0	0	0
<b>Case 3</b>	✓						
>1,3[%]	11,8	13,7	-	-	-	-	-
<0,9[%]	5,3	0	-	-	-	-	-
nº tests	<b>4368</b>	1848	0	0	0	0	0
<b>Case 4</b>	✓						
>1,3[%]	12,2	22,2	-	-	-	-	-
<0,9[%]	3,5	0	-	-	-	-	-
nº tests	<b>4368</b>	1848	0	0	0	0	0
<b>Case 5</b>							
>1,3[%]	22,2	-	-	-	-	-	-
<0,9[%]	19,1	-	-	-	-	-	-
nº tests	<b>2268</b>	0	0	0	0	0	0
<b>Case 6</b>							
>1,3[%]	29,2	-	-	-	-	-	-
<0,9[%]	18,7	-	-	-	-	-	-
nº tests	<b>2268</b>	0	0	0	0	0	0
<b>Case 7</b>							
>1,3[%]	12,6	-	-	-	-	-	-
<0,9[%]	3,5	-	-	-	-	-	-
nº tests	<b>5220</b>	0	0	0	0	0	0
<b>Case 8</b>							
>1,3[%]	-	-	-	-	-	-	-
<0,9[%]	-	-	-	-	-	-	-
nº tests	0	0	0	0	0	0	0
<b>Case 9</b>				✓			
>1,3[%]	27,8	-	-	6,9	-	-	-
<0,9[%]	1,9	-	-	0	-	-	-
nº tests	108	0	0	<b>216</b>	0	0	0
<b>Case 10</b>				✓			
>1,3[%]	28,7	-	-	7,9	-	-	-
<0,9[%]	1,9	-	-	0	-	-	-
nº tests	180	0	0	<b>216</b>	0	0	0

## 5 CONCLUSION AND FUTURE RESEARCH

### 5.1 Conclusion

In this thesis, a wide comparison between the most common and accepted solutions and numerical models for the determination of the elastic critical moment of I-section steel beams was carried out. Based on the observed results, it is notorious that all solutions have a good approximation to the numerical results. It can also be noted that the higher the difference from the basic case, the higher the error is. One can verify this by the high number of inaccurate results obtained by some solution for mono symmetric cross section and for tests with rotations about z axis restricted. Nevertheless, in structural design, the rotation about z axis and warping are usually considered free, once the real behavior of connections is unknown. Therefore, considering the basic case of beams with fork conditions and double symmetric cross section, it was seen that all solutions lead to a very good and equivalent level of safety.

### 5.2 Future Research

In order to obtain a consistent, thorough, practical and accurate standardized procedure based on these solutions; some goals have to be accomplished in further research.

- Clarification with the authors of the correct procedure for some of issues/inconsistencies found in some solutions as discussed in section 3.2 of this thesis;
- Standardization of all solutions in a practical and simplified C factors format allowing the use of only one main 3-factor formula;
- Application and validation of a new solution based in all C factors values that obtain the best accuracy in this study;
- Calibration of some C values with numerical models in order to adjust some evident errors detected in this study. As well as, definition of better ranges or C values for mono symmetric cross sections, as discussed along the Chapter 5.
- Application and validation of possible combinations between the more accurate  $C_1$ ,  $C_2$  and  $C_3$  values of different solutions, in order to increase the number of possible solutions, with more mono symmetric cross sections cases and load positions relatively to the shear center.

- Finally, calibration of some practical expressions of the C factors, in order to improve the computation process.

### 5.3 Original Contributions

This study is part of the goals of the supervisor's activity within the ECCS Technical Committee 8 – Stability, TC8, where the need to validate existing expressions for determination of the elastic critical moment of steel beams has been discussed. With the aim to give answer to this question, this work was presented and discussed in a TC8 meeting:

Simões da Silva, L., Canha, J., and Marques, L. "Comparison between C factors for determination of the elastic critical moment of steel beams", Technical Committee 8, ECCS, Document TC8-2013-06-009, Stuttgart, Germany, June 21<sup>st</sup>, 2013;

In addition, the following conference proceeding resulted from the work presented:

Canha, J., Marques, L., and Simões da Silva, L. "Análise comparativa de métodos simplificados de cálculo do momento crítico". IX Congresso em Construção Metálica e Mista e o I Congresso Luso-Brasileiro de Construção Metálica Sustentável, Porto, Portugal, 24-25 October (2013) (accepted for publication)

Finally, a journal paper will be including this study as well as some of the described Future Research goals.

## 6 REFERENCES

- AISC, American Institute of Steel Construction (1994) "Load and Resistance Factor Design". Chicago : AISC, 1994.
- Andrade, A., Camotim, D. and Providência e Costa, P. (2006) "On the evaluation of elastic critical moments in doubly and singly symmetric I-section cantilevers". Journal Of Constructional Steel Research. Portugal : Elsevier, 2006. Vol. 63, pp. 894-908.
- ANSYS. ANSYS V5.6. Pennsylvania : Ansys, Inc.
- Baláz, Ivan and Koleková, Yvona. (2012). "LTB resistance of beam influenced by plastic reserve or local buckling". 18th International Conference Engineering Mechanics 2012. Svatka, Czech Republic : Academy of Sciences of the Czech Republic, 2012. pp. 639-655.
- Baláz, Ivan and Koleková, Yvona. (1999). "Stability of Monosymmetric Beams". Stability and Ductility of Steel Structures. 1999, Vol. SDSS'99.
- CEN. (2007). "Eurocode 3: Design of Steel Structure, Part 1-1: General rules and rules for buildings." EN 1999-1-1. Brussels : European Committee for Standardization, 2007.
- CEN. (2003). "Eurocode 3: Design of Steel Structure, Part 1-1: General rules and rules for buildings." ENV 1993-1-1. Brussels : European Committee for Standardization, 2003.
- CEN. (2007). "Eurocode 9: Design of Aluminium Structure, Part 1-1: General structure rules." EN 1999-1-1. Brussels : European Committee for Standardization, 2007.
- Clark, J. W. and Hill, H. N. (1960). "Lateral buckling of beams". Journal of Structural Division. s.l. : American Society of Civil Engineers, 1960. Vol. 68, pp. 175-196.
- DIN. (1990). "Steel Structures - Part 2: Stability - Buckling of bars and skeletal structures". DIN 18800-2. Berlin : Deutsches Institut für Normung, 1990.
- Djalaly, H. (1974). "Calcul de la résistance ultime au déversement.". s.l. : Construction Métallique, 1974. Vols. 1,3,4, pp. 58-77, 43-56, 54-61.
- ECCS. (2006). "ECCS Technical Committee 8 - Stability" - Rules for Member Stability in 1993-1-1: Background documentation and design guidelines. s.l. : ECCS, 2006. Vol. 119.
- Galéa, Y. (2002). "Déversement Élastique d'une Poutre à Section Bi-Symétrique Soumise à des Moments d'Extrémité et une Charge Répartie ou Concentrée". 2 s.l. : Centre Technique Industriel de la Construction Métallique, 2002.
- Galéa. (2002). "LTBeam - Report on Validation Test". LTBeam Installation Package. s.l. : CTICM, 2002.

- Galéa. (2010). "LTBeam Version 1.0.11". CTICM. France : s.n., 2010.
- Mrázik, A. and Djubek, J. (1958). "Stability of Thin-Walled Member Structures". Bratislava : ÚSTARCH - Slovak Academy of Sciences, 1958. Vol. Research Report IX.3 S/58.
- Serna, A. Miguel, et al. (2006). "Equivalent uniform moment factor for lateral-torsional buckling of steel members". Journal of Constructional Steel Research. s.l. : Elsevier, 2006. Vol. 62, pp. 566-580.
- Trahair, Nicholas. (1993). "Flexural-Torsion Buckling of Structures" . London : E&FN Spon (Chapman & Hall), 1993.

## ANNEX

Annex A – C Factors

Annex B – Statistical Analysis

## ANNEX A – C Factors

In this Annex is presented all the solutions for C factors values considered in the study. The main formulae are presented in the Chapter 3, thus they are not presented here.

### A.1 – General Formulae

- **Parameter  $\psi_f$**

$$\psi_f = \frac{I_{fc} - I_{ft}}{I_{fc} + I_{ft}} \quad (\text{A.1})$$

Where  $I_{fc}$  and  $I_{ft}$  are the second moment of area of the compression flange and tension flange about the minor axis of the section respectively.

- **Parameter  $\bar{K}$**

$$\bar{K} = \frac{\pi}{L} \sqrt{\frac{EI_z h_m^2}{4GI_T}} \quad (\text{A.2})$$

- **Torsion Parameter K**

$$K = \frac{\pi}{L} \sqrt{\frac{EI_w}{GI_T}} \quad (\text{A.3})$$

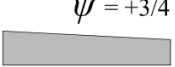
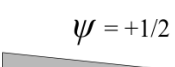
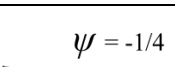
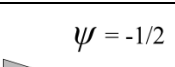
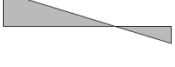
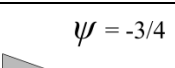
- **Dimensionless distance of load from centroid  $\varepsilon$**

$$\varepsilon = \frac{2z_a K}{h_m \pi} \quad (\text{A.4})$$

## A.2 – Baláž and Koleková

- End Moment Loading

Table A.1 – Values of factors  $C_1$  and  $C_3$  corresponding to various end moment ratio  $\psi$ , values of buckling length factor  $k_z$  and cross-section parameters  $\psi_f$  and  $k_{wt}$  ( $k_w=1$ ).

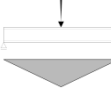
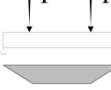
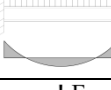
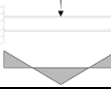
Loading and Support Conditions	Bending Moment Diagram	$\psi$	$k_z^{(2)}$	Values of factors				
				$C_1^{(1)}$		$C_3$		
				$C_{1,0}$	$C_{1,1}$	$\psi_f = -1$	$-0,9 \leq \psi_f \leq 0$	$0 \leq \psi_f \leq 0,9$
		1	1	1	1,000	1,000	1,000	
				<b>0,7L</b>	1,016	1,100	1,025	1,000
				<b>0,7R</b>	1,016	1,100	1,025	1,000
				<b>0,5</b>	1,000	1,127	1,019	
		0,75	0,75	1	1,139	1,141	1,000	
				<b>0,7L</b>	1,210	1,313	1,050	1,000
				<b>0,7R</b>	1,109	1,201	1,000	
				<b>0,5</b>	1,139	1,285	1,017	
		0,5	0,5	1	1,312	1,320	1,150	1,000
				<b>0,7L</b>	1,480	1,616	1,160	1,000
				<b>0,7R</b>	1,213	1,317	1,000	
				<b>0,5</b>	1,310	1,482	1,150	1,000
		0,25	0,25	1	1,522	1,551	1,290	1,000
				<b>0,7L</b>	1,853	2,059	1,600	1,260
				<b>0,7R</b>	1,329	1,467	1,000	
				<b>0,5</b>	1,516	1,730	1,350	1,000
		0	0	1	1,770	1,847	1,470	1,000
				<b>0,7L</b>	2,331	2,683	2,000	1,420
				<b>0,7R</b>	1,453	1,592	1,000	
				<b>0,5</b>	1,753	2,027	1,500	1,000
		-0,25	-0,25	1	2,047	2,207	1,65	1,000
				<b>0,7L</b>	2,827	3,322	2,40	1,550
				<b>0,7R</b>	1,582	1,748	1,38	0,850
				<b>0,5</b>	2,004	2,341	1,75	1,000
		-0,5	-0,5	1	2,331	2,591	1,85	1,000
				<b>0,7L</b>	3,078	3,399	2,70	1,450
				<b>0,7R</b>	1,711	1,897	1,45	0,780
				<b>0,5</b>	2,230	2,579	2,00	0,950
		-0,75	-0,75	1	2,547	2,852	2,00	1,000
				<b>0,7L</b>	2,592	2,770	2,00	0,850
				<b>0,7R</b>	1,829	2,027	1,55	0,700
				<b>0,5</b>	2,352	2,606	2,00	0,850
		-1	-1	1	2,555	2,733	2,00	$-\psi_f$
				<b>0,7L</b>	1,921	2,103	1,55	0,380
				<b>0,7R</b>	1,921	2,103	1,55	0,580
				<b>0,5</b>	2,223	2,390	1,88	$0,125 - 0,7\psi_f$

<sup>1)</sup>  $C_1 = C_{1,0} + (C_{1,1} - C_{1,0})k_{wt} \leq C_{1,1}$ , ( $C_1 = C_{1,0}$  for  $k_{wt} = 0$ ,  $C_1 = C_{1,1}$  for  $k_{wt} \geq 1$ )

<sup>2)</sup> 0,7L = Left end fixed, 0,7R = Right End Fixed

• Transverse Loading

Table A.2 – Values of factors  $C_1$ ,  $C_2$  and  $C_3$  corresponding to various transverse loading cases, values of buckling length factors  $k_y$ ,  $k_z$  and  $k_w$ , cross section mono symmetry factor  $\psi_f$  and torsion parameter  $k_{wt}$ .

Loading and Support Conditions	Buckling length factors			Values of factors							
				$C_1$ <sup>1)</sup>		$C_2$				$C_3$	
	$k_y$	$k_z$	$k_w$	$C_{1,0}$	$C_{1,1}$	$\psi_f = -1$	$-0,9 \leq \psi_f \leq 0,9$	$\psi_f = 1$	$\psi_f = -1$	$-0,9 \leq \psi_f \leq 0,9$	$\psi_f = 1$
	1	1	1	1,127	1,132	0,33	0,459	0,50	0,93	0,525	0,38
	1	1	0,5	1,128	1,231	0,33	0,391	0,50	0,93	0,806	0,38
	1	0,5	1	0,947	0,997	0,25	0,407	0,40	0,84	0,478	0,44
	1	0,5	0,5	0,947	0,970	0,25	0,310	0,40	0,84	0,674	0,44
	1	1	1	1,348	1,363	0,52	0,553	0,42	1,00	0,411	0,31
	1	1	0,5	1,349	1,452	0,52	0,580	0,42	1,00	0,666	0,31
	1	0,5	1	1,030	1,087	0,40	0,449	0,42	0,80	0,338	0,31
	1	0,5	0,5	1,031	1,067	0,40	0,437	0,42	0,80	0,516	0,31
	1	1	1	1,038	1,040	0,33	0,431	0,39	0,93	0,562	0,39
	1	1	0,5	1,039	1,148	0,33	0,292	0,39	0,93	0,878	0,39
	1	0,5	1	0,922	0,960	0,28	0,404	0,30	0,88	0,539	0,50
	1	0,5	0,5	0,922	0,945	0,28	0,237	0,30	0,88	0,772	0,50
				$C_{1,0}$	$C_{1,1}$	$\psi_f = -1$	$-0,5 \leq \psi_f \leq 0,5$	$\psi_f = 1$	$\psi_f = -1$	$-0,5 \leq \psi_f \leq 0,5$	$\psi_f = 1$
	0,5	1	1	2,576	2,608	1,00	1,562	0,15	1,00	-0,859	-1,99
	0,5	0,5	1	1,490	1,515	0,56	0,900	0,08	0,61	-0,516	-1,20
	0,5	0,5	0,5	1,494	1,746	0,56	0,825	0,08	0,61	0,002712	-1,20
	0,5	1	1	1,683	1,726	1,20	1,388	0,07	1,15	-0,716	-1,35
	0,5	0,5	1	0,936	0,955	0,69	0,763	0,03	0,64	-0,406	-0,76
	0,5	0,5	0,5	0,937	1,057	0,69	0,843	0,03	0,64	-0,0679	-0,76

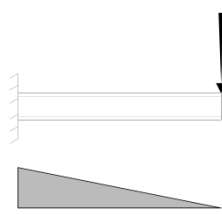
<sup>1)</sup>  $C_1 = C_{1,0} + (C_{1,1} - C_{1,0})k_{wt} \leq C_{1,1}$ , ( $C_1 = C_{1,0}$  for  $k_{wt} = 0$ ,  $C_1 = C_{1,1}$  for  $k_{wt} \geq 1$ )

2) Parameter  $\psi_f$  refers to the middle of the span.

3) Values of critical moments  $M_{cr}$  refer to the cross section, where  $M_{max}$  is located.

- Cantilever loaded by concentrated tip load F

Table A.3 – Relative non-dimensional critical moment  $\mu_{cr}$  for cantilever loaded by concentrated tip load F ( $k_z = k_w = 2$ ).

Loading and Support Conditions	$k_w k_{wt} = k_{wt0}$	$k_z \xi_g = \xi_{g0}$	Values of non-dimensional critical moment						
			$k_z \xi_j = \xi_{j0}$						
			-4	-2	-1	0	1	2	4
	<b>0</b>	4	0,107	0,156	0,194	0,245	0,316	0,416	0,759
		2	0,123	0,211	0,302	0,463	0,759	1,312	4,024
		0	0,128	0,254	0,478	1,280	3,178	5,590	10,730
		-2	0,129	0,258	0,508	1,619	3,894	6,500	11,860
		-4	0,129	0,258	0,511	1,686	4,055	6,740	12,240
	<b>0,5</b>	4	0,151	0,202	0,240	0,293	0,367	0,475	0,899
		2	0,195	0,297	0,393	0,560	0,876	1,528	5,360
		0	0,261	0,495	0,844	1,815	3,766	6,170	11,295
		-2	0,329	0,674	1,174	2,423	4,642	7,235	12,595
		-4	0,364	0,723	1,235	2,529	4,843	7,540	13,100
	<b>1</b>	4	0,198	0,257	0,301	0,360	0,445	0,573	1,123
		2	0,268	0,391	0,502	0,691	1,052	1,838	6,345
		0	0,401	0,750	1,243	2,431	4,456	6,840	11,920
		-2	0,629	1,326	2,115	3,529	5,635	8,115	13,365
		-4	0,777	1,474	2,264	3,719	5,915	8,505	13,960
	<b>2</b>	4	0,335	0,428	0,496	0,588	0,719	0,916	1,795
		2	0,461	0,657	0,829	1,111	1,630	2,698	7,815
		0	0,725	1,321	2,079	3,611	5,845	8,270	13,285
		-2	1,398	3,003	4,258	5,865	7,845	10,100	15,040
		-4	2,119	3,584	4,760	6,360	8,385	10,715	15,825
	<b>4</b>	4	0,845	1,069	1,230	1,443	1,739	2,168	3,866
		2	1,159	1,614	1,992	2,569	3,498	5,035	10,345
		0	1,801	3,019	4,231	6,100	8,495	11,060	16,165
		-2	3,375	6,225	8,035	9,950	11,975	14,110	18,680
		-4	5,530	8,130	9,660	11,375	13,285	15,365	19,925

a) For  $z_j = 0$ ,  $z_g = 0$  and  $k_{wt0} \leq 8$ :  $\mu_{cr} = 1,27 + 1,14k_{wt0} + 0,017k_{wt0}^2$

b) For  $z_j = 0$ ,  $-4 \leq \xi_g \leq 4$  and  $k_{wt} \leq 4$ ,  $\mu_{cr}$  may be calculated also from C factors, where the following approximate values of the factors  $C_1$  and  $C_2$  should be used for the cantilever under tip load F:

$C_1 = 2,56 + 4,675k_{wt} - 2,62k_{wt}^2 + 0,5k_{wt}^3$ , if  $k_{wt} \leq 2$

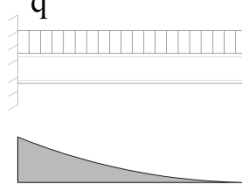
$C_1 = 5,55$ , if  $k_{wt} > 2$

$C_2 = 1,255 + 1,566k_{wt} - 0,931k_{wt}^2 + 0,245k_{wt}^3 - 0,024k_{wt}^4$ , if  $\xi_g \geq 0$

$C_2 = 0,192 + 0,585k_{wt} - 0,054k_{wt}^2 - (0,032 + 0,102k_{wt} - 0,013k_{wt}^2)\xi_g$ , if  $\xi_g < 0$

- Cantilever loaded by uniformly distributed load  $q$

Table A.4 – Relative non-dimensional critical moment  $\mu_{cr}$  for cantilever loaded by uniformly distributed load  $q$  ( $k_z = k_w = 2$ ).

Loading and Support Conditions	$k_w k_{wt} = k_{wt0}$	$k_z \xi_g = \xi_{g0}$	Values of non-dimensional critical moment						
			$k_z \xi_j = \xi_{j0}$						
			-4	-2	-1	0	1	2	4
	0	4	0,113	0,173	0,225	0,304	0,431	0,643	1,718
		2	0,126	0,225	0,340	0,583	1,165	2,718	13,270
		0	0,132	0,263	0,516	2,054	6,945	12,925	25,320
		-2	0,134	0,268	0,537	3,463	10,490	17,260	30,365
		-4	0,134	0,270	0,541	4,273	12,715	20,135	34,005
	0,5	4	0,213	0,290	0,352	0,443	0,586	0,823	2,046
		2	0,273	0,421	0,570	0,854	1,505	3,229	14,365
		0	0,371	0,718	1,287	3,332	8,210	14,125	26,440
		-2	0,518	1,217	2,418	6,010	12,165	18,685	31,610
		-4	0,654	1,494	2,950	7,460	14,570	21,675	35,320
	1	4	0,336	0,441	0,522	0,636	0,806	1,080	2,483
		2	0,449	0,663	0,865	1,224	1,977	3,873	15,575
		0	0,664	1,263	2,172	4,762	9,715	15,530	27,735
		-2	1,109	2,731	4,810	8,695	14,250	20,425	33,075
		-4	1,623	3,558	6,025	10,635	16,880	23,555	36,875
	2	4	0,646	0,829	0,965	1,152	1,421	1,839	3,865
		2	0,885	1,268	1,611	2,185	3,282	5,700	18,040
		0	1,383	2,550	4,103	7,505	12,770	18,570	30,570
		-2	2,724	6,460	9,620	13,735	18,755	24,365	36,365
		-4	4,678	8,635	11,960	16,445	21,880	27,850	40,400
	4	4	1,710	2,168	2,500	2,944	3,565	4,478	8,260
		2	2,344	3,279	4,066	5,285	7,295	10,745	23,150
		0	3,651	6,210	8,845	13,070	18,630	24,625	36,645
		-2	7,010	13,555	17,850	22,460	27,375	32,575	43,690
		-4	12,270	18,705	22,590	26,980	31,840	37,090	48,390

a) For  $z_j = 0$ ,  $z_g = 0$  and  $k_{wt0} \leq 8$ :  $\mu_{cr} = 2,04 + 2,68k_{wt0} + 0,021k_{wt0}^2$

b) For  $z_j = 0$ ,  $-4 \leq z_g \leq 4$  and  $k_{wt} \leq 4$ ,  $\mu_{cr}$  may be calculated also from C factors, where the following approximate values of the factors  $C_1$  and  $C_2$  should be used for the cantilever under tip load F:

$$C_1 = 4,11 + 11,2k_{wt} - 5,65k_{wt}^2 + 0,975k_{wt}^3, \text{ if } k_{wt} \leq 2$$

$$C_1 = 12, \text{ if } k_{wt} > 2$$

$$C_2 = 1,661 + 1,068k_{wt} - 0,609k_{wt}^2 + 0,153k_{wt}^3 - 0,014k_{wt}^4, \text{ if } z_g \geq 0$$

$$C_2 = 0,535 + 0,426k_{wt} - 0,029k_{wt}^2 - (0,061 + 0,074k_{wt} - 0,0085k_{wt}^2)\zeta_g, \text{ if } z_g < 0$$

- Combined loading of end moments and transverse load

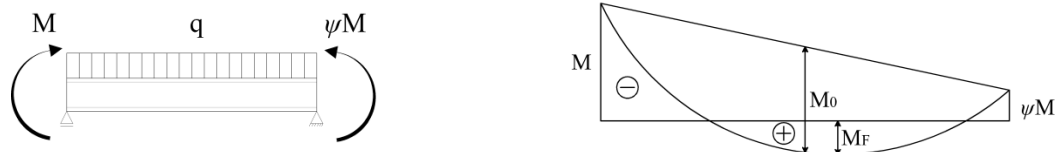


Figure A.1 – Loading case.

Considerations:

$$M_0 = \frac{1}{8}qL^2 \geq 0 \quad -1 \leq \psi \leq 1 \quad M_0 \leq 0 \quad M_F = M_0 + \frac{1+\psi}{2}M + \frac{(1-\psi)^2}{16}\frac{M^2}{M_0} \quad (\text{A.5})$$

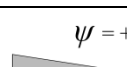
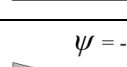
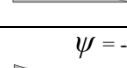
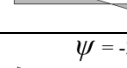
Table A.5 – Values of factor  $C_1$  ( $k_{wt} = 0.235$ ;  $\psi$ ;  $M_0/M$ ) ( $k_z=k_w=1$ ).

$C_1$	$M_0/M$										
	0	-0,25	-0,5	-0,75	-1	-1,25	-1,5	-1,75	-2	-10	$-\infty$
$\psi$	<b>1</b>	1,00	1,28	1,75	2,67	4,36	4,61	2,59	1,69	1,24	
	<b>0,9</b>	1,06	1,37	1,93	3,03	4,70	4,14	2,36	1,58	1,23	
	<b>0,8</b>	1,11	1,46	2,11	3,40	5,05	3,66	2,14	1,47	1,22	
	<b>0,7</b>	1,17	1,56	2,29	3,77	5,31	3,19	1,92	1,36	1,21	
	<b>0,6</b>	1,24	1,68	2,52	4,11	5,07	2,78	1,75	1,26	1,21	
	<b>0,5</b>	1,32	1,82	2,77	4,34	4,54	2,48	1,63	1,22	1,20	
	<b>0,4</b>	1,39	1,95	3,01	4,65	4,01	2,18	1,49	1,18	1,19	
	<b>0,3</b>	1,48	2,11	3,26	4,77	3,34	1,98	1,39	1,20	1,19	
	<b>0,2</b>	1,58	2,27	3,49	4,64	2,84	1,80	1,30	1,20	1,19	
	<b>0,1</b>	1,68	2,44	3,73	4,26	2,47	1,64	1,23	1,19	1,18	
	<b>0,0</b>	1,79	2,61	3,83	3,74	2,23	1,53	1,20	1,19	1,18	1,16
	<b>-0,1</b>	1,90	2,79	3,99	3,26	1,96	1,39	1,18	1,18	1,17	
	<b>-0,2</b>	2,03	2,96	3,97	2,76	1,79	1,29	1,19	1,18	1,17	
	<b>-0,3</b>	2,15	3,11	3,75	2,38	1,63	1,23	1,19	1,18	1,17	
	<b>-0,4</b>	2,28	3,28	3,29	2,10	1,49	1,21	1,19	1,18	1,17	
	<b>-0,5</b>	2,40	3,27	2,84	1,92	1,40	1,21	1,19	1,17	1,17	
	<b>-0,6</b>	2,54	3,18	2,47	1,70	1,30	1,20	1,19	1,17	1,16	
	<b>-0,7</b>	2,65	2,93	2,19	1,56	1,25	1,21	1,19	1,17	1,16	
	<b>-0,8</b>	2,65	2,83	1,99	1,49	1,25	1,21	1,19	1,17	1,16	
	<b>-0,9</b>	2,64	2,77	1,81	1,43	1,26	1,21	1,19	1,17	1,16	
	<b>-1</b>	2,62	2,71	1,63	1,36	1,26	1,22	1,19	1,17	1,16	

### A.3 – ECCS – Basis Load Cases

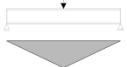
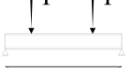
- End Moment Loading

Table A.6 – Values of factors  $C_1$  and  $C_3$  corresponding to various end moment ratio  $\psi$ , values of buckling length factor  $k_z$  and cross-section parameters  $\psi_f$  and  $k_{wt}$  ( $k_w=1$ ).

Loading and Support Conditions	Bending Moment Diagram	$\psi$	$k_z$	Values of factors				
				$C_1$	$C_3$			
					$\psi_f < 0$	$\psi_f > 0$		
	 $\psi = 1$	1	1	1,000	1,000			
			0,5	1,050	1,019			
	 $\psi = +3/4$	0,75	1	1,140	1,000			
			0,5	1,190	1,017			
	 $\psi = +1/2$	0,5	1	1,310	1,000			
			0,5	1,370	1,000			
	 $\psi = +1/4$	0,25	1	1,520	1,000			
			0,5	1,600	1,000			
	 $\psi = 0$	0	1	1,770	1,000			
			0,5	1,860	1,000			
	 $\psi = -1/4$	-0,25	1	2,060	1,000	0,850		
			0,5	2,150	1,000	0,650		
	 $\psi = -1/2$	-0,5	1	2,350	1,000	$1,3 - 1,2\psi_f$		
			0,5	2,420	0,950	$0,77 - \psi_f$		
	 $\psi = -3/4$	-0,75	1	2,600	1,000	$0,55 - \psi_f$		
			0,5	2,450	0,850	$0,35 - \psi_f$		
	 $\psi = -1$	-1	1	2,600	$-\psi_f$	$-\psi_f$		
			0,5	2,450	$0,125 - 0,7\psi_f$	$-0,125 - 0,7\psi_f$		
In this table the factor $C_1$ should be divide by 1,05, when								
$k_{wt} = \frac{\pi}{k_w L} \sqrt{\frac{EI_w}{GI_T}} \leq 1,0 \text{ but } C_1 \geq 1$								

• Transverse Loading

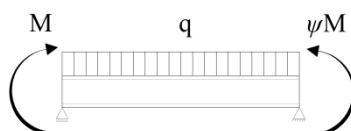
Table A.7 – Values of factors  $C_1$ ,  $C_2$  and  $C_3$  corresponding to various transverse loading cases, values of buckling length factor  $k_z$ , cross section mono symmetry and torsion parameter  $k_{wt}$  ( $k_w=1$ ).

Loading and Support Conditions	$k_z$	Values of factors		
		$C_1$	$C_2$	$C_3$
	<b>1,0</b>	1,120	0,450	0,525
	<b>0,5</b>	0,970	0,360	0,478
	<b>1,0</b>	1,350	0,590	0,411
	<b>0,5</b>	1,050	0,480	0,338
	<b>1,0</b>	1,040	0,420	0,562
	<b>0,5</b>	0,950	0,310	0,539

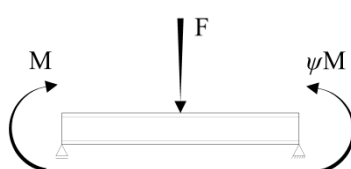
#### A.4 – Galéa

For combined loads cases this solution have  $C_1$  and  $C_2$  values by chart or by tables. ( $k_y=k_w=1$ )

#### Ration of the moment due to transverse load to the maximum moment $\mu$



$$\mu = \frac{qL^2}{8M} \quad (\text{A.6})$$



$$\mu = \frac{FL}{4M} \quad (\text{A.7})$$

The sign convention for  $\mu$  is defined as positive if  $M$  and the transverse load bend the beam in the same direction, and negative in the other situation.

- Combination between end moments and uniformly distributed load  $q$  (by charts)

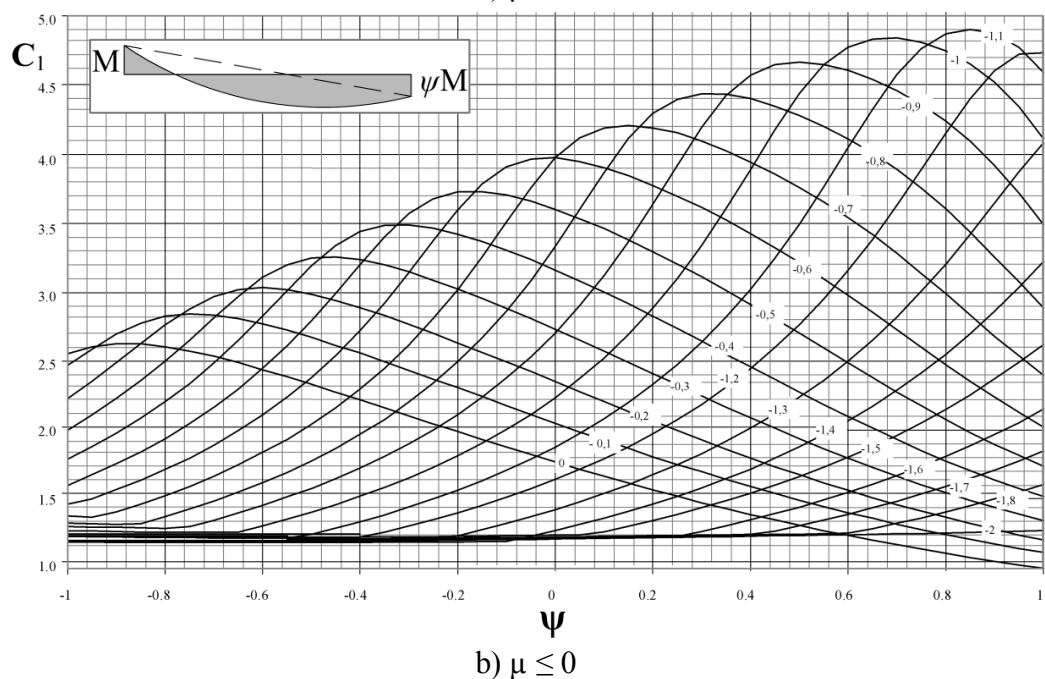
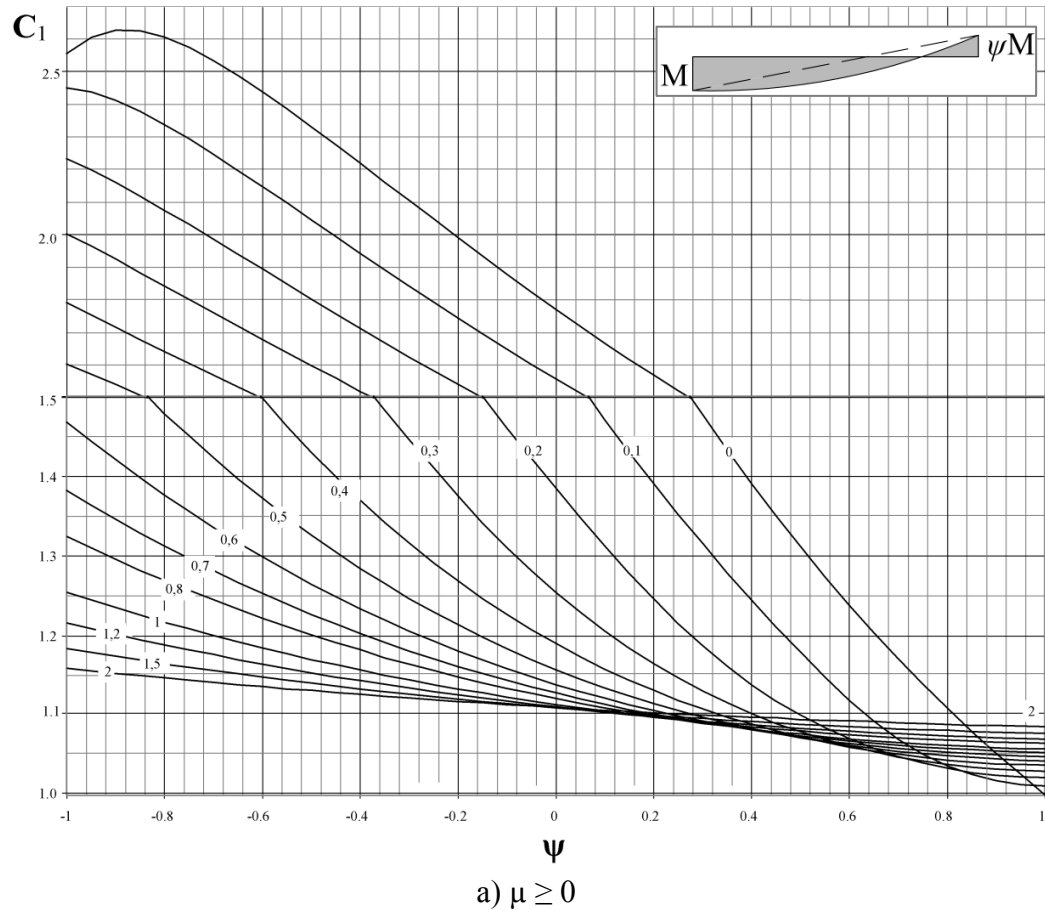


Figure A.2 –  $C_1$  for end moments with uniformly distributed load  $q$ .

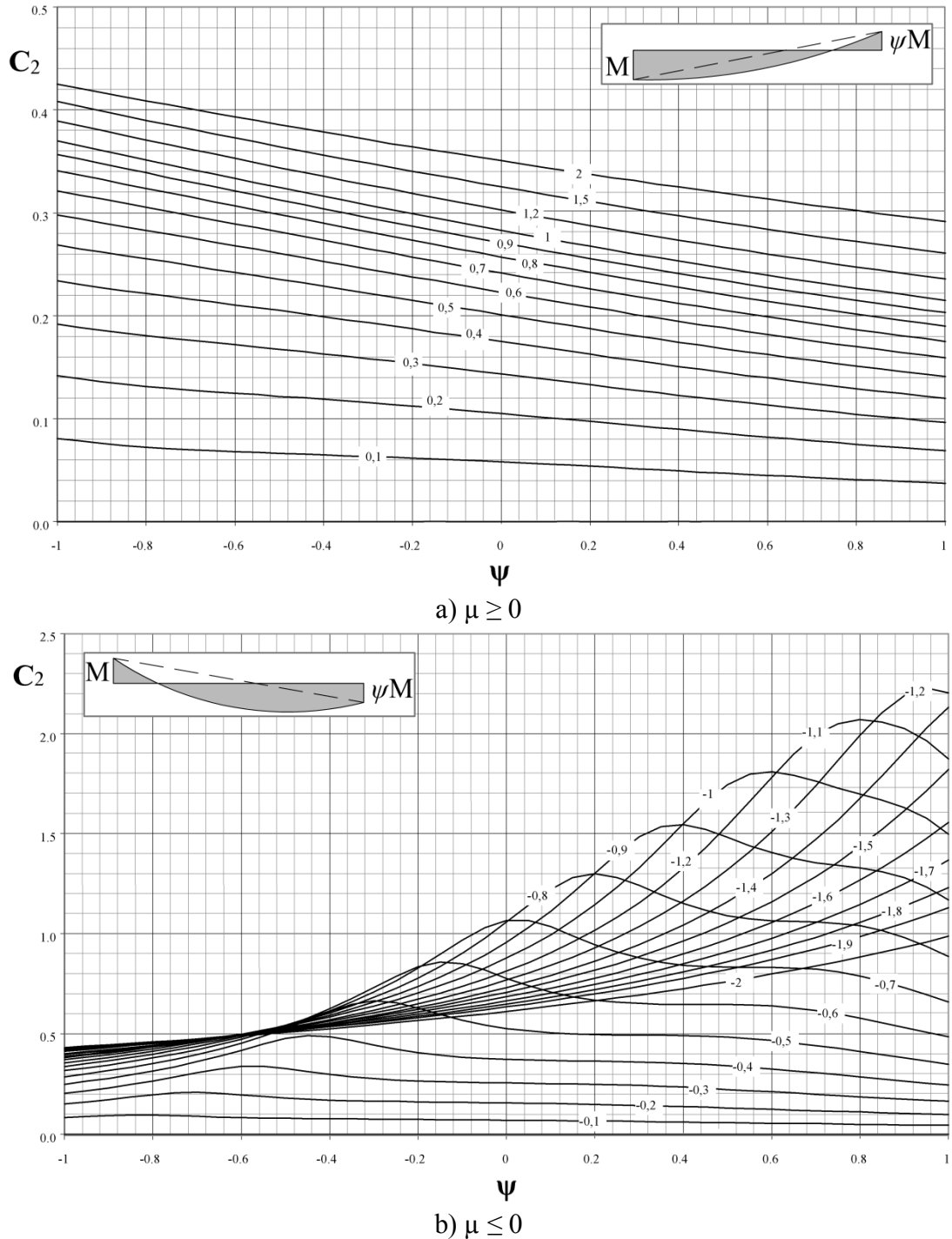


Figure A.3 –  $C_2$  for end moments with uniformly distributed load  $q$ .

- Combination between end moments and concentrated load F (by charts)

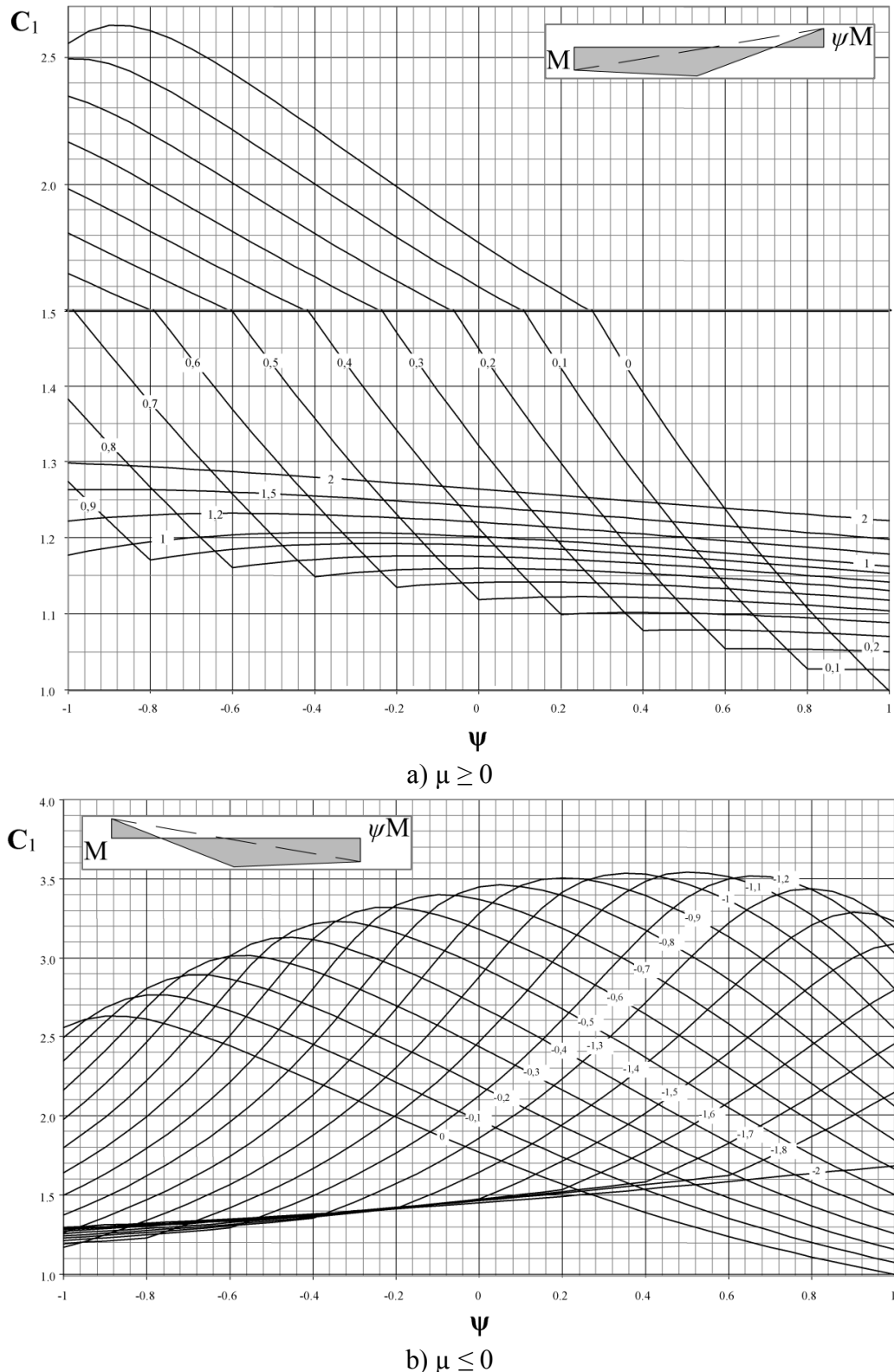


Figure A.4 – C<sub>1</sub> for end moments with concentrated load F.

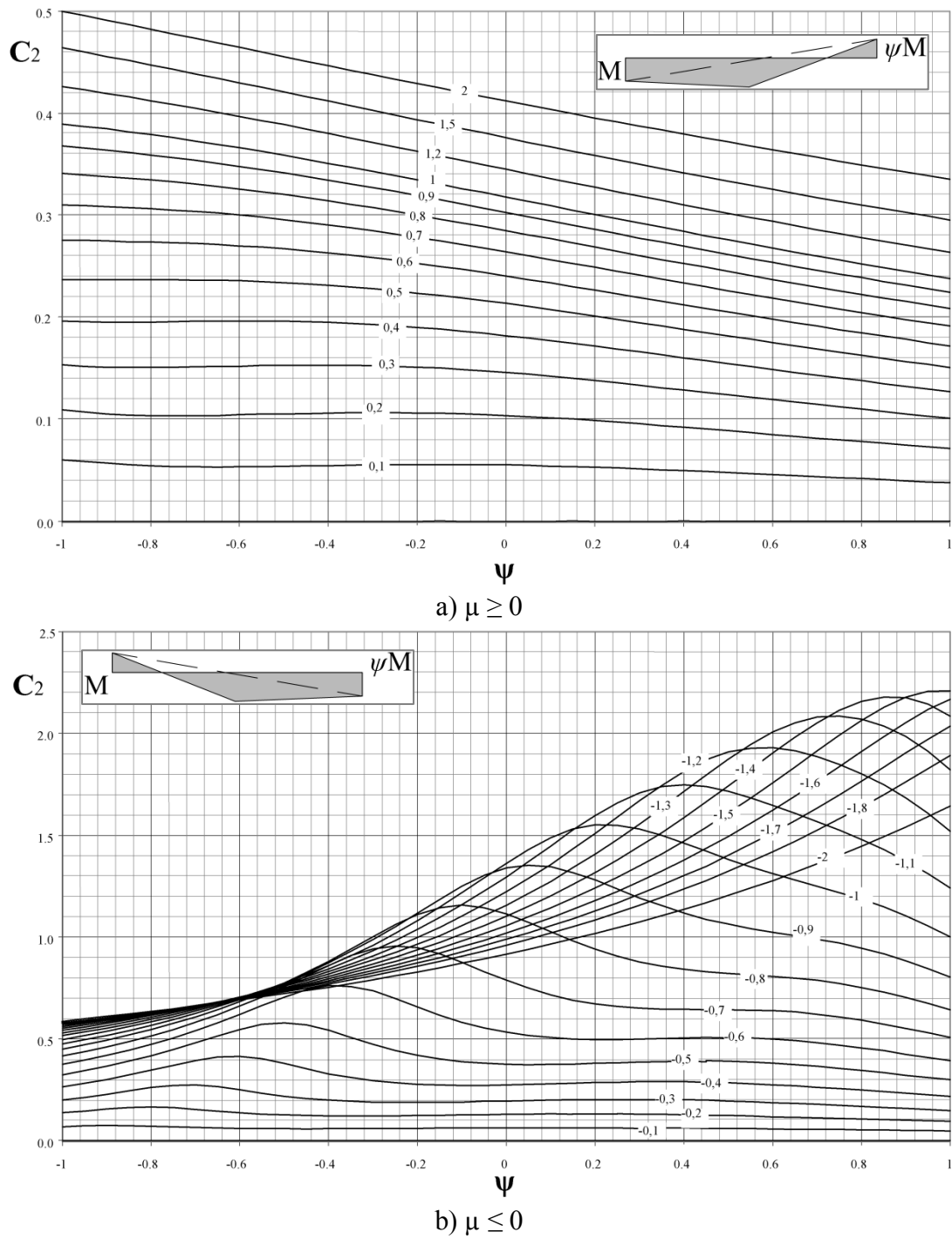


Figure A.5 –  $C_2$  for end moments with concentrated load  $F$ .

- Combination between end moments and uniformly distributed load q (by table)

Table A.8 –  $C_1$  for end moments with uniformly distributed load  $q$  ( $\mu \geq 0$ ).

$C_1$	$\Psi$											$\psi M$									
	-1	-0,9	-0,8	-0,7	-0,6	-0,5	-0,4	-0,3	-0,2	-0,1	0	0,1	0,2	0,3	0,4	0,5	0,6	0,7	0,8	0,9	1
$\infty$	1,127	1,127	1,127	1,127	1,127	1,127	1,127	1,127	1,127	1,127	1,127	1,127	1,127	1,127	1,127	1,127	1,127	1,127	1,127	1,127	1,127
10	1,128	1,127	1,127	1,126	1,125	1,125	1,124	1,123	1,122	1,121	1,120	1,119	1,118	1,118	1,118	1,117	1,117	1,116	1,116	1,116	1,116
7	1,129	1,128	1,127	1,126	1,125	1,124	1,123	1,122	1,121	1,120	1,119	1,118	1,117	1,116	1,115	1,114	1,114	1,113	1,112	1,112	1,112
5	1,132	1,130	1,129	1,127	1,126	1,125	1,124	1,122	1,121	1,119	1,118	1,117	1,116	1,115	1,114	1,112	1,111	1,110	1,108	1,108	1,107
4	1,135	1,133	1,130	1,128	1,126	1,124	1,122	1,121	1,119	1,117	1,115	1,114	1,112	1,111	1,110	1,108	1,107	1,105	1,105	1,104	1,103
3,5	1,137	1,134	1,132	1,130	1,127	1,125	1,122	1,120	1,118	1,116	1,114	1,112	1,111	1,109	1,108	1,106	1,105	1,103	1,102	1,101	1,100
3	1,141	1,138	1,135	1,131	1,128	1,126	1,123	1,120	1,117	1,115	1,113	1,111	1,109	1,107	1,105	1,103	1,102	1,100	1,099	1,098	1,098
2,5	1,148	1,143	1,139	1,135	1,131	1,127	1,124	1,120	1,117	1,114	1,111	1,109	1,107	1,104	1,102	1,100	1,098	1,096	1,094	1,094	1,093
2,2	1,153	1,148	1,143	1,138	1,133	1,129	1,125	1,121	1,117	1,114	1,111	1,107	1,105	1,102	1,100	1,097	1,095	1,093	1,091	1,090	1,089
2	1,159	1,153	1,147	1,141	1,136	1,131	1,126	1,122	1,118	1,114	1,110	1,107	1,103	1,101	1,098	1,095	1,093	1,091	1,089	1,087	1,086
1,8	1,167	1,159	1,153	1,146	1,140	1,134	1,128	1,123	1,118	1,114	1,109	1,106	1,102	1,099	1,096	1,093	1,090	1,088	1,086	1,084	1,083
1,7	1,171	1,164	1,156	1,149	1,142	1,135	1,130	1,124	1,119	1,114	1,109	1,105	1,102	1,098	1,095	1,092	1,089	1,087	1,085	1,083	1,083
1,6	1,177	1,168	1,160	1,152	1,145	1,138	1,131	1,125	1,120	1,114	1,110	1,105	1,101	1,097	1,094	1,091	1,088	1,085	1,083	1,081	1,080
1,5	1,184	1,175	1,165	1,157	1,148	1,141	1,134	1,127	1,121	1,115	1,110	1,105	1,100	1,096	1,092	1,089	1,086	1,083	1,081	1,079	1,078
1,4	1,193	1,181	1,172	1,162	1,153	1,144	1,136	1,129	1,122	1,116	1,110	1,104	1,099	1,095	1,091	1,087	1,084	1,081	1,079	1,077	1,075
1,3	1,203	1,191	1,179	1,168	1,158	1,148	1,139	1,131	1,124	1,117	1,110	1,104	1,099	1,094	1,090	1,086	1,083	1,079	1,077	1,075	1,073
1,2	1,216	1,202	1,189	1,176	1,165	1,154	1,144	1,135	1,126	1,118	1,111	1,104	1,098	1,093	1,088	1,084	1,081	1,077	1,075	1,072	1,071
1,1	1,233	1,217	1,201	1,187	1,174	1,161	1,150	1,139	1,129	1,120	1,112	1,105	1,098	1,092	1,087	1,082	1,078	1,075	1,072	1,070	1,068
1	1,254	1,236	1,217	1,201	1,185	1,170	1,157	1,145	1,133	1,123	1,114	1,105	1,098	1,091	1,085	1,080	1,076	1,072	1,069	1,067	1,065
0,9	1,284	1,261	1,239	1,219	1,201	1,183	1,167	1,153	1,140	1,128	1,117	1,107	1,098	1,091	1,084	1,078	1,073	1,069	1,066	1,063	1,061
0,8	1,324	1,296	1,270	1,245	1,222	1,201	1,182	1,164	1,148	1,134	1,121	1,110	1,100	1,090	1,083	1,076	1,071	1,066	1,062	1,060	1,058
0,7	1,382	1,346	1,313	1,282	1,253	1,227	1,203	1,181	1,161	1,144	1,128	1,114	1,102	1,091	1,082	1,074	1,068	1,063	1,059	1,056	1,054
0,6	1,468	1,421	1,377	1,336	1,299	1,265	1,234	1,206	1,181	1,159	1,139	1,122	1,106	1,093	1,082	1,073	1,065	1,059	1,054	1,051	1,049
0,5	1,604	1,539	1,479	1,423	1,373	1,326	1,284	1,247	1,213	1,184	1,157	1,135	1,115	1,098	1,084	1,072	1,063	1,055	1,049	1,046	1,043
0,4	1,790	1,717	1,642	1,569	1,497	1,430	1,370	1,316	1,269	1,227	1,190	1,159	1,131	1,108	1,089	1,073	1,061	1,051	1,044	1,039	1,037
0,3	2,003	1,925	1,843	1,760	1,678	1,598	1,521	1,446	1,375	1,310	1,254	1,206	1,165	1,131	1,102	1,080	1,062	1,048	1,039	1,033	1,030
0,2	2,233	2,160	2,076	1,986	1,894	1,802	1,712	1,625	1,541	1,461	1,385	1,314	1,246	1,187	1,139	1,101	1,071	1,049	1,034	1,025	1,022
0,1	2,450	2,411	2,337	2,246	2,148	2,046	1,943	1,842	1,744	1,648	1,558	1,472	1,391	1,315	1,245	1,179	1,119	1,070	1,037	1,018	1,012
0	2,554	2,627	2,606	2,534	2,438	2,331	2,219	2,104	1,990	1,878	1,770	1,667	1,569	1,477	1,391	1,312	1,238	1,171	1,109	1,052	1,000

Table A.9 –  $C_1$  for end moments with uniformly distributed load  $q$  ( $\mu \leq 0$ )

$C_1$	$\Psi$	$M$										$\psi M$									
		-1	-0.9	-0.8	-0.7	-0.6	-0.5	-0.4	-0.3	-0.2	-0.1	0	0.1	0.2	0.3	0.4	0.5	0.6	0.7	0.8	0.9
0	2,554	2,627	2,606	2,534	2,438	2,331	2,219	2,104	1,990	1,878	1,770	1,667	1,569	1,477	1,391	1,312	1,238	1,171	1,109	1,052	1,000
-0,1	2,450	2,672	2,805	2,815	2,751	2,653	2,538	2,415	2,288	2,160	2,033	1,909	1,791	1,678	1,573	1,475	1,385	1,302	1,227	1,158	1,095
-0,2	2,233	2,490	2,763	2,972	3,034	2,987	2,890	2,770	2,637	2,497	2,354	2,210	2,069	1,932	1,802	1,680	1,567	1,464	1,371	1,286	1,209
-0,3	2,003	2,231	2,505	2,817	3,108	3,249	3,236	3,149	3,027	2,886	2,735	2,576	2,414	2,252	2,094	1,942	1,800	1,670	1,551	1,444	1,348
-0,4	1,790	1,980	2,210	2,491	2,828	3,190	3,440	3,489	3,423	3,306	3,162	3,001	2,829	2,648	2,463	2,279	2,101	1,934	1,781	1,644	1,522
-0,5	1,604	1,759	1,944	2,171	2,450	2,795	3,201	3,570	3,726	3,703	3,601	3,461	3,296	3,113	2,915	2,705	2,490	2,279	2,081	1,902	1,742
-0,6	1,468	1,570	1,719	1,897	2,115	2,385	2,722	3,140	3,598	3,908	3,971	3,902	3,775	3,614	3,426	3,214	2,979	2,728	2,477	2,240	2,027
-0,7	1,382	1,410	1,530	1,671	1,840	2,046	2,300	2,618	3,020	3,507	3,972	4,191	4,192	4,094	3,945	3,760	3,540	3,281	2,989	2,685	2,400
-0,8	1,324	1,316	1,372	1,486	1,618	1,776	1,967	2,201	2,493	2,862	3,326	3,863	4,290	4,433	4,397	4,276	4,104	3,882	3,600	3,253	2,884
-0,9	1,284	1,278	1,271	1,332	1,438	1,562	1,708	1,882	2,095	2,357	2,685	3,101	3,617	4,175	4,550	4,646	4,584	4,438	4,219	3,898	3,471
-1	1,254	1,250	1,245	1,242	1,291	1,389	1,503	1,637	1,796	1,986	2,218	2,505	2,865	3,317	3,865	4,419	4,754	4,820	4,724	4,498	4,089
-1,1	1,233	1,229	1,226	1,223	1,222	1,248	1,339	1,444	1,566	1,709	1,879	2,083	2,331	2,638	3,019	3,491	4,045	4,574	4,869	4,871	4,590
-1,2	1,216	1,213	1,211	1,209	1,208	1,208	1,208	1,290	1,386	1,496	1,625	1,775	1,954	2,168	2,428	2,746	3,136	3,607	4,133	4,583	4,712
-1,3	1,203	1,201	1,199	1,198	1,197	1,197	1,198	1,200	1,241	1,329	1,429	1,544	1,678	1,834	2,019	2,239	2,504	2,823	3,207	3,648	4,084
-1,4	1,193	1,191	1,190	1,189	1,189	1,189	1,190	1,190	1,195	1,199	1,274	1,364	1,467	1,586	1,723	1,883	2,070	2,292	2,555	2,865	3,221
-1,5	1,184	1,183	1,182	1,182	1,182	1,183	1,184	1,185	1,188	1,191	1,196	1,221	1,303	1,303	1,396	1,501	1,621	1,760	1,920	2,107	2,325
-1,6	1,177	1,176	1,176	1,176	1,176	1,177	1,178	1,180	1,183	1,186	1,190	1,194	1,200	1,245	1,328	1,422	1,528	1,649	1,788	1,946	2,128
-1,7	1,171	1,171	1,171	1,171	1,171	1,172	1,174	1,176	1,178	1,181	1,185	1,189	1,194	1,199	1,207	1,266	1,350	1,444	1,550	1,670	1,805
-1,8	1,167	1,166	1,166	1,167	1,167	1,168	1,170	1,171	1,174	1,177	1,180	1,184	1,189	1,194	1,200	1,207	1,214	1,283	1,366	1,460	1,564
-2	1,159	1,159	1,159	1,160	1,161	1,162	1,163	1,165	1,167	1,170	1,173	1,176	1,180	1,185	1,190	1,195	1,201	1,208	1,215	1,223	1,232
-2,2	1,153	1,154	1,154	1,155	1,156	1,157	1,159	1,160	1,162	1,165	1,167	1,170	1,174	1,178	1,182	1,186	1,192	1,197	1,203	1,209	1,217
-2,5	1,148	1,148	1,148	1,149	1,151	1,152	1,153	1,155	1,157	1,159	1,161	1,164	1,167	1,170	1,173	1,177	1,181	1,185	1,189	1,195	1,201
-3	1,141	1,142	1,143	1,143	1,144	1,144	1,146	1,147	1,148	1,150	1,152	1,154	1,156	1,158	1,160	1,163	1,166	1,169	1,172	1,175	1,179
-3,5	1,137	1,138	1,139	1,140	1,141	1,142	1,143	1,144	1,146	1,147	1,149	1,151	1,152	1,155	1,157	1,159	1,161	1,164	1,167	1,170	1,173
-4	1,135	1,136	1,136	1,137	1,138	1,139	1,140	1,142	1,143	1,144	1,145	1,147	1,149	1,151	1,152	1,154	1,156	1,158	1,160	1,163	1,165
-5	1,132	1,133	1,133	1,134	1,135	1,135	1,136	1,137	1,138	1,139	1,140	1,141	1,142	1,144	1,145	1,146	1,148	1,149	1,151	1,152	1,154
-7	1,129	1,130	1,130	1,131	1,132	1,133	1,133	1,134	1,135	1,136	1,137	1,137	1,138	1,139	1,140	1,141	1,142	1,143	1,144	1,145	1,146
-10	1,128	1,129	1,129	1,130	1,130	1,131	1,131	1,132	1,132	1,133	1,133	1,134	1,134	1,135	1,136	1,136	1,137	1,138	1,139	1,140	1,140
$-\infty$	1,127	1,127	1,127	1,127	1,127	1,127	1,127	1,127	1,127	1,127	1,127	1,127	1,127	1,127	1,127	1,127	1,127	1,127	1,127	1,127	1,127

Table A.10 –  $C_2$  for end moments with uniformly distributed load  $q$  ( $\mu \geq 0$ ).

$C_2$	$\Psi$	$\frac{\psi M}{M}$									
		-1	-0,9	-0,8	-0,7	-0,6	-0,5	-0,4	-0,3	-0,2	-0,1
$\infty$	0,454	0,454	0,454	0,454	0,454	0,454	0,454	0,454	0,454	0,454	0,454
10	0,449	0,447	0,445	0,442	0,440	0,438	0,436	0,433	0,431	0,429	0,427
7	0,448	0,445	0,442	0,439	0,435	0,432	0,429	0,426	0,423	0,420	0,418
5	0,446	0,442	0,437	0,433	0,429	0,425	0,421	0,417	0,413	0,409	0,406
4	0,444	0,438	0,433	0,428	0,424	0,419	0,414	0,409	0,405	0,400	0,396
3,5	0,441	0,436	0,430	0,425	0,419	0,414	0,409	0,404	0,398	0,393	0,389
3	0,438	0,432	0,426	0,420	0,413	0,408	0,402	0,396	0,390	0,385	0,380
2,5	0,433	0,426	0,419	0,412	0,406	0,399	0,392	0,386	0,380	0,374	0,368
2,2	0,429	0,421	0,414	0,406	0,399	0,392	0,385	0,378	0,371	0,365	0,358
2	0,425	0,417	0,409	0,401	0,393	0,386	0,378	0,371	0,364	0,357	0,351
1,8	0,420	0,411	0,403	0,394	0,386	0,379	0,371	0,363	0,356	0,349	0,342
1,7	0,416	0,408	0,399	0,391	0,383	0,375	0,367	0,359	0,351	0,344	0,337
1,6	0,413	0,404	0,395	0,386	0,378	0,370	0,362	0,354	0,346	0,339	0,331
1,5	0,408	0,399	0,390	0,381	0,373	0,364	0,356	0,348	0,340	0,333	0,325
1,4	0,403	0,394	0,385	0,376	0,367	0,359	0,350	0,342	0,334	0,326	0,318
1,3	0,397	0,387	0,378	0,369	0,360	0,352	0,343	0,335	0,327	0,319	0,311
1,2	0,389	0,380	0,371	0,362	0,353	0,344	0,336	0,327	0,319	0,311	0,303
1,1	0,380	0,371	0,362	0,353	0,344	0,335	0,327	0,318	0,310	0,302	0,294
1	0,370	0,361	0,352	0,342	0,334	0,325	0,316	0,308	0,299	0,291	0,283
0,9	0,357	0,348	0,339	0,330	0,321	0,313	0,304	0,296	0,287	0,279	0,271
0,8	0,341	0,332	0,324	0,315	0,307	0,298	0,290	0,282	0,273	0,265	0,257
0,7	0,322	0,313	0,305	0,297	0,289	0,281	0,273	0,265	0,257	0,249	0,241
0,6	0,298	0,290	0,283	0,276	0,268	0,261	0,253	0,245	0,238	0,230	0,223
0,5	0,269	0,262	0,255	0,249	0,242	0,236	0,229	0,222	0,215	0,208	0,201
0,4	0,224	0,227	0,222	0,216	0,211	0,205	0,199	0,193	0,187	0,181	0,174
0,3	0,192	0,186	0,181	0,176	0,172	0,167	0,163	0,158	0,154	0,149	0,144
0,2	0,142	0,136	0,131	0,128	0,125	0,122	0,119	0,116	0,112	0,109	0,105
0,1	0,081	0,076	0,072	0,070	0,068	0,066	0,065	0,063	0,062	0,060	0,058
0	0,000	0,000	0,000	0,000	0,000	0,000	0,000	0,000	0,000	0,000	0,000

Table A.11 –  $C_2$  for end moments with uniformly distributed load  $q$  ( $\mu \leq 0$ ).

$C_2$	$\Psi$	$\psi M$									
		-1	-0.9	-0.8	-0.7	-0.6	-0.5	-0.4	-0.3	-0.2	-0.1
0	0	0,000	0,000	0,000	0,000	0,000	0,000	0,000	0,000	0,000	0,000
-0,1	0,083	0,094	0,096	0,089	0,083	0,080	0,077	0,076	0,074	0,073	0,071
-0,2	0,150	0,172	0,197	0,209	0,181	0,171	0,165	0,161	0,159	0,156	0,153
-0,3	0,205	0,232	0,265	0,307	0,338	0,328	0,298	0,277	0,266	0,259	0,256
-0,4	0,250	0,279	0,315	0,360	0,418	0,477	0,487	0,445	0,406	0,384	0,372
-0,5	0,287	0,316	0,352	0,396	0,453	0,526	0,612	0,665	0,629	0,567	0,526
-0,6	0,317	0,345	0,380	0,421	0,474	0,540	0,625	0,731	0,834	0,849	0,777
-0,7	0,340	0,368	0,400	0,439	0,486	0,544	0,617	0,710	0,829	0,968	1,067
-0,8	0,358	0,385	0,415	0,451	0,493	0,544	0,606	0,683	0,780	0,904	1,058
-0,9	0,373	0,398	0,427	0,460	0,498	0,542	0,596	0,660	0,738	0,836	0,938
-1	0,385	0,409	0,435	0,465	0,500	0,540	0,586	0,640	0,705	0,783	0,878
-1,1	0,394	0,417	0,442	0,469	0,501	0,536	0,577	0,624	0,678	0,742	0,819
-1,2	0,402	0,423	0,446	0,472	0,500	0,532	0,569	0,609	0,656	0,710	0,773
-1,3	0,409	0,428	0,448	0,474	0,500	0,529	0,561	0,597	0,638	0,685	0,737
-1,4	0,414	0,433	0,453	0,475	0,499	0,525	0,555	0,587	0,623	0,664	0,709
-1,5	0,419	0,436	0,455	0,475	0,498	0,522	0,549	0,578	0,610	0,646	0,685
-1,6	0,422	0,439	0,457	0,476	0,497	0,519	0,543	0,570	0,599	0,631	0,666
-1,7	0,426	0,441	0,458	0,476	0,495	0,516	0,539	0,563	0,589	0,618	0,650
-1,8	0,428	0,443	0,459	0,476	0,494	0,513	0,534	0,557	0,581	0,607	0,635
-2	0,433	0,446	0,461	0,476	0,492	0,509	0,527	0,546	0,567	0,589	0,612
-2,2	0,436	0,448	0,461	0,475	0,489	0,504	0,520	0,537	0,555	0,574	0,594
-2,5	0,440	0,451	0,462	0,474	0,486	0,499	0,513	0,527	0,542	0,558	0,574
-3	0,444	0,453	0,462	0,472	0,482	0,492	0,503	0,514	0,526	0,538	0,551
-3,5	0,447	0,454	0,462	0,470	0,479	0,487	0,496	0,505	0,515	0,525	0,545
-4	0,448	0,455	0,462	0,469	0,476	0,483	0,491	0,499	0,507	0,515	0,524
-5	0,450	0,455	0,461	0,466	0,472	0,478	0,483	0,490	0,496	0,502	0,508
-7	0,452	0,456	0,459	0,463	0,467	0,471	0,475	0,479	0,483	0,487	0,492
-10	0,453	0,455	0,458	0,461	0,463	0,466	0,469	0,471	0,474	0,477	0,480
$-\infty$	0,454	0,454	0,454	0,454	0,454	0,454	0,454	0,454	0,454	0,454	0,454

- Combination between end moments and concentrated load F (by tables)

Table A.12 – C<sub>1</sub> for end moments with concentrated load F ( $\mu \geq 0$ ).

C <sub>1</sub>	$\Psi$	$\mu M$	M									
			-1	-0.9	-0.8	-0.7	-0.6	-0.5	-0.4	-0.3	-0.2	-0.1
$\infty$	1,348	1,348	1,348	1,348	1,348	1,348	1,348	1,348	1,348	1,348	1,348	1,348
10	1,346	1,344	1,342	1,341	1,339	1,337	1,336	1,334	1,332	1,331	1,329	1,327
7	1,343	1,341	1,339	1,337	1,334	1,332	1,330	1,328	1,326	1,323	1,321	1,319
5	1,339	1,337	1,334	1,334	1,331	1,328	1,325	1,322	1,320	1,317	1,314	1,311
4	1,335	1,332	1,328	1,325	1,322	1,319	1,316	1,312	1,309	1,306	1,303	1,300
3,5	1,331	1,328	1,324	1,321	1,317	1,314	1,311	1,307	1,304	1,300	1,297	1,293
3	1,325	1,322	1,318	1,315	1,311	1,307	1,304	1,300	1,296	1,293	1,289	1,285
2,5	1,315	1,312	1,309	1,305	1,302	1,298	1,294	1,290	1,287	1,283	1,279	1,275
2,2	1,306	1,303	1,300	1,297	1,294	1,290	1,286	1,282	1,278	1,274	1,270	1,266
2	1,298	1,296	1,293	1,290	1,287	1,283	1,279	1,276	1,272	1,268	1,264	1,260
1,8	1,287	1,286	1,283	1,281	1,278	1,275	1,271	1,268	1,264	1,260	1,256	1,252
1,7	1,280	1,279	1,277	1,275	1,273	1,270	1,266	1,263	1,259	1,255	1,251	1,247
1,6	1,273	1,272	1,271	1,269	1,267	1,264	1,261	1,258	1,254	1,250	1,246	1,242
1,5	1,263	1,263	1,263	1,262	1,260	1,258	1,255	1,252	1,248	1,245	1,243	1,239
1,4	1,252	1,253	1,254	1,253	1,252	1,250	1,248	1,245	1,242	1,238	1,235	1,231
1,3	1,238	1,241	1,243	1,243	1,243	1,241	1,240	1,237	1,235	1,231	1,227	1,223
1,2	1,222	1,227	1,230	1,231	1,232	1,231	1,230	1,229	1,226	1,223	1,219	1,216
1,1	1,202	1,209	1,214	1,217	1,219	1,220	1,219	1,218	1,217	1,214	1,211	1,208
1	1,177	1,187	1,194	1,200	1,203	1,206	1,207	1,206	1,205	1,204	1,201	1,199
0,9	1,273	1,221	1,170	1,179	1,185	1,189	1,191	1,192	1,192	1,190	1,188	1,184
0,8	1,383	1,324	1,267	1,213	1,161	1,168	1,173	1,175	1,177	1,175	1,173	1,170
0,7	1,508	1,442	1,378	1,317	1,258	1,203	1,150	1,155	1,158	1,160	1,159	1,157
0,6	1,650	1,577	1,505	1,436	1,370	1,306	1,246	1,189	1,136	1,140	1,142	1,143
0,5	1,809	1,730	1,651	1,573	1,498	1,426	1,358	1,293	1,231	1,174	1,120	1,122
0,4	1,983	1,901	1,816	1,730	1,646	1,564	1,486	1,412	1,342	1,276	1,213	1,155
0,3	2,168	2,089	2,000	1,908	1,815	1,724	1,636	1,551	1,470	1,394	1,322	1,192
0,2	2,348	2,285	2,200	2,105	2,006	1,906	1,807	1,711	1,619	1,532	1,449	1,371
0,1	2,494	2,475	2,408	2,317	2,216	2,109	2,002	1,896	1,792	1,693	1,597	1,507
0	2,554	2,627	2,606	2,534	2,438	2,331	2,219	2,104	1,990	1,878	1,770	1,667

Table A.13 – C<sub>1</sub> for end moments with concentrated load F ( $\mu \leq 0$ ).

$C_1$	$\psi M$									
	-1	-0,9	-0,8	-0,7	-0,6	-0,5	-0,4	-0,3	-0,2	-0,1
0	2,554	2,627	2,606	2,534	2,438	2,331	2,219	2,104	1,990	1,878
-0,1	2,494	2,682	2,760	2,737	2,663	2,563	2,451	2,333	2,212	2,090
-0,2	2,348	2,597	2,804	2,889	2,868	2,792	2,690	2,575	2,451	2,324
-0,3	2,168	2,417	2,689	2,916	3,012	2,994	2,919	2,817	2,700	2,573
-0,4	1,983	2,207	2,472	2,763	3,012	3,124	3,114	3,044	2,943	2,826
-0,5	1,809	2,000	2,231	2,505	2,811	3,083	3,219	3,225	3,163	3,067
-0,6	1,650	1,811	2,004	2,236	2,514	2,828	3,122	3,291	3,322	3,274
-0,7	1,508	1,643	1,802	1,992	2,222	2,496	2,811	3,122	3,332	3,399
-0,8	1,383	1,496	1,627	1,783	1,968	2,189	2,453	2,760	3,080	3,332
-0,9	1,273	1,368	1,478	1,605	1,754	1,931	2,141	2,390	2,681	2,998
-1	1,177	1,258	1,349	1,454	1,576	1,718	1,884	2,080	2,312	2,583
-1,1	1,202	1,220	1,239	1,327	1,427	1,542	1,675	1,831	2,012	2,225
-1,2	1,222	1,239	1,258	1,329	1,427	1,542	1,675	1,831	2,012	2,472
-1,3	1,238	1,255	1,273	1,293	1,314	1,338	1,363	1,465	1,581	1,713
-1,4	1,252	1,268	1,285	1,304	1,324	1,346	1,369	1,395	1,424	1,531
-1,5	1,263	1,278	1,295	1,312	1,331	1,351	1,374	1,397	1,423	1,451
-1,6	1,273	1,287	1,302	1,319	1,337	1,356	1,376	1,398	1,422	1,447
-1,7	1,280	1,294	1,309	1,325	1,341	1,359	1,378	1,398	1,420	1,443
-1,8	1,287	1,300	1,314	1,329	1,345	1,361	1,379	1,398	1,418	1,439
-2	1,298	1,310	1,323	1,336	1,350	1,364	1,380	1,396	1,413	1,431
-2,2	1,306	1,317	1,329	1,341	1,353	1,366	1,380	1,394	1,409	1,425
-2,5	1,315	1,325	1,335	1,345	1,356	1,367	1,379	1,391	1,403	1,416
-3	1,325	1,333	1,341	1,349	1,358	1,367	1,376	1,386	1,395	1,405
-3,5	1,331	1,338	1,344	1,351	1,359	1,366	1,373	1,381	1,389	1,397
-4	1,335	1,341	1,346	1,352	1,359	1,365	1,371	1,378	1,384	1,391
-5	1,339	1,344	1,348	1,353	1,358	1,363	1,367	1,372	1,377	1,382
-7	1,343	1,347	1,350	1,353	1,356	1,359	1,363	1,366	1,369	1,372
-10	1,346	1,348	1,350	1,352	1,356	1,358	1,361	1,363	1,365	1,367
$-\infty$	1,348	1,348	1,348	1,348	1,348	1,348	1,348	1,348	1,348	1,348

Table A.14 – C<sub>2</sub> for end moments with concentrated load F ( $\mu \geq 0$ ).

C <sub>2</sub>	$\Psi$	$\psi M$									
		-1	-0,9	-0,8	-0,7	-0,6	-0,5	-0,4	-0,3	-0,2	-0,1
$\infty$	0,630	0,630	0,630	0,630	0,630	0,630	0,630	0,630	0,630	0,630	0,630
10	0,556	0,552	0,549	0,546	0,543	0,539	0,536	0,533	0,530	0,527	0,524
7	0,553	0,549	0,544	0,540	0,535	0,531	0,527	0,522	0,518	0,514	0,510
5	0,548	0,542	0,536	0,531	0,525	0,519	0,514	0,508	0,503	0,497	0,492
4	0,542	0,535	0,529	0,522	0,515	0,509	0,502	0,496	0,490	0,483	0,477
3,5	0,538	0,530	0,523	0,515	0,508	0,501	0,494	0,487	0,480	0,474	0,467
3	0,530	0,523	0,514	0,507	0,499	0,491	0,484	0,476	0,469	0,461	0,454
2,5	0,519	0,511	0,502	0,494	0,485	0,477	0,469	0,460	0,452	0,444	0,436
2,2	0,509	0,500	0,491	0,483	0,474	0,465	0,457	0,448	0,440	0,431	0,423
2	0,500	0,491	0,482	0,473	0,465	0,456	0,447	0,438	0,429	0,421	0,412
1,8	0,489	0,480	0,471	0,462	0,453	0,444	0,435	0,426	0,417	0,408	0,400
1,7	0,482	0,473	0,464	0,455	0,446	0,437	0,428	0,419	0,410	0,401	0,393
1,6	0,473	0,465	0,456	0,448	0,439	0,430	0,421	0,412	0,403	0,394	0,385
1,5	0,464	0,456	0,448	0,439	0,430	0,421	0,412	0,403	0,394	0,385	0,376
1,4	0,453	0,446	0,437	0,429	0,420	0,412	0,403	0,394	0,385	0,376	0,367
1,3	0,441	0,434	0,426	0,418	0,410	0,401	0,392	0,383	0,375	0,366	0,358
1,2	0,426	0,420	0,413	0,405	0,397	0,389	0,380	0,372	0,363	0,354	0,345
1,1	0,410	0,404	0,397	0,390	0,383	0,375	0,367	0,359	0,350	0,341	0,333
1	0,390	0,385	0,379	0,373	0,366	0,359	0,351	0,343	0,335	0,327	0,318
0,9	0,367	0,363	0,358	0,353	0,347	0,341	0,334	0,326	0,319	0,311	0,303
0,8	0,340	0,337	0,334	0,330	0,325	0,320	0,314	0,307	0,300	0,292	0,284
0,7	0,310	0,308	0,306	0,303	0,300	0,295	0,290	0,284	0,278	0,271	0,264
0,6	0,275	0,273	0,272	0,270	0,267	0,263	0,258	0,253	0,247	0,240	0,233
0,5	0,237	0,236	0,236	0,235	0,234	0,231	0,228	0,223	0,219	0,213	0,207
0,4	0,196	0,195	0,195	0,196	0,196	0,195	0,193	0,190	0,186	0,182	0,177
0,3	0,153	0,151	0,150	0,151	0,152	0,153	0,152	0,151	0,149	0,145	0,142
0,2	0,109	0,105	0,103	0,104	0,105	0,106	0,106	0,106	0,103	0,101	0,099
0,1	0,060	0,057	0,054	0,053	0,053	0,054	0,055	0,056	0,055	0,053	0,051
0	0,000	0,000	0,000	0,000	0,000	0,000	0,000	0,000	0,000	0,000	0,000

Table A.15 – C<sub>2</sub> for end moments with concentrated load F ( $\mu \leq 0$ ).

$C_2$	$\Psi$	$\psi M$									
		-1	-0.9	-0.8	-0.7	-0.6	-0.5	-0.4	-0.3	-0.2	-0.1
0	0,000	0,000	0,000	0,000	0,000	0,000	0,000	0,000	0,000	0,000	0,000
-0,1	0,067	0,073	0,069	0,063	0,059	0,057	0,058	0,059	0,061	0,061	0,060
-0,2	0,134	0,154	0,163	0,151	0,135	0,125	0,121	0,120	0,122	0,125	0,128
-0,3	0,202	0,231	0,263	0,277	0,253	0,222	0,202	0,193	0,191	0,194	0,198
-0,4	0,267	0,304	0,349	0,396	0,416	0,382	0,332	0,298	0,280	0,275	0,277
-0,5	0,326	0,368	0,419	0,482	0,548	0,581	0,543	0,475	0,421	0,391	0,378
-0,6	0,377	0,420	0,474	0,541	0,621	0,707	0,761	0,736	0,658	0,583	0,533
-0,7	0,419	0,463	0,516	0,582	0,662	0,757	0,862	0,943	0,947	0,875	0,787
-0,8	0,452	0,496	0,548	0,610	0,684	0,775	0,882	1,002	1,110	1,156	1,113
-0,9	0,480	0,522	0,571	0,629	0,697	0,779	0,876	0,991	1,122	1,252	1,341
-1	0,502	0,542	0,588	0,642	0,704	0,777	0,863	0,965	1,084	1,220	1,364
-1,1	0,520	0,558	0,601	0,651	0,707	0,773	0,849	0,938	1,041	1,161	1,299
-1,2	0,535	0,571	0,611	0,657	0,709	0,767	0,835	0,913	1,002	1,105	1,224
-1,3	0,547	0,581	0,619	0,661	0,708	0,762	0,822	0,890	0,968	1,057	1,159
-1,4	0,557	0,589	0,624	0,664	0,707	0,756	0,810	0,871	0,940	1,017	1,105
-1,5	0,565	0,596	0,629	0,665	0,706	0,750	0,799	0,854	0,915	0,984	1,060
-1,6	0,572	0,601	0,632	0,666	0,704	0,745	0,790	0,839	0,894	0,955	1,022
-1,7	0,578	0,606	0,635	0,667	0,702	0,740	0,781	0,826	0,876	0,930	0,991
-1,8	0,584	0,609	0,637	0,667	0,700	0,735	0,773	0,815	0,860	0,909	0,963
-2	0,592	0,615	0,640	0,667	0,696	0,726	0,760	0,795	0,833	0,875	0,920
-2,2	0,598	0,620	0,642	0,666	0,692	0,719	0,748	0,779	0,812	0,848	0,886
-2,5	0,605	0,624	0,644	0,665	0,686	0,710	0,734	0,760	0,788	0,817	0,847
-3	0,612	0,628	0,644	0,661	0,679	0,698	0,717	0,737	0,759	0,781	0,804
-3,5	0,617	0,630	0,644	0,658	0,673	0,689	0,705	0,721	0,739	0,756	0,775
-4	0,620	0,632	0,644	0,656	0,669	0,682	0,709	0,724	0,739	0,754	0,770
-5	0,624	0,633	0,642	0,652	0,662	0,672	0,693	0,704	0,715	0,727	0,738
-7	0,627	0,633	0,640	0,647	0,653	0,660	0,667	0,675	0,682	0,689	0,697
-10	0,628	0,633	0,637	0,642	0,647	0,651	0,666	0,671	0,676	0,681	0,686
$-\infty$	0,630	0,630	0,630	0,630	0,630	0,630	0,630	0,630	0,630	0,630	0,630

### A.5 – Andrade et al.

In the main formula the length factors  $k_z$  and  $k_w$  are equal to 2 and 1 respectively in both cases. The solution is limited to the range  $0,1 \leq \bar{K} \leq 2,5$ .

- **Cantilever with warping prevented at the fixed end**

Table A.16 – Values of  $C_1$  and  $C_2$  for cantilevers with warping prevent at the fixed end.

Loading	Values of factors		
	$C_1$	$C_2$	
		Top flange loading	Bottom flange loading
	$\frac{2,462}{\sqrt{1+\bar{K}^2}} + \frac{2,383\bar{K}}{\sqrt{1+\bar{K}^2}}$	$0,380 + 2,092\bar{K} - 0,318\bar{K}^2$	$0,512 + 0,370\bar{K} - 0,033\bar{K}^2$
	$\frac{3,962}{\sqrt{1+\bar{K}^2}} + \frac{5,531\bar{K}}{\sqrt{1+\bar{K}^2}}$	$1,130 + 1,539\bar{K} - 0,176\bar{K}^2$	$1,049 + 0,234\bar{K} + 0,020\bar{K}^2$

Table A.17 – Values of  $C_3$  for cantilevers with warping prevent at the fixed end.

Loading	Values of Factors	
	$C_3$	
	<b>Top flange loading</b>	$1,520 - 1,342\psi_f - 0,010\psi_f^2 - 0,424\psi_f^3 +$ $+ (0,162 + 2,419\psi_f + 0,875\psi_f^2 + 0,400\psi_f^3)\bar{K} +$ $+ (0,148 - 0,623\psi_f - 0,216\psi_f^2 + 0,141\psi_f^3)\bar{K}^2$
	<b>Shear center loading</b>	$1,808 - 0,944\psi_f + 0,299\psi_f^2 - 0,061\psi_f^3 +$ $+ (0,060 + 1,235\psi_f - 0,574\psi_f^2 - 0,337\psi_f^3)\bar{K} +$ $+ (0,128 - 0,409\psi_f + 0,047\psi_f^2 + 0,237\psi_f^3)\bar{K}^2$
	<b>Bottom flange loading</b>	$1,966 - 0,792\psi_f + 0,139\psi_f^2 - 0,341\psi_f^3 +$ $+ (0,061 + 0,549\psi_f + 0,077\psi_f^2 - 0,206\psi_f^3)\bar{K} +$ $+ (0,064 - 0,135\psi_f - 0,050\psi_f^2 + 0,058\psi_f^3)\bar{K}^2$
	<b>Top flange loading</b>	$2,441 - 1,589\psi_f + 0,176\psi_f^2 - 0,658\psi_f^3 +$ $+ (-0,412 + 2,442\psi_f + 0,635\psi_f^2 + 0,261\psi_f^3)\bar{K} +$ $+ (0,273 - 0,601\psi_f - 0,140\psi_f^2 + 0,205\psi_f^3)\bar{K}^2$
	<b>Shear center loading</b>	$2,609 - 1,801\psi_f + 0,552\psi_f^2 + 0,461\psi_f^3 +$ $+ (-0,445 + 2,251\psi_f - 0,620\psi_f^2 - 0,1443\psi_f^3)\bar{K} +$ $+ (0,244 - 0,701\psi_f - 0,044\psi_f^2 + 0,611\psi_f^3)\bar{K}^2$
	<b>Bottom flange loading</b>	$2,793 - 1,235\psi_f + 0,428\psi_f^2 - 0,630\psi_f^3 +$ $+ (-0,495 + 1,008\psi_f - 0,134\psi_f^2 - 0,095\psi_f^3)\bar{K} +$ $+ (0,194 - 0,263\psi_f - 0,003\psi_f^2 + 0,060\psi_f^3)\bar{K}^2$

$\psi_f$  is limited to the range  $-0,8 \leq \psi_f \leq 0,8$ .

- Cantilever with warping free at the fixed end

Table A.18 – Values of  $C_1$  and  $C_2$  for cantilevers with warping free at the fixed end.

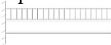
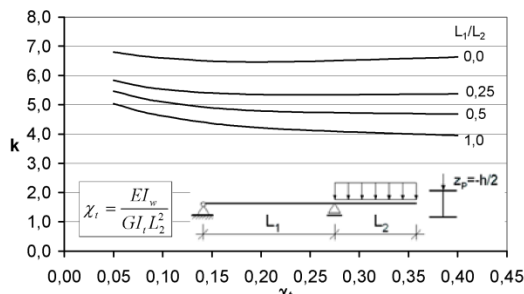
Loading	Values of factors		
	$C_1$	$C_2$	
		Top flange loading	Bottom flange loading
	$\frac{2,437}{\sqrt{1 + \bar{K}^2}} + \frac{0,613\bar{K}}{\sqrt{1 + \bar{K}^2}} - \frac{0,105\bar{K}^2}{\sqrt{1 + \bar{K}^2}}$	$0,409 + 1,444\bar{K} + 0,070\bar{K}^2$	$0,529 + 0,234\bar{K} + 0,149\bar{K}^2$
	$\frac{3,840}{\sqrt{1 + \bar{K}^2}} + \frac{1,496\bar{K}}{\sqrt{1 + \bar{K}^2}} - \frac{0,247\bar{K}}{\sqrt{1 + \bar{K}^2}}$	$0,987 + 1,420\bar{K} + 0,165\bar{K}^2$	$1,028 + 0,388\bar{K} + 0,150\bar{K}^2$

Table A.19 – Values of  $C_3$  for cantilevers with warping free at the fixed end.

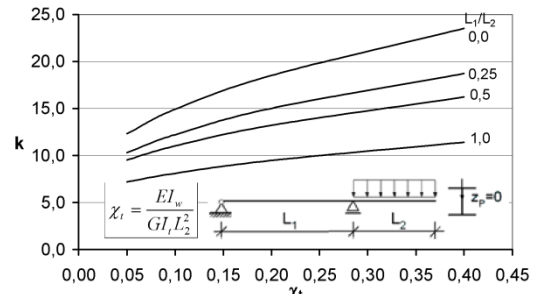
Loading	Values of Factors		
	$C_3$		
	<b>Top flange loading</b>	$1,732 - 0,648\psi_f - 0,062\psi_f^2 + 0,059\psi_f^3 +$ $(0,066 + 1,539\psi_f + 0,520\psi_f^2 - 0,032\psi_f^3)\bar{K} +$ $(0,446 + 0,221\psi_f - 0,037\psi_f^2 + 0,066\psi_f^3)\bar{K}^2$	
		$2,021 + 0,361\psi_f + 0,176\psi_f^2 - 0,655\psi_f^3 +$ $(0,242 + 0,120\psi_f - 0,426\psi_f^2 + 0,891\psi_f^3)\bar{K} +$ $(0,337 + 0,052\psi_f - 0,198\psi_f^2 - 0,099\psi_f^3)\bar{K}^2$	
		$2,156 - 0,055\psi_f + 0,101\psi_f^2 - 0,079\psi_f^3 +$ $(0,435 + 0,168\psi_f - 0,083\psi_f^2 + 0,077\psi_f^3)\bar{K} +$ $(0,238 - 0,022\psi_f - 0,011\psi_f^2 - 0,030\psi_f^3)\bar{K}^2$	
	<b>Shear center loading</b>	$2,669 - 0,815\psi_f + 0,071\psi_f^2 - 0,066\psi_f^3 +$ $(0,113 + 1,812\psi_f + 0,359\psi_f^2 + 0,007\psi_f^3)\bar{K} +$ $(0,499 + 0,289\psi_f + 0,043\psi_f^2 + 0,081\psi_f^3)\bar{K}^2$	
		$3,036 + 0,310\psi_f + 0,306\psi_f^2 - 0,888\psi_f^3 +$ $(0,066 + 0,036\psi_f - 0,585\psi_f^2 + 1,180\psi_f^3)\bar{K} +$ $(0,462 + 0,098\psi_f - 0,227\psi_f^2 - 0,123\psi_f^3)\bar{K}^2$	
		$3,277 - 0,350\psi_f + 0,348\psi_f^2 - 0,263\psi_f^3 +$ $(0,190 + 0,348\psi_f - 0,195\psi_f^2 - 1,137\psi_f^3)\bar{K} +$ $(0,395 + 0,071\psi_f - 0,009\psi_f^2 + 0,009\psi_f^3)\bar{K}^2$	
$\psi_f$ is limited to the range $-0,8 \leq \psi_f \leq 0,8$ .			

## A.6 – Lindner

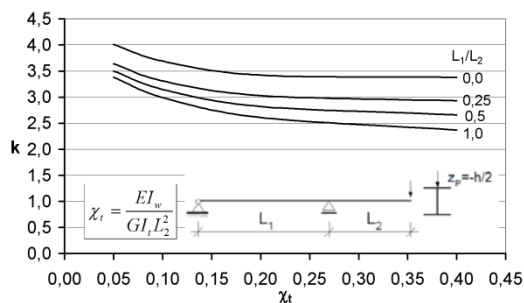
- Single beam with cantilever



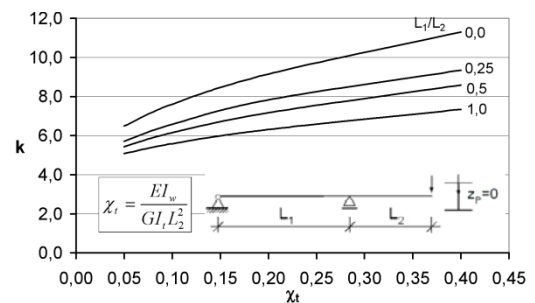
a) Distributed load at flange



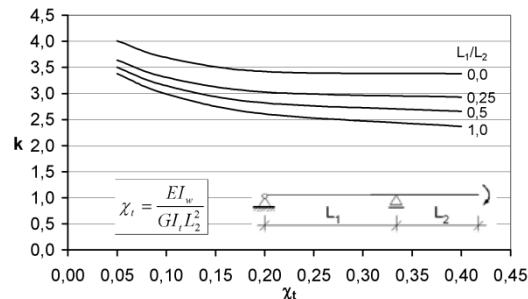
b) Distributed load at shear center



c) Point load at top flange



d) Point load at shear center



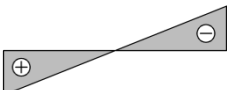
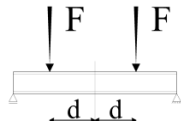
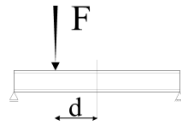
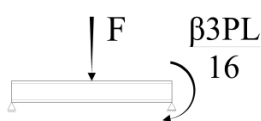
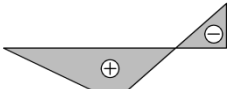
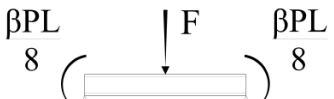
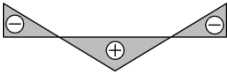
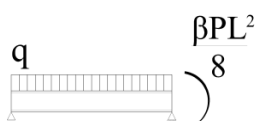
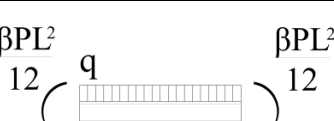
e) End moment at tip of cantilever

Figure A.6 – Values of  $k$  for single double symmetric beams with cantilever.

### A.7 – Trahair

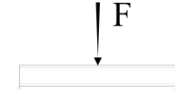
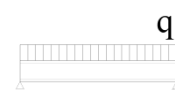
- Simply supported beams

Table A.20 – Values of  $\alpha_m$  for doubly symmetric beams with loads at shear center ( $k_z=k_w=1$ ).

Loading and Support Conditions	Bending Moment Diagram	$\alpha_m$	Range
		$1,75 + 1,05\beta + 0,3\beta^2 \leq 2,5$	$-1 \leq \beta \leq 1$
		$1,0 + 0,35(1 - \frac{2d}{L})^2$	$0 \leq \frac{2d}{L} \leq 1$
		$1,35 + 0,4(\frac{2d}{L})^2$	$0 \leq \frac{2d}{L} \leq 1$
		$1,35 + 0,15\beta$	$0 \leq \beta \leq 0,89$
		$-1,2 + 3,0\beta$	$0,89 \leq \beta \leq 1$
		$1,35 + 0,36\beta$	$0 \leq \beta \leq 1$
		$1,13 + 0,10\beta$	$0 \leq \beta \leq 0,7$
		$-1,25 + 3,5\beta$	$0,7 \leq \beta \leq 1$
		$1,13 + 0,12\beta$	$0 \leq \beta \leq 0,75$
		$-2,38 + 4,8\beta$	$0,75 \leq \beta \leq 1$

- Mono symmetric beam

Table A.21 – Critical moment for mono symmetric beams with loads at shear center  
( $k_z = k_w = 1$ ).

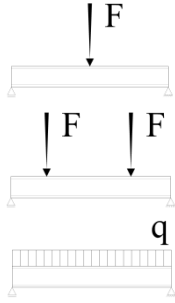
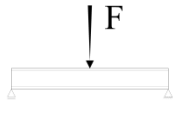
Mono Symmetric	
Loading and Support Conditions	Formulation
End Moments	$M_{cr} = \alpha_m \frac{\pi}{L} \sqrt{EI_T GI_z} \left\{ \sqrt{1 + 4 \left( \frac{I_{fc}}{I_z} \right) \left( 1 - \left( \frac{I_{fc}}{I_z} \right) \right)} f_1 \bar{K}^2 + \left( \frac{f_2 \bar{K} \beta_y^*}{h_m} \right)^2 + \frac{f_2 \bar{K}^2 \beta_y^*}{h_m} \right\}$
	$f_1 = 1 + 3 \left( \frac{\beta_y^*}{h_m} \right)^2 \frac{(1 + \beta)^n}{2^n}$
	$f_2 = \alpha_m \frac{(1 - \beta)}{2} + 2 \left( \frac{\beta_y^*}{h_m} \right) \frac{(1 + \beta)^n}{2^n}$
	$n = 9 \frac{\left( 1 + \left( \frac{I_{fc}}{I_z} \right) \right)}{1 + \bar{K}}$
Transverse Loads	$M_{cr} = \alpha_m M_{cr}^{basic} \left\{ \sqrt{1 + \left( \frac{0,4 \alpha_m f_3 \beta_y^*}{2 M_{cr}^{basic} / N_{cr,z}} \right)^2} + \frac{0,4 \alpha_m f_3 \beta_y^*}{2 M_{cr}^{basic} / N_{cr,z}} \right\}$
	$f_3 = \frac{\pi^2}{8} - \frac{1}{2}$
	$f_3 = \frac{\pi^2}{6} - \frac{1}{2}$

Where  $\beta_y^*$  is given by

$$\beta_y^* = \int_A (y^2 + z^2) \frac{z}{I_y} dA + z_s \Leftrightarrow \beta_y^* = -2z_j \quad (\text{A.8})$$

- Load out of shear center

Table A.22 – Critical moment for doubly and mono symmetric beams with loads out of shear center ( $k_z=k_w=1$ ).

Load Position	
Loading and Support Conditions	Formulation
<b>Double Symmetric</b> 	$M_{cr} = \alpha_m M_{cr}^{basic} \left\{ \sqrt{1 + \left( \frac{0,4\alpha_m z_a}{M_{cr}^{basic}/N_{cr,z}} \right)^2} + \frac{0,4\alpha_m z_a}{M_{cr}^{basic}/N_{cr,z}} \right\}$
<b>Mono Symmetric</b> 	$M_{cr} = \alpha_m M_{cr}^{basic} \left\{ \sqrt{1 + \gamma^2} + \gamma \right\}$ $\text{with } \gamma = \frac{0,4\alpha_m(z_a - z_s) + f_3\beta_y^*/2}{M_{cr}^{basic}/N_{cr,z}}$

- **Restrictions at the supports**

Table A.23 – Critical moment for doubly and mono symmetric beams with loads out shear center and subjected to uniform bending moment.

<b>Restrictions at the supports</b>	
<b>Main Formula</b>	$M_{cr} = k_\phi \frac{\pi}{k_1 L} \sqrt{G I_T E I_z \left( 1 + \frac{\pi^2 E I_w}{k_2^2 L^2 G I_T} \right)}$
<b>Rotations about axis z restricted</b>	$k_1 = k_2 \approx \frac{4 + \frac{\alpha_z L}{E I_z}}{4 + \frac{2 \alpha_z L}{E I_z}}$ and $k_\phi = 1$
<b>Warping free</b>	
<b>Rotations about axis z restricted</b>	
<b>Rotations about axis z free</b>	$k_1 = 1$ and $k_2 \approx \frac{4 + \frac{\alpha_w L}{E I_w}}{4 + \frac{2 \alpha_w L}{E I_w}}$ and $k_\phi = 1$
<b>Warping restricted</b>	
<b>Rotations about axis x restricted</b>	
<b>Rotations about axis z restricted</b>	$k_1 = \frac{4 + \frac{\alpha_z L}{E I_z}}{4 + \frac{2 \alpha_z L}{E I_z}}$ and $k_2 \approx \frac{4 + \frac{\left(\alpha_w + \frac{\alpha_z h_m^2}{4}\right) L}{E I_w}}{2 \left(\alpha_w + \frac{\alpha_z h_m^2}{4}\right) L}$ and $k_\phi = 1$
<b>Warping restricted</b>	
<b>Rotations about axis x restricted</b>	
<b>Rotations about axis z free</b>	$k_1 = 1$ and $k_2 = 1$ and $k_\phi = \sqrt{\frac{\frac{\alpha_x L}{G I_T}}{\left(\frac{4,9 + 4,5\pi^2 E I_w}{G I_T L^2}\right) \alpha_x L}}$
<b>Warping free</b>	
<b>Rotations about axis x restricted</b>	
$\alpha_z$ is the stiffness of the bending restriction about z $\alpha_w$ is the stiffness of warping restraints $\alpha_x$ is the stiffness of the bending restriction about x	

• Cantilevers

Table A.24 – Critical moment for doubly symmetric cantilevers.

Cantilevers	
<b>Warping restricted</b> <b>Rotations about axis z restricted</b>	
$M_{cr} = 11 \frac{\sqrt{EI_z GI_T}}{L} \left[ 1 + \frac{1,2\varepsilon}{\sqrt{1 + 1,44\varepsilon^2}} \right] + 4(K - 2) \frac{\sqrt{EI_z GI_T}}{L} \left[ 1 + \frac{1,2(\varepsilon - 0,1)}{\sqrt{1 + 1,44(\varepsilon - 0,1)^2}} \right]$	
<b>Warping restricted</b> <b>Rotations about axis z restricted</b>	
$M_{cr} = 27 \frac{\sqrt{EI_z GI_T}}{L} \left[ 1 + \frac{1,4(\varepsilon - 0,1)}{\sqrt{1 + 1,96(\varepsilon - 0,1)^2}} \right] + 10(K - 2) \frac{\sqrt{EI_z GI_T}}{L} \left[ 1 + \frac{1,3(\varepsilon - 0,1)}{\sqrt{1 + 1,69(\varepsilon - 0,1)^2}} \right]$	
<b>Warping free</b> <b>Rotations about axis z restricted</b>	
$M_{cr} = 6 \frac{\sqrt{EI_z GI_T}}{L} \left[ 1 + \frac{1,5(\varepsilon - 0,1)}{\sqrt{1 + 2,25(\varepsilon - 0,1)^2}} \right] + 1,5(K - 2) \frac{\sqrt{EI_z GI_T}}{L} \left[ 1 + \frac{3(\varepsilon - 0,3)}{\sqrt{1 + 9(\varepsilon - 0,3)^2}} \right]$	
<b>Warping free</b> <b>Rotations about axis z restricted</b>	
$M_{cr} = 15 \frac{\sqrt{EI_z GI_T}}{L} \left[ 1 + \frac{1,8(\varepsilon - 0,3)}{\sqrt{1 + 3,24(\varepsilon - 0,3)^2}} \right] + 4(K - 2) \frac{\sqrt{EI_z GI_T}}{L} \left[ 1 + \frac{2,8(\varepsilon - 0,4)}{\sqrt{1 + 7,84(\varepsilon - 0,4)^2}} \right]$	

### A.8 – Serna et al.

For a general moment diagram, the coefficient  $C_1$  is obtained by

$$C_1 = \frac{\sqrt{kA_1 + \left[ \frac{(1-\sqrt{k})}{2} A_2 \right]^2} + \frac{(1-\sqrt{k})}{2} A_2}{A_1} \quad (\text{A.9})$$

Where  $k$  depends on the lateral bending and warping conditions coefficient  $k_1$  and  $k_2$ . Free lateral bending and warping at the left end is represented by  $k_1=1$ , prevented support conditions at the left end by  $k_1=0,5$ ;  $k_2$  is the corresponding support conditions coefficient for the right end. On the other hand the length factors in the main formula  $k_z$  and  $k_w$  are equal to 1 for free lateral bending and free warping and 0,5 for prevented lateral bending and prevented warping.

$$k = \sqrt{k_1 k_2} \quad (\text{A.10})$$

And  $A_1$  and  $A_2$  are given by

$$A_1 = \frac{M_{max}^2 + \alpha_1 M_1^2 + \alpha_2 M_2^2 + \alpha_3 M_3^2 + \alpha_4 M_4^2 + \alpha_5 M_5^2}{(1 + \alpha_1 + \alpha_2 + \alpha_3 + \alpha_4 + \alpha_5) M_{max}^2} \quad (\text{A.11})$$

$$A_2 = \left| \frac{M_1 + 2M_2 + 3M_3 + 2M_4 + M_5}{9M_{max}} \right| \quad (\text{A.12})$$

Where

$$\alpha_1 = (1 - k_2) \quad \alpha_2 = 5 \frac{k_1^3}{k_2^2} \quad \alpha_3 = 5 \left( \frac{1}{k_1} + \frac{1}{k_2} \right) \quad (\text{A.13})$$

$$\alpha_4 = 5 \frac{k_2^3}{k_1^2} \quad \alpha_5 = (1 - k_1) \quad (\text{A.14})$$

$M_{max}$  is the maximum moment, and  $M$ ,  $M_2$ ,  $M_3$ ,  $M_4$  and  $M_5$  are the values of the moment at different sections of the beam as indicated in Figure A.7, each of them with the corresponding sign.

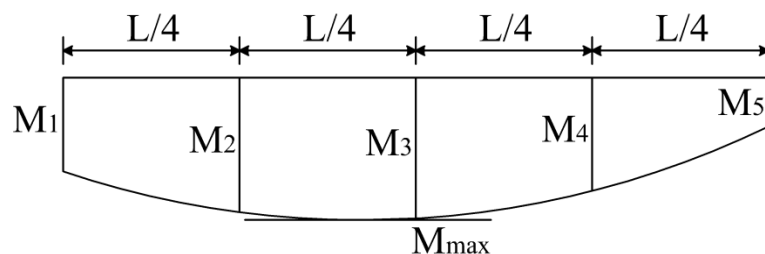


Figure A.7 – Moment diagram and moment values.

## ANNEX B – Statistical Analysis

In this Annex is presented the complete tables of the statistical analysis.

### B.1 – Baláž and Koleková

- Case 1

Table B.1 – Baláž and Koleková – Case 1.

Case 1	Baláž and Koleková	n	Mean	St.Dev	CoV%	Min.	Max.	<0,9%	>1,03	
Double Symmetric	Var.	All	3280	0,998	0,019	1,948	0,944	1,036	0,0	0,6
		1	820	0,997	0,010	1,044	0,960	1,009	0,0	0,0
	k <sub>z</sub>	0,5	820	0,980	0,018	1,841	0,944	1,008	0,0	0,0
		0,7L	820	1,001	0,020	2,047	0,945	1,031	0,0	0,4
		0,7R	820	1,014	0,008	0,773	0,995	1,036	0,0	2,2
		[0,5;1]	880	1,005	0,014	1,361	0,969	1,029	0,0	0,0
	Ψ	[0;0,5[	800	1,003	0,017	1,671	0,960	1,036	0,0	2,6
		]0,5;0]	800	0,992	0,021	2,157	0,945	1,024	0,0	0,0
		[-1;-0,5]	880	0,991	0,020	2,062	0,944	1,029	0,0	0,0
	λ <sup>LTBeam</sup>	[0;0,5[	873	0,995	0,023	2,294	0,946	1,035	0,0	1,5
Mono Symmetric		[0,5;1[	1676	0,996	0,019	1,954	0,944	1,036	0,0	0,5
		[1;∞[	731	1,004	0,012	1,237	0,960	1,029	0,0	0,0
	Profile	IPE	1640	0,998	0,019	1,941	0,944	1,036	0,0	0,5
		HEB	1640	0,998	0,020	1,956	0,946	1,035	0,0	0,8
	Var.	All	8528	1,003	0,078	7,817	0,571	1,556	6,1	20,8
		1	2132	0,995	0,062	6,190	0,625	1,556	5,3	12,7
	k <sub>z</sub>	0,5	2132	1,010	0,091	9,008	0,571	1,467	6,2	27,9
		0,7L	2132	0,997	0,086	8,588	0,583	1,415	8,0	18,7
		0,7R	2132	1,008	0,071	7,012	0,641	1,415	5,0	24,0
		[0,5;1]	2288	1,010	0,017	1,721	0,951	1,088	0,0	9,9
	Ψ	[0;0,5[	2080	1,010	0,033	3,287	0,886	1,148	0,6	20,8
		]0,5;0]	2080	0,982	0,097	9,874	0,571	1,556	12,2	22,3
		[-1;-0,5]	2288	1,008	0,113	11,193	0,625	1,415	11,3	31,0
	λ <sup>LTBeam</sup>	[0;1[	3356	0,987	0,073	7,442	0,571	1,556	7,5	15,6
Ψ <sub>f</sub>		[1;1,5[	3302	1,009	0,082	8,127	0,625	1,415	5,8	23,3
		[1,5;∞[	1870	1,019	0,076	7,409	0,767	1,390	4,3	25,7
	-1	656	0,967	0,050	5,193	0,808	1,147	9,0	9,9	
	[-0,9;-0,6]	1968	1,056	0,079	7,475	0,925	1,415	0,0	49,1	
	]-0,6;0[	1312	0,993	0,026	2,617	0,910	1,066	0,0	4,7	
	0	656	0,999	0,017	1,662	0,944	1,027	0,0	0,0	
	[0;0,6[	1312	0,982	0,045	4,585	0,726	1,081	5,3	6,8	
	[0,6;0,9]	1968	1,009	0,082	8,095	0,736	1,467	8,1	28,5	
	1	656	0,925	0,126	13,645	0,571	1,556	35,7	4,9	

• Case 2

Table B.2 – Baláž and Koleková – Case 2.

Case 2	Baláž and Koleková	n	Mean	St.Dev	CoV%	Min.	Max.	<0,9%	>1,03%	
Double Symmetric	Var.	All	1680	0,998	0,010	1,030	0,972	1,044	0,0	0,9
	$k_w=1$	$k_z=1$	420	1,000	0,001	0,083	0,998	1,002	0,0	0,0
	$k_w=1$	$k_z=0,5$	420	0,999	0,016	1,576	0,972	1,044	0,0	3,6
	$k_w=0,5$	$k_z=1$	420	0,995	0,003	0,255	0,973	1,008	0,0	0,0
	$k_w=0,5$	$k_z=0,5$	420	0,998	0,006	0,632	0,990	1,015	0,0	0,0
	$h_l$	$[0,5;1]$	800	0,994	0,008	0,824	0,972	1,008	0,0	0,0
	$h_l$	$0,5$	80	0,997	0,007	0,688	0,977	1,006	0,0	0,0
	$h_l$	$[0;0,5]$	800	1,002	0,011	1,099	0,973	1,044	0,0	1,9
	$\bar{\lambda}^{LTBeam}$	$[0;0,5]$	237	1,004	0,009	0,940	0,986	1,044	0,0	3,8
	$\bar{\lambda}^{LTBeam}$	$[0,5;1]$	839	0,999	0,010	1,010	0,973	1,042	0,0	0,7
	$\bar{\lambda}^{LTBeam}$	$[1;\infty[$	604	0,995	0,010	0,969	0,972	1,024	0,0	0,0
Mono Symmetric	Profile	IPE	840	0,997	0,010	1,010	0,972	1,042	0,0	0,7
	Profile	HEB	840	0,998	0,010	1,049	0,973	1,044	0,0	1,1
	Var.	All	4368	0,994	0,027	2,760	0,827	1,116	1,0	3,8
	$k_w=1$	$k_z=1$	1092	0,997	0,022	2,244	0,893	1,048	0,6	1,9
	$k_w=1$	$k_z=0,5$	1092	0,992	0,030	3,013	0,879	1,116	0,8	7,7
	$k_w=0,5$	$k_z=1$	1092	0,994	0,029	2,922	0,827	1,066	1,1	3,8
	$k_w=0,5$	$k_z=0,5$	1092	0,993	0,028	2,776	0,860	1,061	1,6	1,8
	$h_l$	$[0,5;1]$	2288	0,990	0,025	2,574	0,827	1,066	1,3	1,4
	$h_l$	$[0;0,5]$	2288	0,997	0,029	2,873	0,879	1,116	0,7	5,9
	$\bar{\lambda}^{LTBeam}$	$[0;1]$	1287	0,996	0,028	2,786	0,847	1,066	1,5	4,0
	$\bar{\lambda}^{LTBeam}$	$[1;1,5]$	1364	0,996	0,024	2,377	0,827	1,115	0,7	3,1
	$\bar{\lambda}^{LTBeam}$	$[1,5;\infty[$	1717	0,990	0,030	2,981	0,879	1,116	1,0	4,2
	$\Psi_f$	-1	336	0,945	0,027	2,880	0,879	1,006	4,8	0,0
	$\Psi_f$	$[-0,9;-0,6]$	1008	1,006	0,021	2,060	0,961	1,116	0,0	9,6
	$\Psi_f$	$[-0,6;0]$	672	1,001	0,010	1,005	0,973	1,037	0,0	1,3
	$\Psi_f$	0	336	1,000	0,008	0,849	0,972	1,038	0,0	1,2
	$\Psi_f$	$[0;0,6]$	672	0,999	0,009	0,893	0,969	1,043	0,0	1,0
	$\Psi_f$	$[0,6;0,9]$	1008	1,004	0,016	1,584	0,962	1,066	0,0	4,9
	$\Psi_f$	1	336	0,945	0,029	3,092	0,827	0,994	8,6	0,0

Table B.3 – Baláž and Koleková – Case 2 –  $\psi_f$  limits analysis.

Case 2	Baláž and Koleková	n	Mean	St.Dev	CoV%	Min.	Max.	<0,9%	>1,03%	
Mono Symmetric	$\Psi_f$	-0,9	336	1,009	0,027	2,687	0,961	1,116	0,0	19,0
		-0,8	336	1,006	0,019	1,876	0,966	1,074	0,0	6,8
		-0,6	336	1,004	0,014	1,355	0,975	1,049	0,0	3,0
		0,6	336	1,001	0,011	1,107	0,967	1,046	0,0	1,2
		0,8	336	1,003	0,014	1,385	0,965	1,040	0,0	0,9
		0,9	336	1,007	0,021	2,042	0,962	1,066	0,0	12,5

• Case 3

Table B.4 – Baláž and Koleková – Case 3.

Case 3	Baláž and Koleková	n	Mean	St.Dev	CoV%	Min.	Max.	<0,9%	>1,03%
Double Symmetric	Var.	All	1680	0,997	0,007	0,733	0,978	1,009	0,0
	$k_w=1$	$k_z=1$	420	1,000	0,004	0,413	0,993	1,008	0,0
	$k_w=1$	$k_z=0,5$	420	0,995	0,007	0,654	0,984	1,006	0,0
	$k_w=0,5$	$k_z=1$	420	0,996	0,010	1,041	0,978	1,009	0,0
	$k_w=0,5$	$k_z=0,5$	420	0,997	0,006	0,588	0,984	1,005	0,0
	$h_l$	$[0,5;1]$	800	0,999	0,007	0,710	0,978	1,009	0,0
	$h_l$	$0,5$	80	0,996	0,007	0,674	0,978	1,005	0,0
	$h_l$	$[0;0,5]$	800	0,995	0,007	0,704	0,978	1,005	0,0
	$\bar{\lambda}^{LTBeam}$	$[0;0,5]$	293	1,001	0,004	0,368	0,985	1,007	0,0
	$\bar{\lambda}^{LTBeam}$	$[0,5;1]$	830	0,997	0,007	0,715	0,978	1,009	0,0
	$\bar{\lambda}^{LTBeam}$	$[1;\infty[$	557	0,995	0,008	0,815	0,978	1,009	0,0
Mono Symmetric	Profile	IPE	840	0,997	0,007	0,722	0,978	1,009	0,0
	Profile	HEB	840	0,997	0,007	0,742	0,978	1,009	0,0
	Var.	All	4368	0,994	0,043	4,283	0,811	1,138	5,3
	$k_w=1$	$k_z=1$	1092	0,998	0,042	4,232	0,811	1,096	4,0
	$k_w=1$	$k_z=0,5$	1092	0,991	0,042	4,227	0,812	1,108	3,2
	$k_w=0,5$	$k_z=1$	1092	0,995	0,047	4,712	0,838	1,138	8,2
	$k_w=0,5$	$k_z=0,5$	1092	0,995	0,039	3,901	0,846	1,063	5,8
	$h_l$	$[0,5;1]$	2288	0,996	0,037	3,702	0,838	1,088	3,1
	$h_l$	$[0;0,5]$	2288	0,993	0,047	4,783	0,811	1,138	7,3
	$\bar{\lambda}^{LTBeam}$	$[0;1]$	1484	0,994	0,041	4,144	0,838	1,138	4,7
	$\bar{\lambda}^{LTBeam}$	$[1;1,5]$	1533	0,995	0,036	3,598	0,839	1,103	4,4
	$\bar{\lambda}^{LTBeam}$	$[1,5;\infty[$	1351	0,995	0,051	5,076	0,811	1,108	6,9
	$\Psi_f$	-1	336	0,915	0,041	4,505	0,811	0,991	36,6
	$\Psi_f$	$[-0,9;-0,6]$	1008	1,025	0,024	2,337	0,968	1,108	0,0
	$\Psi_f$	$[-0,6;0]$	672	1,003	0,007	0,652	0,982	1,021	0,0
	$\Psi_f$	0	336	0,999	0,004	0,429	0,984	1,007	0,0
	$\Psi_f$	$[0;0,6]$	672	0,997	0,008	0,752	0,974	1,015	0,0
	$\Psi_f$	$[0,6;0,9]$	1008	1,009	0,028	2,729	0,961	1,138	0,0
	$\Psi_f$	1	336	0,910	0,026	2,900	0,838	0,965	32,1

Table B.5 – Baláž and Koleková – Case 3 –  $\psi_f$  limits analysis.

Case 3	Baláž and Koleková	n	Mean	St.Dev	CoV%	Min.	Max.	<0,9%	>1,03%
Mono Symmetric	$\Psi_f$	-0,9	168	1,042	0,032	3,037	0,959	1,119	0,0
		-0,8	168	1,014	0,027	2,652	0,940	1,069	0,0
		-0,6	168	0,994	0,023	2,274	0,930	1,036	0,0
		0,6	168	0,997	0,021	2,121	0,945	1,059	0,0
		0,8	168	1,008	0,027	2,663	0,961	1,098	0,0
		0,9	168	1,017	0,034	3,323	0,966	1,138	0,0
		1	168	1,017	0,034	3,323	0,966	1,138	0,0

• Case 4

Table B.6 – Baláž and Koleková – Case 4.

Case 4	Baláž and Koleková	n	Mean	St.Dev	CoV%	Min.	Max.	<0,9%	>1,03%
Double Symmetric	Var.	All	1,002	0,022	2,216	0,963	1,127	0,0	8,8
	$k_w=1$	$k_z=1$	420	1,001	0,005	0,522	0,995	1,019	0,0
	$k_w=1$	$k_z=0,5$	420	1,009	0,038	3,759	0,963	1,127	0,0
	$k_w=0,5$	$k_z=1$	420	0,996	0,013	1,290	0,969	1,014	0,0
	$k_w=0,5$	$k_z=0,5$	420	1,003	0,016	1,637	0,983	1,055	0,0
	$h_l$	$[0,5;1]$	800	0,991	0,010	1,005	0,963	1,009	0,0
	$h_l$	$0,5$	80	0,997	0,007	0,700	0,975	1,008	0,0
	$h_l$	$[0;0,5]$	800	1,014	0,026	2,531	0,969	1,127	0,0
	$\bar{\lambda}^{LTBeam}$	$[0;0,5]$	221	1,013	0,029	2,882	0,981	1,127	0,0
	$\bar{\lambda}^{LTBeam}$	$[0,5;1]$	830	1,004	0,023	2,261	0,963	1,123	0,0
	$\bar{\lambda}^{LTBeam}$	$[1;\infty[$	629	0,997	0,016	1,634	0,964	1,091	0,0
	Profile	IPE	840	1,002	0,022	2,148	0,964	1,123	0,0
	Profile	HEB	840	1,003	0,023	2,280	0,963	1,127	0,0
Mono Symmetric	Var.	All	4368	0,995	0,042	4,213	0,826	1,190	3,5
	$k_w=1$	$k_z=1$	1092	0,995	0,029	2,955	0,877	1,065	0,8
	$k_w=1$	$k_z=0,5$	1092	1,002	0,055	5,497	0,844	1,190	2,9
	$k_w=0,5$	$k_z=1$	1092	0,990	0,037	3,738	0,826	1,088	4,2
	$k_w=0,5$	$k_z=0,5$	1092	0,994	0,041	4,144	0,857	1,091	5,9
	$h_l$	$[0,5;1]$	2288	0,984	0,034	3,406	0,826	1,091	4,1
	$h_l$	$[0;0,5]$	2288	1,005	0,046	4,608	0,844	1,190	3,1
	$\bar{\lambda}^{LTBeam}$	$[0;1]$	1163	1,007	0,051	5,034	0,830	1,190	4,6
	$\bar{\lambda}^{LTBeam}$	$[1;1,5]$	1336	1,001	0,036	3,554	0,826	1,151	1,8
	$\bar{\lambda}^{LTBeam}$	$[1,5;\infty[$	1869	0,984	0,037	3,760	0,844	1,150	4,0
	$\Psi_f$	-1	336	0,927	0,031	3,363	0,844	0,994	19,9
	$\Psi_f$	$[-0,9;-0,6]$	1008	1,000	0,027	2,736	0,957	1,151	0,0
	$\Psi_f$	$[-0,6;0]$	672	1,002	0,022	2,176	0,961	1,108	0,0
	$\Psi_f$	0	336	1,005	0,023	2,334	0,964	1,123	0,0
	$\Psi_f$	$[0;0,6]$	672	1,009	0,026	2,547	0,964	1,151	0,0
	$\Psi_f$	$[0,6;0,9]$	1008	1,021	0,031	3,073	0,964	1,190	0,0
	$\Psi_f$	1	336	0,921	0,033	3,606	0,826	1,019	25,0

Table B.7 – Baláž and Koleková – Case 4 –  $\psi_f$  limits analysis.

Case 4	Baláž and Koleková	n	Mean	St.Dev	CoV%	Min.	Max.	<0,9%	>1,03%
Mono Symmetric	$\Psi_f$	-0,9	336	1,001	0,033	3,253	0,957	1,151	0,0
		-0,8	336	0,999	0,026	2,610	0,959	1,109	0,0
		-0,6	336	1,000	0,023	2,257	0,961	1,086	0,0
		0,6	336	1,015	0,029	2,809	0,965	1,168	0,0
		0,8	336	1,021	0,031	3,008	0,965	1,182	0,0
		0,9	336	1,028	0,033	3,259	0,964	1,190	0,0
		1	336	0,921	0,033	3,606	0,826	1,019	25,0

• Case 5

Table B.8 – Baláž and Koleková – Case 5.

Case 5	Baláž and Koleková	n	Mean	St.Dev	CoV%	Min.	Max.	<0,9%	>1,03%
Double Symmetric	Var.	All	1260	0,996	0,015	1,518	0,944	1,019	0,0
		$k_z=1$	420	1,001	0,004	0,424	0,996	1,013	0,0
		$k_z=0,5$	420	0,998	0,007	0,707	0,990	1,019	0,0
		$k_w=0,5$	420	0,990	0,023	2,375	0,944	1,016	0,0
		$ 0,5;1 $	600	0,998	0,014	1,428	0,950	1,019	0,0
	$h_l$	$0,5$	60	0,993	0,014	1,403	0,949	1,008	0,0
		$ 0;0,5 $	600	0,994	0,016	1,593	0,944	1,016	0,0
		$ \bar{\lambda}^{LTBeam} $	436	0,999	0,013	1,302	0,945	1,016	0,0
		$ 0,5;1 $	610	0,995	0,016	1,605	0,944	1,019	0,0
		$ 1;\infty $	214	0,993	0,016	1,581	0,950	1,018	0,0
Mono Symmetric	Profile	IPE	630	0,995	0,015	1,522	0,944	1,019	0,0
		HEB	630	0,997	0,015	1,510	0,945	1,019	0,0
	Var.	All	2268	0,963	0,130	13,447	0,337	1,198	19,1
		$k_z=1$	756	0,972	0,105	10,815	0,640	1,198	18,8
		$k_z=0,5$	756	0,980	0,114	11,631	0,611	1,193	19,0
		$k_w=0,5$	756	0,937	0,159	16,964	0,337	1,112	19,4
	$h_l$	$ 0,5;1 $	1188	0,969	0,107	11,021	0,362	1,114	16,2
		$ 0;0,5 $	1188	0,957	0,149	15,559	0,337	1,198	22,2
		$ \bar{\lambda}^{LTBeam} $	1104	1,010	0,082	8,111	0,484	1,198	3,0
		$ 1;1,5 $	818	0,937	0,150	15,985	0,337	1,150	27,3
Mono Symmetric		$ 1,5;\infty $	346	0,875	0,138	15,763	0,542	1,077	13,0
		-1	252	0,833	0,079	9,544	0,685	0,985	74,6
		$ -0,5;0 $	756	1,044	0,040	3,821	0,971	1,198	0,0
	$\Psi_f$	0	252	1,000	0,008	0,760	0,983	1,020	0,0
		$ 0;0,5 $	756	1,006	0,026	2,556	0,974	1,166	0,0
		1	252	0,688	0,138	20,106	0,337	0,931	97,2
									0,0

Table B.9 – Baláž and Koleková – Case 5 –  $\psi_f$  limits analysis.

Case 5	Baláž and Koleková	n	Mean	St.Dev	CoV%	Min.	Max.	<0,9%	>1,03%
Mono Symmetric	Var.	All	3276	1,031	0,257	24,917	0,269	3,752	19,6
		$[-0,9;-0,5 $	756	1,110	0,209	18,846	0,700	2,440	11,1
		$[-0,5;0 $	756	1,044	0,040	3,821	0,971	1,198	0,0
		0	252	1,000	0,008	0,760	0,983	1,020	0,0
		$ 0;0,5 $	756	1,006	0,026	2,556	0,974	1,166	0,0
		$ 0,5;0,9 $	756	1,156	0,448	38,771	0,269	3,752	16,5
	$\Psi_f$	-0,5	252	1,066	0,048	4,488	0,971	1,198	0,0
		-0,4	252	1,048	0,034	3,226	0,974	1,143	0,0
		-0,2	252	1,018	0,014	1,410	0,979	1,058	0,0
		0,2	252	0,992	0,008	0,802	0,974	1,009	0,0
		0,4	252	1,004	0,019	1,926	0,974	1,086	0,0
		0,5	252	1,020	0,034	3,323	0,980	1,166	0,0
									17,9

• Case 6

Table B.10 – Baláž and Koleková – Case 6.

Case 6	Baláž and Koleková	n	Mean	St.Dev	CoV%	Min.	Max.	<0,9%	>1,03%	
Double Symmetric	Var.	All	1260	0,999	0,016	1,598	0,961	1,030	0,0	0,2
	$k_w=1$	$k_z=1$	420	1,000	0,014	1,351	0,977	1,025	0,0	0,0
	$k_w=1$	$k_z=0,5$	420	1,003	0,014	1,377	0,984	1,030	0,0	0,7
	$k_w=0,5$	$k_z=0,5$	420	0,995	0,019	1,903	0,961	1,024	0,0	0,0
	$h_l$	$ 0,5;1 $	600	1,009	0,015	1,485	0,963	1,030	0,0	0,5
	$h_l$	$0,5$	60	0,995	0,010	1,047	0,963	1,007	0,0	0,0
	$\bar{\lambda}^{LTBeam}$	$ 0;0,5 $	600	0,991	0,012	1,186	0,961	1,028	0,0	0,0
	$\bar{\lambda}^{LTBeam}$	$ 0,5;1 $	245	1,002	0,009	0,921	0,966	1,028	0,0	0,0
	$\bar{\lambda}^{LTBeam}$	$ 1;\infty $	630	0,999	0,016	1,636	0,962	1,030	0,0	0,3
	$\bar{\lambda}^{LTBeam}$	$ 1;\infty $	385	0,999	0,018	1,845	0,961	1,030	0,0	0,3
Mono Symmetric	Profile	IPE	630	0,999	0,016	1,586	0,961	1,030	0,0	0,2
	Profile	HEB	630	1,000	0,016	1,606	0,962	1,030	0,0	0,3
	Var.	All	2268	0,972	0,126	12,911	0,470	1,410	18,7	29,2
	$k_w=1$	$k_z=1$	756	0,977	0,109	11,189	0,618	1,246	18,4	30,7
	$k_w=1$	$k_z=0,5$	756	0,988	0,119	12,063	0,645	1,410	19,0	35,1
	$k_w=0,5$	$k_z=0,5$	756	0,953	0,143	15,038	0,470	1,147	18,8	21,8
	$h_l$	$ 0,5;1 $	1187	0,980	0,102	10,374	0,480	1,108	15,5	27,3
	$h_l$	$ 0;0,5 $	1188	0,964	0,145	15,027	0,470	1,410	22,2	30,9
	$\bar{\lambda}^{LTBeam}$	$ 0;1 $	687	1,029	0,074	7,169	0,553	1,410	1,2	36,2
	$\bar{\lambda}^{LTBeam}$	$ 1;1,5 $	902	0,961	0,137	14,281	0,470	1,297	18,1	25,1
Mono Symmetric	$\bar{\lambda}^{LTBeam}$	$ 1,5;\infty $	679	0,930	0,130	14,022	0,553	1,108	37,4	27,5
	$\Psi_f$	-1	252	0,839	0,087	10,379	0,645	1,002	69,4	0,0
	$\Psi_f$	$ -0,5;0 $	756	1,039	0,032	3,056	0,972	1,108	0,0	59,7
	$\Psi_f$	0	252	1,003	0,012	1,211	0,979	1,028	0,0	0,0
	$\Psi_f$	$ 0;0,5 $	756	1,028	0,058	5,678	0,978	1,410	0,0	27,9
	$\Psi_f$	1	252	0,710	0,105	14,764	0,470	0,918	99,2	0,0

Table B.11 – Baláž and Koleková – Case 6 –  $\psi_f$  limits analysis.

Case 6	Baláž and Koleková	n	Mean	St.Dev	CoV%	Min.	Max.	<0,9%	>1,03%	
Mono Symmetric	Var.	All	3276	1,088	0,263	24,185	0,435	4,307	6,8	53,3
	$\Psi_f$	$[-0,9;-0,5 $	756	1,104	0,172	15,553	0,609	1,731	13,1	77,8
	$\Psi_f$	$[-0,5;0 $	756	1,039	0,032	3,056	0,972	1,108	0,0	59,7
	$\Psi_f$	0	252	1,003	0,012	1,211	0,979	1,028	0,0	0,0
	$\Psi_f$	$ 0;0,5 $	756	1,028	0,058	5,678	0,978	1,410	0,0	27,9
	$\Psi_f$	$ 0,5;0,9 $	756	1,211	0,493	40,695	0,435	4,307	16,3	65,5
	$\Psi_f$	-0,5	252	1,060	0,031	2,911	0,973	1,108	0,0	83,3
	$\Psi_f$	-0,4	252	1,042	0,026	2,524	0,972	1,088	0,0	67,5
	$\Psi_f$	-0,2	252	1,015	0,019	1,894	0,978	1,054	0,0	28,2
	$\Psi_f$	0,2	252	1,004	0,019	1,880	0,978	1,107	0,0	7,9
	$\Psi_f$	0,4	252	1,028	0,052	5,069	0,979	1,281	0,0	31,7
	$\Psi_f$	0,5	252	1,052	0,078	7,389	0,980	1,410	0,0	44,0

• Case 7

Table B.12 – Baláž and Koleková – Case 7.

Case 7	Baláž and Koleková	n	Mean	St.Dev	CoV%	Min.	Max.	<0,9%	>1,03%	
Double Symmetric	Var.	All	5220	1,003	0,040	4,034	0,789	1,241	3,5	12,6
		[−1;0]	1800	0,989	0,058	5,840	0,789	1,241	7,8	12,9
	M <sub>0</sub> /M	[−2;−1]	1800	1,005	0,030	3,004	0,812	1,069	2,4	15,8
	μ	[−4;−2]	900	1,018	0,010	0,980	0,996	1,046	0,0	10,8
		[−∞;−4]	720	1,017	0,012	1,210	0,992	1,043	0,0	6,1
		[0,5;1]	1160	1,008	0,043	4,246	0,812	1,069	5,3	27,5
	Ψ	[0;0,5]	1740	1,000	0,045	4,462	0,789	1,065	5,4	12,0
		[−0,5;0]	1740	0,998	0,035	3,483	0,808	1,060	3,0	6,0
		[−1;−0,5]	1160	1,008	0,040	3,966	0,892	1,241	0,5	7,5
	λ <sup>LTBeam</sup>	[0;0,5]	632	0,961	0,066	6,919	0,789	1,182	21,2	10,0
Profile		[0,5;1]	2756	1,005	0,035	3,482	0,816	1,240	1,8	12,1
		[1;∞]	1832	1,015	0,023	2,285	0,921	1,241	0,0	14,3
		IPE	2610	1,004	0,040	3,991	0,789	1,241	3,4	13,0
		HEB	2610	1,002	0,041	4,077	0,790	1,240	3,7	12,2

Table B.13 – Baláž and Koleková – Case 7 – C<sub>2</sub> analysis.

Case 7	Baláž and Koleková	n	Mean	St.Dev	CoV%	Min.	Max.	<0,9%	>1,03%	
Double Symmetric	Var.	All	15660	1,020	0,163	15,959	0,409	2,583	10,8	28,7
		1	5220	1,089	0,224	20,551	0,665	2,583	7,5	48,0
	h <sub>l</sub>	0,5	5220	1,003	0,040	4,034	0,789	1,241	3,5	12,6
		0	5220	0,969	0,142	14,684	0,409	1,449	21,5	25,6

• Case 9

Table B.14 – Baláž and Koleková – Case 9.

Case 9	Baláž and Koleková	n	Mean	St.Dev	CoV%	Min.	Max.	<0,9%	>1,03%	
Double Symmetric	Var.	All	60	1,045	0,097	9,314	0,960	1,302	0,0	28,3
		1	20	1,150	0,105	9,172	1,015	1,302	0,0	85,0
	h <sub>I</sub>	0,5	20	1,009	0,011	1,119	0,991	1,023	0,0	0,0
		0	20	0,976	0,014	1,425	0,960	1,000	0,0	0,0
	λ <sup>LTBeam</sup>	[0;0,5[	7	0,977	0,015	1,567	0,961	0,994	0,0	0,0
		[0,5;1[	26	1,055	0,107	10,183	0,960	1,302	0,0	34,6
		[1;∞[	27	1,053	0,094	8,967	0,966	1,296	0,0	29,6
	Profile	IPE	30	1,043	0,094	9,050	0,960	1,296	0,0	26,7
		HEB	30	1,047	0,102	9,717	0,961	1,302	0,0	30,0
	Var.	All	108	1,034	0,115	11,131	0,445	1,310	1,9	27,8
Mono Symmetric		1	36	1,116	0,172	15,397	0,445	1,310	5,6	80,6
	h <sub>I</sub>	0,5	36	1,002	0,005	0,544	0,996	1,020	0,0	0,0
		0	36	0,983	0,017	1,737	0,958	1,032	0,0	2,8
	λ <sup>LTBeam</sup>	[0;1[	27	0,992	0,016	1,628	0,960	1,023	0,0	0,0
		[1;1,5[	41	1,047	0,105	10,000	0,958	1,303	0,0	26,8
		[1,5;∞[	40	1,048	0,153	14,555	0,445	1,310	5,0	47,5
		[-0,8;-0,4[	24	1,015	0,033	3,274	0,971	1,123	0,0	20,8
		[-0,4;0[	24	1,039	0,081	7,778	0,958	1,216	0,0	33,3
	Ψ <sub>f</sub>	0	12	1,053	0,107	10,162	0,959	1,261	0,0	33,3
		[0;0,4[	24	1,048	0,117	11,178	0,917	1,302	0,0	29,2
		[0,4;0,8]	24	1,023	0,184	17,976	0,445	1,310	8,3	25,0

Table B.15 – Baláž and Koleková – Case 9 – Interpolation analysis.

Case 9	Interpolation	n	Mean	St.Dev	CoV%	Min.	Max.	<0,9%	>1,03%
Double Symmetric	Non-linear	60	1,045	0,097	9,314	0,960	1,302	0,0	28,3
	Linear	60	1,034	0,108	10,422	0,918	1,327	0,0	28,3
Mono Symmetric	Non-linear	108	1,034	0,115	11,131	0,445	1,310	1,9	27,8
	Linear	108	1,100	0,107	9,710	0,918	1,346	0,0	73,1

• Case 10

Table B.16 – Baláž and Koleková – Case 10.

Case 9	Baláž and Koleková	n	Mean	St.Dev	CoV%	Min.	Max.	<0,9%	>1,03%
Double Symmetric	Var.	All	60	1,047	0,112	10,691	0,929	1,297	0,0
		1	20	1,179	0,094	7,941	1,031	1,297	0,0
	h <sub>I</sub>	0,5	20	1,012	0,012	1,191	0,994	1,027	0,0
		0	20	0,950	0,021	2,256	0,929	0,994	0,0
	λ <sup>LTBeam</sup>	[0;0,5]	16	1,015	0,129	12,713	0,930	1,297	0,0
		[0,5;1]	32	1,057	0,114	10,791	0,929	1,296	0,0
		[1;∞[	12	1,063	0,076	7,161	0,971	1,217	0,0
	Profile	IPE	30	1,045	0,109	10,470	0,929	1,296	0,0
		HEB	30	1,049	0,116	11,081	0,930	1,297	0,0
	Var.	All	108	1,035	0,142	13,691	0,348	1,424	1,9
Mono Symmetric		1	36	1,142	0,205	17,917	0,348	1,424	5,6
	h <sub>I</sub>	0,5	36	1,000	0,007	0,696	0,990	1,022	0,0
		0	36	0,961	0,029	2,995	0,925	1,037	0,0
	λ <sup>LTBeam</sup>	[0;1]	47	1,007	0,095	9,478	0,925	1,356	0,0
		[1;1,5]	52	1,032	0,154	14,896	0,348	1,421	3,8
		[1,5;∞[	9	1,194	0,179	14,993	0,994	1,424	0,0
		[-0,8;-0,4]	24	1,007	0,039	3,923	0,937	1,076	0,0
		[-0,4;0]	24	1,034	0,089	8,649	0,925	1,205	0,0
	Ψ <sub>f</sub>	0	12	1,053	0,124	11,785	0,929	1,279	0,0
		[0;0,4]	24	1,053	0,145	13,775	0,921	1,363	0,0
		[0,4;0,8]	24	1,035	0,232	22,447	0,348	1,424	8,3
									25,0

Table B.17 – Baláž and Koleková – Case 10 – Interpolation analysis.

Case 10	Interpolation	n	Mean	St.Dev	CoV%	Min.	Max.	<0,9%	>1,03%
Double Symmetric	Non-linear	60	1,047	0,112	10,691	0,929	1,297	0,0	33,3
	Linear	60	1,063	0,145	13,648	0,916	1,402	0,0	33,3
Mono Symmetric	Non-linear	108	1,035	0,142	13,691	0,348	1,424	1,9	28,7
	Linear	108	1,122	0,161	14,341	0,916	1,578	0,0	62,0

## B.2 – ECCS - Basis Load Cases

- Case 1

Table B.18 – ECCS – Basis Load Cases – Case 1.

Case 1	ECCS	n	Mean	St.Dev	CoV%	Min.	Max.	<0,9%	>1,03%	
	All	3280	0,956	0,148	15,465	0,618	1,344	26,5	20,9	
	Without $k_z=0,7$	1640	0,934	0,032	3,445	0,865	1,032	16,2	0,1	
	1	820	0,937	0,030	3,217	0,865	1,004	13,2	0,0	
$k_z$	0,5	820	0,930	0,034	3,616	0,879	1,032	19,1	0,1	
	0,7L	820	0,818	0,138	16,910	0,618	1,255	73,5	7,8	
	0,7R	820	1,139	0,113	9,960	0,927	1,344	0,0	75,5	
	<b>Without <math>k_z=0,7</math></b>									
Double Symmetric	$\Psi$	[0,5;1]	440	0,947	0,031	3,312	0,885	1,004	7,7	0,0
		[0;0,5]	400	0,937	0,028	2,966	0,879	0,996	9,8	0,0
		[-0,5;0]	400	0,924	0,029	3,101	0,875	1,006	20,5	0,0
		[-1;-0,5]	440	0,925	0,034	3,662	0,865	1,032	26,6	0,2
$\bar{\lambda}^{LTBeam}$		[0;0,5]	449	0,922	0,030	3,246	0,865	1,026	25,4	0,0
		[0,5;1]	827	0,932	0,033	3,553	0,865	1,029	17,7	0,0
		[1; $\infty$ ]	364	0,951	0,025	2,589	0,894	1,032	1,4	0,3
	Profile	IPE	820	0,933	0,032	3,474	0,865	1,032	17,4	0,1
		HEB	820	0,934	0,032	3,418	0,865	1,029	14,9	0,0
	All	7216	0,975	0,140	14,383	0,581	1,450	23,8	26,4	
	Without $k_z=0,7$	3608	0,957	0,079	8,214	0,752	1,381	17,8	10,0	
	1	1804	0,942	0,057	6,056	0,752	1,134	19,5	4,3	
$k_z$	0,5	1804	0,972	0,093	9,571	0,830	1,381	16,1	15,7	
	0,7L	1804	0,866	0,147	16,955	0,581	1,349	59,6	12,0	
	0,7R	1804	1,118	0,108	9,697	0,926	1,450	0,0	73,5	
	<b>Without <math>k_z=0,7</math></b>									
Mono Symmetric	$\Psi$	[0,5;1]	968	0,955	0,027	2,874	0,885	1,006	4,8	0,0
		[0;0,5]	880	0,955	0,034	3,607	0,883	1,111	4,8	2,7
		[-0,5;0]	880	0,942	0,084	8,873	0,759	1,381	30,5	12,7
		[-1;-0,5]	968	0,975	0,121	12,367	0,752	1,376	30,1	24,1
$\bar{\lambda}^{LTBeam}$		[0;1]	1548	0,933	0,062	6,638	0,759	1,381	27,7	4,0
		[1;1,5]	1295	0,967	0,090	9,351	0,752	1,376	16,4	15,1
		[1,5; $\infty$ ]	765	0,988	0,073	7,344	0,910	1,372	0,0	13,7
		[-0,9;-0,6]	984	1,015	0,088	8,705	0,870	1,376	1,0	25,9
$\Psi_f$		[-0,6;0]	656	0,935	0,033	3,551	0,856	1,063	14,9	0,6
		0	328	0,922	0,032	3,499	0,870	1,025	31,7	0,0
		[0;0,6]	656	0,918	0,043	4,642	0,820	1,063	35,7	0,9
		[0,6;0,9]	984	0,952	0,086	9,046	0,752	1,381	19,8	9,9

Table B.19 – ECCS – Basis Load Cases – Case 1 –  $k_z = 0,7$  Method.

Case 1	ECCS	n	Mean	St.Dev.	CoV%	Min.	Max.	<0,9%	>1,03%
Double Symmetric	$k_z=0,7$	Interpolation	1640	0,978	0,204	20,867	0,618	1,344	36,8
		$k_z=1$	1640	0,967	0,211	21,816	0,602	1,366	38,8
	$k_z=0,7$								
	$k_z=0,7L$	Interpolation	820	0,818	0,138	16,910	0,618	1,255	73,5
		$k_z=1$	820	0,809	0,152	18,814	0,602	1,300	77,6
Mono Symmetric	$k_z=0,7R$	Interpolation	820	1,139	0,113	9,960	0,927	1,344	0,0
		$k_z=1$	820	1,125	0,127	11,279	0,902	1,366	0,0
	$k_z=0,7$	Interpolation	3608	0,992	0,180	18,175	0,581	1,450	29,8
		$k_z=1$	3608	0,980	0,187	19,042	0,566	1,423	33,4
$k_z=0,7$									
$k_z=0,7L$	Interpolation	1804	0,866	0,147	16,955	0,581	1,349	59,6	
	$k_z=1$	1804	0,857	0,160	18,718	0,566	1,381	66,9	
$k_z=0,7R$	Interpolation	1804	1,118	0,108	9,697	0,926	1,450	0,0	
	$k_z=1$	1804	1,104	0,116	10,515	0,906	1,423	0,0	
	$k_z=0,7$								

• Case 2

Table B.20 – ECCS – Basic Load Cases – Case 2.

Case 2	ECCS	n	Mean	St.Dev	CoV%	Min.	Max.	<0,9%	>1,03%	
Double Symmetric	Var.	All	840	0,993	0,015	1,486	0,949	1,031	0,0	0,2
	k <sub>z</sub>	1	420	0,991	0,003	0,253	0,984	0,996	0,0	0,0
		0,5	420	0,995	0,021	2,068	0,949	1,031	0,0	0,5
	h <sub>l</sub>	[0,5;1]	400	0,999	0,010	1,026	0,980	1,031	0,0	0,5
		0,5	40	0,991	0,011	1,107	0,974	1,021	0,0	0,0
		[0;0,5[	400	0,987	0,016	1,656	0,949	1,025	0,0	0,0
	λ <sup>LTBeam</sup>	[0;0,5[	84	0,977	0,017	1,762	0,950	1,018	0,0	0,0
		[0,5;1]	425	0,993	0,015	1,516	0,949	1,031	0,0	0,5
		[1;∞[	331	0,997	0,010	1,042	0,973	1,025	0,0	0,0
	Profile	IPE	420	0,993	0,015	1,466	0,949	1,030	0,0	0,2
		HEB	420	0,992	0,015	1,506	0,950	1,031	0,0	0,2
Mono Symmetric	Var.	All	1848	0,996	0,028	2,780	0,935	1,122	0,0	11,1
	k <sub>w</sub> =1	k <sub>z</sub> =1	924	0,996	0,011	1,126	0,980	1,040	0,0	1,4
		k <sub>z</sub> =0,5	924	0,995	0,038	3,769	0,935	1,122	0,0	20,8
	h <sub>l</sub>	[0,5;1]	968	1,000	0,023	2,275	0,937	1,069	0,0	11,6
		[0;0,5[	968	0,991	0,031	3,138	0,935	1,122	0,0	10,4
	λ <sup>LTBeam</sup>	[0;1[	411	0,970	0,020	2,109	0,935	1,030	0,0	0,2
		[1;1,5[	619	0,993	0,022	2,252	0,948	1,122	0,0	5,2
		[1,5;∞[	818	1,011	0,024	2,401	0,982	1,119	0,0	21,0
		[-0,9;-0,6[	504	1,026	0,024	2,375	0,975	1,122	0,0	39,3
		]-0,6;0[	336	0,998	0,015	1,481	0,948	1,037	0,0	1,5
Mono Symmetric	ψ <sub>f</sub>	0	168	0,988	0,016	1,669	0,942	1,035	0,0	0,6
		[0;0,6[	336	0,981	0,016	1,680	0,938	1,030	0,0	0,3
		[0,6;0,9]	504	0,976	0,018	1,853	0,935	1,016	0,0	0,0

Table B.21 – ECCS – Basic Load Cases – Case 2 – ψ<sub>f</sub> limits analysis.

Case 2	Baláž and Koleková	n	Mean	St.Dev	CoV%	Min.	Max.	<0,9%	>1,03%	
Mono Symmetric	ψ <sub>f</sub>	-0,9	168	1,042	0,027	2,590	1,011	1,122	0,0	57,7
		-0,8	168	1,026	0,019	1,842	0,959	1,046	0,0	26,2
		-0,6	168	1,011	0,014	1,400	0,975	1,046	0,0	18,5
		0,6	168	0,976	0,017	1,705	0,936	1,015	0,0	0,0
		0,8	168	0,976	0,018	1,836	0,935	1,008	0,0	0,0
		0,9	168	0,977	0,020	2,014	0,936	1,016	0,0	0,0

• Case 3

Table B.22 – ECCS – Basic Load Cases – Case 3.

Case 3	ECCS	n	Mean	St.Dev	CoV%	Min.	Max.	<0,9%	>1,03%
Double Symmetric	Var.	All	840	0,990	0,018	1,770	0,931	1,017	0,0
	k <sub>z</sub>	1	420	0,995	0,009	0,862	0,972	1,017	0,0
		0,5	420	0,985	0,022	2,246	0,931	1,017	0,0
	h <sub>l</sub>	[0,5;1]	400	0,981	0,020	1,997	0,931	1,015	0,0
		0,5	40	0,989	0,013	1,274	0,967	1,015	0,0
		[0;0,5]	400	0,999	0,009	0,904	0,972	1,017	0,0
	λ <sup>LTBeam</sup>	[0;0,5]	105	0,987	0,021	2,144	0,940	1,017	0,0
		[0,5;1]	432	0,988	0,019	1,877	0,931	1,017	0,0
		[1;∞[	303	0,995	0,013	1,338	0,941	1,017	0,0
	Profile	IPE	420	0,991	0,017	1,730	0,931	1,017	0,0
		HEB	420	0,989	0,018	1,808	0,931	1,017	0,0
Mono Symmetric	Var.	All	1848	1,000	0,030	2,997	0,925	1,138	0,0
	k <sub>w</sub> =1	k <sub>z</sub> =1	924	1,008	0,024	2,348	0,969	1,138	0,0
		k <sub>z</sub> =0,5	924	0,992	0,033	3,369	0,925	1,119	0,0
	h <sub>l</sub>	[0,5;1]	968	0,988	0,027	2,759	0,925	1,079	0,0
		[0;0,5]	968	1,012	0,027	2,657	0,951	1,138	0,0
	λ <sup>LTBeam</sup>	[0;1[	515	1,003	0,031	3,129	0,931	1,138	0,0
		[1;1,5[	677	0,993	0,027	2,688	0,925	1,119	0,0
		[1,5;∞[	656	1,006	0,031	3,043	0,930	1,117	0,0
		[-0,9;-0,6[	504	1,017	0,034	3,321	0,930	1,119	0,0
		]-0,6;0[	336	0,985	0,020	2,048	0,925	1,019	0,0
Ψ <sub>f</sub>	0	168	0,983	0,020	2,025	0,926	1,019	0,0	0,0
		[0;0,6[	336	0,989	0,019	1,967	0,929	1,040	0,0
		[0,6;0,9]	504	1,007	0,029	2,867	0,945	1,138	0,0
									17,3

Table B.23 – ECCS – Basic Load Cases – Case 3 –  $\psi_f$  limits analysis.

Case 3	ECCS	n	Mean	St.Dev	CoV%	Min.	Max.	<0,9%	>1,03%
Mono Symmetric	Ψ <sub>f</sub>	-0,9	168	1,042	0,032	3,037	0,959	1,119	0,0
		-0,8	168	1,014	0,027	2,652	0,940	1,069	0,0
		-0,6	168	0,994	0,023	2,274	0,930	1,036	0,0
		0,6	168	0,997	0,021	2,121	0,945	1,059	0,0
		0,8	168	1,008	0,027	2,663	0,961	1,098	0,0
		0,9	168	1,017	0,034	3,323	0,966	1,138	0,0

• Case 4

Table B.24 – ECCS – Basic Load Cases – Case 4.

Case 4	ECCS	n	Mean	St.Dev	CoV%	Min.	Max.	<0,9%	>1,03%	
Double Symmetric	Var.	All	840	1,009	0,021	2,122	0,960	1,107	0,0	13,0
	k <sub>z</sub>	1	420	1,002	0,002	0,231	1,000	1,010	0,0	0,0
		0,5	420	1,016	0,029	2,809	0,960	1,107	0,0	26,0
	h <sub>l</sub>	[0,5;1]	400	1,017	0,024	2,331	1,000	1,107	0,0	20,3
		0,5	40	1,002	0,009	0,889	0,990	1,028	0,0	0,0
		[0;0,5]	400	1,002	0,016	1,645	0,960	1,042	0,0	7,0
	λ <sup>LTBeam</sup>	[0;0,5]	73	0,997	0,027	2,747	0,961	1,078	0,0	13,7
		[0,5;1]	415	1,011	0,024	2,397	0,960	1,107	0,0	15,4
		[1;∞]	352	1,009	0,015	1,444	0,987	1,087	0,0	9,9
	Profile	IPE	420	1,009	0,021	2,049	0,960	1,106	0,0	12,6
		HEB	420	1,009	0,022	2,196	0,961	1,107	0,0	13,3
Mono Symmetric	Var.	All	1848	1,015	0,034	3,397	0,942	1,160	0,0	22,2
	k <sub>w</sub> =1	k <sub>z</sub> =1	924	1,007	0,009	0,907	0,998	1,064	0,0	3,4
		k <sub>z</sub> =0,5	924	1,022	0,047	4,574	0,942	1,160	0,0	41,1
	h <sub>l</sub>	[0,5;1]	968	1,019	0,036	3,560	0,943	1,121	0,0	27,3
		[0;0,5]	968	1,009	0,031	3,120	0,942	1,160	0,0	16,5
	λ <sup>LTBeam</sup>	[0;1]	352	0,991	0,029	2,970	0,942	1,094	0,0	8,8
		[1;1,5]	635	1,010	0,030	2,957	0,958	1,160	0,0	16,7
		[1,5;∞]	861	1,028	0,034	3,274	0,998	1,156	0,0	31,8
		[-0,9;-0,6]	504	1,045	0,036	3,431	0,996	1,160	0,0	53,4
		[-0,6;0]	336	1,018	0,028	2,754	0,961	1,117	0,0	23,8
Ψ <sub>f</sub>	0	168	1,007	0,028	2,756	0,951	1,116	0,0	13,7	
		[0;0,6]	336	0,998	0,024	2,355	0,944	1,108	0,0	7,4
		[0,6;0,9]	504	0,996	0,021	2,087	0,942	1,077	0,0	2,8

Table B.25 – ECCS – Basic Load Cases – Case 4 –  $\psi_f$  limits analysis.

Case 4	ECCS	n	Mean	St.Dev	CoV%	Min.	Max.	<0,9%	>1,03%	
Mono Symmetric	Ψ <sub>f</sub>	-0,9	168	1,059	0,040	3,748	1,012	1,160	0,0	61,3
		-0,8	168	1,045	0,033	3,152	1,009	1,118	0,0	55,4
		-0,6	168	1,032	0,029	2,805	0,996	1,117	0,0	43,5
		0,6	168	0,993	0,020	2,019	0,942	1,077	0,0	3,0
		0,8	168	0,995	0,020	2,021	0,943	1,062	0,0	1,2
		0,9	168	0,999	0,022	2,187	0,947	1,062	0,0	4,2

### B.3 – Galéa

- Case 1 to 6

Table B.26 – Galéa – Case 1 to 6.

Double Symmetric	Galéa	n	Mean	St.Dev	CoV%	Min.	Max.	<0,9%	>1,03%	
Case 1	Var.	All	820	0,973	0,029	3,032	0,898	1,001	0,6	0,0
		[0,5;1]	220	0,999	0,002	0,153	0,994	1,001	0,0	0,0
	$\Psi$	[0;0,5]	200	0,988	0,010	0,996	0,960	1,000	0,0	0,0
		[-0,5;0]	200	0,961	0,024	2,512	0,907	0,998	0,0	0,0
		[-1;-0,5]	220	0,944	0,028	2,987	0,898	0,995	2,3	0,0
	$\bar{\lambda}^{\text{LTBeam}}$	[0;0,5]	113	0,943	0,029	3,114	0,899	0,996	1,8	0,0
		[0,5;1]	439	0,971	0,029	3,019	0,898	1,001	0,7	0,0
		[1; $\infty$ ]	268	0,988	0,017	1,690	0,932	1,001	0,0	0,0
	Profile	IPE	410	0,974	0,029	2,978	0,898	1,001	0,7	0,0
		HEB	410	0,972	0,030	3,086	0,899	1,001	0,5	0,0
Case 2	Var.	All	420	1,000	0,002	0,203	0,995	1,003	0,0	0,0
		[0,5;1]	200	1,001	0,001	0,100	0,999	1,003	0,0	0,0
	$h_l$	0,5	20	1,000	0,001	0,134	0,998	1,002	0,0	0,0
		[0;0,5]	200	0,999	0,002	0,215	0,995	1,002	0,0	0,0
	$\bar{\lambda}^{\text{LTBeam}}$	[0;0,5]	19	0,996	0,001	0,074	0,995	0,997	0,0	0,0
		[0,5;1]	199	0,999	0,002	0,192	0,995	1,003	0,0	0,0
		[1; $\infty$ ]	202	1,001	0,001	0,148	0,997	1,003	0,0	0,0
	Profile	IPE	210	1,000	0,002	0,199	0,995	1,003	0,0	0,0
		HEB	210	1,000	0,002	0,207	0,995	1,003	0,0	0,0
	Var.	All	420	0,994	0,020	2,014	0,943	1,045	0,0	4,0
Case 3		[0,5;1]	200	0,978	0,014	1,467	0,943	0,999	0,0	0,0
	$h_l$	0,5	20	0,993	0,003	0,346	0,989	0,999	0,0	0,0
		[0;0,5]	200	1,010	0,012	1,194	0,994	1,045	0,0	8,5
	$\bar{\lambda}^{\text{LTBeam}}$	[0;0,5]	35	1,014	0,019	1,861	0,980	1,045	0,0	25,7
		[0,5;1]	202	0,991	0,022	2,195	0,943	1,044	0,0	4,0
		[1; $\infty$ ]	183	0,993	0,016	1,580	0,943	1,027	0,0	0,0
	Profile	IPE	210	0,994	0,019	1,932	0,943	1,044	0,0	3,8
		HEB	210	0,994	0,021	2,098	0,943	1,045	0,0	4,3
	Var.	All	420	0,995	0,005	0,482	0,983	1,004	0,0	0,0
		[0,5;1]	200	0,996	0,003	0,316	0,990	1,004	0,0	0,0
Case 5	$h_l$	0,5	20	0,992	0,004	0,367	0,988	0,999	0,0	0,0
		[0;0,5]	200	0,993	0,006	0,559	0,983	1,003	0,0	0,0
	$\bar{\lambda}^{\text{LTBeam}}$	[0;0,5]	110	0,992	0,005	0,514	0,983	1,003	0,0	0,0
		[0,5;1]	215	0,995	0,005	0,461	0,984	1,004	0,0	0,0
		[1; $\infty$ ]	95	0,997	0,003	0,290	0,991	1,004	0,0	0,0
	Profile	IPE	210	0,995	0,005	0,471	0,983	1,004	0,0	0,0
		HEB	210	0,995	0,005	0,494	0,984	1,004	0,0	0,0
	Var.	All	420	0,987	0,053	5,400	0,876	1,112	6,0	20,5
		[0,5;1]	200	0,944	0,033	3,548	0,876	0,997	12,5	0,0
	$h_l$	0,5	20	0,983	0,007	0,736	0,976	0,998	0,0	0,0
Case 6		[0;0,5]	200	1,031	0,032	3,127	0,990	1,112	0,0	43,0
	$\bar{\lambda}^{\text{LTBeam}}$	[0;0,5]	53	1,041	0,050	4,843	0,934	1,112	0,0	60,4
		[0,5;1]	216	0,986	0,053	5,428	0,876	1,096	6,0	22,7
		[1; $\infty$ ]	151	0,971	0,041	4,225	0,876	1,056	7,9	3,3
	Profile	IPE	210	0,987	0,055	5,604	0,876	1,112	6,2	21,4
		HEB	210	0,988	0,051	5,202	0,876	1,111	5,7	19,5

• Case 7 and 8

Table B.27 – Galéa – Case 7.

Case 7	Galéa	n	Mean	St.Dev	CoV%	Min.	Max.	<0,9%	>1,03%
$M_0/M$	Var.	All	31860	0,990	0,023	2,305	0,773	1,113	1,3
		[4;∞]	1620	0,998	0,004	0,414	0,986	1,017	0,0
		[2;4]	2700	0,997	0,003	0,310	0,980	1,004	0,0
		[1;2]	5400	0,996	0,005	0,538	0,956	1,005	0,0
		[0;1]	5400	0,988	0,018	1,808	0,893	1,004	0,2
	$\mu$	0	1080	0,973	0,029	3,005	0,903	1,001	0,0
		[-1;0]	5400	0,971	0,042	4,295	0,773	1,113	7,3
		[-2;-1]	5400	0,995	0,015	1,468	0,836	1,101	0,3
		[-4;-2]	2700	0,996	0,003	0,298	0,985	1,002	0,0
		[-∞;-4]	2160	0,997	0,004	0,438	0,968	1,013	0,0
Double Symmetric	ψ	[0,5;1]	7080	0,996	0,020	2,045	0,799	1,113	0,9
		[0;0,5]	10620	0,991	0,025	2,476	0,773	1,102	2,2
		[-0,5;0]	10620	0,987	0,024	2,415	0,786	1,055	1,8
		[-1;-0,5]	7080	0,985	0,020	2,054	0,893	1,013	0,2
		1	10620	0,995	0,014	1,387	0,903	1,102	0,0
$h_l$		0,5	10620	0,987	0,026	2,653	0,773	1,040	2,4
		0	10620	0,988	0,025	2,561	0,786	1,113	1,6
									1,1
$\bar{\lambda}^{LTBeam}$		[0;0,5]	3143	0,966	0,048	4,963	0,773	1,113	9,2
		[0,5;1]	15242	0,989	0,020	2,034	0,822	1,100	0,9
		[1;∞]	13475	0,996	0,008	0,826	0,928	1,041	0,0
Profile		IPE	15930	0,990	0,022	2,246	0,773	1,100	1,2
		HEB	15930	0,990	0,023	2,362	0,774	1,113	1,4
									0,7

Table B.28 – Galéa – Case 8.

Case 8	Galéa	n	Mean	St.Dev	CoV%	Min.	Max.	<0,9%	>1,03%
$M_0/M$	Var.	All	31860	0,992	0,046	4,640	0,794	1,558	1,9
		[4;∞]	1620	0,997	0,020	2,054	0,932	1,087	0,0
		[2;4]	2700	0,995	0,005	0,507	0,973	1,012	0,0
		[1;2]	5400	0,996	0,010	0,971	0,935	1,046	0,0
		[0;1]	5400	0,990	0,022	2,217	0,872	1,066	0,8
	$\mu$	0	1080	0,973	0,029	3,005	0,903	1,001	0,0
		[-1;0]	5400	0,980	0,054	5,509	0,794	1,339	6,6
		[-2;-1]	5400	1,004	0,085	8,514	0,870	1,558	3,4
		[-4;-2]	2700	0,993	0,037	3,716	0,881	1,096	0,7
		[-∞;-4]	2160	0,992	0,028	2,853	0,921	1,065	0,0
Double Symmetric	ψ	[0,5;1]	7080	1,002	0,064	6,346	0,870	1,558	1,8
		[0;0,5]	10620	0,993	0,048	4,814	0,814	1,467	2,7
		[-0,5;0]	10620	0,988	0,036	3,629	0,794	1,208	2,1
		[-1;-0,5]	7080	0,987	0,028	2,805	0,872	1,066	0,8
		1	10620	0,981	0,030	3,089	0,870	1,066	1,7
$h_l$		0,5	10620	0,984	0,024	2,468	0,814	1,040	2,3
		0	10620	1,012	0,065	6,439	0,794	1,558	1,7
									22,9
$\bar{\lambda}^{LTBeam}$		[0;0,5]	3755	1,009	0,098	9,727	0,794	1,558	6,5
		[0,5;1]	15657	0,989	0,039	3,960	0,819	1,434	1,8
		[1;∞]	12448	0,991	0,022	2,248	0,870	1,150	0,6
Profile		IPE	15930	0,992	0,044	4,456	0,794	1,537	1,8
		HEB	15930	0,992	0,048	4,818	0,797	1,558	2,0
									8,6

#### B.4 – Andrade *et al.*

- Case 9

Table B.29 – Andrade *et al.* – Case 9.

Case 9	Andrade <i>et al.</i>	n	Mean	St.Dev	CoV%	Min.	Max.	<0,9%	>1,03%
Double Symmetric	Var.	All	120	1,001	0,010	0,971	0,969	1,018	0,0
	k <sub>w</sub>	0,5	60	1,003	0,007	0,713	0,982	1,013	0,0
		1	60	1,000	0,012	1,170	0,969	1,018	0,0
		1	40	1,001	0,006	0,597	0,980	1,009	0,0
	h <sub>l</sub>	0,5	40	0,999	0,009	0,857	0,972	1,009	0,0
		0	40	1,005	0,013	1,273	0,969	1,018	0,0
		]0;0,5[	10	1,008	0,008	0,770	0,997	1,016	0,0
	λ <sup>LTBeam</sup>	[0,5;1[	54	1,004	0,007	0,656	0,986	1,018	0,0
		[1;∞[	56	0,998	0,011	1,131	0,969	1,016	0,0
	Profile	IPE	60	1,000	0,010	0,969	0,969	1,016	0,0
		HEB	60	1,002	0,010	0,972	0,971	1,018	0,0
Mono Symmetric	Var.	All	216	1,007	0,015	1,490	0,968	1,118	0,0
	k <sub>w</sub>	0,5	108	1,006	0,012	1,152	0,979	1,044	0,0
		1	108	1,009	0,018	1,757	0,968	1,118	0,0
		1	72	1,006	0,022	2,178	0,968	1,118	0,0
	h <sub>l</sub>	0,5	72	1,003	0,007	0,665	0,985	1,018	0,0
		0	72	1,013	0,010	0,986	0,995	1,044	0,0
		]0;1[	40	1,008	0,018	1,756	0,968	1,044	0,0
	λ <sup>LTBeam</sup>	[1;1,5[	66	1,002	0,010	0,988	0,979	1,026	0,0
		[1,5;∞[	110	1,010	0,016	1,553	0,993	1,118	0,0
		[-0,8;-0,4[	48	1,006	0,018	1,751	0,968	1,044	0,0
ψ <sub>f</sub>		[-0,4;0[	48	1,003	0,009	0,937	0,982	1,023	0,0
		0	24	1,003	0,005	0,547	0,995	1,016	0,0
		]0;0,4[	48	1,007	0,006	0,561	0,997	1,019	0,0
		]0,4;0,8]	48	1,016	0,022	2,129	0,993	1,118	0,0

Table B.30 – Andrade *et al.* – Case 9 – ψ<sub>f</sub> limits analysis.

Case 2	Andrade <i>et al.</i>	n	Mean	St.Dev	CoV%	Min.	Max.	<0,9%	>1,03%
Mono Symmetric	ψ <sub>f</sub>	-0,8	24	1,009	0,020	1,959	0,968	1,044	0,0
		-0,6	24	1,003	0,015	1,481	0,979	1,028	0,0
		0,6	24	1,013	0,012	1,138	0,997	1,042	0,0
		0,8	24	1,019	0,028	2,781	0,993	1,118	0,0

• Case 10

Table B.31 – Andrade *et al.* – Case 10.

Case 10	Andrade <i>et al.</i>	n	Mean	St.Dev	CoV%	Min.	Max.	<0,9%	>1,03%
Double Symmetric	Var.	All	120	1,003	0,011	1,091	0,963	1,018	0,0
		0,5	60	1,005	0,006	0,589	0,993	1,014	0,0
	k <sub>w</sub>	1	60	1,000	0,014	1,393	0,963	1,018	0,0
		1	40	1,001	0,009	0,891	0,970	1,011	0,0
	h <sub>l</sub>	0,5	40	1,001	0,011	1,060	0,965	1,013	0,0
		0	40	1,006	0,013	1,252	0,963	1,018	0,0
	λ <sup>LTBeam</sup>	[0;0,5[	24	1,007	0,007	0,682	0,996	1,018	0,0
		[0,5;1[	64	1,003	0,010	1,023	0,966	1,017	0,0
		[1;∞[	32	0,998	0,013	1,325	0,963	1,013	0,0
	Profile	IPE	60	1,002	0,011	1,105	0,963	1,015	0,0
		HEB	60	1,003	0,011	1,080	0,966	1,018	0,0
Mono Symmetric	Var.	All	216	1,009	0,017	1,670	0,974	1,132	0,0
		0,5	108	1,007	0,012	1,192	0,981	1,063	0,0
	k <sub>w</sub>	1	108	1,011	0,020	2,019	0,974	1,132	0,0
		1	72	1,008	0,023	2,278	0,974	1,132	0,0
	h <sub>l</sub>	0,5	72	1,004	0,008	0,801	0,981	1,025	0,0
		0	72	1,016	0,014	1,372	0,999	1,068	0,0
	λ <sup>LTBeam</sup>	[0;1[	75	1,009	0,012	1,190	0,983	1,063	0,0
		[1;1,5[	100	1,009	0,014	1,385	0,981	1,070	0,0
		[1,5;∞[	41	1,010	0,028	2,756	0,974	1,132	0,0
		[-0,8;-0,4[	48	1,010	0,022	2,149	0,974	1,068	0,0
Ψ <sub>f</sub>		[-0,4;0[	48	1,004	0,009	0,918	0,986	1,025	0,0
		0	24	1,004	0,005	0,529	0,995	1,014	0,0
		[0;0,4]	48	1,008	0,006	0,607	0,996	1,022	0,0
		[0,4;0,8]	48	1,018	0,024	2,364	0,996	1,132	0,0

Table B.32 – Andrade *et al.* – Case 10 –  $\psi_f$  limits analysis.

Case 10	Andrade <i>et al.</i>	n	Mean	St.Dev	CoV%	Min.	Max.	<0,9%	>1,03%
Mono Symmetric	Ψ <sub>f</sub>	-0,8	24	1,016	0,025	2,427	0,974	1,068	0,0
		-0,6	24	1,003	0,016	1,628	0,981	1,034	0,0
		0,6	24	1,015	0,013	1,300	0,999	1,047	0,0
		0,8	24	1,020	0,032	3,095	0,996	1,132	0,0

## B.5 – Lindner

- Case 9

Table B.33 – Lindner – Case 9.

Case 9	Lindner	n	Mean	St.Dev	CoV%	Min.	Max.	<0,9%	>1,03%
All	Interpolation	612	1,012	0,016	1,606	0,976	1,074	0,0	14,7
	Formula	612	1,012	0,017	1,656	0,975	1,077	0,0	13,2
<b><math>L_1/L</math></b>									
0	Interpolation	68	1,002	0,013	1,277	0,989	1,048	0,0	2,9
	Formula	68	1,002	0,013	1,298	0,989	1,050	0,0	2,9
]0;0,5[	Interpolation	68	1,027	0,011	1,049	1,013	1,069	0,0	27,9
	Formula	68	1,015	0,012	1,211	0,994	1,061	0,0	11,8
0,25	Interpolation	68	1,000	0,013	1,294	0,976	1,043	0,0	1,5
	Formula	68	1,000	0,013	1,297	0,975	1,046	0,0	1,5
]0,25;0,5[	Interpolation	68	1,012	0,014	1,356	0,995	1,065	0,0	10,3
	Formula	68	1,005	0,015	1,444	0,984	1,062	0,0	8,8
0,5	Interpolation	68	1,008	0,014	1,359	0,996	1,064	0,0	8,8
	Formula	68	1,008	0,014	1,378	0,996	1,066	0,0	8,8
]0,5;1[	Interpolation	204	1,020	0,015	1,437	0,994	1,074	0,0	26,5
	Formula	204	1,026	0,013	1,249	1,006	1,077	0,0	27,5
1	Interpolation	68	1,001	0,012	1,180	0,991	1,043	0,0	1,5
	Formula	68	1,001	0,012	1,180	0,991	1,043	0,0	1,5
<b><math>h_1</math></b>									
Top Flange	Interpolation	306	1,022	0,016	1,554	0,993	1,074	0,0	29,4
	Formula	306	1,020	0,016	1,598	0,993	1,077	0,0	25,2
Shear Center	Interpolation	306	1,003	0,010	1,007	0,976	1,026	0,0	0,0
	Formula	306	1,004	0,013	1,267	0,975	1,043	0,0	1,3
<b><math>\lambda^{LTBeam}</math></b>									
]0;0,6[	Interpolation	204	1,012	0,020	1,957	0,976	1,074	0,0	16,7
	Formula	204	1,012	0,020	2,006	0,975	1,077	0,0	18,1
]0,6;0,9[	Interpolation	225	1,016	0,016	1,528	0,989	1,056	0,0	23,6
	Formula	225	1,016	0,016	1,543	0,990	1,055	0,0	18,2
]0,9;∞[	Interpolation	183	1,008	0,011	1,065	0,989	1,032	0,0	1,6
	Formula	183	1,007	0,012	1,168	0,990	1,036	0,0	1,6
<b>Profile</b>									
IPE	Interpolation	288	1,007	0,011	1,131	0,983	1,044	0,0	2,4
	Formula	288	1,007	0,012	1,225	0,984	1,046	0,0	2,4
HEB	Interpolation	324	1,017	0,018	1,813	0,976	1,074	0,0	25,6
	Formula	324	1,017	0,019	1,840	0,975	1,077	0,0	22,8

• Case 10

Table B.34 – Lindner – Case 10.

Case 10	Lindner	n	Mean	St.Dev	CoV%	Min.	Max.	<0,9%	>1,03%
All	Interpolation	612	1,016	0,020	1,970	0,985	1,089	0,0	24,0
	Formula	612	1,022	0,017	1,710	0,991	1,086	0,0	34,2
<b><math>L_1/L</math></b>									
0	Interpolation	68	1,006	0,011	1,077	0,997	1,052	0,0	2,9
	Formula	68	1,007	0,011	1,082	0,997	1,053	0,0	2,9
$ 0;0,5 $	Interpolation	68	1,052	0,009	0,858	1,035	1,089	0,0	100,0
	Formula	68	1,034	0,009	0,899	1,019	1,073	0,0	73,5
$0,25$	Interpolation	68	1,004	0,009	0,922	0,990	1,040	0,0	1,5
	Formula	68	1,004	0,009	0,939	0,991	1,044	0,0	1,5
$ 0,25;0,5 $	Interpolation	68	1,024	0,012	1,176	1,012	1,080	0,0	27,9
	Formula	68	1,015	0,012	1,179	1,003	1,072	0,0	8,8
$0,5$	Interpolation	68	1,020	0,012	1,151	1,007	1,078	0,0	16,2
	Formula	68	1,020	0,012	1,176	1,007	1,080	0,0	17,6
$ 0,5;1 $	Interpolation	204	1,012	0,020	1,994	0,985	1,080	0,0	22,1
	Formula	204	1,036	0,012	1,205	1,010	1,086	0,0	67,2
1	Interpolation	68	1,006	0,008	0,829	0,992	1,040	0,0	1,5
	Formula	68	1,006	0,008	0,829	0,992	1,040	0,0	1,5
<b><math>h_l</math></b>									
Top Flange	Interpolation	306	1,024	0,019	1,834	0,990	1,089	0,0	35,6
	Formula	306	1,024	0,018	1,781	0,991	1,086	0,0	35,0
Shear Center	Interpolation	306	1,008	0,018	1,782	0,985	1,055	0,0	12,4
	Formula	306	1,019	0,016	1,606	0,997	1,049	0,0	33,3
<b><math>\lambda^{LTBeam}</math></b>									
$ 0;0,6 $	Interpolation	255	1,019	0,023	2,270	0,985	1,089	0,0	29,8
	Formula	255	1,024	0,019	1,816	0,997	1,086	0,0	41,2
$ 0,6;0,9 $	Interpolation	275	1,016	0,018	1,792	0,986	1,061	0,0	23,6
	Formula	275	1,022	0,016	1,597	0,993	1,056	0,0	34,2
$ 0,9;∞ $	Interpolation	82	1,010	0,013	1,262	0,985	1,044	0,0	7,3
	Formula	82	1,013	0,014	1,428	0,991	1,049	0,0	12,2
<b>Profile</b>									
IPE	Interpolation	288	1,011	0,017	1,653	0,985	1,057	0,0	13,5
	Formula	288	1,016	0,016	1,545	0,991	1,054	0,0	23,6
HEB	Interpolation	324	1,021	0,021	2,102	0,985	1,089	0,0	33,3
	Formula	324	1,026	0,018	1,723	0,997	1,086	0,0	43,5

## B.6 – Trahair

- Case 1 to 6

Table B.35 – Trahair – Case 1 to 4.

Double Symmetric	Trahair	n	Mean	St.Dev	CoV%	Min.	Max.	<0,9%	>1,03%	
Case 1	Var.	All	820	0,963	0,033	3,412	0,875	1,015	6,2	0,0
		[0,5;1]	220	0,993	0,004	0,391	0,985	1,000	0,0	0,0
	ψ	[0;0,5]	200	0,977	0,010	1,040	0,949	0,991	0,0	0,0
		[-0,5;0]	200	0,954	0,023	2,367	0,910	0,999	0,0	0,0
		[-1;-0,5]	220	0,928	0,034	3,630	0,875	1,015	23,2	0,0
	λ <sup>LTBeam</sup>	[0;0,5]	113	0,932	0,032	3,384	0,875	0,988	18,6	0,0
		[0,5;1]	439	0,960	0,033	3,459	0,875	1,014	6,8	0,0
		[1;∞]	268	0,980	0,019	1,985	0,905	1,015	0,0	0,0
	Profile	IPE	410	0,964	0,032	3,364	0,875	1,015	5,6	0,0
		HEB	410	0,962	0,033	3,461	0,875	1,014	6,8	0,0
Case 2	Var.	All	420	1,000	0,002	0,203	0,995	1,003	0,0	0,0
		[0,5;1]	200	1,001	0,001	0,100	0,999	1,003	0,0	0,0
	h <sub>l</sub>	0,5	20	1,000	0,001	0,134	0,998	1,002	0,0	0,0
		[0;0,5]	200	0,999	0,002	0,215	0,995	1,002	0,0	0,0
	λ <sup>LTBeam</sup>	[0;0,5]	19	0,996	0,001	0,074	0,995	0,997	0,0	0,0
		[0,5;1]	199	0,999	0,002	0,192	0,995	1,003	0,0	0,0
		[1;∞]	202	1,001	0,001	0,148	0,997	1,003	0,0	0,0
	Profile	IPE	210	1,000	0,002	0,199	0,995	1,003	0,0	0,0
		HEB	210	1,000	0,002	0,207	0,995	1,003	0,0	0,0
	Var.	All	600	0,995	0,010	1,035	0,963	1,020	0,0	0,0
Case 3		[0,5;1]	200	1,002	0,005	0,452	0,992	1,010	0,0	0,0
	h <sub>l</sub>	0,5	200	0,996	0,013	1,351	0,963	1,020	0,0	0,0
		[0;0,5]	200	0,989	0,005	0,525	0,980	1,000	0,0	0,0
	d	[0,25;0,5]*	100	0,988	0,013	1,276	0,963	1,015	0,0	0,0
	(h <sub>l</sub> = 0,5)*	[0;0,25]*	100	0,999	0,010	1,033	0,977	1,020	0,0	0,0
		0	420	0,996	0,009	0,892	0,980	1,019	0,0	0,0
	λ <sup>LTBeam</sup>	[0;0,5]	59	0,985	0,010	0,970	0,963	1,008	0,0	0,0
		[0,5;1]	289	0,995	0,010	1,012	0,963	1,017	0,0	0,0
		[1;∞]	252	0,999	0,009	0,881	0,973	1,020	0,0	0,0
	Profile	IPE	300	0,996	0,010	1,023	0,963	1,020	0,0	0,0
Case 4		HEB	300	0,995	0,010	1,047	0,963	1,020	0,0	0,0
	Var.	All	580	1,044	0,013	1,269	1,003	1,068	0,0	87,6
		[0,5;1]	200	1,043	0,002	0,214	1,038	1,047	0,0	100,0
	h <sub>l</sub>	0,5	180	1,035	0,018	1,777	1,003	1,060	0,0	60,0
		[0;0,5]	200	1,054	0,005	0,513	1,047	1,068	0,0	100,0
	d	[0,25;0,5]*	80	1,018	0,012	1,189	1,003	1,036	0,0	25,0
	(h <sub>l</sub> = 0,5)*	0,25	420	1,048	0,007	0,633	1,038	1,068	0,0	100,0
		[0;0,25]*	80	1,048	0,011	1,024	1,027	1,060	0,0	85,0
	λ <sup>LTBeam</sup>	[0;0,5]	11	1,060	0,012	1,086	1,028	1,068	0,0	90,9
		[0,5;1]	271	1,045	0,013	1,287	1,003	1,068	0,0	87,1
Case 4			[1;∞]	318	1,043	0,013	1,220	1,003	1,063	0,0
	Profile	IPE	290	1,044	0,013	1,260	1,003	1,068	0,0	87,9
		HEB	290	1,044	0,013	1,280	1,003	1,068	0,0	87,2

Table B.36 – Trahair – Case 5 to 6.

Double Symmetric	Trahair	n	Mean	St.Dev	CoV%	Min.	Max.	<0,9%	>1,03%		
Case 5	$\bar{\lambda}^{\text{LTBeam}}$	Var.	All	20	0,931	0,003	0,367	0,927	0,938	0,0	0,0
			$[0;0,5]$	4	0,928	0,001	0,100	0,927	0,929	0,0	0,0
			$[0,5;1]$	13	0,931	0,003	0,351	0,927	0,937	0,0	0,0
			$[1;\infty]$	3	0,934	0,003	0,366	0,931	0,938	0,0	0,0
	Profile	IPE		10	0,931	0,004	0,385	0,927	0,938	0,0	0,0
		HEB		10	0,931	0,003	0,368	0,927	0,937	0,0	0,0
	$\bar{\lambda}^{\text{LTBeam}}$	Var.	All	20	0,999	0,007	0,736	0,991	1,014	0,0	0,0
			$[0;0,5]$	3	0,992	0,000	0,032	0,991	0,992	0,0	0,0
			$[0,5;1]$	10	0,998	0,007	0,730	0,991	1,013	0,0	0,0
			$[1;\infty]$	7	1,002	0,007	0,713	0,995	1,014	0,0	0,0
	Profile	IPE		10	0,999	0,008	0,770	0,991	1,014	0,0	0,0
		HEB		10	0,998	0,007	0,739	0,991	1,013	0,0	0,0

Table B.37 – Trahair – Case 3 to 6 –  $h_l$  analysis.

	Trahair	n	Mean	St.Dev	CoV%	Min.	Max.	<0,9%	>1,03%	
Case 3	$h_l=1$	$d \in [0,25;0,5]$	100	0,878	0,099	11,248	0,637	1,016	49,0	0,0
		$d \in [0;0,25]$	100	0,995	0,029	2,875	0,913	1,028	0,0	0,0
		$d = 0$	20	1,008	0,001	0,085	1,007	1,010	0,0	0,0
		$d \in [0,25;0,5]$	100	0,990	0,015	1,497	0,963	1,020	0,0	0,0
	$h_l=0,5$	$d \in [0;0,25]$	100	1,003	0,009	0,943	0,986	1,020	0,0	0,0
		$d = 0$	20	0,994	0,003	0,346	0,991	1,001	0,0	0,0
	$h_l=0$	$d \in [0,25;0,5]$	100	1,160	0,113	9,773	1,020	1,485	0,0	96,0
		$d \in [0;0,25]$	100	1,029	0,034	3,338	0,995	1,135	0,0	36,0
Case 4	$h_l=1$	$d = 0,25$	20	0,985	0,005	0,500	0,980	0,996	0,0	0,0
		$d \in [0,25;0,5]$	80	1,114	0,060	5,425	1,032	1,276	0,0	100,0
		$d=0,25$	20	1,061	0,006	0,525	1,051	1,068	0,0	100,0
		$d \in [0;0,25]$	80	1,032	0,017	1,692	0,998	1,057	0,0	52,5
	$h_l=0,5$	$d \in [0,25;0,5]$	80	1,018	0,012	1,189	1,003	1,036	0,0	25,0
		$d=0,25$	20	1,046	0,001	0,052	1,046	1,047	0,0	100,0
	$h_l=0$	$d \in [0;0,25]$	80	1,048	0,011	1,024	1,027	1,060	0,0	85,0
		$d \in [0,25;0,5]$	80	0,944	0,063	6,659	0,794	1,029	25,0	0,0
Case 5	$h_l$	$d=0,25$	20	1,041	0,002	0,225	1,038	1,045	0,0	100,0
		$d \in [0;0,25]$	80	1,068	0,011	1,076	1,044	1,089	0,0	100,0
	$h_l$	$[0,5;1]$	200	1,073	0,100	9,280	0,942	1,312	0,0	56,5
		$0,5$	20	0,931	0,003	0,367	0,927	0,938	0,0	0,0
Case 6	$h_l$	$[0;0,5]$	200	0,819	0,072	8,773	0,672	0,933	85,0	0,0
		$[0,5;1]$	200	1,205	0,143	11,874	1,022	1,567	0,0	96,5
	$h_l$	$0,5$	20	0,999	0,007	0,736	0,991	1,014	0,0	0,0
		$[0;0,5]$	200	0,845	0,098	11,562	0,642	1,006	66,0	0,0

• Case 7 and 8

Table B.38 – Trahair – Case 7 and 8.

Double Symmetric	Trahair	n	Mean	St.Dev	CoV%	Min.	Max.	<0,9%	>1,03%	
	Var.	All	700	1,000	0,016	1,561	0,927	1,035	0,0	0,7
		1	300	0,998	0,021	2,130	0,927	1,035	0,0	1,7
		0	400	1,001	0,009	0,919	0,968	1,027	0,0	0,0
$\psi = 1$										
Case 7	M0/M	[ -2;-1 ]	220	0,999	0,012	1,197	0,968	1,027	0,0	0,0
		[ -4;-2 ]	100	1,004	0,002	0,238	0,999	1,008	0,0	0,0
	$\mu$	[ $-\infty$ ; -4 ]	80	1,003	0,002	0,168	1,000	1,007	0,0	0,0
						$\psi = 0$				
	M0/M	[ -2;-1,5 ]	120	0,993	0,033	3,283	0,927	1,035	0,0	4,2
		[ -4;-2 ]	100	0,999	0,006	0,562	0,987	1,008	0,0	0,0
	$\mu$	[ $-\infty$ ; -4 ]	80	1,003	0,002	0,188	1,000	1,008	0,0	0,0
	$\bar{\lambda}^{\text{LTBeam}}$	[ 0;0,5 ]	34	0,993	0,028	2,795	0,927	1,023	0,0	0,0
		[ 0,5;1 ]	375	0,998	0,016	1,635	0,927	1,034	0,0	0,5
		[ 1; $\infty$ ]	291	1,002	0,012	1,190	0,931	1,035	0,0	1,0
	Profile	IPE	350	1,000	0,016	1,563	0,927	1,035	0,0	0,9
		HEB	350	1,000	0,016	1,562	0,927	1,034	0,0	0,6
	Var.	All	520	1,000	0,014	1,431	0,981	1,036	0,0	3,5
		1	200	1,015	0,010	1,028	0,991	1,036	0,0	9,0
		0	320	0,990	0,006	0,559	0,981	1,001	0,0	0,0
						$\psi = 1$				
Case 8	M0/M	[ -4;-2 ]	120	1,015	0,012	1,185	0,991	1,036	0,0	13,3
		[ $-\infty$ ; -4 ]	80	1,014	0,007	0,734	1,001	1,031	0,0	2,5
						$\psi = 0$				
	M0/M	[ -2;-1,4 ]	140	0,988	0,006	0,584	0,981	1,001	0,0	0,0
		[ -4;-2 ]	100	0,990	0,005	0,500	0,982	1,000	0,0	0,0
	$\mu$	[ $-\infty$ ; -4 ]	80	0,994	0,004	0,386	0,989	1,001	0,0	0,0
	$\bar{\lambda}^{\text{LTBeam}}$	[ 0;0,5 ]	75	0,994	0,013	1,348	0,981	1,019	0,0	0,0
		[ 0,5;1 ]	242	0,999	0,014	1,406	0,981	1,035	0,0	2,1
		[ 1; $\infty$ ]	203	1,003	0,014	1,418	0,984	1,036	0,0	6,4
	Profile	IPE	260	1,000	0,014	1,437	0,981	1,036	0,0	3,8
		HEB	260	0,999	0,014	1,427	0,981	1,036	0,0	3,1

• Case 9 and 10

Table B.39 – Trahair – Case 9 and 10.

Double Symmetric	Trahair	n	Mean	St.Dev	CoV%	Min.	Max.	<0,9%	>1,03%
Case 9	Var.	All	1,039	0,071	6,814	0,966	1,338	0,0	40,0
	k <sub>z</sub>	0,5	1,045	0,097	9,312	0,966	1,338	0,0	25,0
		1	1,032	0,024	2,278	0,982	1,084	0,0	55,0
		1	1,093	0,097	8,916	1,005	1,338	0,0	65,0
	h <sub>l</sub>	0,5	1,009	0,019	1,922	0,976	1,039	0,0	20,0
		0	1,014	0,029	2,870	0,966	1,058	0,0	35,0
	λ <sup>LTBeam</sup>	0;0,5	0,983	0,011	1,079	0,969	1,000	0,0	0,0
		0,5;1	1,042	0,078	7,469	0,966	1,336	0,0	38,9
		[1;∞]	1,046	0,066	6,310	0,994	1,338	0,0	48,2
	Profile	IPE	1,037	0,068	6,532	0,966	1,338	0,0	40,0
		HEB	1,040	0,074	7,136	0,969	1,336	0,0	40,0
Case 10	Var.	All	0,964	0,074	7,637	0,850	1,223	10,0	11,7
	k <sub>z</sub>	0,5	1,006	0,080	7,985	0,940	1,223	0,0	23,3
		1	0,921	0,029	3,097	0,850	0,975	20,0	0,0
		1	1,014	0,102	10,024	0,915	1,223	0,0	35,0
	h <sub>l</sub>	0,5	0,930	0,043	4,607	0,850	0,974	30,0	0,0
		0	0,947	0,017	1,845	0,920	0,975	0,0	0,0
	λ <sup>LTBeam</sup>	0;0,5	0,971	0,090	9,265	0,852	1,215	16,7	12,5
		0,5;1	0,967	0,077	8,009	0,850	1,223	9,4	12,5
		[1;∞]	0,952	0,049	5,136	0,889	1,115	6,3	9,4
	Profile	IPE	0,962	0,072	7,434	0,850	1,223	8,3	11,7
		HEB	0,966	0,076	7,891	0,852	1,222	11,7	11,7

## B.7 – Serna et al.

- Case 1 and 4

Table B.40 – Serna et al. – Case 1 and 6.

Double Symmetric		Serna et al.	n	Mean	St.Dev	CoV%	Min.	Max.	<0,9%	>1,03%
Case 1	$\psi$	Var.	All	0,973	0,031	3,203	0,890	1,026	3,8	0,0
		[0,5;1]	220	0,994	0,004	0,390	0,986	1,000	0,0	0,0
		[0;0,5]	200	0,984	0,008	0,800	0,965	1,004	0,0	0,0
		[-0,5;0]	200	0,980	0,023	2,306	0,934	1,026	0,0	0,0
		[-1;-0,5]	220	0,936	0,034	3,633	0,890	1,023	14,1	0,0
	$\bar{\lambda}^{\text{LTBeam}}$	[0;0,5]	113	0,945	0,031	3,322	0,890	0,989	15,0	0,0
		[0,5;1]	439	0,970	0,032	3,280	0,890	1,025	3,2	0,0
		[1;∞[	268	0,989	0,017	1,769	0,914	1,026	0,0	0,0
	Profile	IPE	410	0,974	0,031	3,170	0,890	1,026	3,4	0,0
		HEB	410	0,972	0,031	3,236	0,890	1,025	4,1	0,0
Case 2	$k_w=k_z$	Var.	All	1,020	0,026	2,585	0,993	1,056	0,0	50,0
		1	20	0,994	0,001	0,134	0,993	0,997	0,0	0,0
		0,5	20	1,046	0,004	0,346	1,044	1,056	0,0	100,0
		[0;0,5[	4	1,044	0,000	0,036	1,044	1,045	0,0	100,0
		[0,5;1]	22	1,020	0,027	2,624	0,993	1,055	0,0	50,0
	Profile	[1;∞[	14	1,014	0,027	2,644	0,993	1,056	0,0	35,7
		IPE	20	1,020	0,027	2,613	0,993	1,055	0,0	50,0
		HEB	20	1,021	0,027	2,626	0,993	1,056	0,0	50,0
		Var.	All	220	0,988	0,033	3,326	0,915	1,055	0,0
		$k_w=k_z$	1	200	0,990	0,034	3,422	0,915	1,055	0,0
Case 3	$d$ ( $k=1$ )	0,5	20	0,969	0,005	0,542	0,966	0,983	0,0	0,0
		[0,25;0,5[	100	0,983	0,019	1,968	0,948	1,021	0,0	0,0
		[0;0,25[	100	1,005	0,029	2,888	0,948	1,055	0,0	20,0
		0	20	0,919	0,003	0,346	0,915	0,925	0,0	0,0
		[0;0,5[	30	0,978	0,029	2,933	0,915	1,039	0,0	6,7
	$\bar{\lambda}^{\text{LTBeam}}$	[0,5;1]	109	0,987	0,033	3,313	0,915	1,052	0,0	9,2
		[1;∞[	81	0,994	0,034	3,402	0,917	1,055	0,0	9,9
		IPE	110	0,989	0,033	3,337	0,915	1,055	0,0	9,1
		HEB	110	0,988	0,033	3,329	0,915	1,054	0,0	9,1
		Var.	All	200	1,002	0,024	2,378	0,962	1,053	0,0
Case 4	$k_w=k_z$	1	180	0,997	0,020	2,040	0,962	1,034	0,0	4,4
		0,5	20	1,043	0,004	0,353	1,041	1,053	0,0	100,0
		[0,25;0,5[	80	0,992	0,008	0,763	0,980	1,000	0,0	0,0
		0,25	20	0,962	0,000	0,052	0,962	0,963	0,0	0,0
		[0;0,25[	80	1,011	0,019	1,857	0,977	1,034	0,0	10,0
	$\bar{\lambda}^{\text{LTBeam}}$	[0;0,5[	5	1,028	0,028	2,759	0,978	1,042	0,0	80,0
		[0,5;1]	101	1,002	0,024	2,439	0,962	1,052	0,0	12,9
		[1;∞[	94	1,000	0,022	2,224	0,962	1,053	0,0	11,7
		Profile	IPE	100	1,002	0,024	2,389	0,962	1,053	0,0
		HEB	100	1,002	0,024	2,379	0,962	1,052	0,0	13,0

• Case 5 and 6

Table B.41 – Serna *et al.* – Case 5 and 6.

Double Symmetric	Serna <i>et al.</i>	n	Mean	St.Dev	CoV%	Min.	Max.	<0,9%	>1,03%
Case 5	Var.	All	40	0,940	0,026	2,759	0,918	1,024	0,0
	$k_w = k_z$	1	20	0,922	0,003	0,367	0,918	0,929	0,0
		0,5	20	0,959	0,025	2,617	0,941	1,024	0,0
	$\bar{\lambda}^{LTBeam}$	0;0,5	15	0,940	0,016	1,712	0,918	0,980	0,0
		0,5;1	20	0,938	0,027	2,847	0,918	1,018	0,0
		[1;∞[	5	0,955	0,044	4,647	0,922	1,024	0,0
	Profile	IPE	20	0,941	0,027	2,896	0,918	1,024	0,0
		HEB	20	0,940	0,025	2,685	0,918	1,018	0,0
	Var.	All	40	0,861	0,057	6,579	0,801	0,965	50,0
	$k_w = k_z$	1	20	0,807	0,006	0,736	0,801	0,819	100,0
Case 6		0,5	20	0,916	0,019	2,105	0,901	0,965	0,0
	$\bar{\lambda}^{LTBeam}$	0;0,5	7	0,859	0,054	6,306	0,801	0,906	42,9
		0,5;1	22	0,865	0,056	6,456	0,801	0,961	45,5
		[1;∞[	11	0,855	0,064	7,526	0,804	0,965	63,6
	Profile	IPE	20	0,862	0,058	6,720	0,801	0,965	50,0
		HEB	20	0,861	0,057	6,608	0,801	0,961	50,0

• Case 7 and 8

Table B.42 – Serna *et al.* – Case 7 and 8.

Double Symmetric	Galéa	n	Mean	St.Dev	CoV%	Min.	Max.	<0,9%	>1,03%		
Case 7	$M_0/M_\mu$	Var.	All	10620	0,979	0,053	5,366	0,666	1,047	8,0	0,8
		[4; $\infty$ ]	540	0,995	0,001	0,128	0,993	0,998	0,0	0,0	
		[2;4]	900	0,995	0,002	0,188	0,993	1,005	0,0	0,0	
		[1;2]	1800	0,998	0,004	0,448	0,994	1,024	0,0	0,0	
		[0;1]	1800	0,999	0,015	1,503	0,909	1,047	0,0	3,3	
		0	360	0,972	0,032	3,311	0,897	1,023	4,4	0,0	
		[-1;0]	1800	0,916	0,083	9,025	0,666	1,047	36,6	1,7	
		[-2;-1]	1800	0,975	0,061	6,268	0,704	1,024	9,8	0,0	
	$\bar{\lambda}^{LTBeam}$	[-4;-2]	900	0,997	0,003	0,263	0,993	1,008	0,0	0,0	
		[-∞;-4]	720	0,995	0,002	0,153	0,993	0,999	0,0	0,0	
		[0,5;1]	2360	0,967	0,066	6,806	0,666	1,012	11,8	0,0	
		[0;0,5]	3540	0,972	0,059	6,042	0,676	1,010	10,0	0,0	
		[-0,5;0]	3540	0,982	0,045	4,577	0,737	1,033	7,7	0,2	
		[-1;-0,5]	2360	0,995	0,028	2,791	0,865	1,047	2,2	3,5	
Case 8	$M_0/M_\mu$	[0;0,5]	777	0,883	0,095	10,720	0,666	1,003	50,2	0,0	
		[0,5;1]	5677	0,980	0,046	4,708	0,690	1,046	7,2	0,5	
		[1;∞]	4166	0,995	0,022	2,210	0,760	1,047	1,2	1,4	
		Profile	IPE	5310	0,979	0,052	5,324	0,666	1,047	7,9	0,9
			HEB	5310	0,978	0,053	5,407	0,666	1,046	8,2	0,8
		Var.	All	10620	0,922	0,059	6,365	0,691	1,042	21,7	0,1
		[4; $\infty$ ]	540	0,924	0,005	0,530	0,915	0,938	0,0	0,0	
	$\bar{\lambda}^{LTBeam}$	[2;4]	900	0,934	0,007	0,776	0,918	0,952	0,0	0,0	
		[1;2]	1800	0,947	0,008	0,862	0,925	0,965	0,0	0,0	
		[0;1]	1800	0,970	0,015	1,553	0,902	1,017	0,0	0,0	
		0	360	0,972	0,032	3,311	0,897	1,023	4,4	0,0	
		[-1;0]	1800	0,916	0,075	8,189	0,707	1,042	35,6	0,6	
		[-2;-1]	1800	0,853	0,073	8,534	0,691	0,965	64,5	0,0	
		[-4;-2]	900	0,897	0,023	2,522	0,821	0,936	49,3	0,0	
	$\Psi$	[-∞;-4]	720	0,912	0,007	0,727	0,892	0,926	5,3	0,0	
		[0,5;1]	2360	0,918	0,079	8,646	0,691	1,003	28,3	0,0	
		[0;0,5]	3540	0,915	0,067	7,297	0,691	1,042	30,4	0,1	
		[-0,5;0]	3540	0,921	0,049	5,303	0,733	1,042	22,9	0,3	
		[-1;-0,5]	2360	0,934	0,021	2,223	0,860	1,002	4,2	0,0	
		[0;0,5]	1248	0,882	0,074	8,386	0,691	1,002	45,8	0,0	
		[0,5;1]	5473	0,921	0,059	6,412	0,691	1,040	21,7	0,1	
	Profile	[1;∞]	3899	0,936	0,045	4,815	0,713	1,042	13,9	0,1	
		IPE	5310	0,922	0,059	6,353	0,691	1,042	21,5	0,1	
			HEB	5310	0,921	0,059	6,377	0,691	1,040	21,9	0,1